

This PDF was created from the British Library's microfilm copy of the original thesis. As such the images are greyscale and no colour was captured.

Due to the scanning process, an area greater than the page area is recorded and extraneous details can be captured.

This is the best available copy

D 37667'81

Attention is drawn to the fact that the copyright of this thesis rests with its author.

This copy of the thesis has been supplied on condition that anyone who consults it is understood to recognise that its copyright rests with its author and that no quotation from the thesis and no information derived from it may be published without the author's prior written consent.

I

D 37667/81

BRADY F

PP

361

**REPRODUCED
FROM THE
BEST
AVAILABLE
COPY**

MULTINUCLEAR NUCLEAR MAGNETIC RESONANCE INVESTIGATIONS
IN ORGANOTALLIUM CHEMISTRY

A thesis submitted to the
Council for National Academic Awards
in partial fulfilment of the requirements for the degree of
Doctor of Philosophy

By
Frank Brady

The work described was carried out in the Department of
Chemistry, The Polytechnic of North London and in Royal
Holloway College, University of London.

May 1980.

MULTINUCLEAR NUCLEAR MAGNETIC RESONANCE INVESTIGATIONS
IN ORGANOThALLIUM CHEMISTRY

F. BRADY

ABSTRACT

Thallium-205 chemical shifts have been determined for organothallium(III) derivatives $RTlX_2$ and R_2TlX (R = alkyl, alicyclic, alkenyl, aryl; X = anion). $\delta(^{205}Tl)$ is sensitive to hybridisation at thallium, the nature of R, X and the solvent. Relationships between $\delta(^{205}Tl)$ and Taft's σ^* and Es parameters for R are shown for alkyl derivatives. Substitution of electronegative atoms in R causes increased thallium shielding.

$^nJ(Tl-C)$, ($n = 1-4$) and $^{n+1}J(Tl-H)$, ($n = 2-4$) were measured for $RTlX_2$ and R_2TlX and the relative signs of the couplings determined in many cases. Coupling is sensitive to hybridisation at thallium and carbon. A stereochemical dependence of $^3J(Tl-C)$ and $^3J(Tl-H)$ and the effect of heteroatom substitution in R on coupling were examined.

Thallium-205 spin lattice relaxation times have been measured as a function of temperature for a selection of $RTlX_2$ and R_2TlX compounds. Correlation times and associated energies of activation were calculated in a number of cases. Chemical shift anisotropy is proposed as being an important relaxation mechanism for these compounds. Spin rotation is important for chloromethylbis(acetato)-thallium(III).

The X-ray crystal structures of cyclopropylbis(isobutyrate)thallium(III), the first available for an $RTlX_2$ compound, and bis(trimethylsilylmethyl)chlorothallium(III) have been determined.

Cyclopropylbis(isobutyrate)thallium(III) contains two types of carboxylate groups, bridging and chelating and chelating only. Thallium is, unusually, seven coordinate in the polymeric structure which contains a near linear (168°) $O-Tl-C$ unit. The structure allowed rationalisation of infra-red spectroscopic data, presented for organothallium(III) carboxylates in the solid state and in chloroform solution.

Bis(trimethylsilylmethyl)chlorothallium(III) is dimeric with bridging chlorine atoms. Thallium is four coordinate with a $C-Tl-C$ angle of 168° contrary to previous suggestions.

Twenty four new organothallium(III) derivatives have been synthesised and a number of existing syntheses modified.

PREFACE

The results and conclusions presented in this thesis represent original work by the author unless specific reference is made. This work has not been used in any other submission for an academic award except as noted below.

Several results in TABLES 3.4;4.4, and 4.10 have previously been used in submission for the degree of B.Sc. (B.Sc.(CNAA) Chemistry Project by F. Brady, The Polytechnic of North London, 1976). These have been clearly referenced in the tables.

ACKNOWLEDGEMENTS

I would like to thank Dr. Ray Matthews for his encouragement and guidance during this project. I would also like to thank Dr. Duncan Gillies for many helpful discussions, for assistance in running some of the thallium-205 spectra and for obtaining the high field proton spectra. I am grateful to Dr. Kim Henrick and Dr. Mary McPartlin for assistance with the X-ray crystal structures.

I gratefully acknowledge the award of a Research Studentship from the Science Research Council.

TABLE OF CONTENTS

	Page
LIST OF TABLES.....	1
LIST OF FIGURES.....	4
 1. INTRODUCTION.....	 9
1.1. Thallium-205 chemical shift studies.....	12
1.1.1. Organothallium(III) compounds.....	12
1.1.2. Thallium(I) compounds.....	16
1.2. Thallium-carbon and thallium proton coupling constants.....	 18
1.2.1. General survey.....	18
1.2.2. Relative sign determinations.....	20
1.2.3. Influence of the number of organo groups bonded to thallium.....	 21
1.2.4. Influence of anion and solvent.....	23
1.3. Thallium-205 relaxation studies.....	27
1.4. Solid-state structures of organothallium(III) compounds.....	 29
1.5. Syntheses of organothallium(III) compounds.....	31
1.5.1. Bis(organo)thallium(III) compounds.....	31
1.5.1.1. Alkyl and alicyclic compounds.....	31
1.5.1.2. Alkenyl compounds.....	33
1.5.1.3. Aryl compounds.....	34
1.5.2. Monoorganothallium(III) compounds.....	35
1.6. Aims of the project.....	37
 2. EXPERIMENTAL	
2.1. Instrumental measurements.....	39
2.1.1. Proton NMR spectra.....	39
2.1.2. Carbon-13 NMR spectra.....	40

	Page
2.1.3. Thallium-205 NMR spectra.....	40
2.1.3.1. Calculation of $\Xi(^{205}\text{Tl})$	44
2.1.4. Infra-red spectra.....	45
2.1.5. X-Ray crystal structure determinations..	45
2.2. Preparations.....	45
2.2.1. Purification of solvents.....	45
2.2.2. List of preparations.....	46
2.2.3. Starting materials.....	49
2.2.4. Organothallium(III) compounds..	50
3. THALLIUM-205 CHEMICAL SHIFTS IN ORGANOThALLIUM(III) COMPOUNDS.	
3.1. Results.....	70
3.2. Discussion.....	78
3.2.1. Origin of the chemical shift....	78
3.2.2. Range of thallium chemical shifts..	82
3.2.3. The effect of concentration and temperature.....	87
3.2.4. The effect of the solvent.....	88
3.2.5. The effect of the anion.....	92
3.2.6. The effect of the organo group....	93
3.2.6.1. Alkyl derivatives.....	93
3.2.6.2. Alicyclic derivatives.....	103
3.2.6.3. Alkenyl derivatives.....	106
3.2.6.4. Aryl derivatives.....	111
3.2.6.5. The effect of heteroatom substitution.	112
3.2.6.6. Monoorganothallium(III)derivatives...	115
4. THALLIUM-CARBON AND THALLIUM-PROTON SPIN-SPIN COUPLING CONSTANTS IN ORGANOThALLIUM(III) COMPOUNDS.	
4.1. Introduction.....	118
4.2. Results.....	119
4.2.1. Determination of the relative signs of coupling constants.....	153

	Page
4.2.2. Assignment of carbon-13 and proton spectra..	158
4.2.2.1. Comparison of carbon-13 spectra obtained at two different magnetic fields.....	158
4.2.2.2. Use of the general nuclear Overhauser effect.....	165
4.2.2.3. Assignment of the proton spectrum of bis(cyclopropyl)isobutyrate to thallium(III)...	166
4.3. Discussion.....	170
4.3.1. The origin of nuclear spin-spin coupling.....	170
4.3.2. Effects of solvent and anion on the NMR parameters.....	174
4.3.3. Effect of orbital hybridisation on spin-spin coupling constants involving thallium.....	176
4.3.4. Relative signs of coupling constants involving thallium.....	182
4.3.5. The influence of the organo group on spin- spin coupling constants involving thallium..	185
4.3.5.1. Alkyl derivatives.....	185
4.3.5.2. Alkenyl derivatives.....	190
4.3.5.3. Aryl derivatives.....	193
4.3.6. The effect of heteroatom substitution on spin-spin coupling constants involving thallium.....	193
4.3.6.1. Alkyl derivatives.....	193
4.3.6.2. Alkenyl derivatives.....	196
4.3.7. Influence of stereochemistry on spin-spin coupling constants involving thallium.....	199
4.3.7.1. Alicyclic derivatives.....	199
(a) Carbon-13 NMR results.....	200
(b) Proton NMR results.....	210

	Page
4.3.7.2. Alkyl derivatives.....	217
4.3.7.3. Alkenyl derivatives.....	220
5. THALLIUM-205 SPIN LATTICE RELAXATION IN ORGANO-THALLIUM(III) DERIVATIVES	
5.1. Introduction.....	224
5.2. Results.....	224
5.2.1. Measurement of T_1	231
5.2.2. Energy of activation.....	231
5.3. Relaxation mechanisms.....	234
5.3.1. Dipole-Dipole.....	234
5.3.2. Spin-rotation.....	235
5.3.3. Chemical shift anisotropy.....	237
5.3.4. Scalar relaxation.....	239
5.3.5. Quadrupolar relaxation.....	240
5.3.6. Electron-nuclear relaxation.....	241
5.4. Discussion.....	244
5.4.1. Evidence for the CSA mechanism in organo-thallium(III) compounds.....	249
5.4.2. Chloromethylbis(acetato)thallium(III).....	260
6. CRYSTAL AND MOLECULAR STRUCTURES OF CYCLOPROPYLBIS (ISOBUTYRATO)THALLIUM(III) AND BIS(TRIMETHYLSILYLMETHYL) CHLOROTHALLIUM(III) AND INFRA-RED SPECTROSCOPIC STUDIES OF ORGANO-THALLIUM(III) CARBOXYLATES.	
6.1. Crystal structure determination.....	264
6.1.1. Patterson synthesis.....	265
6.1.2. Fourier synthesis.....	266
6.1.3. Difference Fourier synthesis.....	267
6.1.4. Temperature factors.....	267
6.1.5. Structure refinement.....	268

	Page
6.2. Crystallography.....	269
6.2.1. Cyclopropylbis(isobutyrate)thallium(III).....	269
6.2.2. Bis(trimethylsilylmethyl)chlorothallium(III)....	272
6.3. Discussion of the structures.....	279
6.3.1. Cyclopropylbis(isobutyrate)thallium(III).....	279
6.3.1.1. Infra-red spectroscopic studies.....	285
6.3.2. Bis(trimethylsilylmethyl)chlorothallium(III)....	294
REFERENCES	300
PUBLICATIONS	322
APPENDIX I Abbreviations used.	
APPENDIX II Computer output from iterative calculation of ¹ H spectrum of bis(cyclopropyl)isobutyra- tothallium(III)	
APPENDIX III T-Values used in thallium-205 spin-lattice relaxation measurements	
APPENDIX IV Observed and calculated structure factors for cyclopropylbis(isobutyrate)thallium(III) and bis(trimethylsilylmethyl)chlorothallium(III).	

LIST OF TABLES

<u>Table</u>		<u>Page</u>
1.1.	Relative receptivity to the NMR experiment of some nuclei of spin $I = \frac{1}{2}$	11
3.1.	^{205}Tl Chemical shifts for straight-chain bis(alkyl)thallium(III) compounds..	71
3.2.	^{205}Tl Chemical shifts for branched-chain bis(alkyl)thallium(III) compounds.....	72
3.3.	^{205}Tl Chemical shifts for bis(alicyclic)thallium(III) compounds.....	73
3.4.	^{205}Tl Chemical shifts for bis(alkenyl)thallium(III) compounds.....	74
3.5.	^{205}Tl Chemical shifts for bis(aryl)-thallium(III) compounds.....	75
3.6.	^{205}Tl Chemical shifts for monoorganothallium(III) compounds.....	76
3.7.	Taft's σ^* constants and steric parameters, E_s for organo groups.....	95
3.8.	Thallium-fluorine coupling constants for $(\text{C}_6\text{F}_5)_2\text{TlBr}$ and $(p\text{-HC}_6\text{F}_4)_2\text{TlBr}$ in various solvents.....	114
4.1.	^{13}C NMR Parameters for straight-chain bis(alkyl)thallium(III) compounds.....	120
4.2.	^{13}C NMR Parameters for branched-chain bis(alkyl)thallium(III) compounds.....	122
4.3.	^{13}C NMR Parameters for bis(alicyclic)thallium(III) compounds.....	126

<u>Table</u>	<u>Page</u>
4.4. ^{13}C NMR Parameters for bis(alkenyl)thallium-(III) compounds.....	129
4.5. ^{13}C NMR Parameters for monoorganothallium(III) compounds.....	132
4.6. ^{13}C NMR Parameters for arylthallium(III) compounds.....	135
4.7. ^1H NMR Parameters for straight-chain bis-(alkyl)thallium(III) compounds.....	137
4.8. ^1H NMR Parameters for branched-chain bis-(alkyl)thallium(III) compounds.....	138
4.9. ^1H NMR Parameters for bis(alicyclic)thallium-(III) compounds.....	143
4.10 ^1H NMR Parameters for bis(alkenyl)thallium-(III) compounds.....	146
4.11. ^1H NMR Parameters for monoorganothallium(III) compounds.....	149
4.12. Observed ratios of $ J(\text{Tl-C}) $ and $ J(\text{Tl-H}) $ respectively in RTlX_2 and RTlX derivatives..	178
4.13. Dependence of $^3J(\text{Tl-C})$ on dihedral angle in norbornane derivatives RTlX_2	204
5.1 ^{205}Tl Spin-lattice relaxation times (T_1) and activation energies (E_{act}) for RTlX_2 derivatives at 34.7 MHz.....	226
5.2. ^{205}Tl Spin-lattice relaxation times (T_1), activation energies (E_{act}) and correlation times (τ_c) for R_2TlX derivatives at 34.7 MHz.....	227

<u>Table</u>	<u>Page</u>
5.3. Variation of linewidth in the proton spectra of R_2TlX derivatives with spectrometer operating frequency.....	229
5.4. Variation of linewidth in the proton spectra of $(CH_3)_2TlOCOCH_3$ with temperature at 80,220 and 360 MHz.....	229
5.5. Variation of linewidth in the proton spectra of $[(CH_3)_3CCH_2]_2TlCl$ with temperature at 360 MHz.....	230
6.1. Summary of crystal data and intensity collection for $(CH_2)_2CHTl[OCOCH(CH_3)_2]_2$ and $\{[(CH_3)_3SiCH_2]_2TlCl\}_2$	274
6.2. Final fractional coordinates and isotropic thermal parameters for $(CH_2)_2CHTl[OCOCH(CH_3)_2]_2$	275
6.3. Final fractional coordinates and isotropic thermal parameters for $\{[(CH_3)_3SiCH_2]_2TlCl\}_2$...	276
6.4. Interatomic distances and angles for $(CH_2)_2CHTl[OCOCH(CH_3)_2]_2$	277
6.5. Least squares planes for $(CH_2)_2CHTl[OCOCH(CH_3)_2]_2$	286
6.6. Infra-red absorption bands in the region $1350-1650\text{ cm}^{-1}$ for alkylthallium(III) carboxylates in the solid state and in chloroform solution....	288
6.7. Infra-red absorption bands in the region $1350-1750\text{ cm}^{-1}$ of a range of organothallium(III) carboxylates in the solid state and in chloroform solution.....	290
6.8. Interatomic distances and angles for $\{[(CH_3)_3SiCH_2]_2TlCl\}_2$	295

LIST OF FIGURES

<u>Figure</u>		<u>Page</u>
3.1.	Factors influencing thallium shielding...	82
3.2.	^{205}Tl Chemical shift range for thallium compounds in solution.....	83
3.3.	^{205}Tl Chemical shift range for organo-thallium(III) compounds R_2TlX and RTlX_2 in solution.....	85
3.4.	Variation of $\delta(\text{M})$; $\text{M} = ^{205}\text{Tl}, ^{199}\text{Hg}, ^{113}\text{Cd}$, with alkyl group for dialkylmetal compounds.....	98
3.5	Broad-band proton decoupled ^{205}Tl spectra at 34.7 MHz of $[\text{CH}_3\text{CH}_2(\text{CH}_3)\text{CH}]_2\text{TlCl}$ and $[\text{CH}_3\text{CH}_2\text{CH}_2(\text{CH}_3)\text{CH}]_2\text{TlCl}$	102
3.6.	^{205}Tl spectra at 34.7 MHz in DMSO of $(\text{CH}_2)_2\text{CHTl}[\text{OCOCH}(\text{CH}_3)_2]_2$ and $[(\text{CH}_2)_2\text{CH}]_2\text{TlBr}$	105
3.7.	Plot of $\delta(^{205}\text{Tl})$ against $^1\text{J}(^{205}\text{Tl}-^{13}\text{C})$ for alkenylthallium(III) compounds.....	107
3.8.	Plot of $\delta(^{13}\text{C}_\alpha)$ against $\delta(^{205}\text{Tl})$ for alkenylthallium(III) compounds.....	108
3.9.	Broad-band proton decoupled ^{205}Tl spectrum of $(\text{CH}_3\text{CH}=\text{CH})_2\text{TlNO}_3$ at 34.7 MHz in pyridine- d_5	110
3.10.	^{205}Tl Spectrum at 34.7 MHz of $(\text{C}_6\text{F}_5)_2\text{TlBr}$ in pyridine- d_5	113
4.1.	Energy level diagram for $\text{CH}_3\text{Tl}^{2+}$ as an AMX_3 spin system.....	155
4.2.	Assignment of ^1H , ^{205}Tl , ^{13}C transitions in the spectra of $\text{CH}_3\text{Tl}^{2+}$ for all possible relative sign combinations.....	156

<u>Figure</u>		<u>Page</u>
4.3.	^1H spectra at 60MHz of $[(\text{CH}_2)_2\text{CH}]_2\text{TlOCOCH}-(\text{CH}_3)_2$	159
4.4.	^{13}C spectra at 22.63 MHz of $[(\text{CH}_2)_2\text{CH}]_2\text{TlBr}$.	160
4.5.	Experimental and calculated spectra of $[(\text{CH}_2)_2\text{CH}]_2\text{TlOCOCH}(\text{CH}_3)_2$ at 60 MHz.....	161
4.6.	Determination of relative signs of thallium-proton coupling constants for $[(\text{CH}_3)_2\text{CHCH}_2]_2\text{TlCl}$ in DMSO-d_6	162
4.7.	Proton decoupled ^{13}C spectrum of (cyclo- $\text{C}_6\text{H}_{13}\text{CH}_2$) $_2\text{TlBr}$ at 22.63 MHz.....	163
4.8.	Proton decoupled ^{13}C spectrum of $\text{CH}_3\text{CH}(\text{OCH}_3)\text{CH}_2\text{Tl}(\text{CH}_3)\text{OCOCH}_3$	164
4.9.	Plot of $^1\text{J}(\text{Tl-C})$ against σ^* for R_2TlX derivatives.....	189
4.10.	^1H spectrum at 60 MHz of (<u>trans</u> - ClCH=CH) $_2\text{TlCl}$ and <u>trans</u> - $\text{ClCH=CH}_2\text{TlCl}_2$	198
4.11.	Plot of $^1\text{J}(\text{Tl-C})$ against ring size for R_2TlX (R = alicyclic; X = anion) in DMSO-d_6 ..	201
4.12.	Conformations of bis(cyclohexyl)thallium....	203
4.13.	Dihedral angles for $^3\text{J}(\text{Tl-C})$ for axial and equatorial thallium in cyclohexylthallium....	204
4.14.	Conformations of cyclopentane.....	207
4.15.	Dihedral angles for $^3\text{J}(\text{Tl-C})$ in cyclopentyl-thallium.....	208
4.16.	Conformations and dihedral angles for $^3\text{J}(\text{Tl-C})$ in cycloheptylthallium.....	209

<u>Figure</u>		<u>Page</u>
4.17.	Dihedral angles for $^3J(\text{Tl-H})$ in cyclopropylthallium.....	210
4.18.	Plot of $^3J(\text{Tl-H})$ against dihedral angle for RTlX_2 derivatives.....	212
4.19.	Dihedral angles for $^3J(\text{Tl-H})$ in cyclohexylthallium.....	213
4.20.	Dihedral angles for $^3J(\text{Tl-H})$ in cyclopentylthallium.....	215
4.21.	Dihedral angles for $^3J(\text{Tl-H})$ in cycloheptylthallium(quasi-equatorial thallium)...	216
4.22.	^1H spectrum at 60 MHz of $[\text{CH}_3\text{CH}_2(\text{CH}_3)\text{CH}]_2\text{TlCl}$ in DMSO-d_6	218
4.23.	Newman projections of a <u>sec</u> -alkyl-thallium (III) derivative.	217
5.1	Determination of T_1 by the inversion recovery method using the $(180^\circ-\tau-90^\circ)$ pulse sequence..	232
5.2.	Typical results of a ^{205}Tl T_1 determination at 34.7MHz using the $(180^\circ-\tau-90^\circ)$ pulse sequence.....	233
5.3.	Temperature dependence of spin-lattice relaxation.....	243
5.4.	Plot of $\ln T_1(^{205}\text{Tl})$ against temperature for $(\text{C}_6\text{H}_5)_2\text{TlCl}$	247
5.5.	Proton spectra of $(\text{CH}_3)_2\text{TlOCOCH}_2$ in D_2O at different frequencies.....	250

<u>Figure</u>		<u>Page</u>
5.6.	Dependence of $V_{\frac{1}{2}}$ on operating frequency for proton spectra of $(\text{CH}_3)_2\text{TlOCOCH}_3$ in D_2O	251
5.7.	Proton spectra at 360 MHz of $[(\text{CH}_3)_3\text{CCH}_2]_2\text{TlCl}$ in pyridine- d_5	253
5.8.	Plot of $\ln R_1(\text{OC } V_{\frac{1}{2}}(^1\text{H}))$ against temperature for $(\text{CH}_3)_2\text{TlOCOCH}_3$ in D_2O at 80, 220 and 360 MHz.....	256
5.9.	Plot of $\ln R_1(^{205}\text{Tl})$ against temperature for $(\text{CH}_3)_2\text{TlOCOCH}_3$ in D_2O at 34.7 MHz.....	257
5.10.	Plot of $\ln T_1(^{205}\text{Tl})$ against temperature for $\text{Cl CH}_2\text{Tl}(\text{OCOCH}_3)_2$ in CD_3OD	261
6.1.	The structure of a monomer unit of $(\text{CH}_2)_2\text{-CHTl}[\text{OCOCH}(\text{CH}_3)_2]_2$ without disorder.....	280
6.2.	The structure of a monomer unit of $(\text{CH}_2)_2\text{CHTl}[\text{OCOCH}(\text{CH}_3)_2]_2$ showing disorder in atoms C(2), C(7) and C(10).....	281
6.3.	Coordination geometry around thallium in $(\text{CH}_2)_2\text{CHTl}[\text{OCOCH}(\text{CH}_3)_2]_2$	282
6.4.	A section of the polymer chain in $(\text{CH}_2)_2\text{CHTl}[\text{OCOCH}(\text{CH}_3)_2]_2$	284
6.5.	The coordinating modes of the carboxylate anion in organothallium(III) compounds...	292
6.6.	The structure of a monomer unit of $\{[(\text{CH}_3)_3\text{SiCH}_2]_2\text{TlCl}\}_2$ showing disorder in one of the trimethylsilylmethyl groups....	296

Figure

Page

- 6.7. The structure of $\{[(CH_3)_3SiCH_2]_2TiCl\}_2$.
 (The disorder in the trimethylsilylmethyl
 groups not shown) 297

CHAPTER ONE

INTRODUCTION

The use of the pulse Fourier transform (PFT) nuclear magnetic resonance (NMR) method has allowed direct observation of many nuclei with low sensitivity in the NMR experiment and/or low natural abundance (e.g. nuclei with spin $I = \frac{1}{2}$, ^{13}C , ^{29}Si , ^{77}Se , ^{113}Cd , ^{119}Sn , ^{125}Te , ^{195}Pt , ^{199}Hg and ^{207}Pb). NMR spectra for the majority of isotopes in the periodic table with $I > 0$ have now been observed.¹

Thallium is particularly favourable for study by the NMR method. It possesses two isotopes of spin $I = \frac{1}{2}$, (^{205}Tl , natural abundance 70.5% and ^{203}Tl , natural abundance 29.5%) coupled with relatively high sensitivity in the NMR experiment. The relative receptivities of some nuclei with spin $I = \frac{1}{2}$ are given in TABLE 1.1. In addition to studying the chemical shift and relaxation behaviour of the thallium nucleus another way of utilising its favourable spin property is to examine nuclear spin-spin coupling with carbon and protons in organothallium(III) compounds. Thus organothallium(III) derivatives are particularly appropriate for study by the NMR method, having the advantage that three nuclei having spin $I = \frac{1}{2}$ (^1H , ^{13}C , ^{205}Tl) are contained in relatively simple molecules.

To provide a background for the NMR results, structural determinations and synthetic methods described herein, surveys of relevant work in each of these areas are given in the following sections.

Details of experimental methods, instrumentation and theoretical background of the NMR experiment are given in a number of reviews²⁻⁴ and comprehensive texts,^{1,5-9} and no attempt will be made to reiterate this information here. However, to facilitate discussion of the NMR results, discussions of the origins of the chemical shift and spin-spin coupling constants

TABLE 1.1.

Relative receptivity to the NMR experiment of some nuclei
of spin $I=\frac{1}{2}$ ^a

<u>Isotope</u>	<u>Natural abundance(%)</u>	<u>Relative receptivity^b</u>
¹ H	99.985	1.000
¹³ C	1.108	1.76×10^{-4}
¹⁵ N	0.37	3.85×10^{-6}
¹⁹ F	100	0.8328
²⁹ Si	4.70	3.69×10^{-4}
³¹ P	100	0.0663
⁷⁷ Se	7.58	5.26×10^{-4}
⁸⁹ Y	100	1.18×10^{-4}
¹⁰³ Rh	100	3.12×10^{-5}
¹⁰⁹ Ag	48.18	4.86×10^{-5}
¹¹³ Cd	12.26	1.34×10^{-3}
¹¹⁹ Sn	8.58	4.44×10^{-3}
¹²⁵ Te	6.99	2.21×10^{-3}
¹⁸³ W	14.4	1.04×10^{-5}
¹⁹⁵ Pt	33.8	3.36×10^{-3}
¹⁹⁹ Hg	16.84	9.54×10^{-4}
²⁰⁵ Tl	70.5	0.1355
²⁰³ Tl	29.5	5.51×10^{-2}
²⁰⁷ Pb	22.6	2.07×10^{-3}

a. Data from ref 1.

b. An approximate guide to the ease of observing a signal for a given concentration of the relevant nucleus in solution at a constant magnetic field, B_0 .¹ Values are relative to the proton.

are given in Chapters 3 and 4 respectively. The mechanisms of nuclear relaxation are discussed in some detail (Chapter 5). A brief outline of the theory underlying the determination of solid state structures by X-ray diffraction will be given in Chapter 6.

1.1. Thallium-205 chemical shift studies

A detailed survey of reports of thallium-205 chemical shifts in organothallium(III) compounds will be given followed by a brief selective survey for Tl(I) compounds.

1.1.1. Organothallium(III) compounds

There have been relatively few studies of $\delta(^{205}\text{Tl})$ for organothallium(III) derivatives and the detailed factors influencing the chemical shift are largely unknown. Schneider and Buckingham¹⁰ showed the paramagnetic contribution to be the dominant factor influencing thallium, mercury and lead chemical shifts. They predicted decreased thallium shielding for covalently bonded organothallium(III) compounds and found that the thallium nucleus in $(\text{CH}_3)_3\text{Tl}$, in diethyl ether ca. 25°C , was much less shielded than in a number of Tl(I) compounds. The thallium-205 chemical shifts reported by Hildenbrand and Dreeskamp¹¹ for $(\text{CH}_3)_3\text{Tl}$ in acetone at -70°C , $(\text{CH}_3)_2\text{TlBr}$ in liquid ammonia at -30°C and for $(\text{C}_6\text{H}_5)_2\text{TlCl}$ in the same solvent at -20°C , were also shown to be at higher frequency than those found in Tl(I) compounds. Variation of $\delta(^{205}\text{Tl})$ in the series R_3Tl , R_2TlX , RTlX_2 ($\text{R} = \text{CH}_3$; $\text{X} = \text{anion}$) in various solvents was examined by Hoad, Matthews et al.¹² Increased methyl substitution was found to cause decreased thallium shielding with a total shift range of 1424 ppm, but the factors influencing $\delta(^{205}\text{Tl})$ could not be elucidated due to the limited amount of data

available. Koppell et al.¹³ reported $\delta(^{205}\text{Tl})$ for several R_3Tl derivatives; $(\text{CH}_3)_3\text{Tl}$ in diethyl ether and in pentane, $(\text{CH}_3\text{CH}_2)_3\text{Tl}$ in pentane and $(\text{C}_6\text{H}_5)_3\text{Tl}$ in diethyl ether all at 24°C . Shift values were also reported for R_2TlX ($\text{R} = \text{C}_2\text{H}_5$, $n\text{-C}_3\text{H}_7$; $\text{X} = \text{Br}, \text{NO}_3$) in DMSO and for Ph_2TlBr in DMSO, PhTlCl_2 and PhTlCl_2L ($\text{L} = \text{bipyridyl}$, triphenylphosphine) in pyridine and methanol solutions.¹³ A review of the chemical shift ranges of the various classes of thallium compounds was presented.¹³ For organothallium(III) compounds the relative order of thallium shielding

$$\text{R}_3\text{Tl} < \{\text{R}'\text{TlX}\}_2 < \text{R}''\text{TlX} < \text{R}'''\text{TlX}_2$$

($\text{R} = \text{CH}_3, \text{C}_2\text{H}_5, \text{C}_6\text{H}_5$; $\text{R}' = \text{CH}_3$, $\text{R}'' = \text{CH}_3, \text{C}_2\text{H}_5, n\text{-C}_3\text{H}_7, \text{C}_6\text{H}_5$; $\text{R}''' = \text{C}_6\text{H}_5$) was established based on the limited data available. To a first approximation, $\delta(^{205}\text{Tl})$ depends upon the state of hybridisation and effective nuclear charge at thallium. It was proposed that inductive effects of the organo group are important in influencing the thallium shielding.¹³ The effect of electronic factors in the organo group on $\delta(^{205}\text{Tl})$ was examined by Hinton and Briggs¹⁴ for a series of mono-, di- and trisubstituted arylthallium(III) derivatives $\text{ArTl}(\text{OCOCF}_3)_2$. A correlation between $\delta(^{205}\text{Tl})$ and the Hammett σ parameter was interpreted in terms of the substituent altering the ionic character of the thallium-anion interaction. A trend of increased thallium shielding with increasing electron donating ability of the substituent for a series of arylthallium(III) derivatives $\text{XC}_6\text{H}_4\text{Tl}(\text{OCOCF}_3)_2$ ($\text{X} = \text{alkyl}$, halogen, H , Ph , OCH_3 , $\text{C}_6\text{H}_4\text{CH}_2\text{CO}_2\text{H}$) was noted by Zink et al.¹⁵

The majority of other studies of $\delta(^{205}\text{Tl})$ have been concerned with the influence of anion and solvent in $(\text{CH}_3)_2\text{TlX}$ ($\text{X} = \text{anion}$) derivatives. Burke, Matthews and Gillies¹⁶ have investigated the influence of solute concentration, anion and solvent (H_2O , DMSO, CH_2Cl_2 , pyridine, toluene) on $\delta(^{205}\text{Tl})$ for $(\text{CH}_3)_2\text{TlX}$

(X = NO₃, I, O₆H₄) compounds. The shifts spanned ca. 300ppm and depended mainly on the nature of anion and solvent. A smaller concentration dependence was found in all cases except for (CH₃)₂TlNO₃ in H₂O. It was proposed that the thallium chemical shift depends primarily upon the degree of contact ion pair formation between (CH₃)₂Tl⁺ and X⁻ and/or the average number of anions and solvent molecules surrounding the cation or ion-pair. No correlations between $\delta(^{205}\text{Tl})$ and either $\delta(^1\text{H})$ or $\delta(^{13}\text{C})$ were observed. As an extension of this study the infinite dilution thallium chemical shifts of (CH₃)₂TlNO₃ in a number of donor solvents has been reported by Hinton and Briggs.¹⁷ Although the authors find no correlation between $\delta(^{205}\text{Tl})$ and solvent Gutmann donor number, a plot of the reported values yields a value of $r = 0.92$.¹⁸ Contrary to the previous study¹⁶ they also report a very small concentration dependence of $\delta(^{205}\text{Tl})$ for (CH₃)₂TlNO₃ in H₂O. The results are in otherwise good agreement. The concentration dependence of $\delta(^{205}\text{Tl})$ for (CH₃)₂TlNO₃ in aqueous solution has been studied by Chan and Reeves¹⁹ who found a small concentration dependent solvent isotope shift for $\delta(^{205}\text{Tl})$ between H₂O and D₂O which they interpreted in terms of differential penetration of the D₂O/H₂O solvation spheres of the solvated (CH₃)₂Tl⁺ ion by the anion. The thallium-205 resonance position was independent of dissolved oxygen.

Koppell et al.¹³ examined the influence of solvent, anion and concentration of solute on $\delta(^{205}\text{Tl})$ for (CH₃)₂TlX derivatives. Anion dependence is discussed in terms of the degree of covalency in the metal-anion bonding interaction and solvent effects are interpreted in terms of solvent basicity and dielectric constants. Concentration effects were rationalised in terms of differential disturbance of the first solvation sphere

through ion-pair formation. The solute and anion concentration dependence of $\delta(^{205}\text{Tl})$ for $(\text{CH}_3)_2\text{TlX}$, ($\text{X} = \text{NO}_3, \text{I}, \text{BF}_4, \text{F}, \text{OCOCH}_3$) has been studied by Burke.¹⁸ Variations in $\delta(^{205}\text{Tl})$ were interpreted in terms of equilibria between fully dissociated species and contact ion pairs. A curve fitting procedure was used to estimate equilibrium constants for ion-pair formation. Briggs et al.²⁰ reported a similar study in several solvents for $(\text{CH}_3)_2\text{TlX}$ ($\text{X} = \text{NO}_3, \text{ClO}_4$). In general increased ion-pairing caused a low-frequency shift of the ^{205}Tl resonance, except for $(\text{CH}_3)_2\text{TlNO}_3$ in *n*-butylamine. Ion pair formation constants were calculated. Burke¹⁸ also determined $\delta(^{205}\text{Tl})$ for several dimethylthallium(III) compounds in binary solvent mixtures of varying solvent composition. In all cases $\delta(^{205}\text{Tl})$ was found to vary non-linearly with solvent composition. The results were discussed in terms of a model for preferential solvation of the dimethylthallium(III) ion and in some cases equilibrium constants for the solvent replacement process were determined. The solvent dependence of $\delta(^{205}\text{Tl})$ for $(\text{CH}_3)_2\text{TlX}$, ($\text{X} = \text{NO}_3, \text{ClO}_4$) has been examined by Schramm and Zink²¹, who found a range of ca. 200ppm in a series of donor solvents. A correlation of $\delta(^{205}\text{Tl})$ with solvent pK_a has been suggested. Binary solvent mixtures were investigated to obtain data on relative solvating abilities.

The chemical shifts were dependent upon whether the solvents were O or N donors. Ion-pairing was also found to have a large effect on the shift. Results were discussed in terms of a molecular-orbital model of thallium-solvent interaction. Zink, Srivanavit and Dechter¹⁵ found a relationship between solvent dielectric constant and the differences in $\delta(^{205}\text{Tl})$ for solutions of Me_2TlX ; $\text{X} = \text{NO}_3$ or ClO_4 , in various donor solvents. The result was indicative of the importance of ion-pairing on the

chemical shift.

A variable temperature study of oligomeric dimethylthallium(III) compounds by Sheldrick and Yesinowski²² revealed $J(^{205}\text{Tl}-^{203}\text{Tl})$ coupling for $(\text{CH}_3)_2\text{TlOC}_2\text{H}_5$ in benzene and toluene at low temperatures. $(\text{CH}_3)_2\text{TlN}(\text{CH}_3)_2$ was also studied. The temperature dependence of the thallium-205 chemical shift was examined by Burke et al²³ for R_2TlX ($\text{R} = \text{CH}_3$; $\text{X} = \text{NO}_3, \text{OCOCH}_3, \text{BF}_4$; $\text{R} = \text{CH}_3(\text{CH}_2)_n-$ ($n = 1$ to 5), $\text{X} = \text{NO}_3$). The temperature coefficient ($d\delta(^{205}\text{Tl})/dT$) was less than 0.7ppm per degree in all cases. The variations in $\delta(^{205}\text{Tl})$ with temperature were ascribed to changes in vibrational effects both within the $(\text{CH}_3)_2\text{Tl}^+$ moiety and for interactions of this species with coordinated solvent. The infinite dilution chemical shifts for the methyl derivatives were also reported.

1.1.2. Thallium(I) compounds

The majority of studies on Tl(I) compounds have been concerned with the effect of anion and solvent on the thallium-205 chemical shift. Gutowsky and McGarvey²⁴ studied the thallium-205 chemical shift, $\delta(^{205}\text{Tl})$, for aqueous solutions of Tl(I)NO_3 and Tl(I)OCOCH_3 . The linear concentration dependence of $\delta(^{205}\text{Tl})$ on concentration of solute was interpreted in terms of inter-ionic interactions occurring as the anion penetrated the solvation sphere of the Tl(I) ion. Freeman et al²⁵ carried out a more detailed study of the anion and concentration dependence of $\delta(^{205}\text{Tl})$ in Tl(I)X , ($\text{X} = \text{OH}, \text{F}, \text{OAc}, \text{NO}_3, \text{ClO}_4, \text{HCOO}$), derivatives. The effect of added anion was also examined. The non-linear concentration dependence of $\delta(^{205}\text{Tl})$ at low concentrations of anion was correlated with ion pair formation. The linear behaviour at higher anion concentrations was attributed to interaction between ion-pairs and added anions.

Gasser and Richards²⁶ found further evidence for the importance of ion pairs on $\delta(^{205}\text{Tl})$ by studying Tl(I) ions in the presence of ferricyanide and citrate ions. The concentration dependence of $\delta(^{205}\text{Tl})$ for Tl(I)ClO_4 in water and in a range of non-aqueous solvents has been studied by Dechter and Zink²⁷ who reported $\delta(^{205}\text{Tl})$ at infinite dilution. The shift range was 2600ppm and changes were discussed in terms of site symmetry of the Tl(I) ion as anions penetrated its solvation sphere. Hinton and Briggs²⁸ found a correlation between solvent Gutmann donor number and $\delta(^{205}\text{Tl})$ for Tl(I) ions. A linear correlation between relative solvating ability of solvent and $\delta(^{205}\text{Tl})$ for Tl(I)ClO_4 in binary solvent mixtures has been reported.²⁹ Numerous other studies of the solvent dependence of $\delta(^{205}\text{Tl})$ for the thallous ion have been reported for aqueous solutions, 13,30-39, non-aqueous solutions^{27,29,47-50} and in binary solvent mixtures.^{20,27-29,49} The thallous ion has similarities to Na^+ and K^+ and this has led to its use as a probe of complex formation in crown ethers, cryptands and biological systems^{48,51-60} using thallium-205 NMR.

1.2. Thallium-carbon and thallium-proton coupling constants

1.2.1. General survey

There have been a limited number of reports of Tl-C coupling constants in organothallium(III) compounds. The majority of these have been for methyl-derivatives with $^1J(\text{Tl-C})$ reported for $(\text{CH}_3)_3\text{Tl}$ ¹¹; $(\text{CH}_3)_2\text{TlX}$ ^{11,12,16,21,61-64,78} and CH_3TlX_2 ¹² (X=anion). The only other reports for alkylthallium(III) derivatives have been for $(\text{CH}_3)_2\text{TlCH}_2\text{P}(\text{CH}_3)_3$ ⁶⁴ and $[(\text{CH}_3)_2\text{TlCH}_2\text{P}(\text{CH}_3)_2\text{CH}_2]_2$.⁶⁵ Several authors^{14,66-71} have reported values of $^nJ(\text{Tl-C})$ (n=1-7) for aryl derivatives RTlY_2 (R=aryl, substituted aryl; Y=OCOCF₃). These aryl compounds are notable for the extremely large values of $^1J(\text{Tl-C})$, (8841 to 10718 Hz) observed.

In some cases reported thallium-carbon coupling appears to be sensitive to the geometry of the system. Ernst⁶⁶ studied $^nJ(\text{Tl-C})$, (n=2-6) for a series of alkyl-substituted arylthallium(III)bistrifluoroacetates. For the aryl ring $|J(\text{Tl-C})|$ was found to increase in the order $\text{C}_{\text{para}} < \text{C}_{\text{meta}} < \text{C}_{\text{ortho}} < \text{C}_1$. The effect of alkyl group substitution in the aromatic ring on the couplings was examined. Couplings over five and six bonds were observed and these were shown to exhibit a geometrical dependence, the exact nature of which was not established. This sensitivity of thallium-carbon coupling to molecular geometry has been suggested in studies of thallium adducts of D-galactal acetate,⁷² norbornane and norbornene derivatives⁷³⁻⁷⁶ and in a Tl(I)salt of an ionophoric antibiotic.⁷⁷ However in none of these cases was the detailed nature of the dependence established and this area clearly requires further investigation.

Thallium-carbon coupling has also been noted in a number of compounds without thallium-carbon bonds. Abraham et al⁷⁹⁻⁸¹ and Henrick et al⁶¹ reported coupling in thallium(III) porphyrin derivatives. Bystrov et al⁸² and Hinton and Briggs⁵⁷ noted thallium-carbon coupling in Tl(I)/valinomycin complexes. Krommes and Lorberth⁸³ found $^3J(\text{Tl-C})=83 \text{ Hz}$ in $\{[(\text{CH}_3)_3\text{Si}]_2\text{N}\}_3\text{Tl}$. Thallium-carbon couplings, up to and including four bonds, to the carboxylate groups in the complexes $\text{PdTl}(\text{OCOR})_5$, ($\text{R}=\text{CH}_3, \text{CH}_3\text{CH}_2, (\text{CH}_3)_2\text{CH}$) have been noted.⁸⁴ These will be further discussed in Chapter 4.

Although there have been a large number of studies of proton NMR parameters of alkylthallium(III) compounds⁸⁵ the majority of these have been concerned with the effects of anion and solvent on $^nJ(\text{Tl-H})$ ($n=2,3$) in $(\text{CH}_3)_2\text{TlX}$ and $(\text{CH}_3\text{CH}_2)_2\text{TlX}$ ($\text{X}=\text{anion}$) derivatives.⁸⁵ Longer-chain and branched-chain alkyl derivatives have received relatively little attention. Thallium-proton coupling constants have been noted for R_2TlX compounds, $\text{R}=\text{n-propyl}$ ^{86,13}; iso-propyl⁸⁶; n-Butyl⁸⁶; iso-butyl⁸⁶; neo-pentyl⁸⁷; trimethylsilylmethyl⁸⁸ and cyclopentyl.⁸⁶ A number of scattered reports of thallium-proton coupling in RTlX_2 derivatives have appeared for $\text{R}=\text{methyl}$ ^{12,89-91}, ethyl⁸⁹⁻⁹⁰, neopentyl⁸⁷, trimethylsilylmethyl⁸⁸ and various acetoxy thallation products of olefins.⁹²⁻⁹⁴ Anet⁹² proposed a stereochemical dependence of thallium-proton coupling constants in thallium(III) adducts of norbornane and norbornene. Thallium-proton couplings are known for several vinyl- and substituted alkenylthallium(III)^{86,95-100} compounds. Maher and Evans⁹⁵ demonstrated a large geometrical dependence of thallium-proton coupling in these systems and the couplings were generally much larger than in alkyl systems.

Thallium-proton coupling in bis(aryl)- and mono(aryl)-thallium(III) derivatives has received wide attention.⁸⁵ The ${}^6J(\text{Tl-H})$ in alkyl-substituted monoarylthallium(III) compounds was found to have a similar stereochemical dependence to ${}^5J(\text{Tl-C})$ in such systems. Maher and Evans¹⁰¹ argued that for alkyl-substituted arylthallium(III) derivatives R_2TlX , ($\text{R}=\text{e.g. CH}_3\text{C}_6\text{H}_4$), coupling to protons in ortho- and meta substituents, $J(\text{Tl-CH}_3)$, is transmitted mainly via σ -electrons but that transmission via the π -electrons becomes important in coupling to the protons in para-substituents. This rationalisation accounts for the fact that ${}^6J(\text{Tl-CH}_3)_{\text{para}}$ is larger than ${}^5J(\text{Tl-CH}_3)_{\text{meta}}$ in $(\text{CH}_3\text{-C}_6\text{H}_4)_2\text{Tl}^+$ systems.^{101,102}

1.2.2. Relative sign determinations

A limited number of relative sign determinations have been reported for thallium-carbon and thallium-proton coupling constants in organothallium(III) compounds. Hildenbrand and Dreeskamp¹¹ determined the signs of coupling constants in several organothallium(III) derivatives relative to ${}^1J(\text{CH})$ and ${}^3J(\text{HH})$. ${}^1J(\text{Tl-C})$ is positive in $(\text{CH}_3)_3\text{Tl}$ and $(\text{CH}_3)_2\text{TlBr}$ while ${}^2J(\text{Tl-H})$ in these compounds is negative. A similar situation was found in $(\text{CH}_3)_2\text{Cd}$ where ${}^1J(\text{Cd-C})$ is positive and ${}^2J(\text{Cd-H})$ is negative. Thallium-proton couplings; ${}^3J(\text{Tl-H})$, ${}^4J(\text{Tl-H})$ and ${}^5J(\text{Tl-H})$ in $(\text{C}_6\text{H}_5)_2\text{TlBr}$ all have positive signs. Ernst⁶⁶ found that for a series of alkyl substituted arylthallium(III)bistrifluoroacetates ${}^2J(\text{Tl-C})_{\text{o}}$ and ${}^3J(\text{Tl-C})_{\text{m}}$ are positive while ${}^4J(\text{Tl-C})_{\text{p}}$ is negative. Maher and Evans⁸⁶⁻⁹⁵ determined the relative signs of thallium-proton coupling constants in some alkyl, alkenyl, and arylthallium(III) systems. All thallium-proton coupling constants in phenylthallium(III) compounds, R_3Tl ; R_2Tl^+ ; RTl^{2+} , ($\text{R}=\text{phenyl}$), were found to have the same signs. Similarly all thallium-proton couplings in

vinylthallium(III) derivatives R_2Tl^+ ; RTl^{2+} (R =vinyl) have the same sign, but for alkylthallium(III) compounds R_2Tl^+ (R =ethyl, n-propyl, iso-butyl) $^2J(Tl-H)$ and $^3J(Tl-H)$ are of opposite signs,

while $^3J(Tl-H)$ and $^4J(Tl-H)$ have the same sign.

The relative signs of thallium - proton coupling constants have been reported by Anet⁹² for the oxythallation adducts $RTl(OCOCH_3)_2$ (R =norbornane; norbornene). Shier and Drago¹⁰³ explained the fact that in $(CH_3CH_2)_2Tl^+$ $|^3J(Tl-H)| > |^2J(Tl-H)|$ on the following basis. $^2J(Tl-H)$ is the difference between two large Fermi contact terms and $^3J(Tl-H)$ is the sum. This is by analogy with proton-proton coupling in which the Fermi term dominates and couplings alternate in sign through an odd or even number of bonds.¹⁰⁴ The Fermi term transmitted through the $Tl-C$ bond to the CH_2 protons in the $(CH_3CH_2)_2Tl^+$ derivative will be of opposite sign to that due to direct thallium-proton through space interaction. For coupling to the CH_3 protons both contributions will have the same sign.

1.2.3. Influence of the number of organo groups bonded to thallium

Few investigations of the variation of coupling constants in the series R_3Tl ; R_2Tl^+ ; RTl^{2+} , have been reported. Hoad et al¹² studied the variation of $^1J(Tl-C)$ and $^2J(Tl-H)$ in the series; R_3Tl ; R_2TlX ; $RTlX_2$ ($R=CH_3$; X =anion). Both $^1J(Tl-C)$ and $^2J(Tl-H)$ decrease with increasing number of methyl groups on thallium. A linear correlation between $^1J(Tl-C)$ and $^2J(Tl-H)$ was found for the above series, with close approach of the line to the origin, for gross changes dependent on the extent of methyl substitution. However there appeared to be no detailed correlation between $^1J(Tl-C)$ and $^2J(Tl-H)$ for a particular

type of methylthallium(III) derivative. The ratios of $^1J(\text{Tl-C})$ and $^2J(\text{Tl-H})$ respectively in the series R_3Tl , R_2TlX , RTlX_2 and the linear correlation between $^1J(\text{Tl-C})$ and $^2J(\text{Tl-H})$ were taken as evidence for the dominance of the Fermi contact interaction. (This will be discussed in more detail in Chapter 4).

Maher and Evans^{86,95,101} examined the variation of $^nJ(\text{Tl-H})$ ($n=2-6$) in the series $\text{R}_3\text{Tl}; \text{R}_2\text{Tl}^+; \text{RTl}^{2+}$ ($\text{R}=\text{aryl, alkenyl}$) and for $\text{R}_3\text{Tl}; \text{R}_2\text{Tl}^+$ ($\text{R}=\text{methyl, ethyl}$). $^nJ(\text{Tl-H})$ was found to increase in the order $\text{R}_3\text{Tl} < \text{R}_2\text{Tl}^+ < \text{RTl}^{2+}$ in the ratios 1:1.7:4.0. This was in close agreement with ratios they predicted (1:1.8:4.3) based on the assumption that coupling was dominated by the Fermi contact term.

However Hoad et al¹² recalculated the ratios using the method of Maher and Evans⁸⁶ and found their predicted ratios to be in error. The recalculated ratios; 1.0:1.7:3.7 were found to be in better agreement with observed ratios for $^1J(\text{Tl-C})$ and $^2J(\text{Tl-H})$ respectively in the series R_3Tl , $\text{R}_2\text{Tl}^+; \text{RTl}^{2+}$. Using a simplified model for the contact interaction employing optical hyperfine splitting constants, Hatton¹⁰⁵ made an estimate of the contact contribution to the total thallium-proton coupling constant for the series $\text{R}_3\text{Tl}; \text{R}_2\text{Tl}^+; \text{RTl}^{2+}$. ($\text{R}=\text{organo group}$). It was found that irrespective of the nature of R ($\text{R}=\text{alkyl, alkenyl, aryl}$) (using published values of thallium-proton coupling constants), $J(\text{Tl-H})$ increased in the relative proportions predicted by the model. The results were consistent with the dominance of the Fermi contact term.

1.2.4. Influence of anion and solvent

The majority of coupling constant studies for organo-thallium(III) compounds have been concerned with the influence of anion and solvent on $^1J(\text{Tl-C})$ and $^2J(\text{Tl-H})$ in $(\text{CH}_3)_2\text{TlX}$ derivatives and these will now be examined in some detail.

Burke et al¹⁶ have examined the dependence of $^1J(\text{Tl-C})$ and $^2J(\text{Tl-H})$, in $(\text{CH}_3)_2\text{TlX}$ ($\text{X}=\text{I}, \text{NO}_3, \text{OC}_6\text{H}_5$), on solute concentration, the nature of the anion X and the solvent. The concentration and anion dependence of $^1J(\text{Tl-C})$ ($<2\%$ and $<6\%$ respectively) were similar to those observed for $^2J(\text{Tl-H})$. The solvent had the largest influence with an increase in $^1J(\text{Tl-C})$ of ca. 20% in going from H_2O to pyridine for $(\text{CH}_3)_2\text{TlNO}_3$. An increase in $^2J(\text{Tl-H})$ of ca. 14% for the solvent change toluene to DMSO was observed for $(\text{CH}_3)_2\text{TlOC}_6\text{H}_5$. Solvent induced changes were discussed in terms of the Fermi contact term. It was suggested that changes in ΔE and the s-electron density at the nuclei as well as changes in s-character of the metal-carbon bond could collectively account for solvent dependent changes of the magnitudes observed. Values obtained for $^1J(\text{Tl-C})$ did not support the assumptions often used in rationalising solvent effects, namely that increasing the coordinating ability of the solvent causes rehybridisation at the metal in such a way that $\alpha^2(\text{M})$ increases. The factors influencing $^1J(\text{Tl-C})$ and $^2J(\text{Tl-H})$ were not the same. Hoad et al¹² attributed variations in $^1J(\text{Tl-C})$ and $^2J(\text{Tl-H})$ ($<25\%$ for R_2TlX derivatives) to changes in concentration, anion and most importantly solvent. The data presented for RTlX_2 ($\text{R}=\text{CH}_3$) derivatives likewise suggested the importance of anion and solvent in determining $^1J(\text{Tl-C})$

and $^2J(TlH)$. The solvent and anion dependence of thallium-proton coupling in a number of other methyl and ethyl derivatives, R_2TlX , have previously been reported and rationalisations of the observed variations in coupling proposed. Hatton¹⁰⁵ examined $^nJ(Tl-H)$, ($n=2-3$), in $(CH_3)_2TlX$ and $(CH_3CH_2)_2TlX$ ($X=\text{anion}$) in D_2O and pyridine solvents for a wide range of anions. In D_2O $^2J(Tl-H)$ is virtually independent of the anion, (variation $<0.25\%$), whereas in pyridine anion dependent changes of up to 5% were observed. The couplings in pyridine were larger than those in D_2O in all cases (by up to 6.5%). It was suggested on the basis of Raman evidence, that in D_2O solution the $(CH_3)_2Tl^+$ species was present in all cases whereas in pyridine solution a partially dissociated structure: $[(CH_3)_2Tl-N^+C_5H_4 X^-]$ was present. The solvent dependence of $^2J(Tl-H)$ in $(CH_3)_2TlClO_4$ was examined by Shier and Drago¹⁰³ in a range of nitrogen- and oxygen-donor solvents (variations in $^2J(Tl-H)$ ca. 13% found). The increase in $^2J(Tl-H)$ with increasing donor ability of the solvent was explained in terms of an orbital mixing scheme involving thallium 6s and $5d_{z^2}$ orbitals such that increasing solvent interaction decreases the degree of orbital mixing and increases the amount of s-character in the Tl-C bond. The absence of an observable symmetric stretching frequency in the infra-red spectra of solutions of $(CH_3)_2Tl^+$ in oxygen donor solvents indicated the presence of a linear $CH_3-Tl^+-CH_3$ species. This ruled out the possibility that changes in s-character arose from variation of the C-Tl-C angle as different solvent molecules were coordinated to the cation. It was suggested that in pyridine the C-Tl⁺-C moiety is bent and that rehybridisation of thallium

occurs to provide orbitals that overlap effectively with pyridine providing a stronger covalent interaction. This results in a reduction in s-character of the thallium hybrid orbital directed towards the methyl group leading to a smaller C-Tl-C angle. A similar orbital mixing scheme has been proposed to account for the solvent dependence of $^2J(\text{Pb-H})$ in $(\text{CH}_3)_2\text{Pb}^+$ compounds.¹⁰⁶ Similar changes in s-character of the carbon-thallium bond have been invoked to account for variations in $^2J(\text{Tl-H})$ for $(\text{CH}_3)_2\text{TlX}$ (X=anion) between polar and non-polar solvents. Reported values of $^2J(\text{Tl-H})$ ^{11,13,103,105,107-111} for $(\text{CH}_3)_2\text{TlX}$ with few exceptions fall into two ranges: (i) 400-475 Hz for solutions in polar solvents (ii) 340-380Hz for solutions in non-polar solvents. Several solutions of $(\text{CH}_3)_2\text{TlX}$ with values in the latter range have been shown to contain dimers and this range may be characteristic of oligomer formation. Lower values of $^2J(\text{Tl-H})$ in the latter range have been attributed¹⁰⁷ to a reduction in the s-character of the Tl-C bonds as the C-Tl-C angle deviates from linearity. However Burke et al⁶² examined the variation of $^1J(\text{Tl-C})$ and $^2J(\text{Tl-H})$ in $(\text{CH}_3)_2\text{TlX}$ (X=OC₆H₄; ortho-ClC₆H₄; and SC₆H₄) and found that there was no apparent correlation between the C-Tl-C bond angles (<17° deviation from linearity) in these dimeric derivatives as determined from x-ray crystal structures.

The solvent dependence of a number of other metal-proton coupling constants ^{119}Sn ¹¹²⁻¹¹⁶ ^{207}Pb ^{112,117} and metal-carbon ^{119}Sn ^{118,119}, ^{199}Hg ¹¹² couplings have also been interpreted in terms of a change in the hybridisation of the metal atom such that the degree of s-character in the metal-carbon bond varies. In all cases it is thought that the orbital hybridisation is accompanied by a change in the

geometry of the molecule, the extent of which depends on the donorability of the solvent.

In contrast, Aritomi and Kawasaki¹²⁰ proposed that changes in ΔE , the mean singlet-triplet excitation energy (see equation 4.5) are mainly responsible for the observed solvent dependence of $^2J(M-H)$, $M=^{205}Tl, ^{207}Pb$ in oxinato derivatives of $(CH_3)_2Pb^{2+}$ and $(CH_3)_2Tl^+$. This conclusion is based on linear relationships found between the absorption maxima in the ultra-violet spectra of the complexes and $^2J(M-H)$. The same authors have also attributed the variation of $^2J(M-H)$ ($M=Sn, Pb, Tl$) for a number of $(CH_3)_2M$ compounds in solutions of strong acids to changes in ΔE .¹²¹ The previous model of the solvent dependence of $^2J(Tl-H)$ has been criticised by Schramm and Zink.²¹ These authors found a linear correlation between increasing $^2J(Tl-H)$ and increased thallium-205 shielding for $(CH_3)_2TlX$ ($X=NO_3^-, ClO_4^-$) in a range of oxygen- and nitrogen-donor solvents. Schramm and Zink²¹ propose that a decrease in ΔE which would correspond to an increase in $^2J(Tl-H)$ should be accompanied by a decrease in thallium shielding, since according to the Ramsey¹²² equation, a decrease in the energy separation between the ground and excited states will cause the paramagnetic term σ_p to increase. This is contrary to the observed trend and the authors²¹ suggest that changes in ΔE are not primarily responsible for the solvent dependence of $^2J(Tl-H)$. It should be pointed out however that Schramm and Zink²¹ have neglected the relative sign of $^2J(Tl-H)$ (negative) in this rationalisation.

1.3. Thallium-205 relaxation studies

Studies of ^{205}Tl relaxation have been almost exclusively confined to Tl(I) compounds with only one previous report for $(\text{CH}_3)_2\text{TlNO}_3$ in aqueous solution.¹⁹

The thalious ion has figured in biologically related studies in which relaxation rates of ^{205}Tl have been used as structural probes. Reuben and Kayne^{51,52} have examined T_1 and T_2 for Tl^+ in the presence of pyruvate kinase. However Bacon and Reeves¹²³ have criticised the conclusions of Reuben and Kayne,^{51,52} regarding the distances between metal binding sites in the enzyme estimated from relaxation rates for ^{205}Tl , since they ignored the effect of dissolved oxygen which strongly influences both R_1 and R_2 for Tl(I) . Grisham et al^{54,55} have utilised thallium relaxation to study cation binding sites in adenosine triphosphatase. Hinton and Briggs⁵⁶ have carried out T_1 studies, in the presence and absence of oxygen, to elucidate the solution structures of the Tl^+ complexes of the ionophores monesin and nigericin. They report spin-rotation to be the dominant relaxation mechanism for the Tl^+ ion. In a similar study of nonactin, monactin and dinactin the same authors⁵⁸ deduce the relative contributions to thallium-205 spin lattice relaxation as 50% spin-rotation, 40% dipole-dipole and 10% chemical shift anisotropy (CSA). During the course of the present study these authors⁵⁷ reported that in the Tl^+ /valinomycin complex the CSA mechanism made the dominant (90%) contribution to thallium relaxation. Hinton and Ladner¹²⁴ also suggested the importance of a transient chemical shift anisotropy relaxation mechanism for thallium in DMSO solutions of TlNO_3 and TlClO_4 .

A temperature dependent study⁵⁰ of Tl^+ in H_2O and HMPT showed that while spin rotation was the dominant mechanism for T_1 in H_2O , this was not the case in HMPT. The solvent dependence of T_1 was found to vary by an order of magnitude for a series of nine solvents from 0.08s in n-butylamine to 1.8s in water.

The effect of paramagnetic species on ^{205}Tl relaxation rates for $Tl(I)$ was first studied by Gasser and Richards²⁶ who found a linear increase in relaxation rate with added $Fe(CN)_6^{3-}$. Chan and Reeves¹⁹ also found that $Fe(CN)_6^{3-}$ and Cu^{2+} caused such an increase but this was less marked in the presence of chelating agents such as ethylenediamine and o-phenanthroline. Bacon and Reeves¹²³ and Chan and Reeves¹⁹ also noted a large linear increase of R_1 with dissolved oxygen up to an oxygen partial pressure of five atmospheres. Transient spin-rotation, in the absence of dissolved oxygen, was proposed as the dominant relaxation mechanism in both of the former studies. Bangerter¹²⁵ studied R_1 and R_2 for $^{205}Tl^+$ in aqueous solutions of $TlOCOCH_3$ and found that R_2 increased substantially more than R_1 as the partial pressure of oxygen above the solution was increased. He interpreted this in terms of a scalar contribution to R_2 arising from scalar coupling between Tl^+ and dissolved oxygen. Hinton and Briggs found that T_1 was longer in degassed solutions of Tl^+ complexes with valinomycin,⁵⁷ monesin and nigericin⁵⁶ whereas in complexes with actins⁵⁸ T_1 was nearly equal in both degassed and undegassed solutions. They interpreted this in terms of the actin molecule surrounding the Tl^+ ion in such a way as to prevent collisional access by dissolved oxygen. Bangerter and Schwartz¹²⁵ examined the

increase in R_1 and R_2 for Tl^+ with increasing concentration of the radical 4-hydroxy-2,2,6,6-tetramethylpiperidine-1-oxyl ('TANOL'). They found R_2 was more strongly affected and that the TANOL- Tl^+ electron-nuclear interaction dominated R_1 while scalar interactions dominated R_2 . The effect of the nitroxide radical was also examined.

In the only study of an organothallium(III) derivative, $(CH_3)_2TlNO_3$, Chan and Reeves¹⁹ found that R_1 and R_2 were almost the same and increased with partial pressure of oxygen although to a lesser extent than for Tl^+ . They found R_1 for an aqueous degassed solution of $(CH_3)_2TlNO_3$ to be independent of both the solvent isotope composition (D_2O/H_2O) and the isotope observed ($^{205}Tl/^{203}Tl$).

1.4. Solid-state structures of organothallium(III) compounds

The only reported structure for an R_3Tl derivative is for $(CH_3)_3Tl$ ¹²⁶. Twenty six reports of structures for R_2TlX compounds have appeared. However the majority of these have been for $(CH_3)_2TlX$ (X = a variety of anions). The structure of one ethyl compound has been reported.¹²⁷ Four structures where $R = C_6F_5$ or $p-HC_6F_4$ have been determined. There have been no reports of structures for R_2TlX derivatives where R is a longer or branched chain alkyl group. Similarly the structure of an $RTlX_2$ derivative, where X is a simple anionic ligand, has not previously been reported.

Dimethylthallium(III) compounds $(CH_3)_2TlX$ are generally polymeric; ($X = N_3, NCS, NCO, ^{128}OCOCH_3, tropolonato, acetylacetonato, ^{129}C(CN)_3, N(CN)_2, ^{130}methyl-xanthogenato-^{131}, Cl, Br, I, ^{132,139}L-phenylalaninato^{134}, Al(CH_3)_3NCS^{135}$ and $ClO_4^{136,137}$ (also containing a coordinated *o*-phen ligand)).

Similarly bis(ethyl)salicylaldehydatothallium(III)¹²⁷ is polymeric in the solid state. In all these cases the thallium is six-coordinate and polymerisation is achieved by bridging, often involving largely ionic weak bonding, through the N,O,S or halogen atoms of the anion. The C-Tl-C unit in these compounds is essentially linear with bond angles in the range 165-180°. However, several crystal structures of (CH₃)₂TlX derivatives are known where association does not extend beyond the dimer stage; X=C₆H₅O-, *o*-Cl-C₆H₄-, C₆H₅S-;⁶² tryptophanato¹³⁸ and dibenzylmethido.¹²⁹ Dimer formation occurs through bridging O or S atoms of the anion with four coordination around thallium except in the case of (CH₃)₂TlX (X=tryptophanato)¹³⁸ where it is five coordinate. The C-Tl-C bond angles for four or five coordinate thallium in dimeric derivatives are within the same range (163-180°) as those found for essentially six-coordinate thallium in polymeric derivatives.^{127-131,134,136,139} The carborane derivative (η⁴-decaborato)- dimethylthallium(III),¹⁴⁰ exists as a discrete monomer with a C-Tl-C bond angle of 134.1°.

In arylthallium(III) derivatives, R₂TlX, polymer formation has been found for cases where R=C₆F₅ and X=CH¹⁴¹; R=*p*-HC₆F₄ and X=Br¹⁴². The C-Tl-C angle in these perfluorophenyl compounds is in the range 138.5 to 149.9°. However discrete dimers exist in the solid state for R₂TlX where R=C₆H₅ and X=tropolonato.¹⁴³ The C-Tl-C angle in this case is 162.6°. Dimers have also been found in compounds of the type R₂TlXY (R=C₆F₅, X=OCOC₆F₅; Y=(C₆H₅)₃PO);¹⁴⁴ R = *p*-HC₆F₄, X=Cl, Y = (C₆F₅)₃-PO. For these R₂TlXY compounds the C-Tl-C angle is in the range 127 to 140.5°. In all the perfluorophenyl compounds thallium is five-coordinate except in (C₆F₅)₂Tl(OCOC₆F₅)(Ph₃PO) where it is six-coordinate.

The compound $(C_6H_5)_2TlX$ ($X=N,N'$ -diethyldithio carbamate)¹⁴³ exists as a monomer in which thallium is four-coordinate.

Although the solid state structures of two derivatives of CH_3Tl^{2+} , with quadridentate⁶¹ and quinquidentate¹⁴⁶ macrocyclic anionic ligands, have been determined these give no indication of the preferred coordination around thallium in the precursor monoalkylthallium(III) derivatives $RTlX_2$; $R=CH_3$ ⁸⁹, C_2H_5 ⁸⁹, $(CH_3)_3CCH_2$ ⁸⁷, $(CH_3)_3SiCH_2$ ¹⁴⁷; $X=$ carboxylate.

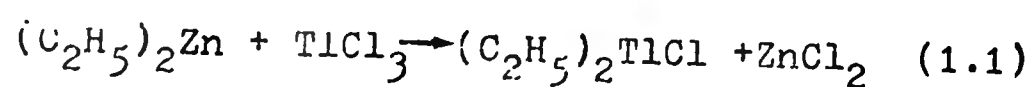
1.5. Synthesis of organothallium(III) compounds

Thallium(III) forms three main classes of organo derivatives; R_3Tl ; R_2TlX and $RTlX_2$. ($R=$ organo group, $X=$ anion). The R_3Tl derivatives are unstable, being light and air sensitive. The organo groups undergo exchange reactions and low temperatures are required for observation of spin-spin coupling to thallium. No R_3Tl derivatives were studied here. R_2TlX compounds form the largest and generally most stable class of organothallium(III) derivatives. $RTlX_2$ compounds are usually less stable than the R_2TlX derivatives. Both R_2TlX and $RTlX_2$ compounds usually exist as solids under ambient conditions. Details of the physical and chemical properties of organothallium(III) compounds are given in a number of texts¹⁴⁸⁻¹⁴⁹ and review articles.¹⁵⁰⁻¹⁵⁴

1.5.1. Bis(organo)thallium(III) compounds R_2TlX ($X=$ anion)

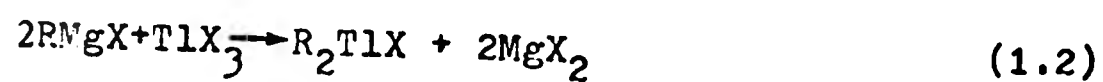
1.5.1.1. Alkyl and alicyclic derivatives

The first reported organothallium(III) compound, $(C_2H_5)_2TlCl$, was prepared by the reaction:¹⁵⁵



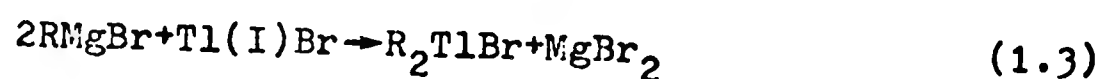
The ethyl, *n*-propyl and *iso*-butyl analogues were made by a

similar reaction using R_3Al .¹⁵⁶ Grignard reagents subsequently have been most widely used for preparing R_2TlX compounds



(X = Cl, Br; R = n-alkyls^{157,159}, branched alkyls,¹⁵⁸ alicyclics.¹⁵⁸)

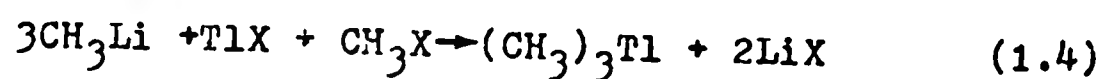
A more convenient one step synthesis has been reported for primary alkyl compounds:¹⁶⁰



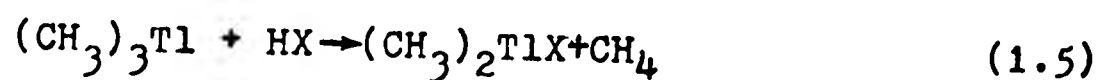
(R = n-alkyl).

Attempted preparation of branched alkyl derivatives by this method gave only coupled organic products R-R.¹⁶¹

Bis(methyl)iodothallium(III) is conveniently prepared by hydrolysis of the tris(methyl)thallium(III) produced in reaction (1.4)¹⁶².



$(CH_3)_3Tl$ reacts with a wide range of compounds containing acidic hydrogen:



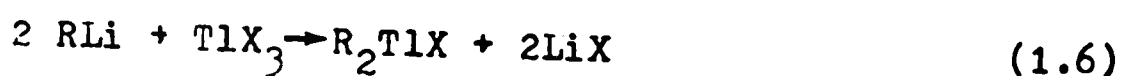
(HX = eg. hydrogen halides,¹⁶³ halomethanes^{148,163}).

Reaction of thallium(III) chloride with alkyl derivatives of boron,¹⁶⁴ tin¹⁶⁵, lead¹⁶⁶ or mercury¹⁶⁷ produce bis(alkyl)thallium(III) derivatives in very low yields. However it has been reported that reaction of thallium(III)acetate with some methyl and ethyltin compounds gives $(CH_3)_2Tl^+$ and $(C_2H_5)_2Tl^+$ derivatives in good yields.¹⁵⁰ Similarly the reaction of thallium(III)chloride with ammonium methylpentafluorosilicate $(NH_4)_2(CH_3SiF_5)$ gives a good yield of $(CH_3)_2TlCl$.¹⁶⁸

1.5.1.2. Alkenyl compounds

Bis(vinyl)halothallium(III), (halo = Cl, Br) compounds were synthesised by Nesmeyanov¹⁶⁹ using the Grignard method (Reaction 1.2) with tetrahydrofuran/ether as solvent.

Organolithium reagents have been used:



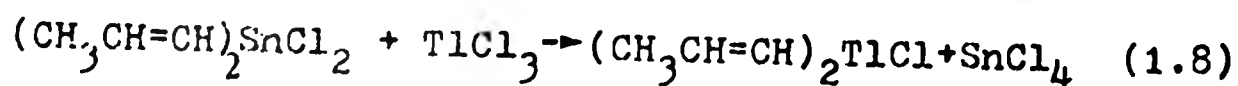
(X=Cl, Br; R=iso-propenyl¹⁷⁰; cis./trans-propenyl¹⁷¹; trans-but-2-enyl,⁸⁶ α -styryl¹⁷²). Exchange reactions with bis(alkenyl)-mercury(II) derivatives have been reported:



(X = Cl, Br; R = vinyl¹⁶⁹; cis- and trans-propenyl¹⁷¹; iso-propenyl¹⁷³; α -styryl¹⁷²; cis- and trans-2-chlorovinyl^{174,175}; cis- and trans-3-acetato-but-2-enyl.¹⁷⁶

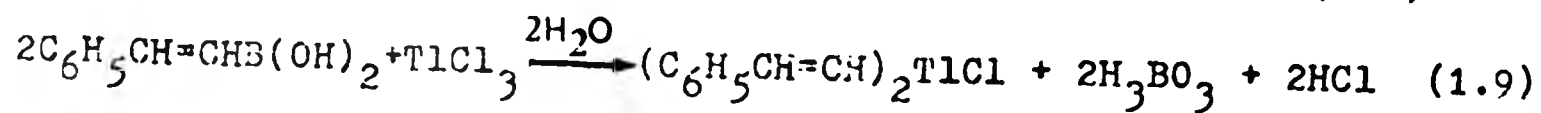
Cleavage of tetra(vinyl)tin(IV) by thallium(III)chloride gave a mixture of bis(vinyl)chlorothallium(III) and vinylbis(chloro)thallium(III)¹⁷⁷ Similarly reaction of tetra(iso-propenyl)tin(IV) with thallium(III)chloride gave either bis(iso-propenyl)chlorothallium(III) or iso-propenylbis(chloro)-thallium(III) depending on the ratio of reactants used.¹⁷⁷

Bis(organo)tin(IV) compounds have also been used:



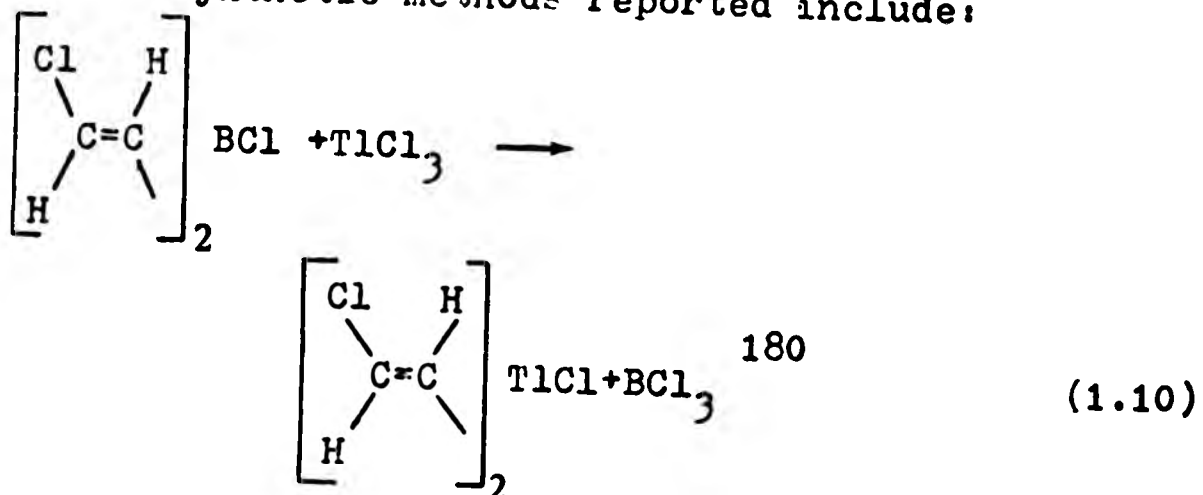
for the cis- and trans-propenyl compounds.

Heating an aqueous solution of β -styrylboronic acid and thallium(III)chloride gives bis(β -styryl)chlorothallium(III):

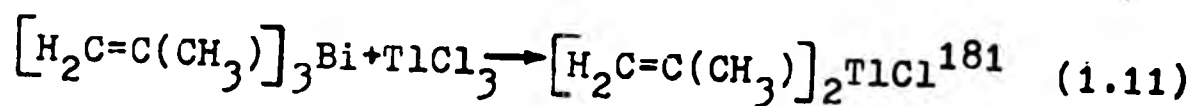


In an analagous reaction cis-propenylboronic acid gives either the bis(alkenyl)- or alkenylbis(chloro)thallium(III) derivative depending on the ratio of reactants used.¹⁷⁹

Other synthetic methods reported include:

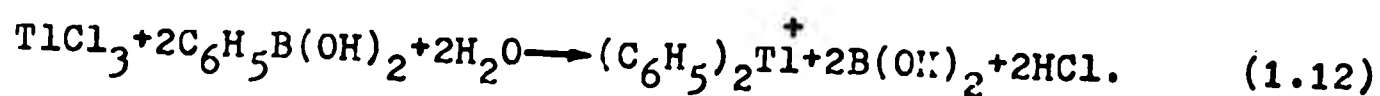


and

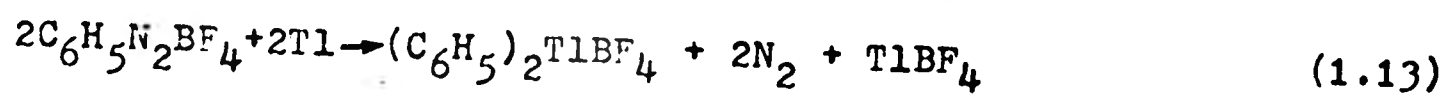


1.5.1.3. Aryl compounds

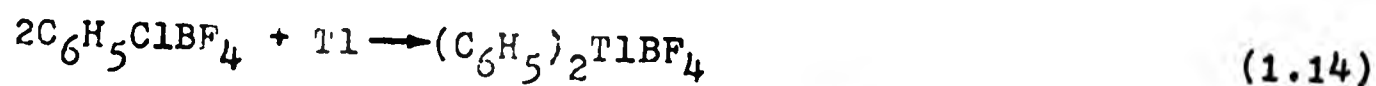
Bis(aryl)thallium(III) derivatives have been reported by the Grignard method (reaction 1.2). R = phenyl¹⁶⁵; pentafluorophenyl¹⁸²; other substituted aryls.^{165,183,184} Organolithium reagents have also been used.^{183,184} However these compounds are most conveniently made by reaction of thallium(III) halides with arylboronic acids^{164,185},



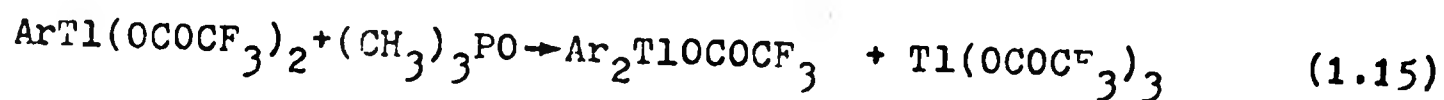
They can also be made by reaction of thallium metal with diazonium fluoroborates¹⁸⁶,



and diphenylhalonium salts¹⁸⁵,

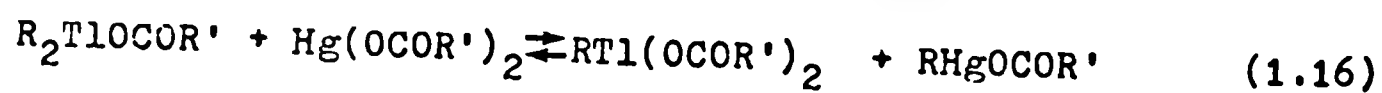


They may also be prepared from ArTlX_2 ($\text{X} = \text{OCOCF}_3$) derivatives, by heating or better by adding trimethylphosphite¹⁸⁸,

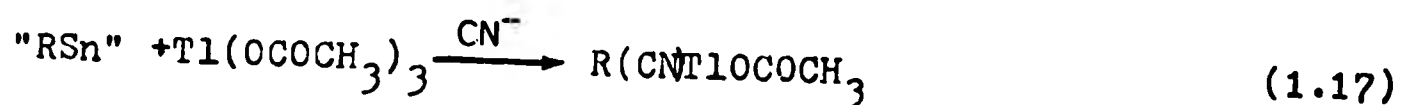


1.5.2. Monoorganothallium(III) compounds

Alkyl derivatives have been prepared by the reaction



($R=CH_3$; $R' = CH_3$.⁸⁹ $R' = CH(CH_3)_2$, $R=C_2H_5$ ⁸⁹, $R=n-C_3H_7$ ¹⁸⁹,
 $R=CH_3$ ⁸⁹). Alkyltin compounds such as $(CH_3)_4Sn$, $(CH_3)_3SnOCOCH_3$,
 $(CH_3)_3SnNO_3$, $(CH_3)_2SnF_2$ or $(C_2H_5)_4Sn$ react with thallium(III)
 -acetate:¹⁹⁰



($R = CH_3; C_2H_5$).

$CH_3(CN)TlOCOCH_3$ has also been prepared from $(NH_4)_2(CH_3SiF_5)$
 and $Tl(OCOCH_3)_3$ in aqueous NaCN solution.¹⁶⁸

Monoaryl- and monovinylthallium(III) derivatives can be
 prepared by the reaction of thallium(III) halides with organo
 derivatives of mercury¹⁹¹ or tin¹⁷⁷.

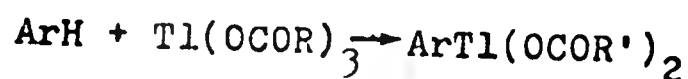


($R = \text{aryl or vinyl}$, $n=2-4$; $M=Hg$ or Sn ; $Y=Cl, Br$ or carboxylate)
 and by the reaction



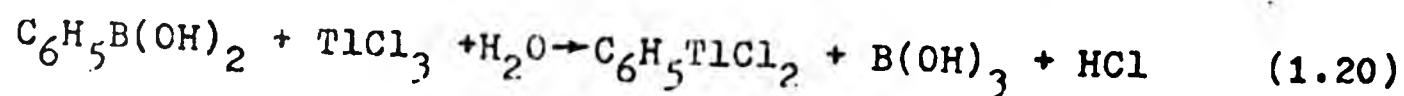
($R=\text{aryl}$ ¹⁸⁵ or vinyl ¹⁶⁹; $X=Cl$ or Br).

However aryl derivatives are more readily prepared by
 either direct thallation:



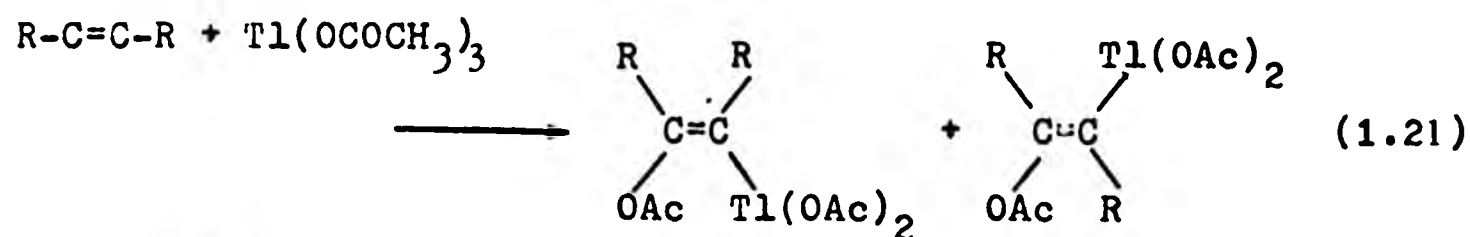
($R=CH(CH_3)_2$ ¹⁹¹; C_2F_5 ¹⁸⁸).

or using arylboronic acids:^{185,164}



In addition to the methods of synthesis of monoalkenyl-
 thallium(III) derivatives previously given, the acetoxy thallation

reaction is a convenient route to these compounds eg.¹⁹²



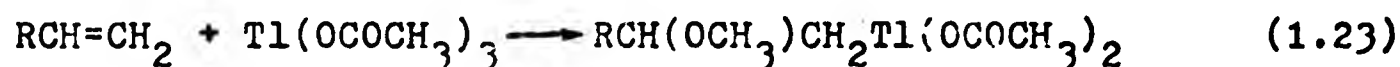
($R=CH_3; C_2H_5$. $OAc=OCOCH_3$).

Uemura carried out similar reactions using alkylphenyl-acetylenes⁹⁹ and Sharma and Martinez used acetoxithallation of allenes.⁹⁶

This reaction has also been used to prepare adducts of norbornene, norbornadiene via:



Preparations of compounds of the type $RCH(OCH_3)CH_2Tl(OCOCH_3)_2$ have been reported by⁹³,

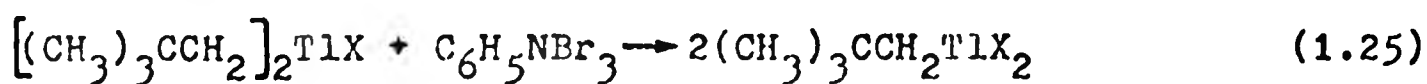


($R=C_6H_5$; o-allyl-phenol; propene; oct-1-ene).

The Pentaquochromium ion has been reported to react with thallium(III)chloride in aqueous solution to give:¹⁹⁴



($R=-CH_2-\text{C}_6\text{H}_4-\text{NH}-Cl$). Johnson⁸⁷ has reported preparation of mononeopentylthallium(III) species by the reaction



($X=Cl, Br$).

1.6. Aims of the project

Reports of the successful application of the NMR method to the study of metal derivatives in solution provided the impetus for using thallium-205 spectroscopy to study a number of organothallium(III) compounds. The overall objectives of the project are to identify and elucidate the relative importance of some of the factors (eg. the number and nature of the organo groups bonded to thallium, heteroatom substitution in the organo group and to a lesser extent anion, solvent and temperature) influencing the NMR parameters (chemical shifts, relaxation times and spin-spin coupling constants) involving the thallium-205 nucleus and to examine the possible use of these parameters as probes for investigating the nature of the species present in solution. Where possible a multinuclear (^{205}Tl , ^{13}C , ^1H) approach has been adopted. The effects of changing the environment of thallium on the NMR parameters for several different nuclei should provide the basis for an integrated approach to critical examination of the factors determining these parameters. Additionally interpretation should bear comparison with results for other heavy metal organometallics (eg. ^{113}Cd , ^{119}Sn , ^{199}Hg , ^{207}Pb) where these are known.

Speculative reports, based on infra-red data, concerning the effect of bulky organo groups on the extent of oligomerisation and C-Tl-C bond angles in R_2TlX derivatives prompted determination of the crystal structure of $[(\text{CH}_3)_3\text{SiCH}_2]_2\text{TlCl}$. It was anticipated that determination of the structure of the new stable compound $(\text{CH}_2)_2\text{CHTl}[\text{OCOCH}(\text{CH}_3)_2]_2$ would allow correlation of much existing infra-red spectroscopic data for organothallium(III) carboxylates with structure.

CHAPTER TWO

EXPERIMENTAL METHODS

2.1. Instrumental measurements

2.1.1. Proton NMR spectra

Proton NMR spectra were obtained on a Perkin Elmer R12B instrument operating at 60MHz with a probe temperature of 35°C. Measurements were made on spinning samples contained in 5mm tubes. Samples were prepared immediately prior to running the spectra. Internal tetramethylsilane (TMS) was used as field-frequency lock and peak positions measured in 100Hz expansions using a Racal digital frequency counter. Homonuclear double resonance experiments were performed using the standard Perkin Elmer Double Resonance Accessory. This equipment did not allow double resonance experiments to be performed under conditions of field-frequency lock. However the resonances to be irradiated were fairly broad (typically ca. 15 Hz) and the field was sufficiently stable for this not to be a problem. Spectral assignment was assisted in several cases by spectra obtained at 90MHz on a Perkin-Elmer R32 (Perkin-Elmer Ltd.) and at 220MHz on a Perkin-Elmer R34 (P.C.M.U. Harwell).

Proton spectra, for $[(CH_3)_3CCH_2]_2TiCl$ in pyridine- d_5 , and $(CH_3)_2TiOCOCH_3$ in D_2O , were obtained in the Pulse Fourier Transform (PFT) mode at 150MHz on a Nicolet NT-150; at 300MHz on a Bruker CXP-300; at 360MHz on a Nicolet NT-360 and at 400MHz on a Bruker WH-400. These spectra were obtained by Dr. D.G. Gillies, Royal Holloway College, University of London. Proton spectra for $(CH_3)_2TiOCOCH_3$ in D_2O were also obtained at 80MHz on a Bruker WP80 (The Polytechnic of North London) and at 220MHz on a Perkin Elmer R34 (P.C.M.U. Harwell).

2.1.2. Carbon-13 NMR spectra

Fourier transform carbon-13 spectra were obtained at 22.63 MHz on a Bruker 90 HXE at 30°C. In several cases assignment was assisted by spectra obtained at 45.28 MHz on a Bruker WH180 (Both at P.C.M.U. Harwell).

A deuterium(solvent) field-frequency lock was used in all cases and spectra were initially obtained with broad-band proton decoupling. Many assignments were assisted by $^{13}\text{C}\{-^1\text{H}\}$ off-resonance spectra and relative signs of $^n\text{J}(\text{Tl}-\text{C})$ and $^{n+1}\text{J}(\text{Tl}-\text{H})$ ($n=1$ to 3) were determined by single frequency off-resonance spectra. Further details of sign determinations are given in Chapter 4. Internal TMS was used as a reference in all cases.

Typical operating conditions, $^{13}\text{C}\{-^1\text{H}\}$ broad band, for an R_2TlX derivative 0.4 mol dm^{-3} in DMSO-d_6 ($\text{R}=\text{iso-butyl-}$; $\text{X}=\text{Cl}$), at 22.3 MHz, are: number of transients 65,536; pulse length $10 \mu\text{sec}$; delay 1 sec; spectral width 6024 Hz. For an RTlX_2 derivative ($\text{R}=(\text{CH})_2\text{CH}$; $\text{X}=\text{OCOCH}(\text{CH}_3)_2$) 0.26 mol dm^{-3} in DMSO-d_6 , 65,536 transients were used with a pulse length of $8 \mu\text{sec}$; a delay of 1 sec and a spectral width of 15152 Hz. In both cases 4096 data points were used and the pre-pulse delay was $143 \mu\text{sec}$.

2.1.3. Thallium-205 spectra

Spectra were obtained in the PFT mode using a Varian HA60-IL spectrometer modified (Dr.D.G. Gillies, Royal Holloway College, University of London) for observation of thallium-205 at 34.7 MHz. The system was interfaced to a DEC PDP-11(28K) computer incorporating dual drive floppy disks for data handling and storage.

All measurements were made on spinning samples. Samples were held in 12mm tubes containing a 5mm insert of D_2O , coaxially held by teflon spacers, the 2H resonance of which was used as a field-frequency lock. The lock was always to the first upfield sideband, (1KHz). In several cases the deuterated solvent containing the sample was used as the lock signal, in which cases a teflon vortex suppressor was inserted into the solutions. Samples were run within 24 hours of solution preparation. No attempt was made to exclude oxygen or atmospheric moisture during sample preparation except for samples for T_1 determinations. These latter solutions were made up under argon and deoxygenated by purging with argon for approximately thirty minutes.

Spectra were obtained at ambient probe temperature (ca, $30^\circ C$), except for the T_1 experiments where the temperature was controlled using the standard Varian variable temperature unit. Temperatures were measured, using a thermocouple thermometer immersed in liquid paraffin contained in a 12mm tube, immediately prior to and after obtaining the NMR spectrum. The error in temperature measurement was estimated as $\pm 1^\circ C$. Each sample was allowed to equilibrate for ca 30 minutes until the resonance frequency did not change for successive determinations.

Typical operating conditions for determining thallium-205 spectra were as follows. In the majority of cases broad-band proton decoupling was used. (Exceptions are noted in Chapter 3). The r.f. carrier frequency was entered via the computer keyboard. The system employed a single channel detection system and the carrier frequency was carefully positioned on the low frequency side of the resonance signal. The relative

signal positions and intensities were then determined automatically under computer control. Accumulation and Fourier transformation of each FID were carried out automatically under software control. In a typical experiment, using 1000 transients, $(90^\circ - \tau)_n$, 8192 data points were collected at a rate of $10,000\text{s}^{-1}$ (giving a spectral width of 5000Hz) with a 90° pulse length of $57\text{ }\mu\text{sec}$ and a post pulse delay of 0.09sec . After digitisation the FID's were apodised (using a cosine function) and filtered (using an exponential weighting function) then Fourier transformed. The resulting frequency spectrum was displayed on a visual display unit where the phase was corrected manually. Hard copies of spectra were obtained using an XY recorder.

Typically linewidths were $< 50\text{Hz}$. The error on the ^{205}Tl chemical shift is estimated to be better than $\pm 1\text{ppm}$ based on reproducibility over a period of several months. Subjective estimates of errors on individual measurements were typically $< \pm 25\text{Hz}$ at 34.7MHz .

In the T_1 experiment using the inversion-recovery method, the pulse timers controlling the 180° and 90° pulse lengths, the acquisition rate and the overall repetition rate of the experiment, were set manually. The fifth timer for τ , the delay between 180° and 90° pulses, was under computer control with up to ten different τ values being entered via the keyboard. The experiment was then carried out automatically under software control and the resulting FID's and accompanying parameter listings stored on a floppy disk (up to six experiments per side). In a typical T_1 experiment e.g. for a 0.4 mol dm^{-3} solution of RTlX_2 in DMSO-d_6 , 400 transients were used and 1600 data points

collected with an acquisition rate of 2000s^{-1} giving a spectral width of 1000Hz . The 180° pulse length was $114\ \mu\text{sec}$, the 90° pulse length was $57\ \mu\text{sec}$. Details of the τ values used are given in Appendix III. The delay after the $(180^\circ - \tau - 90^\circ)$ sequence was 1.0s . The T_1 value obtained was 0.097s .

A major source of potential error in determining the thallium resonance frequency using this spectrometer system was found as follows. Spurious signals of reduced intensity were observed at $\pm 10\text{KHz}$ from the 'real' signal, especially with the more concentrated solutions and/or when a large number of transients were used. The signal at $+10\text{KHz}$ was found to be more intense than that at -10KHz . However in some cases both signals were capable of being mistaken for the 'real' signal. Discovery of this phenomenon made it necessary to repeat measurements for all samples run up till that time (40 samples). Rechecking showed a number of cases in which spurious signals were previously mistaken for 'real' signals. A system of checking was thereafter followed and in cases of doubt all three spectra were recorded (in some cases only one spurious signal could be observed, especially at the lower concentrations) along with appropriate parameter listings of intensity and scale factor so that the 'real' signal could be identified. However in most cases this was obvious due to the poorer signal to noise ratio and reduced intensity of the spurious signal(s).

2.1.3.1. Calculation of $\Xi(^{205}\text{Tl})$ values from spectra locked to deuterium

Thallium-205 resonance frequencies, $\Xi(^{205}\text{Tl})$, have been reported as suggested by McFarlane¹⁹⁵ and Harris¹⁹⁶ such that $\Xi(^{205}\text{Tl})$ is the frequency (Hz) for a field in which TMS gives a proton resonance at exactly 100MHz. The method of calculation used is as follows.

At an observation field B_0 Tesla the measured ^2H lock frequency is $\nu^2\text{H}$ MHz. If modulation of the lock is 1KHz on upfield sideband, then ^2H will be observed at $(\nu^2\text{H} + 0.001)\text{MHz}$. At the field, B_0 , the thallium-205 resonance frequency is νTl . The shift of the lock signal from TMS is xppm. Then at $(\nu^2\text{H} + 0.001)\text{MHz}$, ^2H of the lock material resonates at B_0 Tesla. So at $(\nu^2\text{H} + 0.001)\text{MHz}$, TMS- d_{12} resonates at $B_0(1 + 0.001 \times 10^{-6})$ Tesla.

At a field of 1 Tesla, ^1H resonates at 42.5759MHz and ^2H resonates at 6.53566MHz.¹⁹⁷ $(\gamma^1\text{H}/\gamma^2\text{H}) = 6.51439(9)$ ^{197,198} Therefore ^1H resonates at 100 MHz when ^2H resonates at $(6.53566 \times 100)/42.5759 = 15.3506\text{MHz}$.

Since TMS- d_{12} resonates at $(\nu^2\text{H} + 0.001)\text{MHz}$ in field $B_0(1 + x \times 10^{-6})$ Tesla, then TMS- d_{12} resonates at 15.3506MHz in a field $B_0(1 + x \times 10^{-6})$ $15.3506/(\nu^2\text{H} + 0.001)$. Therefore at a field $B_0(1 + x \times 10^{-6})/15.3506/(\nu^2\text{H} + 0.001)$, ^{205}Tl resonates at:-

$$\Xi(^{205}\text{Tl}) = \nu\text{Tl} \left\{ \frac{1 + x \times 10^{-6}}{\nu^2\text{H} + 0.001} \right\} \cdot 15.3506.$$

Note on the accuracy of $\gamma^2\text{H} \times 100/\gamma^1\text{H}$ (=15.3506). Using the expression $\mu = \gamma(I \hbar)^2$ and the value reported²⁰⁹ for $\mu^2\text{H}/\mu^1\text{H} = 0.307012192 \pm 0.000000015$, a value for $(\gamma^2\text{H} \times 100/\gamma^1\text{H}) = 15.3506006 \pm 0.000000075$ is calculated. For a typical thallium resonance frequency of 34,700,000 Hz use of this value gives $\Xi(^{205}\text{Tl}) = 57,898,698 \pm 3\text{Hz}$.

The value of 15.3506 used here results in $\Xi(^{205}\text{Tl})$
=57,898,661Hz (a difference of ca. 0.5ppm).

Bulk susceptibility corrections have not been applied in cases where D_2O inserts were used for locking.

2.1.4. Infra-red spectra

These were recorded on a Pye-Unicam SP2000 spectrophotometer as mulls in Nujol and HCB and in chloroform solution using KBr plates. The absorption of a polystyrene film at 1602cm^{-1} was used to calibrate the spectra. Samples and solutions were prepared immediately prior to running the spectra.

2.1.5. X-ray structure determination

A suitable crystal was chosen under the microscope and fixed to the end of a quartz fibre with 'Araldite', with one of the morphological crystal axes approximately coincident with the axis of rotation of the fibre. The quartz fibre was mounted on a goniometer head which in turn was mounted on a Phillips PW1100 four circle X-ray diffractometer.

Weissenberg photographs of cyclopropylbis(isobutyrate)-thallium(III) were obtained from a Weissenberg camera using standard techniques. Further details are given in Chapter 6.

2.2. Preparations

2.2.1. Purification of solvents

Dimethylsulphoxide was refluxed for three hours over calcium hydride under reduced pressure. It was then distilled under reduced pressure onto activated 4A molecular sieves and stored under nitrogen.

Pyridine was refluxed over potassium hydroxide pellets under dry nitrogen. It was then distilled under nitrogen and stored over 4A molecular sieves and stored under nitrogen. Methanol was dried by reaction with magnesium methoxide and distilled under dry nitrogen. It was stored over 4A molecular sieves under nitrogen.

Chloroform was dried over 4A molecular sieves.

Diethyl ether and Tetrahydrofuran were refluxed with sodium wire and benzophenone for several hours. In the case of diethyl ether the development of a deep blue colouration indicated the absence of water. The dry solvents were distilled under argon and stored over 4A molecular sieves under nitrogen.

Benzene was dried by standing in contact with sodium wire.

2.2.2. List of Preparations

Starting Materials

1. Thallium(III)chloride
 - (a) In aqueous solution
 - (b) In acetonitrile.
2. Thallium(III) bromide.
3. Isobutyrosilver(I).
4. Isobutyromercury(II).

Organothallium(III) derivatives

- a) Alkylthallium(III) compounds
 5. Bis(methyl)iodothallium(III).
 6. Bis(methyl)nitratothallium(III).
 7. Bis(methyl)acetatothallium(III).
 8. Methylbis(acetato)thallium(III)
 9. Bis(ethyl)bromothallium(III).

10. Bis(ethyl)nitratothallium(III)
11. Bis(ethyl)isobutyratothallium(III)
12. Ethylbis(isobutyrate)thallium(III)
13. Bis(n-propyl)bromothallium(III)
14. Bis(n-propyl)nitratothallium(III).
15. Bis(iso-propyl)chlorothallium(III).
16. Bis(iso-propyl)acetatothallium(III) (nc)
17. Bis(n-butyl)bromothallium(III)
18. Bis(n-butyl)nitratothallium(III).
19. Bis(iso-butyl)chlorothallium(III).
20. Bis(iso-butyl)isobutyratothallium(III) (nc)
21. iso-butylbis(isobutyrate)thallium(III). (nc)
22. Bis(sec-butyl)chlorothallium(III).
23. Bis(n-pentyl)bromothallium(III).
24. Bis(n-pentyl)nitratothallium(III).
25. Bis(iso-amyl)chlorothallium(III).
26. Bis(iso-amyl)nitratothallium(III) (nc)
27. Bis(iso-amyl)acetatothallium(III) (nc)
28. iso-amylbis(acetate)thallium(III). (nc)
29. Bis(iso-amyl)tetrafluoroboratothallium(III) (nc)
30. Bis(sec-amyl)chlorothallium(III) (nc)
31. Bis(neo-pentyl)chlorothallium(III).
32. neo-pentylbis(halogeno)thallium(III).
33. Bis(neo-pentyl)isobutyratothallium(III) (nc)
34. neo-pentylbis(isobutyrate)thallium(III). (nc)
35. Bis(trimethylsilylmethyl)chlorothallium(III)
36. Bis(trimethylsilylmethyl)isobutyratothallium(III).
37. Trimethylsilylmethylbis(isobutyrate)thallium(III).
38. Bis(cyclohexylmethyl)bromothallium(III) (nc).
39. Bis(cyclohexylmethyl)isobutyratothallium(III) (nc).
40. Methyl(2-methoxypropyl)acetatothallium(III).

b) Alicyclithallium(III) compounds

- 41. Bis(cyclopropyl)bromothallium(III) (nc).
- 42. Bis(cyclopropyl)isobutyrate-thallium(III) (nc).
- 43. Cyclopropylbis(isobutyrate)thallium(III) (nc).
- 44. Bis(cyclopentyl)chlorothallium(III).
- 45. Bis(cyclopentyl)isobutyrate-thallium(III)(nc)
- 46. Bis(cyclopentyl)tetrafluoroborate-thallium(III) (nc).
- 47. Bis(cyclohexyl)chlorothallium(III).
- 48. Bis(cyclohexyl)isobutyrate-thallium(III) (nc).
- 49. Bis(cyclohexyl)tetrafluoroborate-thallium(III) (nc).
- 50. Bis(cycloheptyl)bromothallium(III). (nc).
- 51. Bis(cycloheptyl)tetrafluoroborate-thallium(III). (nc).
- 52. (2-acetatonorbornane)bis(acetate)thallium(III).
- 53. (2-acetatonorbornene)bis(acetate)thallium(III).

c) Alkenylthallium(III) compounds

- 54. Bis(vinyl)chlorothallium(III).
- 55. Bis(vinyl)acetate-thallium(III) (nc).
- 56. Bis(vinyl)isobutyrate-thallium(III)(nc).
- 57. Vinylbis(chloro)thallium(III).
- 58. Bis(iso-propenyl)bromothallium(III).
- 59. Bis(trans- β -styryl)bromothallium(III).
- 60. Bis(trans- β -styryl)nitrate-thallium(III). (nc).
- 61. Bis(trans- β -chlorovinyl)chlorothallium(III).
- 62. trans- β -chlorovinylbis(chloro)thallium(III).
- 63. (trans-2-acetate, but-2-enyl)bis(acetate)thallium(III).

d) Arylthallium(III) compounds

- 64. Bis(phenyl)nitrate-thallium(III).
- 65. Bis(phenyl)acetate-thallium(III).

The use of the designation (nc) indicates a new compound.

2.2.3. Starting Materials

1. Thallium(III)chloride.

(a) Preparation in aqueous solution.

This was prepared as reported by Meyer¹⁹⁹ with the modification that the product was dehydrated over P_2O_5 under vacuum (3 days). After this time infra-red spectroscopy showed the absence of water. The product was not analysed.

(b) Preparation in acetonitrile.

This was prepared according to the method of Cotton et.al.²⁰⁰ The solvent was removed on the rotary evaporator at 25°C. It was not analysed but used immediately after preparation.

2. Thallium(III) bromide.

$TlBr_3$ was prepared as a solution in tetrahydrofuran by the method of Maher.⁸⁶ Reaction of equimolar amounts of $Tl(I)Br$ and bromine in THF under argon at 0°C gave a solution of $TlBr_3$ which was used immediately after preparation.

3. Isobutyrosilver(I).

Isobutyric acid (150cm³) was heated to ca. 150°C and silver(I)oxide (21.6g; 0.09mol) was added in small portions over 30 mins. A further 20cm³ of isobutyric acid was added to the thick greyish suspension and the mixture heated for a further 2h. A colourless crystalline solid was obtained on cooling. After standing overnight the product was filtered and washed with several portions of diethyl ether and then dried under vacuum. The product was obtained as colourless plates and was not analysed. (Yield 33g; 91% based on silver(I)oxide).

4. Isobutyromercury(II).

Freshly prepared orange mercuric oxide²⁰¹ (4.2g; 0.02mol) was added in small portions to hot (ca. 150°C) isobutyric

acid(10cm³) giving a clear solution. On cooling the product crystallised out as colourless plates. These were filtered off, washed with ether and dried under reduced pressure over potassium hydroxide pellets. The product was not analysed. (Yield 6.5g; 90% based on mercuric oxide).

2.2.4. Organothallium(III) derivatives

(a) Alkylthallium(III) compounds

All preparations involving Grignard or organolithium reagents were carried out in dry solvents under argon. Alkylhalides were distilled prior to use and stored over 4A molecular sieves.

5. Bis(methyl)iodothallium(III).

This was prepared according to the published method with the modification¹⁰³ that methanol was used instead of aqueous acid to solvolyse the tris(methyl)thallium(III) solution giving a more tractable precipitate. Recrystallisation from pyridine gave colourless crystals. (Found: C, 6.9; H, 1.8. C₂H₆TlI calc.: C, 6.6; H, 1.7%).

A sample of (¹³CH₃)₂TlI (approx. 60% ¹³C enrichment) was prepared by this method using a mixture of ¹³CH₃I, (91.3 atom % ¹³C, Prochem B.O.C. Ltd.), and CH₃I (unlabelled) in the ratio 2:1 w/w. The product was shown to be pure by proton NMR. The % ¹³C enrichment was calculated from integration of the proton spectrum.

6. Bis(methyl)nitratothallium(III)

This was prepared according to the published method.¹⁰⁵ The product was obtained as colourless crystals. (Found: C, 8.1; H, 1.9; N, 4.6. C₂H₆TlNO₃ calc: C, 8.1; H, 2.0; N, 4.7%).

7. Bis(methyl)acetatothallium(III)

Metathesis of bis(methyl)iodothallium(III) with acetato-silver(I) according to the method of Goddard²⁰² gave this compound as colourless crystals. (Found: C, 16.2; H, 3.1.

$C_4H_9TlO_2$ calc: C, 16.6; H, 3.1%).

8. Methylbis(acetato)thallium(III)

This compound was prepared as described by Kurosawa,⁸⁹ by reaction between bis(methyl)acetatothallium(III) and bis(acetato)mercury(II) in methanol, with the modification that the product was obtained by precipitation from chloroform solution by addition of diethyl ether. The reported method of recrystallisation was found to result in a product contaminated with methyl(acetato)mercury(II), (up to 50%). Proton spectra of the product indicated purity >90%. The product was not analysed.

9. Bis(ethyl)bromothallium(III)

This was prepared by the method of McKillop and Taylor¹⁶⁰ by refluxing a mixture of $Tl(I)Br$ and *n*-alkylmagnesium bromide (2:1 molar ratio) in a mixture of tetrahydrofuran/benzene(1:1v/v) for five hours. Filtration and extraction with pyridine, followed by recrystallisation from the same solvent gave the product as colourless crystals. The product was not analysed but proton NMR showed the absence of impurities.

10. Bis(ethyl)nitratothallium(III).

Reaction of bis(ethyl)bromothallium(III) with nitratothallium(I) in methanol according to the published method²⁰³ gave the product as colourless crystals. (Found: C, 14.9; H, 3.2; N, 4.4. $C_4H_{10}TlNO_3$ calc.: C, 14.8; H, 3.1; N, 4.3%).

11. Bis(ethyl)isobutyratothallium(III).

Metathesis of bis(ethyl)bromothallium(III) with isobutyrate-silver(I) in methanol according to the method

of Kurosawa and Okawara⁸⁹ gave the product as colourless crystals. (Found: C, 27.2; H, 4.7. $C_8H_{17}TlO_2$ calc.: C, 27.5; H, 4.9%).

12. Ethylbis(isobutyrate)thallium(III).

This compound was prepared by the reported method⁸⁹ by reaction between bis(ethyl)isobutyrate thallium(III) and bis(isobutyrate)mercury(II). The product was not analysed but proton NMR indicated purity > 95%.

13. Bis(n-propyl)bromothallium(III).

This was prepared as described by McKillop and Taylor¹⁶⁰ in a manner analogous to that detailed for the ethyl-analogue (Prep 9). The product was not analysed but proton NMR showed the absence of impurities.

14. Bis(n-propyl)nitratothallium(III).

This was prepared by the published method²⁰³ as described for the ethyl analogue (Prep 10). (Found: C, 20.5; H, 3.9; N, 3.8. $C_6H_{14}TlNO_3$ calc: C, 20.4; H, 3.9; N, 3.9%).

15. Bis(iso-propyl)chlorothallium(III).

A modification of the method of Krause and Grosse¹⁵⁸ was used. The reaction mixture from reaction of iso-propylmagnesium chloride and $Tl(III)Cl$ was hydrolysed with aqueous (5%) ammonium chloride solution instead of with aqueous acid. The product was filtered off, washed with water and ether and dried over P_2O_5 . It was then stirred with absolute ethanol, (ca. 200 cm³ ethanol per 5g of product), filtered and the filtrate evaporated at 25°C on the rotary evaporator. Recrystallisation from ethanol gave the product as colourless needles. (Found: C, 22.0; H, 4.4. $C_6H_{14}TlCl$ calc.: C, 22.1; H, 4.3%).

16. Bis(iso-propyl)acetatothallium(III). (nc)

Bis(iso-propyl)chlorothallium(III), (0.7g, 0.002mol), was stirred overnight with acetatosilver(I), (0.40g, 0.002mol) in methanol (250 cm³). Removal of silver halide by filtration followed by evaporation of the filtrate on the rotary evaporator at 25°C, gave the product. Recrystallisation from methanol gave colourless needles. (Yield 0.4g, 52% based on acetatosilver(I)). The product was not analysed but was shown to be pure by proton NMR.

17. Bis(n-butyl)bromothallium(III).

This was prepared by the published method²⁰³ as described for the ethyl-analogue (Prep.9). The product was not analysed but proton nmr indicated the absence of impurities.

18. Bis(n-butyl)nitratothallium(III) .

Reaction of bis(n-butyl)bromothallium(III) with nitratothallium(I) in pyridine by the published method¹⁸ gave the product as a white solid which was recrystallised from a pyridine-water mixture (1:4 v/v) and dried under vacuum over P₂O₅. (Found: C, 25.2; H, 4.7; N, 3.7. C₈H₁₈TlNO₃ calc.: C, 25.2; H, 4.7; N, 3.7%).

19. Bis(iso-butyl)chlorothallium(III).

The reported method¹⁵⁸ was used with the following modifications. The ether layer, present after hydrolysis of the reaction mixture, was removed by evaporation because the product was found to be soluble in it. The remaining aqueous suspension was filtered and the white product was washed with water and dried over P₂O₅. Recrystallisation from diethyl ether gave colourless needles. The product was found to be unstable at room temperature. (Proton spectra indicated ca. 50% decomposition within 48h). Satisfactory analysis (C,H) could

not be obtained but proton spectra of a freshly prepared sample showed no impurities. The product was stored in the fridge.

20. Sis(iso-butyl)isobutyrate-thallium(III).(nc)

Reaction of bis(iso-butyl)chlorothallium(III), (0.71g, 0.002 mol), with isobutyrate-silver(I), (0.40g, 0.002mol), in methanol(100cm³) for 4h at room temperature followed by filtration and evaporation of the filtrate on the rotary evaporator at ca. 25°C gave the product as a white solid. Recrystallisation from methanol gave colourless needles. (Yield 0.3g, 38% based on isobutyrate-silver(I)). The product was not analysed but proton spectra of a freshly prepared sample showed no impurities. The compound was stored in the fridge.

21. iso-butylbis(isobutyrate)thallium(III). (nc)

Reaction of equimolar amounts of bis(iso-butyl)isobutyrate-thallium(III) and bis(isobutyrate)mercury(II) in methanol-d₄ in an nmr tube for approximately two hours at 35°C gave iso-butylbis(isobutyrate)thallium(III). Proton NMR indicated the reaction had gone to ca. 60% completion. The product was not isolated and decomposed completely within four hours. Proton spectra were determined on the reaction mixture.

22. Bis(sec-butyl)chlorothallium(III).

This was prepared by modification of the published¹⁵⁸ method as described for the iso-butyl-analogue (Prep.19). The product was obtained as colourless light sensitive needles. Slow decomposition occurs at room temperature and the product was stored in the fridge. (Found: C, 26.0; H, 5.0. C₈H₁₈TlCl calc.: C, 27.1; H, 5.1%).

23. Bis(n-pentyl)bromothallium(III).

This compound was prepared by the method of McKillop and Taylor¹⁶⁰ as described for the ethyl-analogue(Prep.9). The product was not analysed but proton NMR did not reveal any impurities.

24. Bis(n-pentyl)nitratothallium(III).

This was prepared by the method¹⁸ described for the n-butyl-analogue (Prep.18). (Found: C, 29.5; H, 5.4; N, 3.4. $C_{10}H_{22}TlNO_3$ calc.: C, 29.4; H, 5.4; N, 3.4%).

25. Bis(iso-amyl)chlorothallium(III).

This compound was prepared according to the method of Krause and Grosse.¹⁵⁸ The iso-amylchloride used in preparing the alkylmagnesium halide was made from iso-amylalcohol using the method of Vogel.²⁰⁴ (Found: C, 31.1; H, 5.9. $C_{10}H_{24}TlCl$ calc.: C, 31.4; H, 5.8%).

26. Bis(iso-amyl)nitratothallium(III). (nc)

Bis(iso-amyl)chlorothallium(III), (4.0g; 0.01mol) and nitrat silver(I) (1.6g; 0.009mol) were stirred in methanol (300cm³) for 5h at ca. 40°C. After standing for 3 days at room temperature the mixture was filtered and the filtrate evaporated. The white solid obtained was recrystallised from methanol giving colourless crystals. (Yield 2.9g, 72% based on nitrat silver(I)). (Found: C, 29.2; H, 5.4. $C_{10}H_{22}TlNO_3$ calc.: C, 29.4; H, 5.4%).

27. Bis(iso-amyl)acetatothallium(III) (nc)

Bis(iso-amyl)chlorothallium(III), (2.0g; 0.005mol), and acetat silver(I), (0.8g; 0.0048mol) were stirred in methanol(450cm³) for 24 h. Filtration gave a colourless filtrate which was evaporated to low bulk (ca. 20 cm³) on the rotary evaporator. Cooling in ice gave fine needles.

(Yield 0.9g; 60% based on acetatosilver (I)). (Found: C, 35.6; H, 6.2. $C_{12}H_{27}TlO_2$ calc.: C, 35.5; H, 6.2%).

28. iso-amylbis(acetato)thallium(III) (nc)

Reaction of equimolar amounts of bis(iso-amyl - acetatothallium(III) and bis(acetato)mercury(II) in methanol- d_4 solution in an NMR tube at $35^\circ C$ for ca. 4 hours gave the product. Proton NMR indicated that the reaction had gone to about 60% completion. The compound was not isolated and was found to have decomposed completely within 24 h. Proton NMR spectra were determined on the reaction mixture.

29. Bis(iso-amyl)tetrafluoroboratothallium(III). (nc)

This compound was prepared by the reaction of bis(iso-amyl)chlorothallium(III) with tetrafluoroboratosilver(I) in methanol in a manner analogous to that described for the acetato-analogue (Prep. 27) (Yield 68%, based on tetrafluoroboratosilver(I)). (Found: C, 27.8; H, 5.3. $C_{10}H_{22}TlBF_4$ Calc.: C, 27.7; H, 5.1%).

30. Bis(sec-amyl)chlorothallium(III). (nc)

A solution of sec-amylmagnesium bromide (0.13 mol), prepared from magnesium (3.1g; 0.13 mol) and sec-amylbromide (19.2g; 0.13 mol) in diethyl ether (100cm^3), was added during 1h to a solution of $TlCl_3$ (19.6g; 0.06 mol) in diethyl ether (50cm^3) at $-20^\circ C$. Hydrolysis of the reaction mixture at 0° with 50cm^3 of dilute (2 mol dm^{-3}) aqueous HCl, followed by evaporation of the ether layer and subsequent filtration of the reaction mixture gave the product as a pale yellow solid which was dried over conc. H_2SO_4 . Recrystallisation from diethyl ether gave colourless needles. (Yield 0.6g ; 2% based on $TlCl_3$). (Found: C, 30.9; H, 5.5. $C_{10}H_{24}TlCl$ calc.: C, 31.4; H, 5.8%). The product was light sensitive and decomposed slowly at room temperature. It was stored in the fridge.

31. Bis(neo-pentyl)chlorothallium(III).¹⁴⁷

This compound was prepared from neopentylmagnesium chloride and thallium(III) chloride in a similar way to that described for the trimethylsilylmethyl-analogue. (Prep.35). Recrystallisation from pyridine gave colourless needles. (Found: C, 31.6; H, 5.7. $C_{10}H_{22}TlCl$ calc: C, 31.4; H, 5.8%).

32. neo-pentylbis(halogeno)thallium(III).

Equimolar amounts of bis(neo-pentyl)chlorothallium(III) and pyridinium perbromide were mixed together in CH_2Cl_2 .⁸⁷ Evaporation to low bulk followed by filtration and evaporation of the filtrate to dryness gave a pale green solid which was washed with petroleum ether (40/60°) and dried under vacuum. Proton NMR spectra of a number of separately prepared samples indicated the presence of some bis(neo-pentyl)halogenothallium(III) (< 30%) impurity).

33. Bis(neo-pentyl) isobutyrateothallium(III). (nc)

This was prepared by refluxing (3h) equimolar amounts of bis(neo-pentyl)chlorothallium(II) and isobutyrate silver(I) in methanol. Filtration, evaporation and subsequent recrystallisation from methanol gave the product as colourless needles (Yield 72%). (Found: C, 38.8; H, 6.7. $C_{14}H_{29}TlO_2$ calc.: C, 38.8; H, 6.7%).

34. neo-pentylbis(isobutyrate)thallium(III). (nc)

Reaction of equimolar amounts of bis(neo-pentyl)isobutyrate-thallium(III) and bis(isobutyrate)-mercury(II) in methanol- d_4 solution in an NMR tube at 35°C for 24h gave the product. The compound was not isolated but proton NMR measurements were made on the reaction mixture and indicated the reaction had gone to ca. 60% completion.

35. Bis(trimethylsilylmethyl)chlorothallium(III).

This compound was previously prepared by reaction of lithiotrimethylsilane with thallium(III) chloride.⁸⁸ A Grignard reagent was employed in the present work. A solution of trimethylsilylmethylmagnesium chloride,²⁰⁵ prepared from trimethylsilylmethylchloride (20.2g; 0.16mol) and magnesium (4.0g; 0.17mol) in diethyl ether (75cm³) was cooled to -15°C. Thallium(III) chloride (18.5g; 0.06mol) in diethyl ether was added with stirring during 1h. The reaction mixture was allowed to warm to room temperature and stirred for a further 2.5h. Hydrolysis with aqueous ammonium chloride solution, followed by stirring for 0.5h and subsequent filtration gave 25.8g of crude product. Recrystallisation from chloroform gave colourless needles suitable for single crystal X-ray analysis. (Found: C, 22.3; H, 5.2. C₈H₂₂Si₂TlCl calc.: C, 23.2; H, 5.3%).

36. Bis(trimethylsilylmethyl)isobutyrateothallium(III)^{88,147}

This compound was prepared from bis(trimethylsilylmethyl)-chlorothallium(III) and isobutyrate silver(I) in methanol by an analogous method to that described for the neo-pentyl-analogue (Prep. 33). (Found: C, 30.9; H, 5.9. C₁₂H₂₉O₂Si₂Tl calc.: C, 30.9; H, 6.2%).

37. Trimethylsilylmethylbis(isobutyrate)thallium(III).

This compound was prepared as previously reported.¹⁴⁷ (Found: C, 30.9; H, 5.4. C₁₂H₂₅O₄SiTl calc.: C, 30.9; H, 5.4%) Proton and carbon-13 spectra indicated the presence of a small amount of impurity. (< 10%).

38. Bis(cyclohexylmethyl)bromothallium(III) (nc)

A solution of cyclohexylmethylmagnesium bromide (0.14mol), prepared from magnesium (3.4g; 0.14mol) and cyclohexylmethylbromide (25g; 0.14mol) in diethyl ether (100cm³), was added

slowly with stirring to a freshly prepared solution of Tl(III)Br (0.04mol) in THF, prepared from Tl(I)Br (12.7g; 0.04mol) and bromine (7.1g; 0.04mol), at -20°C . Stirring was continued for 1.5h followed by hydrolysis with aqueous ammonium bromide solution. Filtration gave a white solid which was washed with water and ether then dried over P_2O_5 . Extraction with pyridine (200cm³), followed by filtration and evaporation of the filtrate to small volume (ca. 20cm³) on the rotary evaporator, and addition of petroleum ether (30/40^o) resulted in precipitation of the product as colourless plates. (Yield 17g; 82% based on TlBr_3 .) (Found: C, 34.2; H 5.3. $\text{C}_{14}\text{H}_{26}\text{TlBr}$ calc.: C, 35.1; H, 5.4%).

39. Bis(cyclohexylmethyl)isobutyrate-thallium(III).(nc)

Reaction of bis(cyclohexylmethyl)bromothallium(III) (4.8g; 0.01mol) with isobutyrate-silver(I) (1.9g; 0.0097mol) by stirring in a mixture of methanol (300cm³) and chloroform (100cm³) for 24 hours at room temperature followed by filtration and evaporation of the filtrate on the rotary evaporator gave the product as a white solid. Recrystallisation from chloroform gave colourless crystals. (Yield 4.5g; 90% based on isobutyrate-silver(I)). (Found: C, 44.4; H, 6.4. $\text{C}_{16}\text{H}_{29}\text{TlO}_2$ calc.: C, 44.5; H, 6.4%).

40. Methyl(2-methoxypropyl)acetate-thallium(III).

This was prepared according to the method of Kurosawa⁹³ by reaction of propene with Tl(III) OCOCH_3 in methanol followed by derivatisation with $(\text{CH}_3)_4\text{Sn}$. Evaporation and recrystallisation from benzene/n-hexane (5.1 v/v) gave the product as a white solid. (Found: C, 23.9; H, 4.3. $\text{C}_6\text{H}_{15}\text{TlO}_3$ calc.: C, 23.6; H, 4.2%). Carbon-13 NMR spectra suggested the presence of a methyltin impurity (<10%).

Attempts to prepare bis(tert-butyl)chlorothallium(III) via the Grignard method were unsuccessful. Maher⁹⁷ also reported he was unable to prepare this compound.

Chloromethylbis(acetato)thallium(III).²⁰⁶ A sample of this compound was kindly donated by Mrs. M.M. Thakur (The Polytechnic of North London).

Bis(n-hexyl)nitratothallium(III)¹⁶⁰ was donated by Dr. P.J. Burke (The Polytechnic of North London).

b) Alicyclicthallium(III) compounds.

41. Bis(cyclopropyl)bromothallium(III). (nc)

Cyclopropylmagnesium bromide (0.19mol) prepared from cyclopropylbromide, (23g; 0.19 mol) and magnesium (4.6g; 0.19mol) in THF (100cm³) was added slowly (45mins) with stirring to a cooled (-20°C) freshly prepared solution of thallium(III)bromide (0.06mol), prepared from Tl(I)Br (17.1g; 0.06mol) and bromine (9.6g; 0.06mol) in THF (100cm³). Stirring was continued for a further 20min at -20°C and then, after being allowed to warm to room temperature, the mixture was hydrolysed with aqueous ammonium bromide solution (5%). The crude product was collected by filtration, washed with water and ether and dried over P₂O₅. Extraction of this material (14.5g) with pyridine (500cm³) at 45°C and concentration to ca. 25 cm³, followed by addition of petroleum ether, gave the product as a white solid. (Yield 13g; 59% based on TlBr₃). (Found: C, 20.2; H, 2.8. C₆H₁₀TlBr calc. C 19.7; H, 2.7%).

42. Bis(cyclopropyl)isobutyratothallium(III) (nc)

Bis(cyclopropyl)bromothallium(III), (1.85g; 0.005mol) and isobutyrate silver(I), (0.90g; 0.046mol) were stirred in methanol (250cm³) for 24h. Silver bromide was removed by filtration and evaporation of the filtrate gave the product

as a white solid.(1.2g;75% based on isobutyrosilver(I)).
The product was used without further purification. (Found: C,29.7;H,4.0.C₁₀H₁₇O₂Tl calc.: C,32.1;H,4.6%).

43. Cyclopropylbis(isobutyrate)thallium(III) (nc)

A solution of bis(cyclopropyl)isobutyrate thallium(III), (0.8g;0.002mol) and bis(isobutyrate)mercury(II) (0.8g; 0.002mol) in methanol(100cm³) was stirred for 4h. The mixture was filtered and evaporation of the filtrate at 30°C on the rotary evaporator gave a white solid. Then mercury salts were removed by washing with benzene(50cm³). Recrystallisation from methanol gave colourless needles suitable for single crystal X-ray analysis. (Yield 0.4g;44% based on bis(isobutyrate)mercury(II)). (Found: C, 31.6; H ,4.6. C₁₁H₁₉O₄Tl calc: C, 31.5; H,4.5%).

44. Bis(cyclopentyl)chlorothallium(III).

This was prepared according to the published method ⁹⁷ by reaction of cyclopentylmagnesium chloride with Tl(III)Cl (molar ratio 2:1) in diethyl ether at -20°C. Hydrolysis with dilute HCl (0.2 mol dm⁻³) followed by filtration and evaporation of the filtrate gave a white solid which was recrystallised from pyridine. Colourless needles were obtained which disintegrated when dried under vacuum giving a white powder. (Found: C, 28.6;H4.5.C₁₀H₁₈TlCl calc:C,31.7;H,4.8%).

45. Bis(cyclopentyl)isobutyrate thallium(III). (nc)

Reaction of bis(cyclopentyl)chlorothallium(III) (1g 0.0026mol) and isobutyrosilver(I)(0.48g;0.0025mol) in methanol(250cm³) in a manner analogous to that described for the cyclopropyl analogue-(Prep.42) gave the product as colourless needles. (Yield 0.6g,57% based on isobutyrosilver(I)). (Found: C, 39.9; H,5.5.C₁₄H₂₅O₂Tl calc.: C, 39.9; H,3.8%).

46. Bis(cyclopentyl)tetrafluoroboratothallium(III) (nc)
Bis(cyclopentyl)chlorothallium(III) (2.4g; 0.005 mol)
and tetrafluoroborosilver(I) (1g; 0.005mol) were stirred
in methanol(400cm³) for 2 days. Filtration and evaporation
of the filtrate gave a white solid which was recrystallised
from methanol. (Yield 0.3g; 14% based on tetrafluoroborosilver(I)).
Found: C, 27.8; H, 4.1. C₁₀H₁₈TlBF₄ calc.: C, 27.9; H, 4.2%).

47. Bis(cyclohexyl)chlorothallium(III).

This was prepared by the method of Krause and Grosse¹⁵⁸
in a method analogous to that for the cyclopentyl-analogue
(Prep. 44). (Found: C, 35.2; H, 5.4. C₁₂H₂₂TlCl calc.: C, 35.5;
H, 5.4. C₁₂H₂₂TlCl calc.: C, 35.5; H, 5.4%).

48. Bis(cyclohexyl)isobutyrateothallium(III) (nc)

Reaction of bis(cyclohexyl)chlorothallium(III) (0.65g,
0.002 mol) with isobutyrateosilver(I) (0.39g; 0.002mol) in a
mixture of methanol/chloroform, (1:1 v/v), (300 cm³) for 24h
at room temperature followed by filtration and evaporation
of the filtrate on the rotary evaporator gave the product
which was recrystallised from methanol. (Yield 0.65g; 71% based
on isobutyrateosilver(I). (Found: C, 41.7; H, 6.2. C₁₆H₂₉TlO₂
calc.: C, 41.9; H, 6.3%).

49. Bis(cyclohexyl)tetrafluoroboratothallium(III) (nc)

This compound was prepared by reaction of equimolar
(0.001mol) quantities of bis(cyclohexyl)chlorothallium(III)
with tetrafluoroborosilver(I) in methanol (450cm³) for 4
days at room temperature in a manner analogous to that described
for the cyclopentyl-analogue (Prep. 46). The product was
obtained as pale yellow crystals. (Found: C, 31.2; H, 4.7.
C₁₂H₂₂TlBF₄ calc.: C, 31.5; H, 4.3%).

50. Bis(cycloheptyl)bromothallium(III). (nc).

Reaction of cycloheptylmagnesium bromide (0.2mol), prepared from cycloheptylbromide (35.9g; 0.19mol) and magnesium (4.6g; 0.19mol) in diethyl ether (100cm³) with a freshly prepared solution of thallium(III)bromide (0.06mol) (made from Tl(I)Br (17.1g; 0.06mol) and bromine (9.6g; 0.06mol) in THF (100cm³)) in a manner analagous to that described for the cyclopropyl-analogue (Prep.41) gave the product as a white solid. (Found: C, 37.0; H, 5.4. C₁₄H₂₆TlBr calc.: C, 35.1; H, 5.6%). (Yield 4g; 14% based on thallium(III) bromide).

51. Bis(cycloheptyl)tetrafluoroboratothallium(III). (nc)

Reaction of bis(cycloheptyl)bromothallium(III), (3g; 0.006mol) with tetrafluoroborosilver(I) (1.2g; 0.006mol) in methanol (750cm³) in a manner analagous to that described for the cyclopentyl-compound (Prep.46) gave the product as a pale yellow solid. (Yield 20% based on tetrafluoroborosilver(I)). (Found: C, 34.4; H, 5.2. C₁₄H₃₀TlBF₄ calc: C, 34.6; H, 5.4%).

52. (2-acetatonorbornane)bis(acetato)thallium(III).

This was prepared by the reported method¹⁹³ by reaction of thallium(III) acetate with norbornene in chloroform. (Found: C, 32.9; H, 3.9. C₁₃H₁₉O₆Tl calc.: C, 32.8; H, 4.0%).

53. (2-acetatonorbornene)bis(acetato)thallium(III).

This compound was prepared as reported¹⁹³ by reaction of thallium(III) acetate with norbornadiene in chloroform. (Found: C, 32.9; H, 3.8. C₁₃H₁₇O₆Tl calc.: C, 33.0; H, 4.0%).

Attempted preparations of cyclopentylbis(isobutyrate)-thallium(III) and cyclohexylbis(isobutyrate)thallium(III), (by reaction of the bis(alicyclic)isobutyrate-thallium(III) compounds with bis(isobutyrate)mercury(II) in methanol-d₄ in an NMR tube) were unsuccessful.

c) Alkenylthallium(III) compounds.

54. Bis(vinyl)chlorothallium(III)

This was prepared using the following modification of the method reported by Nesmeyanov.¹⁶⁹ Vinylmagnesium bromide (0.22mol) prepared from vinylbromide(23.5g;0.22mol) and magnesium (5.3g;0.22mol) in THF (70cm³) was added slowly (1hr) to a stirred solution of thallium(III) chloride(31g;0.1mol) in diethyl ether (100cm³) at -20°C. After stirring 15min. the mixture was hydrolysed with aqueous HCl (0.2mol dm⁻³), (100cm³). Filtration gave a grey solid which was washed with water and ether and dried over P₂O₅ under vacuum. Recrystallisation from pyridine gave colourless needles which disintegrated with loss of pyridine, when dried under vacuum, giving a white powder. (Yield 17.3g;59% based on thallium(III)chloride). (Found: C,16.1;H,2.1. C₄H₆TlCl calc.: C, 16.3; H, 2.0%).

55. Bis(vinyl)acetatothallium(III). (nc)

This compound was prepared by reaction of bis(vinyl)-chlorothallium(III), (0.5g; 0.002mol) and acetatosilver(I) (0.28g;0.002mol) in methanol(200cm³) as for the iso-propyl-compound (Prep.16). The product was obtained as pale yellow crystals. (Yield 0.3g;47% based on acetatosilver(I)). (Found: C,22.3;H 2.8. C₆H₉O₂Tl calc.:C,22.6;H,3.4).

56. Bis(vinyl)isobutyratothallium(III). (nc).

Reaction of bis(vinyl)chlorothallium(III) (2.9g;0.01mol) with isobutyratosilver(I) (1.9g;0.01mol) in a mixture of methanol(450cm³) and chloroform (50cm³) as described for the analagous iso-butyl-derivative(Prep.20) gave the product as a pale yellow solid. (Yield 2.3g; 71% based on isobutyratosilver(I)). The compound appeared to decompose slowly at room temperature giving rise to a smell similar to acetylene. Satisfactory

analysis could not be obtained(found C,21.5; H, 3.0. $C_8H_{13}TlO_2$ calc.: C, 27.8; H, 3.7%) but proton NMR of a freshly prepared sample showed no impurities. The compound was stored in the fridge.

57. Vinylbis(chloro)thallium(III).

This compound was prepared by modification of the reported method¹⁶⁹ using methanol instead of water as solvent.

Equimolar amounts of bis(vinyl)chlorothallium(III) and thallium(III)chloride were mixed in methanol- d_4 in an NMR tube. After 24h. at 35°C the proton NMR spectrum showed the presence of >90% vinylbis(chloro)thallium(III). The product was not isolated but proton and carbon-13 spectra were recorded using the reaction mixture.

58. Bis(iso-propenyl)bromothallium(III).

This derivative was made by the method of Nesmeyanov¹⁷⁰ with the modification that the organolithium reagent was reacted with thallium(III) bromide in THF instead of with thallium(III)chloride in diethyl ether. The reaction mixture was hydrolysed with aqueous HBr (1%) at -10°C. Filtration gave a grey solid which was recrystallised from methanol giving a white solid. The product was light sensitive. (Found: C,22.0;H,2.9. $C_6H_{10}TlBr$ calc.: C, 19.7;H,2.7%).

59. Bis(trans- β -styryl)bromothallium(III).

Preparation of this compound was previously reported by reaction of $TlBr_3$ with β -styrylboronic acid.¹⁷⁸ It was prepared here using an organolithium reagent. To a solution of β -styryllithium, prepared from β -styrylbromide (ca. 85% trans-isomer; Koch-Light Ltd) (20g;0.1mol) and lithium (1.5g;0.2 mol) in diethyl ether (100cm³) at -5°C, was added a solution of $TlBr_3$ (0.06mol), prepared from $Tl(I)Br$ (17g; 0.06mol) and bromine (9.6g;0.06mol) in THF(100cm³), with

vigorous stirring over one hour at 0°C. The mixture was hydrolysed with aqueous HBr(1%), (100cm³) at 0°C. The reaction was stirred for a further 20 mins. Filtration gave a grey solid which was washed with water and ether. Recrystallisation from pyridine gave the product as a white solid. Yield 5g; 19% based on TlBr₃). (Found: C, 38.9; H, 2.9.

C₁₆H₁₄TlBr calc.: C, 39.2; H, 2.9%).

60. Bis(trans-β-styryl)nitratothallium(III) (nc).

This compound was prepared by refluxing a mixture of bis(trans-β-styryl)bromothallium(2.5g; 0.005mol) and nitrat-silver(I)(0.85g; 0.005mol) in methanol (800cm³) for 5h. Filtration and evaporation of the filtrate gave the product as a white solid, which was recrystallised from methanol. (Yield 1.8g; 76% based on nitrat-silver(I)). (Found: C, 40.9; H, 2.7.

C₁₆H₁₄TlNO₃ calc.: C, 40.7; H, 2.9%).

61. Bis(trans-β-chlorovinyl)chlorothallium(III).

This compound was prepared according to the method of Nesmeyanov et al¹⁷⁵ by reaction of bis(trans-β-chlorovinyl)-mercury(II)²⁰⁷ with thallium(III)chloride in diethyl ether. The product was obtained as colourless crystals. (Yield 89% based on TlCl₃). (Found: C, 13.2; H, 1.1. C₄H₄TlCl₂ calc: C, 13.2; H, 1.1%).

62. trans-β-chlorovinylbis(chloro)thallium(III).

Reaction of equimolar amounts of bis(trans-β-chlorovinyl)-chlorothallium(III) and thallium(III)chloride in methanol-d₄ for 24h. gave the product. Proton NMR spectra indicated the reaction had gone to about 70% completion. The product was not isolated but proton and carbon-13 spectra were recorded using the reaction mixture.

63. (trans-2-acetato, but-2-enyl)bis(acetato)thallium(III).

This compound was prepared according to the method of Sharma et al¹⁹² by reaction of thallium(III)acetate with but-2-yne. The trans-isomer was separated by recrystallisation from chloroform. The product was obtained as a white solid. (Found: C, 26.7; H, 3.4. $C_{10}H_{15}TlO_4$ calc.: C, 29.7; H, 3.7%).

Bis(vinyl)tetrafluoroboratothallium(III), was available from previous work.²⁰⁸

Bis(trans/cis-propenyl)nitratothallium(III) was available from previous work.²⁰⁸

d) Arylthallium(III) compounds

64. Bis(phenyl)nitratothallium(III).¹⁶⁶

Reaction of bis(phenyl)bromothallium(4.4g; 0.01 mol) with nitrat silver(I) (1.7g; 0.009 mol) in methanol as previously described for the trans- β -styryl-analogue (Prep. 60) gave the product as white crystals. (Yield 2.1g; 50% based on nitrat silver(I)). (Found: C, 33.9; H, 2.3; N, 2.9. $C_{12}H_{10}TlNO_3$ calc.: C, 34.3; H, 2.4; N, 3.3%).

65. Bis(phenyl)acetatothallium(III).¹⁶⁶

This was prepared by reaction of bis(phenyl)chlorothallium(III) (3.9g; 0.01 mol) with acetat silver(I) (1.7g; 0.01 mol) in methanol (200 cm³) as previously described for the analogous iso-propyl-compound (Prep. 16). The product was obtained as a white solid. (Yield 3.3g; 79% based on acetat silver(I)). (Found: C, 40.3; H, 3.2. $C_{14}H_{13}TlO_2$ calc.: C, 40.3%; H, 3.1%).

Bis(phenyl)chlorothallium(III) and Bis(phenyl)bromothallium(III) were both donated by Mrs. M.M. Thakur (The Polytechnic of North London).

Bis(pentafluorophenyl)bromothallium(III) and Bis(p-hydro-tetrafluorophenyl)bromothallium(III) were kindly donated by Dr. G.B. Deacon and Mr. R.J. Phillips (Monash University, Clayton, Victoria, Australia).

Microanalyses (C,H,N,) were carried out by the Butterworth Microanalytical Service, London.

CHAPTER THREE

THALLIUM-205 CHEMICAL SHIFTS IN ORGANO-
THALLIUM(III) COMPOUNDS

The majority of thallium-205 chemical shift studies have been for solutions of Tl(I) compounds.^{13,24-30} There have also been several reports of chemical shifts for Tl(III) in TlX_3 (X=anion) compounds.^{10,13,24,210,211} A smaller number of studies have been concerned with thallium chemical shifts in organothallium(III) compounds of the types R_3Tl ,^{10,11,13} R_2TlX ^{11-16,18,19,22} and $RTlX_2$ ¹²⁻¹⁵ (R=organic group, X=anionic species).

3.1. Results

The ^{205}Tl chemical shifts for alkyl, alicyclic, alkenyl and arylthallium(III) derivatives are presented in Tables 3.1 to 3.5 respectively. Shifts for monoorganothallium(III) compounds are shown in Table 3.6.

A number of references have been proposed as shift standards for ^{205}Tl chemical shifts, eg. $TlOCCCH_3$ ²⁴, TlF in H_2O ⁴¹, $TlCOCH$ in H_2O ,^{27,47} infinitely dilute $TlOCOCH_3$.⁴²⁻⁴³ A 0.3 mol dm^{-3} solution of $TlNO_3$ in H_2O has been widely used^{10,19,25,36,45}. Some authors relate chemical shifts by convention to the proton resonance of H_2O ⁴⁶ or TMS^{12,16,18,22,23} (as proposed by McFarlane¹⁹⁵ and Harris¹⁹⁶), and express the shifts as the frequency ratio $\nu(^{205}Tl)/\nu(^1H)$. Use of the latter approach and reporting of the resonance frequency as $\Xi(^{205}Tl)$ (see 2.1.3.1) obviates the need for a reference standard.

Values of $\Xi(^{205}Tl)$ are reported here, however for convenience in discussion $\delta(^{205}Tl)$ has also been reported. The infinite dilution resonance frequency of $(CH_3)_2TlNO_3$ in H_2O at $41 \pm 1^\circ C$, for which $\Xi(^{205}Tl) = 57887038 \text{ Hz}$ ²³ has been arbitrarily chosen as $\delta(^{205}Tl) = 0$. Unusually among the more easily handled and accessible thallium compounds, aqueous solutions of $(CH_3)_2TlNO_3$ exhibit only a very small dependence

TABLE 3.1

^{205}Tl Chemical shifts for straight-chain bis(alkyl)thallium(III) compounds.^a

Compound	Solvent ^b	Conc. ^c	Temp. ^d	$\Xi(^{205}\text{Tl})^{\text{e},\text{f}}$	$\delta(^{205}\text{Tl})^{\text{f},\text{g}}$
$(\text{CH}_3)_2\text{TlNO}_3$	DMSO	0.21	29	57882013	-87
$(\text{CH}_3\text{CH}_2)_2\text{TlNO}_3$	DMSO	0.19	31	57869508	-303
$(\text{CH}_3\text{CH}_2)_2\text{TlBr}$	py	0.14	28	57891859	83
$(\text{CH}_3\text{CH}_2)_2\text{TlOCOCH}(\text{CH}_3)_2$	DMSO	0.06	28	57878946	-140
$(\text{CH}_3\text{CH}_2)_2\text{TlOCOCH}(\text{CH}_3)_2$	py	0.30	31	57881036	-104
$(\text{CH}_3\text{CH}_2)_2\text{TlOCOCH}(\text{CH}_3)_2$	CHCl_3	0.10	31	57884098	-51
$(\text{CH}_3\text{CH}_2\text{CH}_2)_2\text{TlNO}_3$	DMSO	0.11	28	57875079	-207
$[\text{CH}_3(\text{CH}_2)_2\text{CH}_2]_2\text{TlNO}_3$	DMSO	0.19	28	57877048	-173
$[\text{CH}_3(\text{CH}_2)_2\text{CH}_2]_2\text{TlNO}_3$	py	0.21	28	57878801	-142
$[\text{CH}_3(\text{CH}_2)_3\text{CH}_2]_2\text{TlNO}_3$	DMSO	0.17	29	57875498	-199
$[\text{CH}_3(\text{CH}_2)_4\text{CH}_2]_2\text{TlNO}_3$	DMSO	0.11	32	57871958	-261
$[\text{CH}_3(\text{CH}_2)_4\text{CH}_2]_2\text{TlNO}_3$	py	0.12	31	57872514	-251

^a All spectra were obtained in PFT mode at 34.7 MHz with broad-band proton decoupling. ^b Protonated solvents were used.

^c In mol dm⁻³. ^d Error $\pm 1^\circ\text{C}$. ^e Frequency in Hz of ^{205}Tl resonance for a field in which TMS gives a proton resonance at exactly 100 MHz. ^f Error subjectively estimated as ± 57 Hz (i.e. 1ppm) unless otherwise noted.

^g In ppm. $\delta(^{205}\text{Tl}) = 0$ has been arbitrarily taken as the infinite dilution chemical shift of $(\text{CH}_3)_2\text{TlNO}_3$ in H_2O at $41.0 \pm 1^\circ\text{C}$ for which $\Xi(^{205}\text{Tl}) = 57887038\text{Hz}$ (Ref.23).

TABLE 3.2

²⁰⁵Tl Chemical shifts for branched-chain bis(alkyl)thallium(III)compounds^a

Compound	Solvent ^b	Conc. ^c	Temp. ^d	$\bar{\nu}(\text{}^{205}\text{Tl})^{\text{e,f}}$	$\delta(\text{}^{205}\text{Tl})^{\text{f,g}}$
$[(\text{CH}_3)_2\text{CH}]_2\text{TlCl}$	DMSO	0.14	32	57875383	-201
$[(\text{CH}_3)_2\text{CH}]_2\text{TlCl}$	py	0.10	32	57882368	-81
$[(\text{CH}_3)_2\text{CHCH}_2]_2\text{TlCl}$	DMSO	0.21	32	57892363	92
$[(\text{CH}_3)_2\text{CHCH}_2]_2\text{TlCl}$	py	0.18	30	57897917	188
$[(\text{CH}_3)_2\text{CHCH}_2]_2\text{TlOCOR}^{\text{h}}$	py	0.17	29	57886882	-3
$[\text{CH}_3\text{CH}_2(\text{CH}_3)\text{CH}]_2\text{TlCl}$	DMSO	0.12	33	57881123 57881214	-102 -101
$[(\text{CH}_3)_2\text{CHCH}_2\text{CH}_2]_2\text{TlBF}_4$	DMSO	0.15	30	57874374	-219
$[(\text{CH}_3)_2\text{CHCH}_2\text{CH}_2]_2\text{TlNO}_3$	py	0.14	28	57872331	-254
$[\text{CH}_3\text{CH}_2\text{CH}_2(\text{CH}_3)\text{CH}]_2\text{TlCl}$	DMSO	0.17	29	57883348 57883467	-64 -62
$[\text{CH}_3\text{CH}_2\text{CH}_2(\text{CH}_3)\text{CH}]_2\text{TlCl}$	py	0.05	30	57888648	28
$[(\text{CH}_3)_3\text{CCH}_2]_2\text{TlCl}$	py	0.24	30	57897839	187
$[(\text{CH}_3)_3\text{CCH}_2]_2\text{TlCl}$	CHCl_3	0.10	28	57903889	291
$[(\text{CH}_3)_3\text{CCH}_2]_2\text{TlOCOR}^{\text{h}}$	py	0.24	29	57887578	9
$[(\text{CH}_3)_3\text{CCH}_2]_2\text{TlOCOR}^{\text{h}}$	CHCl_3	0.13	31	57890506	169
$[(\text{CH}_3)_3\text{SiCH}_2]_2\text{TlCl}$	py	0.19	30	57903263	280 ⁱ
$[(\text{CH}_3)_3\text{SiCH}_2]_2\text{TlOCOR}^{\text{h}}$	py	0.26	30	57896375	161
$[(\text{CH}_3)_3\text{SiCH}_2]_2\text{TlOCOR}^{\text{h}}$	CHCl_3	0.06	31	57901562	251 ⁱ
$[(\text{CH}_2)_5\text{CHCH}_2]_2\text{TlBr}$	DMSO	0.25	30	57893501	112 ⁱ
$[(\text{CH}_2)_5\text{CHCH}_2]_2\text{TlBr}$	py	0.15	30	57899003	207
$[(\text{CH}_2)_5\text{CHCH}_2]_2\text{TlOCOR}^{\text{h}}$	py	0.22	28	57887924	15
$[(\text{CH}_2)_5\text{CHCH}_2]_2\text{TlOCOR}^{\text{h}}$	CHCl_3	0.16	28	57891217	72
$\text{CH}_3\text{CH}(\text{OCH}_3)\text{CH}_2(\text{CH}_3)\text{TlX}^{\text{j}}$	py	0.36	29	57885932	-19
$\text{CH}_3\text{CH}(\text{OCH}_3)\text{CH}_2(\text{CH}_3)\text{TlX}^{\text{j}}$	CHCl_3	0.07	28	57889609	-14

^aAll spectra were obtained in PFT mode at 34.7 MHz with broadband proton decoupling. ^bProtonated solvents were used. ^cIn mol dm⁻³.^dError $\pm 1^\circ\text{C}$. ^eSee note e, TABLE 3.1. ^fSee note f, TABLE 3.1.^gSee note g, TABLE 3.1. ^hR=CH(CH₃)₂.ⁱError ± 1.5 ppm. ^jX = OCOCH₃

TABLE 3.3

 ^{205}Tl Chemical shifts for bis(alicyclic)thallium(III) compounds.^a

Compound	Solvent ^b	Conc. ^c	Temp. ^d	$\bar{\nu}(^{205}\text{Tl})^{e,f}$	$\delta(^{205}\text{Tl})^{f,g}$
$[(\text{CH}_2)_2\text{CH}]_2\text{TlBr}$	py	0.25	29	57895766	151
$[(\text{CH}_2)_2\text{CH}]_2\text{TlBr}$	DMSO	0.37	35	57889495	42
$[(\text{CH}_2)_2\text{CH}]_2\text{TlOCOR}^h$	py	0.21	29	57884368	-46
$[(\text{CH}_2)_2\text{CH}]_2\text{TlOCOR}^h$	DMSO	0.09	29	57884263	-48
$[(\text{CH}_2)_4\text{CH}]_2\text{TlCl}$	py	0.13	28	57888676	28
$[(\text{CH}_2)_4\text{CH}]_2\text{TlOCOR}^h$	py	0.05	31	57878838	-142
$[(\text{CH}_2)_5\text{CH}]_2\text{TlCl}$	py	0.07	30	57885998	-18 ⁱ
$[(\text{CH}_2)_5\text{CH}]_2\text{TlBF}_4$	DMSO	0.19	31	57859223	-481 ^j
$[(\text{CH}_2)_5\text{CH}]_2\text{TlOCOR}^h$	py	0.10	28	57874882	-210 ^k
$[(\text{CH}_2)_5\text{CH}]_2\text{TlOCOR}^h$	CHCl_3	0.10	28	57877179	-170 ^j
$[(\text{CH}_2)_6\text{CH}]_2\text{TlBF}_4$	py	0.05	29	57861731	-437 ^k

^aAll spectra obtained in PFT mode at 34.7 MHz with broad-band proton decoupling. ^bProtonated solvents were used. ^cIn mol dm^{-3} . ^dError $\pm 1^\circ\text{C}$. ^eSee note e, TABLE 3.1. ^fSee note f, TABLE 3.1. ^gSee note g, TABLE 3.1. ^h $\text{R} = \text{CH}(\text{CH}_3)_2$. ⁱError $\pm 4\text{ppm}$. Signal broad, $\nu_{1/2} \approx 600\text{ Hz}$. ^jError $\pm 3\text{ppm}$. Signal broad, $\nu_{1/2} \approx 400\text{ Hz}$. ^kError $\pm 2\text{ppm}$. Signal broad $\nu_{1/2} \approx 300\text{ Hz}$.

TABLE 3.4

 ^{205}Tl Chemical shifts for bis(alkenyl)thallium(III) compounds.^a

Compound	Solvent ^b	Conc. ^c	Temp. ^d	$\bar{\nu}(^{205}\text{Tl})^{\text{e,f}}$	$\delta(^{205}\text{Tl})^{\text{f,g}}$
$(\text{H}_2\text{C}=\text{CH})_2\text{TlBF}_4^{\text{h}}$	DMSO	0.66	30	57863000	-415
$(\text{H}_2\text{C}=\text{CH})_2\text{TlOCOR}^{\text{i}}$	py	0.27	28	57864644	-387
$(\text{H}_2\text{C}=\text{CH})_2\text{TlOCOCH}_3$	CH_3OH	0.16	31	57858405	-495
$(\text{H}_2\text{C}=\text{CH})_2\text{TlOCOCH}_3$	py	0.29	29	57864891	-383
$(\text{H}_2\text{C}=\text{CH})_2\text{TlOCOCH}_3$	DMSO	0.33	29	57862150	-430
$[\text{H}_2\text{C}=\text{CH}(\text{CH}_3)]_2\text{TlBr}$	DMSO	0.18	29	57867707	-334
$[\text{H}_2\text{C}=\text{CH}(\text{CH}_3)]_2\text{TlBr}$	py	0.37	29	57875633	-197
$\left[\begin{array}{c} \text{CH}_3 \quad \text{H} \\ \diagdown \quad \diagup \\ \text{C}=\text{C} \\ \diagup \quad \diagdown \\ \text{H} \end{array} \right]_2\text{TlNO}_3$	DMSO	j	30	57860832	-453
$\left[\begin{array}{c} \text{H} \quad \text{H} \\ \diagdown \quad \diagup \\ \text{C}=\text{C} \\ \diagup \quad \diagdown \\ \text{CH}_3 \end{array} \right]_2\text{TlNO}_3$	DMSO	j	30	57865234	-377 ^k
$\left[\begin{array}{c} \text{Cl} \quad \text{H} \\ \diagdown \quad \diagup \\ \text{C}=\text{C} \\ \diagup \quad \diagdown \\ \text{H} \end{array} \right]_2\text{TlCl}$	DMSO^{l}	0.33	29	57852911	-590
$\left[\begin{array}{c} \text{Ph} \quad \text{H} \\ \diagdown \quad \diagup \\ \text{C}=\text{C} \\ \diagup \quad \diagdown \\ \text{H} \end{array} \right]_2\text{TlNO}_3$	DMSO	0.24	29	57858167	-499

^aAll spectra obtained in PFT mode at 34.7 MHz with broad-band proton decoupling. ^bProtonated solvents were used unless otherwise noted. ^cIn mol dm⁻³. ^dError $\pm 1^\circ\text{C}$. ^eSee note e, TABLE 3.1. ^fSee note f, TABLE 3.1. ^gSee note g, TABLE 3.1. ^hData from ref. 208. ⁱR=CH(CH₃)₂. ^jMixture of isomers. Total concentration 0.11 mol dm⁻³. ^kError ± 3 ppm. ^lDMSO-d₆.

TABLE 3.5

 ^{205}Tl Chemical shifts for bis(aryl)thallium(III) compounds.^a

Compound	Solvent ^b	Conc. ^c	Temp ^d	$\Xi(^{205}\text{Tl})^{\text{e,f}}$	$\delta(^{205}\text{Tl})^{\text{f,g}}$
$(\text{C}_6\text{H}_5)_2\text{TlCl}$	DMSO	0.12	30	57868176	-326
$(\text{C}_6\text{H}_5)_2\text{TlBr}$	DMSO	0.10	31	57868411	-322
$(\text{C}_6\text{H}_5)_2\text{TlOCOCH}_3$	py	0.06	31	57864884	-383
$(\text{C}_6\text{H}_5)_2\text{TlOCOCH}_3$	DMSO	0.10	31	57860386	-461
$(\text{C}_6\text{H}_5)_2\text{TlNO}_3$	DMSO	0.11	30	57854768	-558
$(\text{C}_6\text{F}_5)_2\text{TlBr}$	py	0.50	33	57863095	-414
$(\text{C}_6\text{F}_5)_2\text{TlBr}$	CH_3OH	0.43	27	57864568	-388
$(\text{C}_6\text{F}_5)_2\text{TlBr}$	C_6H_6	0.26	29	57872314	-254 ^h
$(\text{C}_6\text{F}_5)_2\text{TlBr}$	$(\text{CH}_3)_2\text{CO}$	0.49	30	57868549	-320
$(\text{p-HC}_6\text{F}_4)_2\text{TlBr}$	CH_3OH	0.29	30	57865542	-371
$(\text{p-HC}_6\text{F}_4)_2\text{TlBr}$	$(\text{CH}_3)_2\text{CO}$	0.47	30	57866996	-346

^aAll spectra were obtained in PFT mode at 34.7 MHz with broad-band proton decoupling used only in the cases of the compounds with fully protonated aromatic rings.

^bProtonated solvents were used. ^cIn mol dm⁻³.

^dError $\pm 1^\circ\text{C}$. ^eSee note e, TABLE 3.1. ^fSee note f, TABLE 3.1.

^gSee note g, TABLE 3.1. ^hError ± 2 ppm, signals broad.

TABLE 3.6.

205

Tl Chemical shifts for monoorganothallium(III) compounds.^a

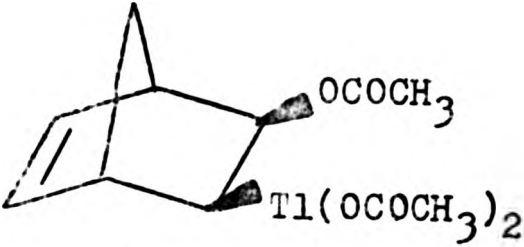
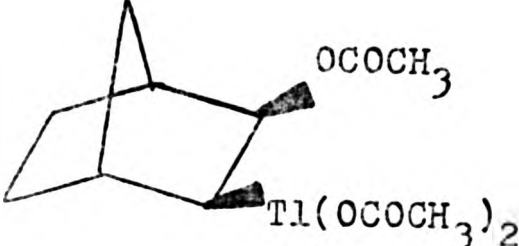
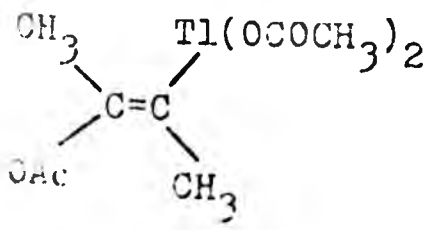
Compound	Solvent ^b	Conc. ^c	Temp. ^d	$\bar{\nu}(^{205}\text{Tl})^{e,f}$	$\delta(^{205}\text{Tl})^{f,g}$
$\text{CH}_3\text{Tl}(\text{OCOCH}_3)_2$	DMSO	0.12	28	57867640	-335
$\text{CH}_3\text{Tl}(\text{OCOCH}_3)_2$	py	0.15	28	57865918	-365
$\text{ClCH}_2\text{Tl}(\text{OCOCH}_3)_2$	CH_3OH	0.40	25	57838917	-832
$\text{CH}_3\text{CH}_2\text{Tl}(\text{OCOR})_2^h$	py	0.25	29	57861151	-447
" "	DMSO	0.14	30	57861126	-448
" "	CHCl_3	0.05	32	57862090	-431
$(\text{CH}_3)_3\text{SiCH}_2\text{Tl}(\text{OCOR})_2^h$	py	0.18	32	57867673	-335
$(\text{CH}_2)_2\text{CHTl}(\text{OCOR})_2^h$	DMSO	0.13	29	57859650	-473
" "	py	0.16	29	57860243	-463
	DMSO	0.01	28	57852515	-597
" "	DMSO	0.13	33	57853038	-588
" "	DMSO	0.56	28	57852502	-597
" "	py	0.12	31	57854906	-555
" "	CHCl_3	0.10	32	57853468	-580
	DMSO	0.06	33	57853913	-573
" "	py	0.08	31	57856067	-535
" "	CHCl_3	0.07	32	57855427	-546
	py	0.23	29	57847960	-676
" "	DMSO	0.29	29	57847525	-683

Table 3.6 continued

^aAll spectra obtained in PFT mode at 34.7MHz using broad-band proton decoupling. ^bProtonated solvents were used.

^cIn mol dm⁻³. ^dError \pm 1°C. ^eSee note e TABLE 3.1.

^fSee note f, TABLE 3.1. ^gSee note g, TABLE 3.1.

^hR = CH(CH₃)₂.

of $\delta(^{205}\text{Tl})$ on concentration.^{17,23} This makes it especially useful in the conversion to a common scale of other ^{205}Tl chemical shift data, which are not reported in terms of $\Xi(^{205}\text{Tl})$. Additionally the thallium resonance in this solution has a well defined linear temperature dependence, $(d\delta(^{205}\text{Tl})/dT = 0.44 \pm 0.01)$.²³

3.2. Discussion

3.2.1. Origin of the chemical shift

When an atom or molecule is placed in a magnetic field (B_0), the local field experienced by a particular nucleus (B_{loc}), will differ from the applied field. The difference depends on the extent to which electrons surrounding the nucleus alter the magnetic field at the nucleus. The local field at a particular nucleus is given by

$$B_{\text{loc}} = B_0 (1 - \sigma) \quad (3.1)$$

where σ is the shielding constant. It is a dimensionless constant independent of the applied field but dependent upon the chemical environment of the nucleus.

The chemical shift is defined⁹ as the difference between the screening constants

$$\delta = \sigma_r - \sigma_s \quad (3.2)$$

where σ_s and σ_r are the shielding constants of sample and reference respectively. Chemical shifts are given in parts per million by

$$\delta = \frac{\nu_s - \nu_r}{\nu_0} \times 10^6 \quad (3.3)$$

where ν_s and ν_r are the resonance frequencies of sample and

reference respectively and ν_0 is the fixed operating frequency of the spectrometer.

Expressions for calculation of the magnetic shielding of nuclei in molecules have been developed by Ramsey.¹²² Saika and Slichter²¹² modified these expressions and proposed that the shielding constant for a given nucleus had three separate atomic contributions.

$$\sigma = \sigma_d + \sigma_p + \sigma_o \quad (3.4)$$

σ_d , the diamagnetic term, arises from the local diamagnetic currents in the molecule. σ_p , the paramagnetic term, represents the contribution to the orbital angular momentum of electrons in the valence orbitals. Only electrons in p, d, f.... orbitals make contributions to σ_p . The paramagnetic term makes a negative contribution to the screening.

σ_o , represents the combined effect of contributions from other atoms in the molecule. A small contribution is also included for the solvent.

Expressions for the diamagnetic and paramagnetic contributions to the shielding constant have been derived by Schneider and Buckingham.¹⁰ For hydrogenlike atomic orbitals a single electron contribution to σ_d is given by

$$\sigma_d = \frac{e^2 Z_{eff}}{3mc^2 A_0 n^2} = 17.8 \times 10^{-6} \cdot \frac{Z_{eff}}{n^2} \quad (3.5)$$

where n is the principal quantum number of the orbital to which an electron is added and Z_{eff} , the effective nuclear charge, is approximated by $(Z_0 Z)^{\frac{1}{2}}$ where Z is the real nuclear charge and Z_0 the Slater²¹³ screened nuclear charge. A_0 is the Bohr radius, c, m and e are the usual constants. For the 6s electrons in thallium, $Z = 81$, $Z_0 = 5.00$ (in TlX_3)

and $\sigma_d = \text{ca. } 10\text{ppm}$ per electron. Contributions of this magnitude are also calculated for Pb, and Hg¹⁰: Considering the large chemical shift ranges of these nuclei this term is relatively unimportant.

The range of chemical shifts possible from changes in σ_p can be calculated using the approximate expressions, Equations 3.6 to 3.8 derived by Schneider and Buckingham¹⁰ using their 'atom in a molecule' model.

$$\sigma_p = - \frac{e^2 \hbar^2 L(L+1)}{12 \pi^2 m^2 c^2 \Delta E} \cdot \langle \psi_o | r^{-3} | \psi_o \rangle \quad (3.6)$$

where $L(L+1)$ represents the electron orbital angular momentum contribution, ΔE is the mean molecular excitation energy and $\langle \psi_o | r^{-3} | \psi_o \rangle$ is the mean value of r^{-3} of an electron that contributes to the orbital angular momentum, approximated by

$$\langle \psi_o | r^{-3} | \psi_o \rangle = \frac{Z_{\text{eff}}^3 A_o^{-3}}{n^3 L(L+1)(L+\frac{1}{2})} \quad (3.7)$$

where A_o is the Bohr radius. Therefore σ_p may be written:

$$\sigma_p = -7.67 \times 10^{-6} \cdot \frac{(Z_o Z)^{3/2} L(L+1)}{n^3 L(L+1)(L+\frac{1}{2}) \Delta E} \quad (3.8)$$

For thallium the paramagnetic contribution calculated using this expression is -5800ppm . The experimentally observed shift range for thallium so far reported covers ca. 5600ppm . for compounds in solution. (See FIG. 3.2).

Saika and Slichter²¹² showed σ_p to be the dominant contribution to fluorine shielding and Schneider and Buckingham¹⁰ found it to be so for Tl, Hg and Pb. It is also considered to dominate the shielding of Sn compounds.^{214,215} Calculations for Pb²¹⁶ and Co²¹⁷ also report the dominance of σ_p .

Using valence-bond formulations Jameson and Gutowsky²¹⁸ derived an expression (Equation 3.9) for σ_p

$$\sigma_p = \frac{-2e^2 \hbar^2}{3\Delta E m^2 c^2} \cdot \left\langle \frac{1}{r^3} \right\rangle_p P_u + \left\langle \frac{1}{r^3} \right\rangle_d D_u \quad (3.9)$$

where ΔE is a mean electronic excitation energy; $\left\langle \frac{1}{r^3} \right\rangle_{p,d}$ are the average values of r^{-3} , where r refers to the separation between the nucleus and the valence p and d electrons respectively. Using the spin orbit interaction as a measure of $\left\langle \frac{1}{r^3} \right\rangle$ the periodic dependence of the range of observed chemical shifts on atomic number was attributed to changes in $\left\langle \frac{1}{r^3} \right\rangle$.²¹⁸ However for a closely related series of compounds changes in the shift were attributed to variations in P_u and D_u .

P_u and D_u represent the amount of electron 'unbalance' associated with the atom's valence p and d orbitals respectively. The values of P_u and D_u depend upon the coordination number of the atom, the hybridisation of its bonding orbitals and the ionicity of its bonds. In the case of spherically symmetric electron shells P_u and D_u both have their minimum values of zero, whereas large values of P_u and D_u correspond to highly imbalanced p and d electron distributions. These two extreme situations may seldom arise but they indicate how changing the relative electronegativities of the substituents will affect the chemical shift.

The expression for σ_p (Equation 3.9) proposed by Jameson and Gutowsky²¹⁸ is similar to that described by Pople and Karplus.^{219,220}

The effects of changing the parameters in equation 3.9 on thallium shielding are summarised in FIG 3.1

FIGURE 3.1

Factors influencing thallium shielding

<u>Higher frequency</u> (Decreased shielding)	<u>Parameter</u>	<u>Lower frequency</u> (Increased shielding)
" ← Decreases	ΔE	Increases → "
" ← Increases	$1/r^3$	Decreases → "
" ← Increases	Pu, Du	Decreases → "
" ← Increases	Z_{eff}	Decreases → "

A number of problems arise when attempts are made to rationalise changes in the thallium chemical shift in terms of variation in these parameters. It is not clear whether changes arise predominantly from variation in one or more parameters. Additionally the validity of making the average energy approximation, even for a related series of compounds, is questionable.

3.2.2. Range of thallium chemical shifts

The ranges of ^{205}Tl chemical shifts for organothallium(III) derivatives of the types R_3Tl ; R_2TlX ; RTlX_2 , (X = anion) are shown in FIG 3.2 compared to the shifts for TlX_3 and Tl(I) compounds in solution. The shifts are relative to the infinite dilution chemical shift of $(\text{CH}_3)_2\text{TlNO}_3$ in H_2O at 41°C . The values reported here considerably extend the known ranges for R_2TlX and RTlX_2 compounds.

A trend of increasing shielding of Tl(III) upon progressive replacement of organo groups by more electronegative substituents (X) can be clearly seen on going from R_3Tl to TlX_3 . The high frequency shifts of the organothallium(III) compounds

^{205}Tl CHEMICAL SHIFT RANGE FOR THALLIUM COMPOUNDS IN SOLUTION

R = ORGANO GROUP
X = ANION

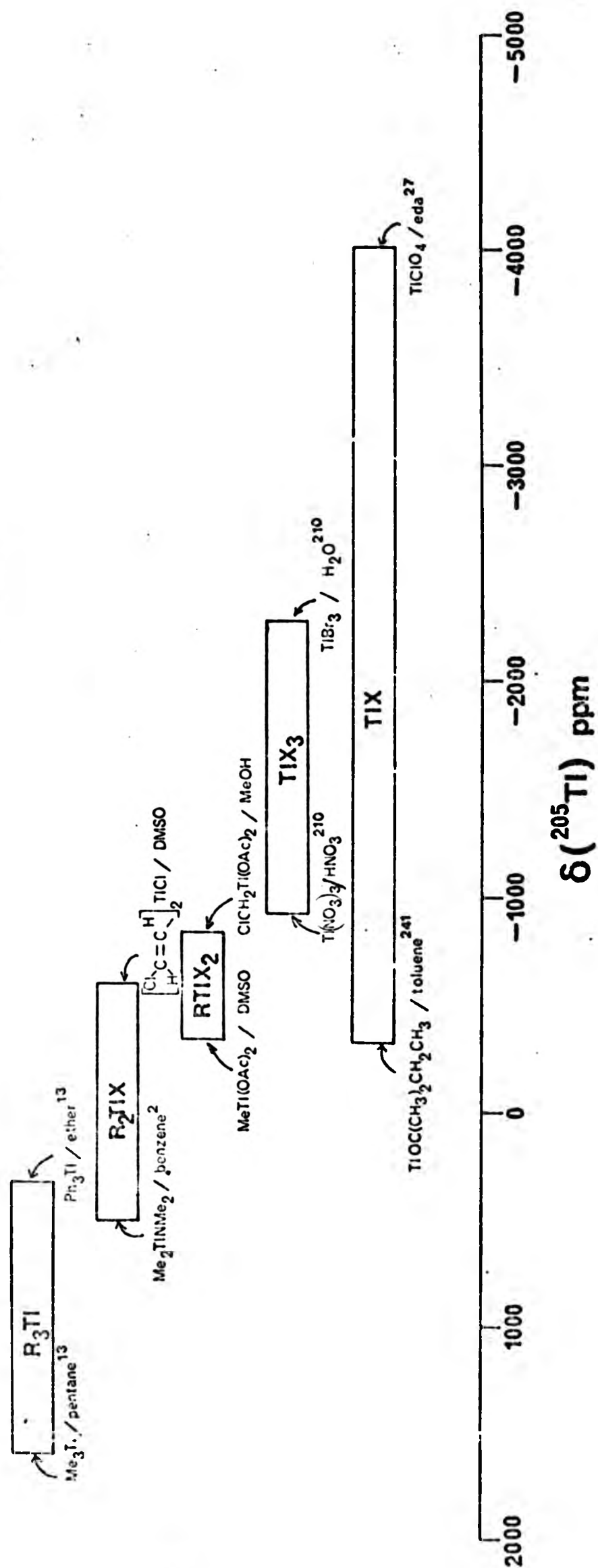


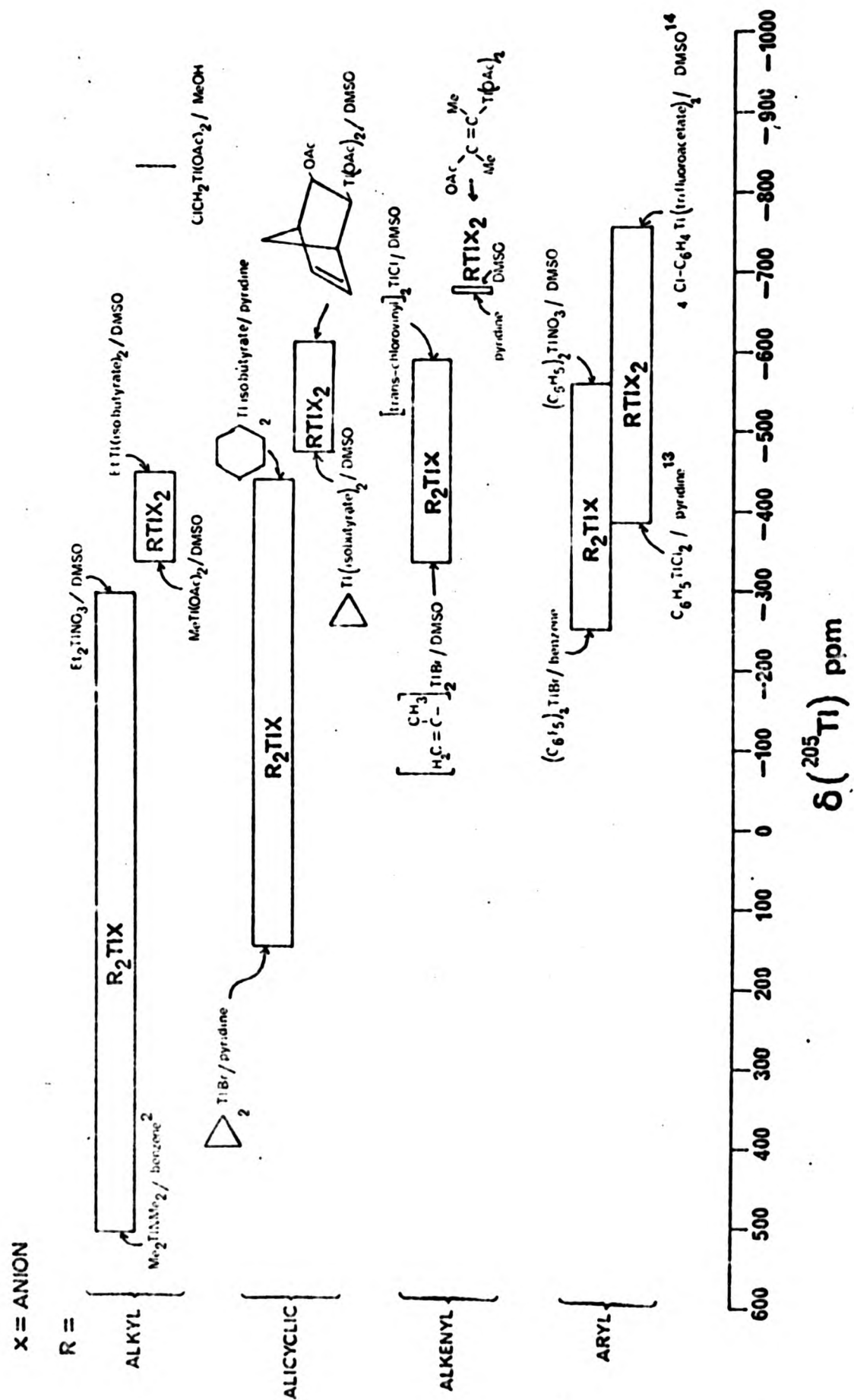
FIG 3.2.

compared to Tl(I) derivatives are in agreement with the model of Schneider and Buckingham¹⁰ which predicted decreased shielding for covalently bonded organothallium(III) compounds. The hybridisation at thallium(in parentheses) changes with increasing ^{205}Tl shielding in the order:
 $\text{R}_3\text{Tl}(\text{sp}^2) < \text{R}_2\text{Tl}^+(\text{sp}) < \text{RTl}^{2+}(\text{s})$ Increasing involvement of p orbitals might be expected to give rise to shifts of $\delta(^{205}\text{Tl})$ to higher frequency on the basis of Equation 3.9 and FIG 3.1, as observed. Only compounds of the types R_2TlX and RTlX_2 were examined in this study. A direct comparison of $\delta(^{205}\text{Tl})$ between R_2TlX and RTlX_2 can be made in only four cases where R and X are common; $\text{R} = \text{CH}_3^{12}$; CH_3CH_2 ; $(\text{CH}_3)_3\text{SiCH}_2$; $(\text{CH}_2)_2\text{CH}$; $\text{X} = \text{carboxylate}$. Replacement of the organic group by a second carboxylate group results in increases in thallium shielding of 174-425ppm.

After the number of organo groups bonded to thallium, the next most important factor influencing the thallium shielding appears to be the nature of the organo group. The effect of changing the organic group R in the series, alkyl, alicyclic, alkenyl, aryl, for compounds R_2TlX and RTlX_2 is shown in FIG 3.3. Although there is considerable overlap of ranges, the trend of increased shielding with increasing electronegativity of the organic group can be seen. Kennedy and McFarlane²¹⁴ have suggested that the increased shielding of organotin compounds having alkenyl and aryl substituents may result from the polarisability of the π -electron systems in these groups.

A wide variety of structural types were examined in an attempt to define the shift range for each type. It is not expected that these ranges are definitive and will be extended

85



as more data becomes available.

The other factors having a major influence on thallium shielding are the nature of the solvent and anion. Temperature and concentration changes produce relatively small changes in $\delta(^{205}\text{Tl})$.^{16,23} After a brief discussion of concentration and temperature dependence the role of solvent, anion and organo group will be examined in more detail.

3.2.3. The effect of concentration and temperature

Burke et al¹⁶ showed that for $(\text{CH}_3)_2\text{TlX}$ ($\text{X} = \text{NO}_3, \text{I}, \text{OC}_6\text{H}_5$) the magnitude and direction of the concentration dependence of $\delta(^{205}\text{Tl})$ varies with the anion and solvent. Concentration induced changes in $\delta(^{205}\text{Tl})$ were within the range 0-14ppm, except for $(\text{CH}_3)_2\text{TlI}$ in DMSO where a change of 50ppm was noted, for changes in the concentration range $0.2\text{--}1.0\text{mol dm}^{-3}$ in $\text{H}_2\text{O}(\text{NO}_3 \text{ only})$, DMSO, pyridine ($\text{NO}_3, \text{OC}_6\text{H}_5$) and $\text{CH}_2\text{Cl}_2(\text{OC}_6\text{H}_5 \text{ only})$.

It has been proposed for $(\text{CH}_3)_2\text{TlX}$ that concentration dependent variations in $\delta(^{205}\text{Tl})$ originate primarily from changes in the degree of contact ion-pair formation between $(\text{CH}_3)_2\text{Tl}^+$ and X^- and/or the average number of anions and solvent molecules surrounding the cation or ion-pair.^{16,18,23} The virtual concentration independence of $\delta(^{205}\text{Tl})$ for $(\text{CH}_3)_2\text{TlNO}_3$ in H_2O has been attributed to complete dissociation of the compound in this solvent and the formation of an undisturbed first solvation sphere for $(\text{CH}_3)_2\text{Tl}^+$.

The thallium chemical shift is also known to be temperature dependent in organothallium(III) derivatives R_2TlX , ($\text{R} = \text{CH}_3$; $\text{X} = \text{NO}_3, \text{OCOCH}_3, \text{BF}_4$; $\text{R} = \text{CH}_3(\text{CH}_2)_n$ ($n=1\text{--}5$), $\text{X} = \text{NO}_3$). The temperature coefficients were less than 0.7 ppm per degree in all cases.²³

To minimise the effects of concentration and temperature dependence of $\delta(^{205}\text{Tl})$ in the present study concentrations were kept in the range $0.1\text{--}0.3\text{mol dm}^{-3}$ as far as possible and temperatures in the range $30 \pm 3^\circ\text{C}$. Based on the behaviour of $(\text{CH}_3)_2\text{TlX}$ compounds^{16,23} this would be expected to give rise to variations in $\delta(^{205}\text{Tl})$ of $< \pm 5\text{ppm}$.

3.2.4. The effect of the solvent

It was not the intention of this study to make a detailed examination of the solvent dependence of $\delta(^{205}\text{Tl})$. This has already been studied by Burke¹⁸ who found a shift range of 227ppm for $(\text{CH}_3)_2\text{TlBF}_4$, in a variety of solvents. However many compounds were investigated in several solvents (usually pyridine and DMSO) to give some idea of likely solvent induced variations.

The largest solvent induced shift was a shielding of 160ppm for bis(neopentyl)isobutyrate thallium(III) (Table 3.2) on going from chloroform to pyridine. On changing the solvent from pyridine to DMSO for R_2TlX compounds (Tables 3.1 to 3.5) thallium shielding is increased by 2-137 ppm, for all classes of compounds. Burke et al¹⁶ noted increased shielding of 26-68 ppm for the same solvent change for $(\text{CH}_3)_2\text{TlX}$ ($\text{X}=\text{I}, \text{OC}_6\text{H}_5$), although a decreased shielding of 5-23ppm was found for $\text{X}=\text{NO}_3$. Koppell et al¹³ observed an increase in thallium shielding of 132 ppm for R_2TlBr ($\text{R}=\text{n-propyl}$) for the solvent change pyridine to DMSO. Changing from chloroform to DMSO also results in increased shielding of ^{205}Tl of 89ppm for R_2TlX and 17-27ppm in the case of RTlX_2 .

However $\text{CH}_3\text{Tl}(\text{OCOCH}_3)_2$ appears to behave anomalously if the reported value¹² for a CHCl_3 solution, $\Xi(^{205}\text{Tl}) = 57861186 \text{ Hz}$ is compared with the value obtained here in DMSO, giving a decrease in thallium shielding of 112 ppm. Increases in shielding of 10-160ppm are observed for the solvent change chloroform to pyridine in R_2TlX compounds, except, $\text{CH}_3\text{CH}(\text{OCH}_3)\text{CH}_2(\text{CH}_3)\text{TlOCOCH}_3$ where a decrease of 25ppm is observed. The monoorganothallium(III) carboxylates similarly show decreases in shielding of 11-82ppm for the same solvent

change, except in the case of the ethyl derivative which shows an increase of 16ppm.

These solvent induced changes are much smaller than those found for Tl(I) compounds²⁷(ca.2600ppm) but larger than the solvent dependent shift ranges of some other metal nuclei, (eg. ^7Li ²²¹(ca. 6ppm), ^{23}Na ²²² (ca. 25 ppm)).

The solvating ability of a solvent may be expressed by means of the Gutmann donor number²²³(D.N.), defined as the enthalpy of formation of the antimony(v)chloride complex with the solvent molecule, the reaction taking place in 1,2-dichloroethane solution. The thallium chemical shifts for solutions of $(\text{C}_6\text{F}_5)_2\text{TlBr}$ in benzene(D.N. 0.1), acetone (D.N. 17.0), methanol(D.N. 23.5) and pyridine (D.N. 33.1) show a trend of increased thallium shielding with increasing solvent donor number for the limited data. Linear regression analysis gave a correlation coefficient $r=0.98$ and the relationship (Equation 3.10):

$$\delta(^{205}\text{Tl}) = -251 + (-5.1 \times \text{D.N.}) \pm 18. \quad (3.10)$$

This trend is in the opposite sense to that found for Tl(I) compounds where increase in

solvent donor number is accompanied by a decrease in shielding.²⁷⁻²⁹ The latter correlation has also been found for infinite dilution shifts of $^{23}\text{Na}^+$ ²²⁴, Cs^+ ²²⁵ and K^+ ²²⁶ and has been rationalised in terms of increased solvent interaction causing a reduction in ΔE and hence a shift to higher frequency.

The decreased shielding shown by some carboxylates RTlX_2 on going from chloroform to pyridine may be due to preservation of the high coordination number of thallium, found in the solid state,²²⁷ in chloroform solution. (see

Chapter 6). Pyridine may be more efficient in causing cleavage of the oligomeric species.

One view of the bonding in the essentially linear R_2Tl^+ unit is that thallium is bonded to the organo groups by predominantly sp hybrid orbitals.⁸⁶ The term Pu (Equation 3.9) has its maximum value which occurs when one p-orbital is filled and two are empty,²¹⁸ in the hypothetical 'unsolvated' or 'free' ion $(CH_3)_2Tl^+$. Increasing coordination of the cation by solvent molecules, as might be expected to occur in going from chloroform to pyridine to DMSO, would be expected to decrease the imbalance of the p-orbitals by increasing donation of electron density into the empty p-orbitals on thallium. This would lead to a lower value of Pu and hence to an increase in thallium shielding, as was observed for these solvents.

An alternative rationalisation of solvent induced changes in $\delta(^{205}Tl)$ involves the role of d orbitals. The role of thallium d orbitals in bonding with the alkyl carbons in these compounds has not been established. Shier and Drago¹⁰³ invoked their use in a model bonding scheme to explain the solvent dependence of $^2J(Tl-H)$ for solutions of Me_2TlClO_4 . They proposed that the $5d_z^2$ and 6s orbitals are mixed, producing two hybrid orbitals, directed along the z axis towards the carbon atoms and in the xy plane respectively. They proposed that the strength of solvent interaction in the xy plane determines the extent of orbital mixing such that increasing interaction increases the s-character in the Tl-C bonds and causes an increase in $^2J(Tl-H)$. By analogy, increased solvent interaction might be expected to reduce the Du term with consequent increased shielding

of thallium. Consequently we might expect a correlation between $\delta(^{205}\text{Tl})$ and coupling between the organo group and thallium.

The use of $^2J(\text{Tl-H})$ as an indication of the s-character in the Tl-C bond as proposed by Shier and Drago¹⁰³ does not appear to support their model. Thallium shielding increases, while $^2J(\text{Tl-H})$ becomes more negative for the solvent change pyridine to DMSO for R_2TlX , $\text{R}=(\text{CH}_3)_2\text{CH}$, $(\text{CH}_3)_2\text{CHCH}_2$; $\text{X}=\text{Cl}$ (Table 3.2); $\text{R}=(\text{CH}_2)_2\text{CH}$; $\text{X}=\text{Br}$ (Table 3.3).

$^1J(\text{Tl-C})$, which is expected to give a more reliable indication of the s-character in the Tl-C bond than $^2J(\text{Tl-H})$, (See Chapter 4), can be compared with variation in $\delta(^{205}\text{Tl})$ for the solvent change pyridine to DMSO in the following four cases. While thallium shielding increases in each case, $^1J(\text{Tl-C})$ does not change in the $[(\text{CH}_3)_2\text{CH}]_2\text{TlCl}$ compound (Table 4.2), shows a decrease in $[\text{cyclo-C}_6\text{H}_{13}\text{CH}_2]_2\text{TlBr}$ (Table 4.3) and increases for $[(\text{CH}_2)_2\text{CH}]_2\text{TlBr}$ (Table 4.3) and $[\text{H}_2\text{C}=\text{C}(\text{CH}_3)]_2\text{TlBr}$ (Table 4.4). In this series steric effects and/or changes in ΔE , and hybridisation at the carbon atom bonded to Tl may be equally or more important however. This serves to emphasise the problems associated with attempting to isolate individual factors influencing the chemical shifts of these compounds.

Studies of the solvent dependence of the shifts for other nuclei in organometallic compounds reveal a similar pattern to that observed here for R_2TlX derivatives.

In organomercury derivatives ^{199}Hg is shifted to low frequency with accompanying increases in $^1J(\text{Hg-C})$ and $^2J(\text{Hg-H})$ as solvent donicity increases.^{228,229} In both $(\text{CH}_3)_2\text{Hg}$ and $(\text{CH}_3)\text{HgCl}$, ^{199}Hg is more shielded in DMSO

than in pyridine. Mitchell²³⁰ observed that the shielding of ^{119}Sn and ^{207}Pb in organoderivatives increase as the donor capacity of the solvent increases. Addition of DMSO to solutions of $(\text{CH}_3)_3\text{PbX}$ ($\text{X} = \text{Cl}, \text{Br}$) in CH_2Cl_2 produces increased shielding of ^{207}Pb up to 270 ppm, attributed to increased coordination at lead.²³¹ Similar changes are observed on adding pyridine to $(\text{CH}_3)_3\text{SnCl}$ in CCl_4 ,²¹⁵ and the ^{119}Sn chemical shift of $(\text{CH}_3)_2\text{SnCl}_2$ in DMSO is almost 400ppm to low frequency of that in CH_2Cl_2 .²³²

3.2.5. The effect of the anion

This study was not extensive regarding the effect of anion on $\delta(^{205}\text{Tl})$ in R_2TlX and RTlX_2 compounds. However several anions were used, mainly as a means of extending and/or enhancing the solubilities of the organothallium(III) compounds.

Anion induced changes in $\delta(^{205}\text{Tl})$ appear to be roughly of the same order of magnitude as solvent shifts, for the compounds and solvents studied here. The largest anion induced change was an increase in shielding of 232ppm for the change $(\text{C}_6\text{H}_5)_2\text{TlCl}$ to $(\text{C}_6\text{H}_5)_2\text{TlNO}_3$ in DMSO (Table 3.5). The anion change, halide to carboxylate, generally results in increased thallium shielding for R_2TlX derivatives.

Replacement of bromide ion by isobutyrate in pyridine causes an increase in thallium shielding of 21-197ppm. Similarly the change from chloride to isobutyrate in the same solvent causes an increase of 119-192 ppm. Increases in thallium shielding are also observed for R_2TlX compounds for the following changes; $\text{R} = \text{C}_6\text{H}_5$; $\text{X} = \text{Cl}$ to $\text{X} = \text{OCOCH}_3$ in DMSO (135ppm). $\text{R} = (\text{CH}_3)_3\text{CCH}_2$; $\text{X} = \text{Cl}$ to $\text{X} = \text{OCOCH}(\text{CH}_3)_2$ in chloroform (122ppm). $\text{R} = \text{H}_2\text{C}=\text{CH}$; $\text{X} = \text{BF}_4$ to $\text{X} = \text{OCOCH}_3$

in DMSO (15ppm). However for R_2TlX the change $X = NO_3$ to $X = \text{carboxylate}$ results in deshielding of thallium of 163ppm for $R = CH_3CH_2$, $X = OCOCH(CH_3)_2$. Similarly for $R = C_6H_5$ and $X = OCOCH_3$ the deshielding is 87ppm. The order of thallium shielding in arylthallium(III) compounds R_2TlX in DMSO is $Br < Cl < OCOCH_3 < NO_3$. (Table 3.5).

It seems likely that the general order of thallium shielding observed for compounds studied here; halide < carboxylate < nitrate, reflects the decreasing ionic character of the thallium-anion bonding interaction for the change nitrate to halide. Burke¹⁶ reports the same shielding order for $(CH_3)_2TlX$ ($X = I, OCOCH_3, NO_3$) in DMSO. Previous studies of $\delta(^{205}Tl)$ in $(CH_3)_2TlX$ compounds in DMSO¹³ reveal that the order of increasing thallium shielding was $I < Br < F < NO_3$. It was proposed that this reflected the degree of covalency in thallium-anion bonds, with increased covalency resulting in shifts to higher frequency.

3.2.6. The effect of the organo group

3.2.6.1. Alkyl derivatives

The previously reported values of $\delta(^{205}Tl)$ for $(CH_3)_2TlNO_3$ in DMSO at 29°C (-91ppm)¹⁶ and for $(CH_3CH_2)_2TlNO_3$ in DMSO at 24°C (-302 ppm)¹³ are close to the values reported here (Table 3.1). However there is a discrepancy of 45ppm between the reported value of -255ppm¹³ for $(CH_3CH_2CH_2)_2TlNO_3$ in DMSO at 24°C and the value of -207ppm found here. (Table 3.1)

The order of increasing thallium shielding for n-alkyl derivatives R_2TlNO_3 in DMSO (Table 3.1) is:- methyl < n-butyl < n-pentyl < n-propyl < n-hexyl < ethyl. Shielding in branched chain compounds R_2TlX ($X = Br, Cl$) in pyridine

(Table 3.2) increases in the order:- trimethylsilylmethyl < cyclohexylmethyl < neo-pentyl < iso-butyl < ethyl < sec-amyl < sec-butyl < iso-propyl. Substitution of a proton in the methyl derivative $(\text{CH}_3)_2\text{TlNO}_3$ to give $(\text{CH}_3\text{CH}_2)_2\text{TlNO}_3$ in DMSO results in an increase in shielding for ^{205}Tl of 216ppm. Further substitution for H at the α -carbon of $(\text{CH}_3\text{CH}_2)_2\text{TlBr}$ in pyridine to give $[(\text{CH}_3)_2\text{CH}]_2\text{TlCl}$ causes a further shielding increase of 162ppm (pyr) substitution of the α -carbon of $(\text{CH}_3\text{CH}_2)_2\text{TlBr}$ to give $[\text{CH}_3\text{CH}_2(\text{CH}_3)\text{CH}]_2\text{TlCl}$ and $[\text{CH}_3\text{CH}_2\text{CH}_2(\text{CH}_3)\text{CH}]_2\text{TlCl}$ similarly results in increased shielding of thallium.

The Taft σ^* constant²³³ is a measure of the inductive effect of an organo group. Values for a number of organo groups are given in Table 3.7. The Taft σ^* constants indicate that the +I effect of the alkyl groups increases in the order: methyl < ethyl < iso-propyl < sec-butyl. Increasing +I would be expected to reduce Z_{eff} and lead to increased thallium shielding. We might expect this to be reflected in the order of shielding if $\delta(^{205}\text{Tl})$ was largely dependent on alkyl group inductive effects. However it is seen that the sec-butyl derivative is less shielded than expected on this basis. Examination of the E_s values (E_s value is a measure of the steric effect of an organo group) (Table 3.7) for the alkyl groups reveals that the value for sec-butyl is larger than for methyl, ethyl or iso-propyl. It would appear that the increasing steric effect of the alkyl group is causing a deshielding of thallium which is of greater magnitude than the shielding effect of the +I inductive effect. Further support for this can be found in the following observations. On the basis of σ^* values increased shielding of

TABLE 3.7

Taft's σ^* constants and steric parameters, E_s , for various
organo groups R^a

<u>R</u>	<u>σ^*</u>	<u>E_s</u>
<u>Alkyls</u>		
CH_3	0.000	0.0
CH_3CH_2	-0.100	-0.07
$\text{CH}_3\text{CH}_2\text{CH}_2$	-0.115	-0.36
$(\text{CH}_3)_2\text{CH}$	-0.19	-0.47
$\text{CH}_3\text{CH}_2\text{CH}_2\text{CH}_2$	-0.130	-0.39
$(\text{CH}_3)_2\text{CHCH}_2$	-0.125	-0.93
$(\text{CH}_3)_3\text{C}$	-0.36	-1.54
$\text{CH}_3\text{CH}_2(\text{CH}_3)\text{CH}$	-0.21	-1.13
$\text{CH}_3\text{CH}_2\text{CH}_2\text{CH}_2\text{CH}_2$	-0.16	-0.40
$(\text{CH}_3)_3\text{CCH}_2$	-0.165	-1.74
$(\text{CH}_3)\text{SiCH}_2$	-0.26	-
$\text{CH}_3\text{CH}_2\text{CH}_2\text{CH}_2\text{CH}_2\text{CH}_2$	-0.16	-
cyclo- $\text{C}_6\text{H}_{13}\text{CH}_2$	-0.06	-0.98
<u>Alicyclics</u>		
C_5H_9	-0.20	-0.51
C_6H_{11}	-0.20	-0.79
C_7H_{13}	-	-1.10
<u>Alkenyls and aryls</u>		
$\text{H}_2\text{C}=\text{CH}$	0.62	-
<u>trans</u> $(\text{CH}_3)\text{HC}=\text{CH}$	0.36	-
<u>cis</u> $(\text{CH}_3)\text{HC}=\text{CH}$	0.36	-
<u>trans</u> $(\text{C}_6\text{H}_5)\text{HC}=\text{CH}$	0.41	-
C_6H_5	0.6	-

^aData from ref. 233.

^{205}Tl might be expected in R_2TlX for the changes, $\text{R}=\text{ethyl} \rightarrow \text{n-propyl} \rightarrow \text{iso-butyl}$. Shifts to higher frequencies are in fact observed as the E_s values for the groups increase. A similar argument can be applied in the case of $[\text{cyclo-C}_6\text{H}_{11}\text{CH}_2]_2\text{TlBr}$ where the σ^* value of -0.06 and E_s of -0.98 result in a large deshielding.

The relative order of $(\text{CH}_3)_3\text{CCH}_2$ shielding can also be rationalised on the basis that the σ^* value (-0.165) might suggest greater shielding than for $(\text{CH}_3)_2\text{CHCH}_2$ ($\sigma^* -0.125$); however the E_s value (-1.74) for the former group causes a larger deshielding compared to $(\text{CH}_3)_2\text{CHCH}_2$ ($E_s -0.93$).

Thus it would appear that a combination of electronic and steric effects of the organo group can be used to explain the observed variations in $\delta(^{205}\text{Tl})$ in these compounds. This would explain why no correlation between $\delta(^{205}\text{Tl})$ and $\sigma^*(\text{R})$ could be found. Such correlations between $\delta(^{119}\text{Sn})$ and $\sigma^*(\text{R})$ have been reported for derivatives of the types, R_4Sn , R_3SnX , R_2SnX_2 ²¹⁵ ($\text{R} = \text{alkyl}$; $\text{X} = \text{anion}$). However Mitchell²³⁴ reported that for $\text{R}_3\text{Sn-SnR}_3$ compounds $\delta(^{119}\text{Sn})$ could not be correlated with $\sigma^*(\text{R})$ although a trend of decreasing tin shielding with decreasing electronegativity of R was observed. Kennedy²³¹ suggested some correlation of $\sigma^*(\text{R})$ with $\delta(^{207}\text{Pb})$ in $(\text{CH}_3)_3\text{PbSR}$ but noted that β and γ substituent effects in R might affect $\delta(^{207}\text{Pb})$ in some way not yet understood. A correlation of $\delta(^{77}\text{Se})$ with $\sigma^*(\text{R})$ has been reported for some organoselenium derivatives in which each organo group makes additive contributions to $\delta(^{77}\text{Se})$ depending on the amount of α chain branching.²³⁵

Multiple regression analysis²³⁶ of the $\delta(^{205}\text{Tl})$, σ^* and E_s data for R_2TlX (R = cyclohexylmethyl, neo-pentyl, iso-butyl, ethyl, iso-propyl, methyl¹⁶; X = halide), derivatives in pyridine solution gave a multiple correlation coefficient $R_m = 0.94$ with the average % relative contributions of σ^* and E_s to $\delta(^{205}\text{Tl})$ as 52 and 48 respectively. (Equation 3.11)

$$\delta(^{205}\text{Tl}) = 191 + (1551 \times \sigma^*) + (-145 \times E_s) \text{ error } \pm 51 \quad (3.11)$$

For R_2TlX in DMSO solution (R = cyclohexylmethyl, iso-butyl, n-propyl, ethyl iso-propyl; X = halide) $R_m = 0.94$ with % relative contributions 63(σ^*) and 37(E_s), (Equation 3.12)

$$\delta(^{205}\text{Tl}) = 127 + (1879 \times \sigma^*) + (-148 \times E_s) \text{ error } \pm 53. \quad (3.12)$$

In the case of R_2TlNO_3 in DMSO (R = methyl, n-butyl, n-pentyl, n-propyl, ethyl) $R_m = 0.91$ and % relative contributions are 56(σ^*) and 44(E_s) (Equation 3.13)

$$\delta(^{205}\text{Tl}) = -105 + (2193 \times \sigma^*) + (-545 \times E_s) \text{ error } \pm 46 \quad (3.13)$$

Previously published values of $\delta(^{199}\text{Hg})$ for R_2Hg ²³⁷, (R = methyl, neo-pentyl, n-butyl, n-propyl, ethyl, iso-propyl, tert-butyl) may be analysed in the same way as described for thallium derivatives and give $R_m = 0.97$ with % relative contributions to $\delta(^{199}\text{Hg})$ of 70(σ^*) and 30(E_s), (Equation 3.14);

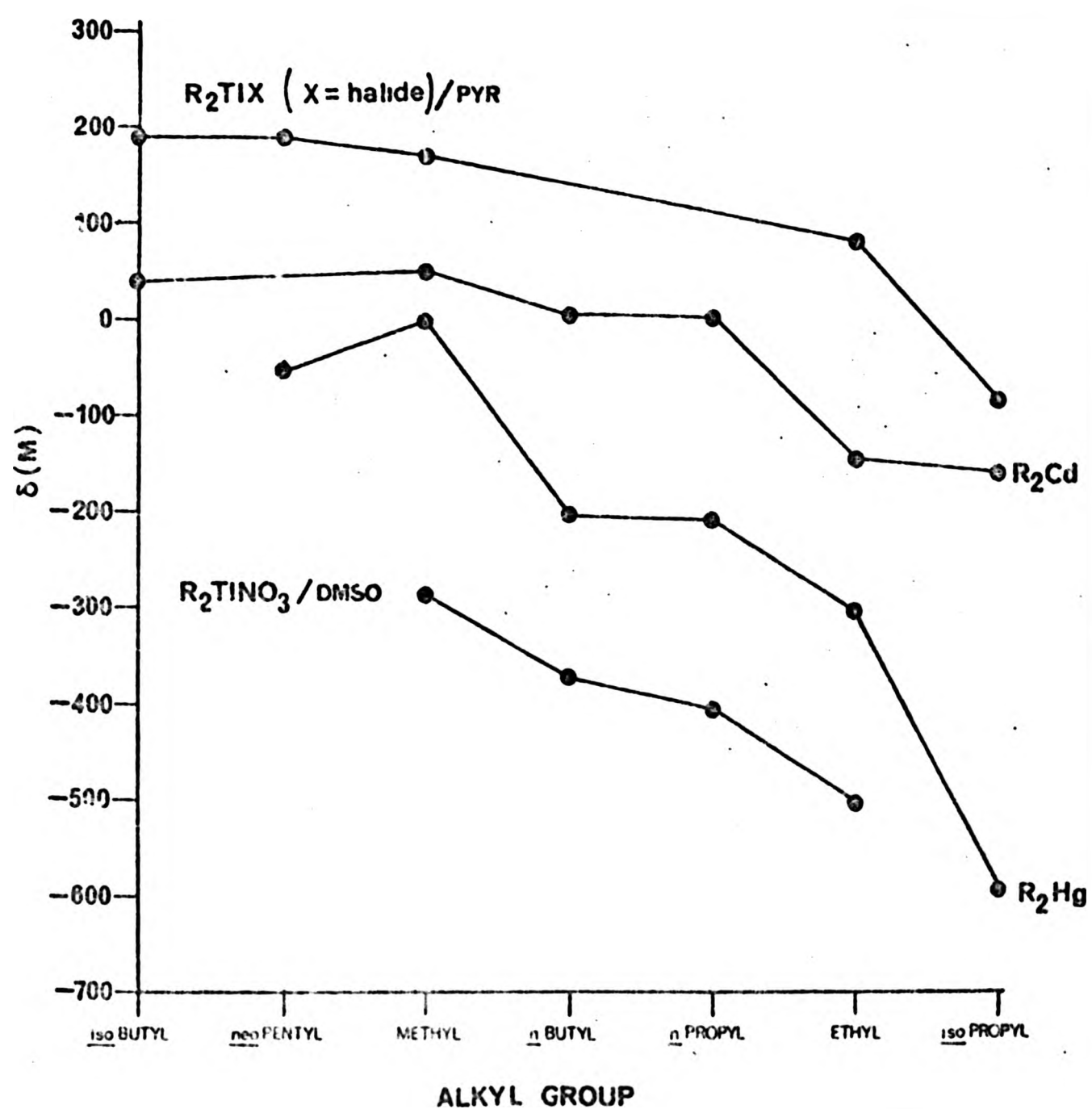
$$\delta(^{199}\text{Hg}) = 33 + (3429 \times \sigma^*) + (-228 \times E_s) \text{ error } \pm 91 \quad (3.14)$$

Similar analysis of $\delta(^{113}\text{Cd})$ data for R_2Cd derivatives²³⁷ carried out here gave a rather poorer correlation of $R_m = 0.88$.

A diagram showing the variation of $\delta(\text{M})$, (M = ^{205}Tl , ^{199}Hg ,²³⁷, ^{113}Cd ²³⁷) with different alkyl groups in R_2M derivatives is shown in FIG 3.4. In order to ensure separation

FIG. 3.4.

VARIATION OF $\delta(M)$; $M = {}^{205}\text{Ti}, {}^{199}\text{Hg}, {}^{113}\text{Cd}$, WITH ALKYL GROUP
FOR DIALKYL METAL COMPOUNDS



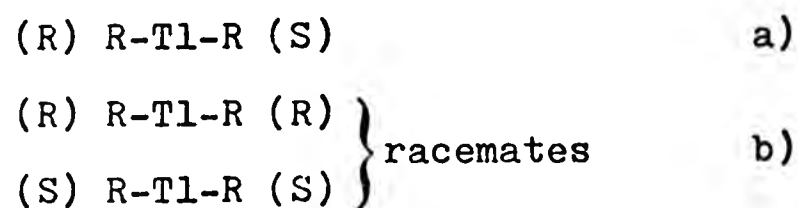
of the plots, for clarity, 50ppm was arbitrarily added to all the $\delta(^{113}\text{Cd})$ values and -200ppm was added to $\delta(^{205}\text{Tl})$ for R_2TlNO_3 in DMSO. The alkyl groups are arranged in order of increasing thallium shielding. Broadly similar trends in shielding can be seen for all three metals on changing the alkyl groups. Mercury is more shielded in $[(\text{CH}_3)_3\text{C}]_2\text{Hg}$ (not shown in FIG 3.4) than in $[(\text{CH}_3)_2\text{CH}]_2\text{Hg}$.²³⁸ This large shielding of the tert-butyl derivative might be predicted on the basis of the σ^* value (-0.36) for this group although the steric factor $E_s = -1.54$ (Table 3.7). is large.

Several authors have noted variations in metal shielding in organometallic derivatives with the amount of substitution at α , β or γ carbon atoms in the alkyl groups. However there have been no previous attempts to quantify the correlation of $\delta(\text{M})$ with electronic (σ^*) and steric (E_s) factors in these compounds. The correlations found here may help explain their observations. Dessey et al²³⁹ found an empirical correlation between $\delta(^{199}\text{Hg})$ and the number of protons on the β -carbon atom in R_2Hg . Turner and White²³⁷ found approximately additive effects on $\delta(^{199}\text{Hg})$ and $\delta(^{113}\text{Cd})$ on substituting methyl groups for protons at the α , β and γ carbon atoms respectively. (See FIG. 3.4). Increased shielding on α substitution can be found for alkyl derivatives of Sn^{214} and Pb^{240} ; however Turner and White²³⁷ could find little regularity in shielding changes induced by β or γ substitution for either Sn , Pb or other elements. Burke²⁴¹ reported that replacement of protons on the α carbon; in Tl(I)alkoxides , TlOR ($\text{R} = \text{alkyl}$), with alkyl groups results in a decrease in thallium shielding of 71-169ppm, whereas substitution at the β carbon increases it by 37-84ppm. It is interesting that substitution at the

α -carbon in the alkoxides, which corresponds to the β carbon in R_2TlX (i.e. two bonds removed from Tl), causes a shielding change in the same direction for both classes of compounds. Multiple regression analysis carried out here for the alkoxide data²⁴¹ revealed no correlation between $\delta(^{205}Tl)$, σ^* and E_s however.

The reasons for the apparent dependence of $\delta(^{205}Tl)$ on steric effects in the alkyl group are unclear at present. Klose^{241a} proposed that the CH_3 and CH_2 protons of an ethyl group interact significantly with the heavy metal to which it is bonded. This interaction might affect the electron density distribution around the metal and consequently influence the paramagnetic contribution to the metal shielding. Replacement of a proton by an alkyl group will give rise to a shielding change which does not necessarily bear a simple relationship to variations of electron density produced by inductive effects, and which varies from one element to another.²³⁷

The sensitivity of the thallium shielding to the stereochemistry of the alkyl group in R_2TlX derivatives is clearly illustrated in the cases where $R = CH_3CH_2(CH_3)^*CH$ and $CH_3CH_2CH_2(CH_3)^*CH$; $X = Cl$ (Table 3.2). The presence of a chiral centre(*) bonded to thallium gives rise to the diastereoisomeric species a) and b):-



The configuration of each alkyl group R is given in parenthesis.

Two signals are observed in the ^{205}Tl spectra of these compounds (FIG 3.5), corresponding to a) and b). Shielding differences of ca. 1ppm for the sec-butyl and ca. 2ppm for the sec-amyl compounds were observed (Table 3.2).

Separate ^{119}Sn resonances have been noted for the diastereoisomers present in R_4Sn and $\text{R}_3\text{SnR}'$ ($\text{R} = \text{CH}_3\text{CH}_2(\text{CH}_3)^*\text{CH}$; $\text{R}' =$ branched alkyl with no chiral centre) ²⁴².

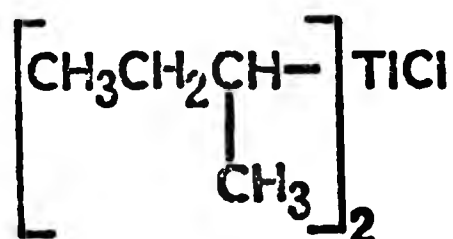
The compound $\text{CH}_3^*\text{CH}(\text{OCH}_3)\text{CH}_2(\text{CH}_3)\text{TlOCOCH}_3$ contains only one chiral centre (*). In solution both enantiomers are present and give rise to only one signal in the ^{205}Tl spectrum. An attempt was made to resolve the signals due to the optical isomers using the chiral shift reagent tris(D-3-heptafluorobutyrylcamphorato)europium. However addition of this reagent to a chloroform solution of the $\text{R}_2\text{TlOCOCH}_3$ compound caused the ^{205}Tl resonance to become so broad as to be undetectable, presumably due to alteration of the ^{205}Tl relaxation rates.

Molecular weight determinations ¹⁴⁷ have shown that the compounds R_2TlCl ($\text{R} =$ neo-pentyl, trimethylsilylmethyl) are dimeric in chloroform solution. The latter compound is also shown to be dimeric in the solid state (Chapter 6). It is interesting to note the large deshielding of thallium in these compounds (Table 3.2). High frequency (relative to $(\text{CH}_3)_2\text{TlNO}_3$ in H_2O) resonances have previously been reported for the dimeric derivatives $\{(\text{CH}_3)_2\text{TlX}\}_2$ $\text{X} = \text{OC}_2\text{H}_5$, ¹³ $\text{N}(\text{CH}_3)_2$ ¹³ ($\delta(^{205}\text{Tl}) = 141\text{--}510\text{ppm}$). In the latter cases the presence of dimeric species was confirmed by observation of $J(^{203}\text{Tl}\text{--}^{205}\text{Tl})$. The compound, $\text{X} = \text{OC}_6\text{H}_5$, known to be dimeric in benzene, ¹⁰⁷ and shown by Burke et al ⁶² to be dimeric in the solid state, gives rise to thallium resonances at high frequencies, especially in CH_2Cl_2 ($\delta(^{205}\text{Tl}) = 220\text{ ppm}$)

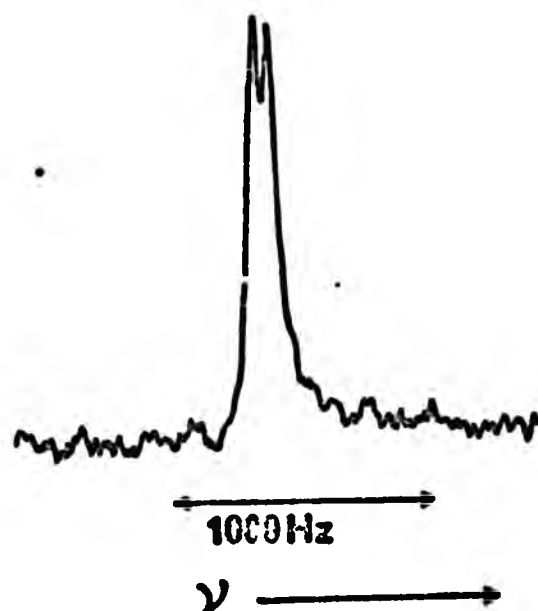
BROAD BAND PROTON DECOUPLED ^{205}TI SPECTRUM

AT 34.7MHz OF

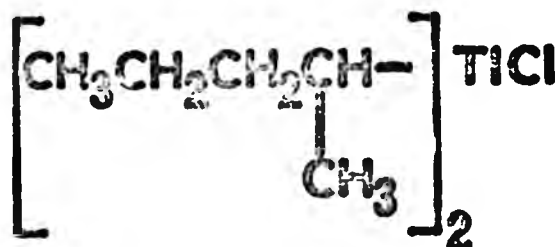
a)

0.12 mol dm⁻³IN DMSO d₆

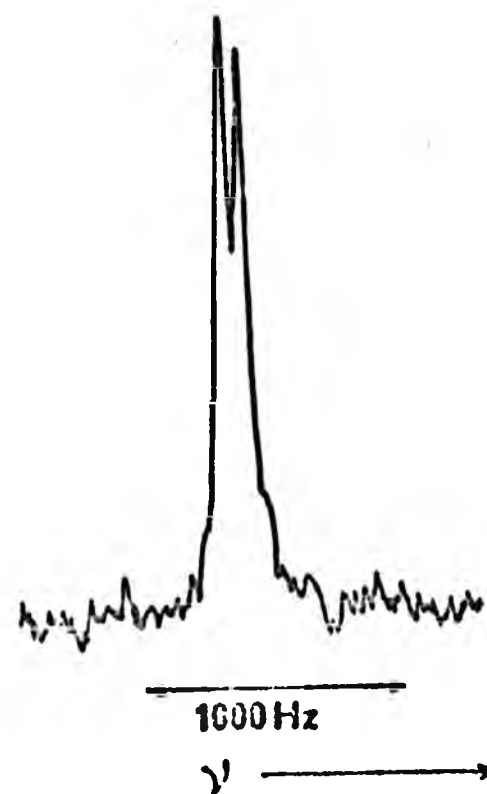
No. of data points = 8192
 No. of pulses = 2000
 Pulse length = 57 μs
 Filter = 5K
 Acq. time = 100 μs
 Delay = 0.09s



b)

0.17 mol dm⁻³IN DMSO d₆

No. of data points = 8192
 No. of pulses = 2500
 Pulse length = 57 μs
 Filter = 5K
 Acq. time = 100 μs
 Delay = 0.09s



and toluene ($\delta(^{205}\text{Tl}) = 204 \text{ ppm}$). Values of $\delta(^{205}\text{Tl})$, (-331 to -934 ppm) reported²⁴¹ for the oligomeric Tl(I) alkoxides, TlOR (R=alkyl group) fall near and extend beyond the high frequency end of the shift range (-606 to -4015 ppm) reported⁸⁵ for Tl(I) compounds.

The coordination number at thallium might be expected to increase on oligomer formation and this appears to be accompanied by a shift of the thallium resonance to a higher frequency. This situation appears to be opposite to that found in organotin derivatives where increased coordination number at tin, resulting from oligomer formation in solution, for R_3SnX and R_2SnX_2 ($\text{X} = \text{Cl}$ ^{243,244}, carboxylate²⁴⁵, alkoxide;²⁴⁶ R = alkyl) results in increased shielding of the tin nucleus compared to cases where the compounds are monomeric.

There were no apparent correlations between $\delta(^{205}\text{Tl})$ and either $\delta(^{13}\text{C}_\alpha)$ or $^1\text{J}(\text{Tl}-\text{C})$ (Tables 4.1, 4.2) for straight-chain or branched chain R_2TlX derivatives. Similarly there appeared to be no correlation between $\delta(^{205}\text{Tl})$ and $\delta(^1\text{H}_\alpha)$ (Table 4.9) for branched-chain alkyls although a trend of $^2\text{J}(\text{Tl}-\text{H})$ becoming more negative as $\delta(^{205}\text{Tl})$ moves to lower frequency was observed, (Table 4.9). Proton NMR parameters for straight chain alkyl derivatives were not examined, except for those reported in Table 4.8.

3.2.6.2. Alicyclic derivatives

Thallium shielding increases with ring size in the sequence cyclopropyl < cyclopentyl < cyclohexyl < cycloheptyl (Table 3.3). (The relative position of the cycloheptyl derivative R_2TlBF_4 , was obtained by assuming that the thallium resonance for this compound in DMSO solution will be to low frequency

of that observed in pyridine by analogy with other systems).

The changes in shielding here are in the opposite sense to those observed for alkyls. Here the thallium resonance shifts to lower frequency as the steric factor E_s (Table 3.7) becomes more negative.

Trends of increasing $^1J(\text{Tl-C})$ (Table 4.3) and $^2J(\text{Tl-H})$ (Table 4.9) with decreased shielding of thallium are noted. Increasing $^1J(\text{Tl-C})$ can be attributed to increasing s-character in the C-Tl bond, (See Chapter 4, equation 4.5) The resulting changes in the thallium bonding orbitals are likely to affect the P_u term in equation 3.9, leading to a decrease in shielding.

Increasing thallium shielding in alicyclic derivatives is accompanied by trends of decreasing shielding for both $\delta(^{13}\text{C}_a)$ (Table 4.3) and $\delta(^1\text{H}_a)$ (Table 4.9) suggesting different factors influence $\delta(^{205}\text{Tl})$.

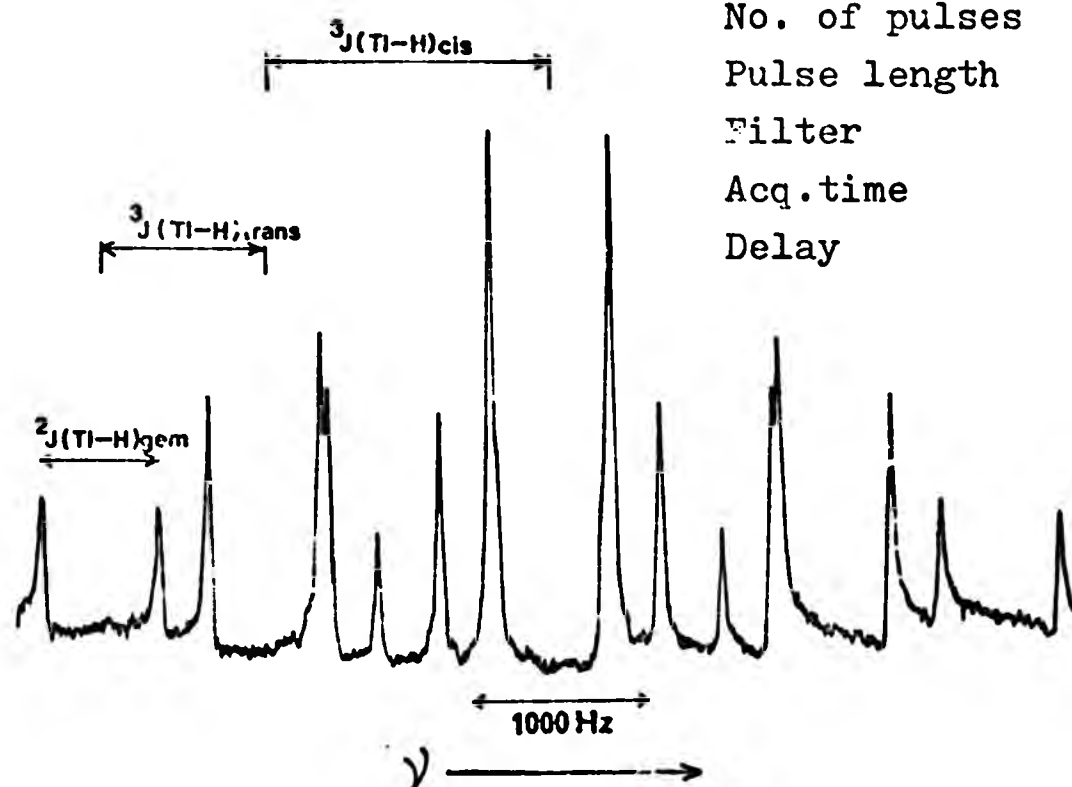
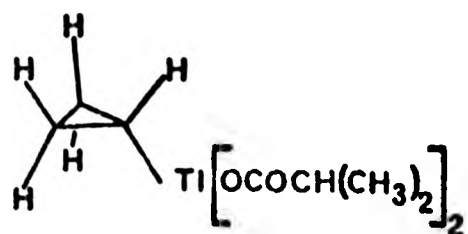
The proton-coupled ^{205}Tl spectra of the cyclopropyl derivatives R_2TlBr and $\text{RTl}[\text{OCOCH}(\text{CH}_3)_2]_2$ are shown in FIG 3.6. First-order analysis of the symmetrical spectrum of the latter yielded values of $^nJ(^{205}\text{Tl-H})$ in DMSO as follows. $^2J(^{205}\text{Tl-H}) = 562\text{Hz}$; $^3J(^{205}\text{Tl-H})_{\text{cis}} = 1328\text{Hz}$; $^3J(\text{Tl-H})_{\text{trans}} = 798\text{Hz}$. The spectrum of $[(\text{CH})_2\text{CH}]_2\text{TlBr}$, although still basically symmetrical, shows some second-order perturbation of the component lines. (See 4.2.2.3. for further discussion of thallium-proton coupling in bis(cyclopropyl)thallium(III)).

The broad-band proton decoupled ^{205}Tl spectra of the five, six and seven membered alicyclic derivatives R_2TlX were generally broad ($V_{\frac{1}{2}} = 300-600\text{Hz}$) (Table 3.3). This may be indicative of conformational changes in the rings. Unfortunately no low temperature studies could be attempted here

FIG 3.6

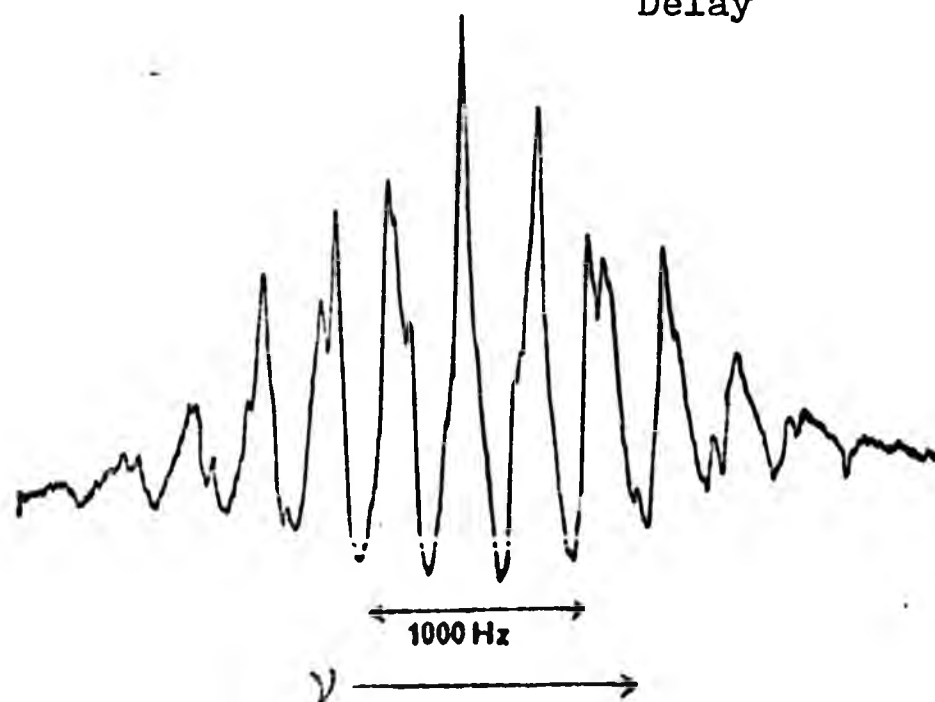
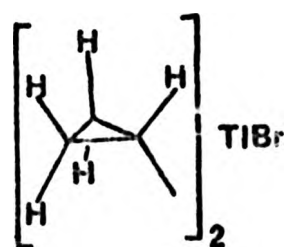
^{205}Ti SPECTRA AT 34.7MHz IN DMSO OF

a)



No. of data points = 8192
 No. of pulses = 10,000
 Pulse length = 30 μs
 Filter = 10K
 Acq. time = 80 μs
 Delay = 0.09s

b)



No. of pulses = 10,000
 Pulse length = 50 μs
 Filter = 10K
 Acq. time = 100 μs
 Delay = 0.09s.

due to the lack of a compound having suitable solubility. Some variable temperature work has been reported for alicyclic derivatives of mercury. Barron et al²⁴⁷ found that cyclohexylmercuric acetate gave a broad signal in the ¹⁹⁹Hg spectrum at ambient temperature. This sharpened considerably on heating to ca.350°K and resolved into two signals, corresponding to the axial and equatorial conformers, at 215°K separated by 77ppm. Due to solubility problems the low temperature ¹⁹⁹Hg spectrum of dicyclohexylmercury²⁴⁸ revealed only two of the expected three signals corresponding to the a,a; e,e; a,e conformers.

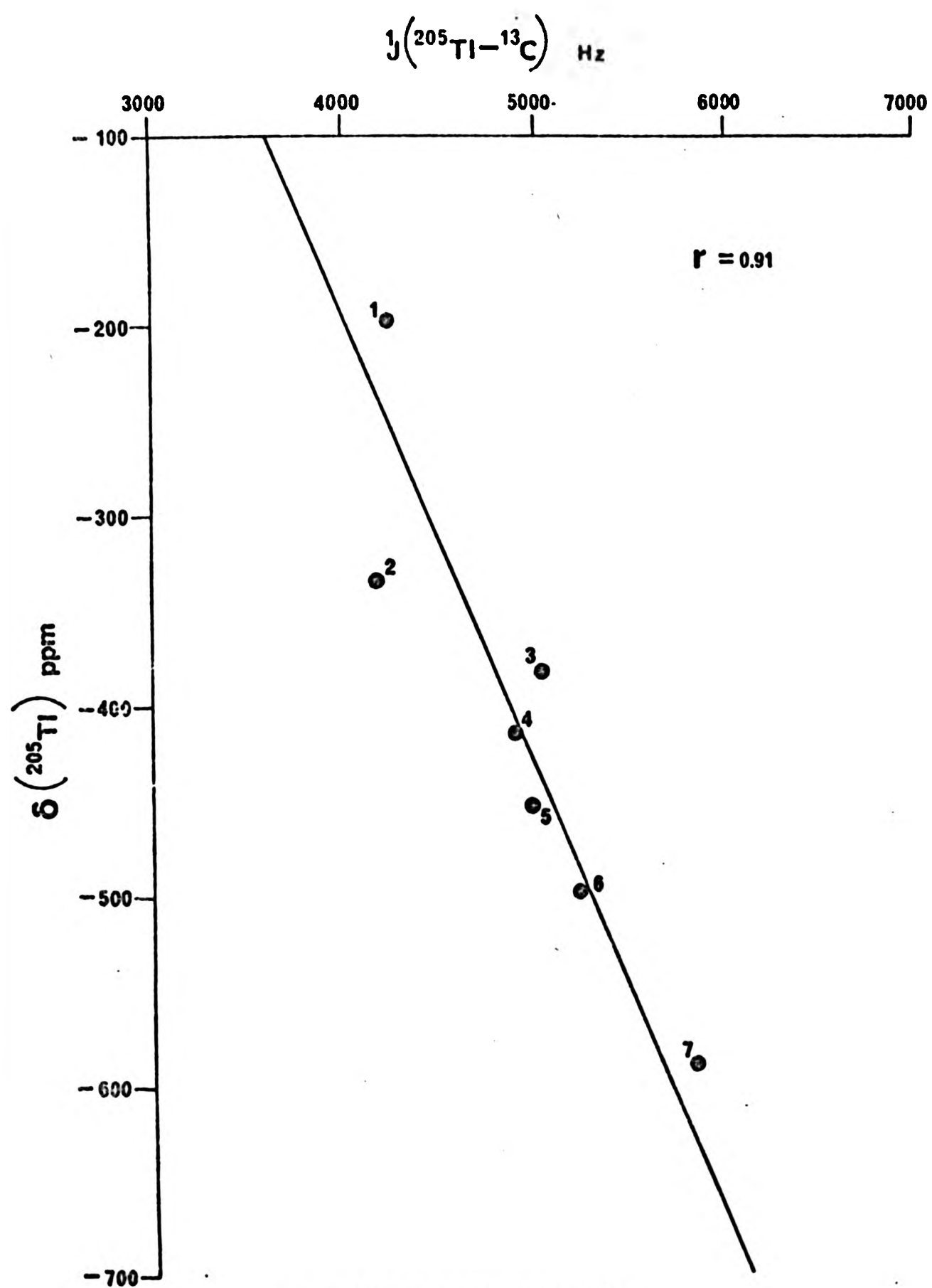
3.2.6.3. Alkenyl derivatives

The order of thallium shielding in alkenyl derivatives (Table 3.4) is difficult to rank in view of the range of anions and solvents involved. A trend of increasing ¹J(Tl-C) (Tables 4.4;4.5) with increasing shielding of thallium in R₂TlX (X = Br, OAc, BF₄, NO₃, Cl) in DMSO and pyridine and RTlX₂ (X = OAc) in DMSO is shown in FIG 3.7. Linear regression analysis gave a correlation coefficient of r = 0.91. Shielding of thallium and ¹J(Tl-C) increase as the electronegativity of the substituent on the β vinyl carbon increases in the series H < CH₃ < C₆H₅ < Cl for the limited data available. Increased shielding of thallium is accompanied by increased shielding of the α-vinyl carbon and linear regression analysis of δ(²⁰⁵Tl) and δ(¹³C_α) (Table 4.4) gave r = 0.92 (See FIG 3.8).

Increased ¹J(Tl-C) can result (See equation 4.5 and discussion in Chapter 4) from either decreases in ΔE, or increases in the s-character of the α-carbon bonded to thallium or the Tl-C bond, or increase in Z_{effective} at thallium.

FIG 3.7

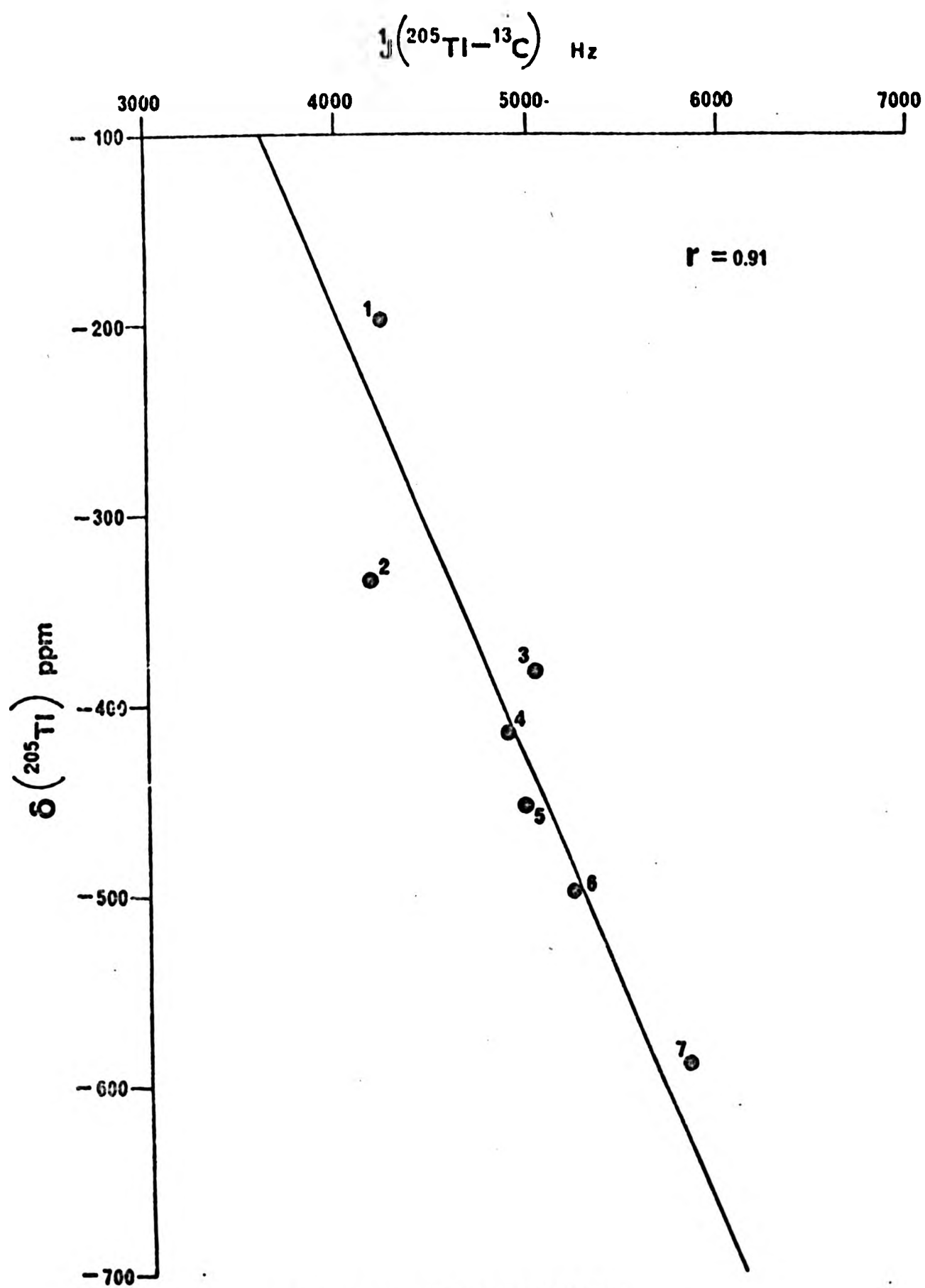
PLOT OF $\delta(^{205}\text{TI})$ AGAINST $J(^{205}\text{TI}-^{13}\text{C})$ FOR ALKENYLTHALLIUM(III) COMPOUNDS



SOLUTIONS NUMBERED AS IN FIG. 3.8.

FIG 3.7

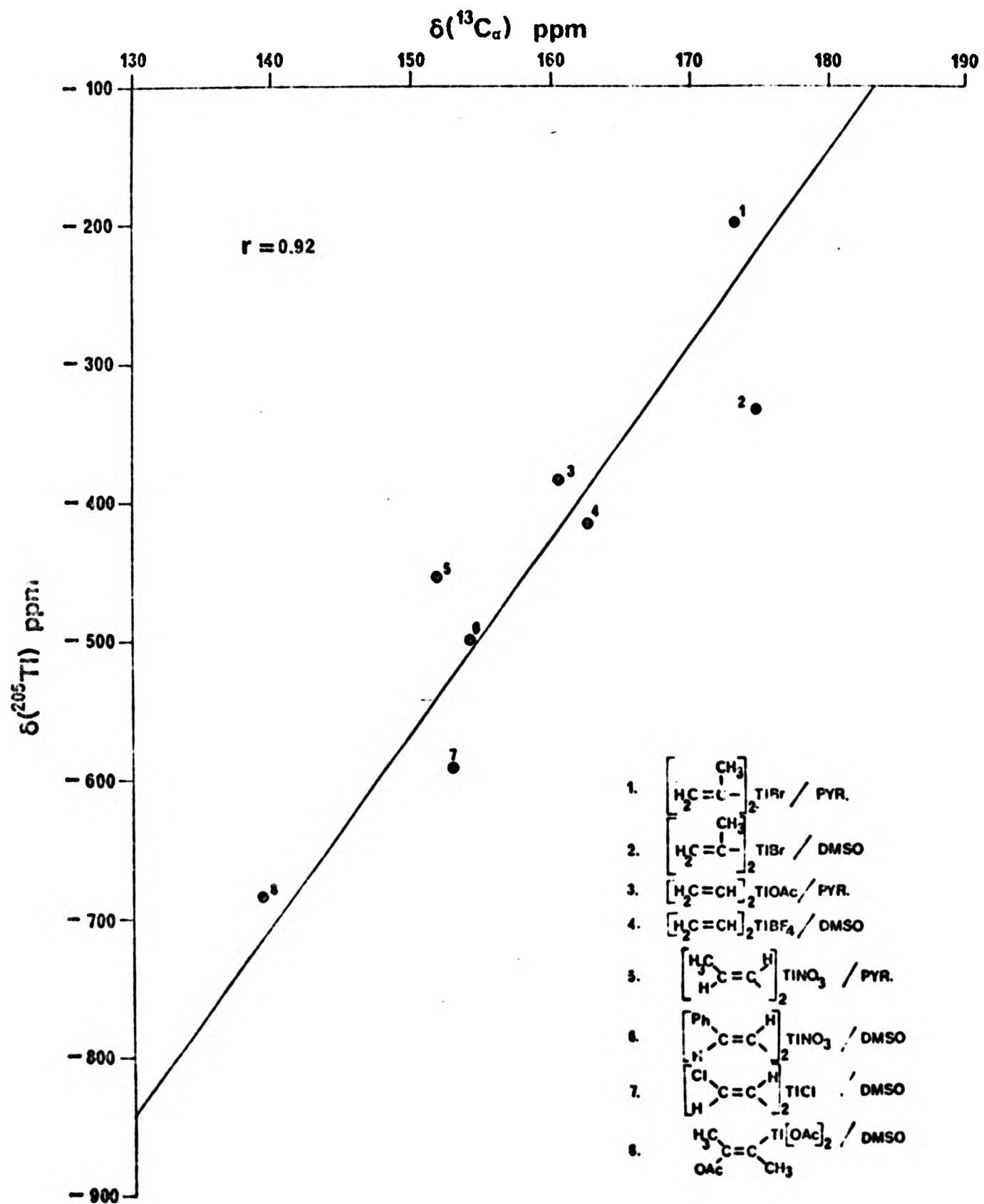
PLOT OF $\delta(^{205}\text{Tl})$ AGAINST $J(^{205}\text{Tl}-^{13}\text{C})$ FOR ALKENYLTHALLIUM(III) COMPOUNDS



SOLUTIONS NUMBERED AS IN FIG. 3.8.

FIG. 3.8

PLOT OF $\delta(^{13}\text{C}_\alpha)$ AGAINST $\delta(^{205}\text{Ti})$ FOR ALKENYLTHALLIUM(III) COMPOUNDS



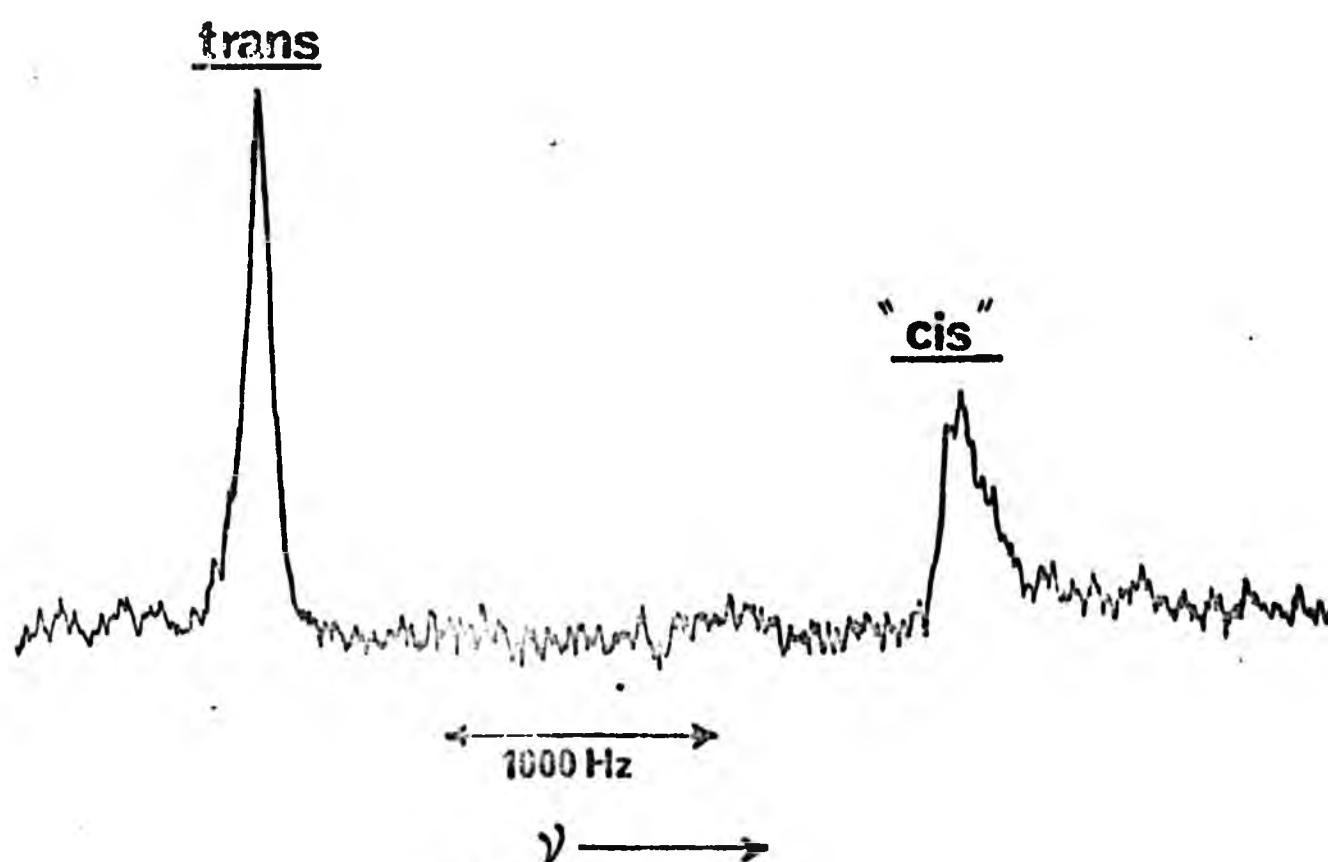
Increased Z_{eff} would however lead to decreased screening contrary to the observed trend. A decrease in ΔE , the average excitation energy, would also lead to decreased shielding and this would appear not to be a factor. The observed changes in $\delta(^{205}\text{Tl})$ might therefore be due to changes in the nature of the Tl-C bonding interaction affecting the Pu and/or possibly the Du term if thallium d orbitals were involved in bonding to these groups.

The sensitivity of the thallium chemical shift to the stereochemistry of substituents is again illustrated by the case of the cis/trans-propenyl derivatives. A mixture of isomers, expected to contain cis/cis;trans/trans and cis/trans isomers, showed two signals in the proton decoupled ^{205}Tl nmr spectrum FIG 3.9. The proton coupled thallium spectrum identified the larger component as the trans/trans isomer by comparison with the known thallium-proton coupling constants.⁸⁶ The smaller component "cis" in FIG.3.9. is assumed to be from the cis/cis-isomer possibly overlapping the cis/trans isomer.

Mitchell²⁴⁹ studied the ^{119}Sn spectra of mixtures of isomeric compounds of the type $(\text{CH}_3)_n\text{Sn}(\text{CH}=\text{CH}\text{CH}_3)_{4-n}$, ($n=0-3$) and found signals for cis, trans and isopropenyl compounds separated by up to 20ppm for a given value of n . (Compared to a difference of ca. 76ppm observed here, probably reflecting the greater range of thallium shifts). The values of $\delta(^{205}\text{Tl})$ found here for the iso-propenyl compound (Table 3.4) cannot be compared directly with those for the cis and trans-propenyl isomers because of the different anions and solvents involved. Mitchell²⁴⁹ noted that in cis- and trans-propenyltin compounds Sn is more shielded than in the unsubstituted vinyltin compound.

FIG 3.9

BROAD BAND PROTON DECOUPLED ^{205}TI SPECTRUM
 OF $[\text{CH}_3\text{CH}=\text{CH}]_2\text{TINO}_3$ AT 34.7 MHz
 ca. 0.1 mol dm^{-3} IN PYRIDINE d_5 .



No. of data points	= 8192
No. of pulses	= 4000
Pulse length	= $57 \mu\text{s}$
Filter	= 5K
Acc. time	= $100 \mu\text{s}$
Delay	= 0.09s

3.2.6.4. Aryl derivatives

The value of $\delta(^{205}\text{Tl})$ reported here for $(\text{C}_6\text{H}_5)_2\text{TlBr}$ (-322ppm) in DMSO at 31°C is compared with the previously reported value of -293ppm in the same solvent at 24°C. The $\delta(^{205}\text{Tl})$ reported here for $(\text{C}_6\text{H}_5)_2\text{TlCl}$ in DMSO (-326ppm) is compared to the value of -377ppm in liquid ammonia at -20°C,¹¹ the only other previous report of $\delta(^{205}\text{Tl})$ in a bis(aryl)-thallium(III) compound.

The effect of substitution of fluorine for protons on the thallium chemical shift in the aryl derivatives cannot be compared directly because of the solvent and anion differences involved. However we might expect $(\text{C}_6\text{H}_5)_2\text{TlBr}$ to give signals at higher frequency in pyridine, relative to DMSO by analogy with other systems and thus the $(\text{C}_6\text{F}_5)_2\text{TlBr}$ compound in DMSO solution would give rise to increased shielding for thallium relative to $(\text{C}_6\text{H}_5)_2\text{TlBr}$. A study of the analogous perfluorophenyl compounds by McFarlane²⁵⁰ revealed that the ^{199}Hg resonance in $(\text{C}_6\text{F}_5)_2\text{Hg}$ was at a lower frequency than in the protonated analogue. Substitution of only one of the rings with fluorine to give $(\text{C}_6\text{F}_5)(\text{C}_6\text{H}_5)\text{Hg}$ ²⁵¹ also results in increased shielding for ^{199}Hg , although not to the same extent as when both rings are substituted. The influence of substituents in the aromatic ring on $\delta(^{205}\text{Tl})$ was examined by Hinton and Briggs¹⁴ for a series of mono-arylthallium(III) compounds $\text{para-XC}_6\text{H}_4\text{Tl}(\text{OCOCF}_3)_2$, ($\text{X} = \text{H}, \text{F}, \text{Cl}, \text{Br}, \text{alkyl}$). A correlation was found between $\delta(^{205}\text{Tl})$ and the Hammett σ constant. The greatest shielding was observed for the halogen derivatives and this was interpreted in terms of their ability to cause an increase in the ionic character of the Tl-O bond. Zink et al¹⁵ also found a correlation of

$\delta(^{205}\text{Tl})$ with the Hammett σ constant for similar compounds but with increased thallium shielding as the electron donating ability of the substituent increased. $(\text{C}_6\text{F}_5)_2\text{TlBr}$ is known to be monomeric in pyridine, methanol, acetone¹⁸² and it is interesting to note that the highest frequency shift observed is for this compound in benzene (Table 3.5) where it is known to be dimeric.¹⁸²

The ^{205}Tl spectrum of $(\text{C}_6\text{F}_5)_2\text{TlBr}$ in pyridine is shown in FIG.3.10. Thallium-fluorine coupling constants $^n\text{J}(^{205}\text{Tl}-^{19}\text{F})$, ($n = 3-5$), obtained from the thallium spectra of $(\text{C}_6\text{F}_5)_2\text{TlBr}$ and $(p\text{-HC}_6\text{F}_4)_2\text{TlBr}$ in various solvents are shown in Table 3.8. These compare well with the published values. There appears to be no correlation between $\delta(^{205}\text{Tl})$ and $^3\text{J}(^{205}\text{Tl}-^{19}\text{F})$.

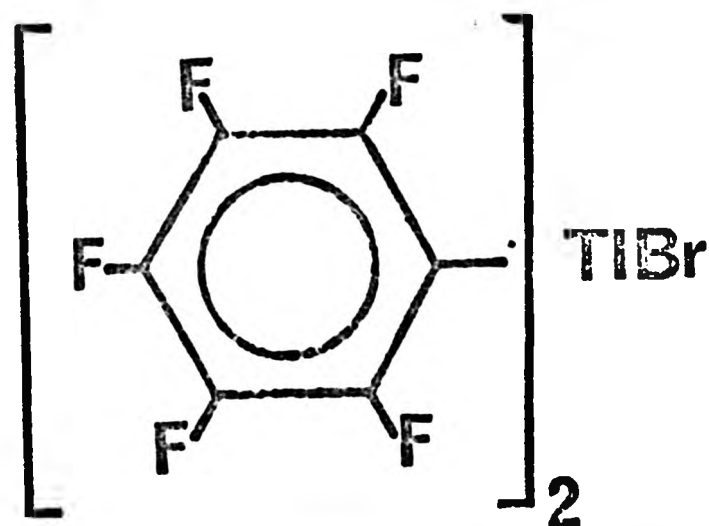
3.2.6.5. The effect of heteroatom substitution

The effect of heteroatom substitution in the alkyl group on thallium chemical shift can be examined using the following examples. Substitution of electronegative atoms or groups appears to cause an increase in thallium shielding. The chloromethyl compound $\text{ClCH}_2\text{Tl}(\text{OCOCH}_3)_2$ is notable in giving rise to the lowest frequency thallium resonance found for an organothallium(III) compound. ($\delta(^{205}\text{Tl}) = -832\text{ppm}$, Table 3.6). Substitution of chlorine for a proton in the methyl compound results in an increase in thallium shielding of 445 ppm compared to $\text{CH}_3\text{Tl}(\text{OAc})_2$ in methanol.¹² $^1\text{J}(\text{Tl}-\text{C})$ simultaneously increases from 5976Hz (Table 4.6) in the methyl compound to 8877Hz in the chloromethyl.²⁵³

Increases in shielding of thallium on substituting chlorine in the vinyl compounds and fluorine in aryl derivatives have previously been noted in the preceding sections. Increased

FIG. 3.10

^{205}Ti SPECTRUM AT 34.7 MHz OF



No. of data points	= 8192
No. of pulses	= 30,000
Pulse length	= 57 μs
Filter	= 5K
Acq. time	= 100 μs
Delay	= 0.09 s

0.5 mol dm $^{-3}$ IN PYRIDINE d $_5$

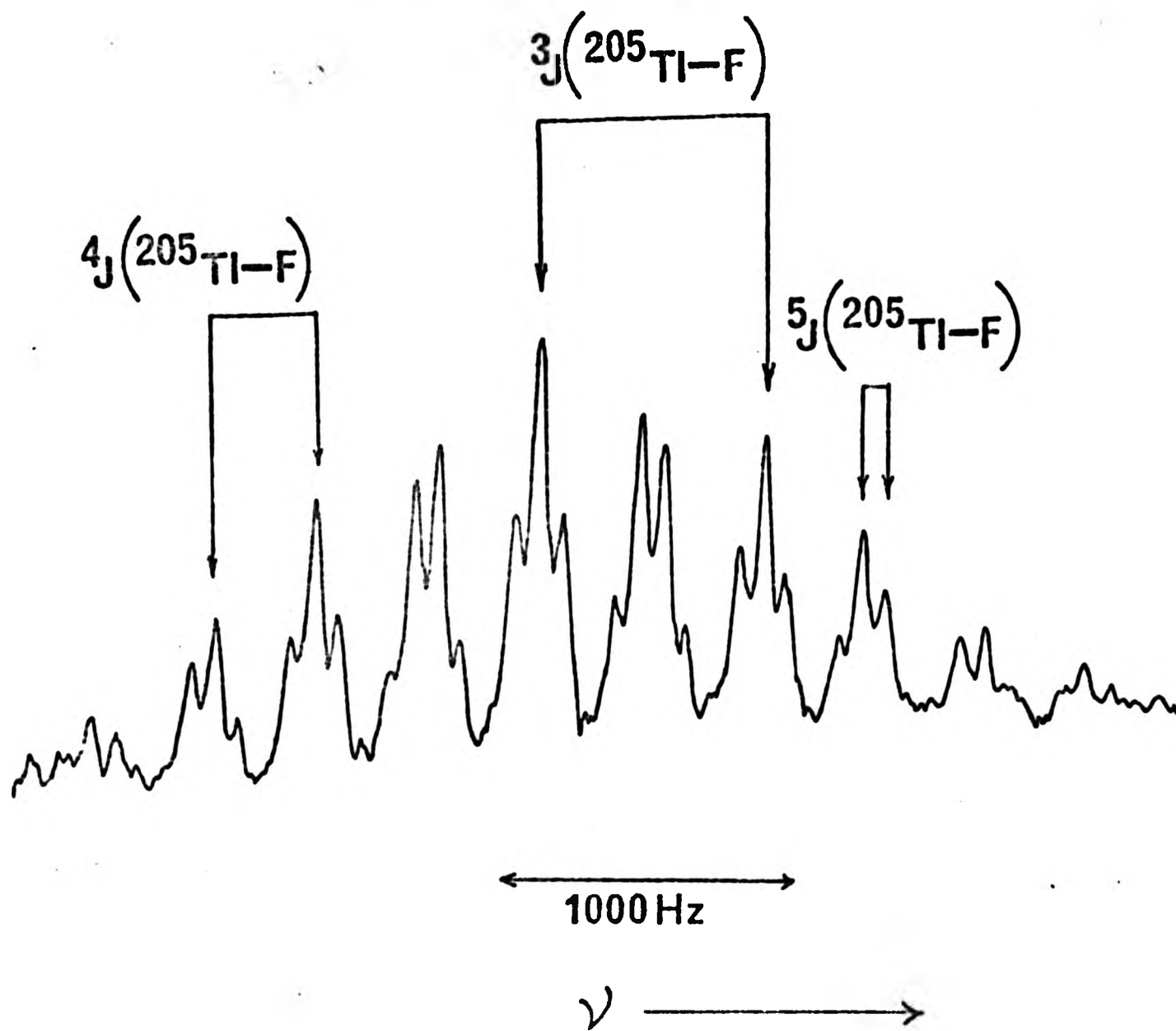


TABLE 3.8

Thallium-fluorine coupling constants for $(C_6F_5)_2TlBr$ and $(p-HC_6F_4)_2TlBr$ in various solvents^a

Solvent ^b	Compound	$^3J(Tl-F)$	$^4J(Tl-F)$	$^5J(Tl-F)$
pyridine	$(C_6F_5)_2TlBr$	772^{+12} (768^{+4})	338^{+12} (341^{+6})	85^{+10} (80^{+2})
methanol	"	803^{+12} (802^{+3})	359^{+12} (340^{+5})	85^{+10} (82^{+1})
acetone	"	(780^{+2})	(339^{+2})	(82^{+2})
benzene	"	(868^{+1})	(345^{+1})	(79^{+1})
acetone	$(p-HC_6F_4)_2TlBr$	786^{+15} (783^{+1})	382^{+15} (369^{+1})	-
methanol	$(p-HC_6F_4)_2TlBr$	830^{+15}	394^{+15}	-

^aValues in Hz obtained from ^{205}Tl spectra at 34.7MHz are for $J(^{205}Tl-^{19}F)$. Concentrations and temperatures are given in Table 3.5. Values in parentheses are from ref.252. and are averages of $J(^{203}Tl-^{19}F)$ and $J(^{205}Tl-^{19}F)$.
^bProtonated solvents were used.

shielding of bis(chlorovinyl)mercury,²⁵⁴ (-840ppm) compared to bis(vinyl)mercury,²²⁸ (-642ppm), has also been observed.

Substitution of the less electronegative silicon to give the trimethylsilylmethyl group causes a decrease in thallium shielding of 82-151ppm relative to the neopentyl compounds. A simultaneous decrease in carbon-thallium coupling is observed, and the α -carbon atom is shielded by ca. 37ppm (Table 4.2).

The increases in thallium-carbon coupling, accompanying increased thallium shielding, on increasing electronegativity of substituents may arise (see equation 4.5 and discussion in Chapter 4) from a decrease in ΔE , increase in Z_{eff} . or increasing s-character in the Tl-C bond. However decrease in ΔE and increase in Z_{eff} would cause decreased shielding of thallium contrary to the observed trend. It is likely that changes in s-character of the hybrid orbital involved in Tl-C bonding affect the P_u term (equation 3.9) leading to increased shielding of thallium.

3.2.6.6. Monoorganothallium(III) derivatives

Some of the trends in thallium shielding observed for R_2TlX compounds may also be seen in $RTlX_2$ derivatives, (Table 3.6), for the limited data in the latter case.

Thallium is more shielded in $CH_3CH_2Tl[OCOCH(CH_3)_2]_2$ than in $CH_3Tl(OCOCH_3)_2$ as a result of the greater +I effect of the CH_3CH_2 group compared to CH_3 (Table 3.7).

Thallium in $(CH_3)_3SiCH_2Tl[OCOCH(CH_3)_2]_2$ is 112ppm less shielded than in the analogous ethyl derivative and 35ppm less than in $CH_3Tl(OCOCH_3)_2$. Kurosawa¹⁴⁷ suggested that the CH_3 and $(CH_3)_3SiCH_2$ groups had similar electronic effects in

organothallium(III) compounds on the basis of ^1H NMR data. However the Taft σ^* values for these groups, CH_3 (0.000); $(\text{CH}_3)_3\text{SiCH}_2$ (-0.26), are markedly different. It is likely that the greater +I effect of the $(\text{CH}_3)_3\text{SiCH}_2$ group would result in a shielding of thallium compared to a methyl group. However the large steric bulk of the $(\text{CH}_3)_3\text{SiCH}_2$ group (an Es value is not available but it is likely to be similar to that of the neo-pentyl group (-1.74), (Table 3.7)) would result in a deshielding. Thus the observed shift value, close to that for the methyl derivative, is coincidental.

The trend of increasing thallium shielding with increasing ring size found for R_2TlX compounds (3.2.6.2.) is reflected here in going from cyclopropyl to the seven membered norbornane derivatives. The increase in $^1\text{J}(\text{Tl}-\text{C})$ (Table 4.5) as thallium becomes less shielded is also paralleled here.

The low-frequency resonance of thallium in the only reported monoalkenyl derivative, (Table 3.6) might be expected on the basis of the presence of electronegative substituents, by analogy with bis(alkenyl)thallium(III) compounds (Table 3.4).

The sensitivity of $\delta(^{205}\text{Tl})$ to structural variations in the organo group is illustrated by the increased shielding of 15-34ppm, caused by the presence of an alkenyl linkage three bonds removed from thallium, in the norbornene compared to the norbornane compound (Table 3.6).

CHAPTER FOUR

THALLIUM-CARBON AND THALLIUM-PROTON SPIN-SPIN COUPLING
IN ORGANOThALLIUM(III) COMPOUNDS

4.1. Introduction

There has been great interest in metal-proton and metal-carbon spin spin coupling constants in organo,(alkyl,alkenyl,aryl) derivatives of heavy metals. Numerous carbon-13 and proton NMR studies on organometallic derivatives of Sn,^{234,242,249,255-259} Hg,^{229,260-265} and to a lesser extent Pb^{230,266-271} and Cd^{11,237,272-275} have been reported. Although the proton NMR parameters for a wide variety of organothallium(III) compounds have been reported,⁸⁵ carbon-13 NMR investigations have been limited to methyl^{11,12,16,21,61-64,78} monophenyl,^{14,66-68,70,71} norbornenyl and norbornyl-thallium(III) derivatives,⁷³⁻⁷⁵ an acetoxythallated sugar,(D-galactal triacetate)⁷² and the compounds $(\text{CH}_3)_3\text{PCH}_2\text{Tl}(\text{CH}_3)_2$; ⁶⁴ $[(\text{CH}_3)_2\text{TlCH}_2\text{P}(\text{CH}_3)_2\text{CH}_2]_2$ ⁶⁵ Thallium-carbon couplings have also been observed in other derivatives not having direct thallium-carbon bonds and these have been reviewed in 1.2.1. Thallium-carbon and thallium-proton coupling constants are generally very large, especially $^1\text{J}(\text{Tl}-\text{C})$ and sensitive to the environment of thallium.^{12,86} This study was undertaken with the objects of characterising the pattern of thallium-carbon and thallium-proton coupling constants in organothallium(III) derivatives and investigating correlations of these with molecular structure and stereochemistry. The variation of $^n\text{J}(\text{Tl}-\text{C})$ and $^{n+1}\text{J}(\text{Tl}-\text{H})$, $n = 1-3$, in R_2TlX and RTlX_2 ($\text{R} = \text{branched-chain alkyl, alicyclic, alkenyl}$; $\text{X} = \text{anion}$) have been studied and compared with available data for analogous n -alkyl and aryl derivatives.

There have been no previous comparative studies of simultaneous variations in both carbon-13 and proton NMR parameters over a whole range of organothallium(III) derivatives. Hoad¹² examined the variation of $^1\text{J}(\text{Tl}-\text{C})$ and $^2\text{J}(\text{Tl}-\text{H})$ in the series: $\text{R}_3\text{Tl}, \text{R}_2\text{TlX}, \text{RTlX}_2$ ($\text{R} = \text{CH}_3$; $\text{X} = \text{anion}$) and Maher⁸⁶

studied the behaviour of $^nJ(\text{Tl-H})$, $n = 2-4$, for this series (where $R = n\text{-alkyl, vinyl, phenyl}$). Weibel and Oliver²⁸⁷ examined the variation of $^2J(\text{Tl-H})$ in the series $\text{Li}[(\text{Me}_3\text{Sn})_n\text{-TlMe}_{4-n}]$, ($n = 0-4$).

A knowledge of the factors influencing thallium-carbon coupling constants might find useful applications in investigations of the solution behaviour of thallium compounds, eg. in elucidating the stereochemistry of biological model systems such as Tl(I) antibiotics^{57,58} and ionophores.^{56,77} The stereochemical dependence of thallium-proton coupling constants has previously been used to suggest the geometry of the products from acetoxythallation of olefins.^{92,93,275}

4.2. Results

Carbon-13 NMR parameters for R_2TlX , ($R = n\text{-alkyl, branched alkyl, alicyclic, alkenyl, aryl}$; $X = \text{anion}$) are given in TABLES 4.1 to 4.5 and for RTlX_2 ($R \neq \text{aryl}$) in TABLE 4.6. Proton NMR parameters for R_2TlX ($R \neq \text{aryl}$) are reported in TABLES 4.7. to 4.11 and those for RTlX_2 ($R \neq \text{aryl}$) in TABLE 4.12. Carbon-13 and proton chemical shifts are reported in these tables for convenience although they are discussed separately in Chapter 3. Some relevant results obtained by other authors are included in the tables.

TABLE 4.1. ^{13}C NMR Parameters for straight-chain bis(alkyl)thallium(III) compounds^a

Compound	Solvent ^b	Conc ^c	$^1J(\text{Tl}-\text{C})$ $\delta(^{13}\text{C})$	$^2J(\text{Tl}-\text{C})$ $\delta(^{13}\text{C})$	$^3J(\text{Tl}-\text{C})$ $\delta(^{13}\text{C})$	$^4J(\text{Tl}-\text{C})$ $\delta(^{13}\text{C})$
$(\text{CH}_3)_2\text{TlNO}_3^{\text{d}}$	py	1.0	+2991 (22.5)			
$(\text{CH}_3\text{CH}_2)_2\text{TlBr}^{\text{e}}$	DMSO	0.3	2519 (40.8)	174 (12.6)		
$(\text{CH}_3\text{CH}_2)_2\text{TlBr}^{\text{e}}$	py	0.2	2552 (39.5)	187 (13.9)		
$(\text{CH}_3\text{CH}_2\text{CH}_2)_2\text{TlBr}^{\text{e}}$	py	0.2	+2436 (49.8)	127 (22.4)	+498 (19.1)	
$(\text{CH}_3\text{CH}_2\text{CH}_2\text{CH}_2)_2\text{TlBr}^{\text{e}}$	py	0.25	2425 (47.4)	131 (31.0)	487 (27.7)	16 (13.7)
$[\text{CH}_3(\text{CH}_2)_3\text{CH}_2]_2\text{TlBr}^{\text{d,f}}$	py	0.18	2427 (47.4)	128 (28.4)	468 (36.9)	18 (22.5)
$[\text{CH}_3(\text{CH}_2)_4\text{CH}_2]_2\text{TlBr}^{\text{d,g}}$	py	0.13	2416 (47.5)	129 (28.8)	468 (34.4)	18 (31.6)

Table 4.1 continued

^aAll spectra were obtained at 22.63MHz and 30[±]2°C. Coupling constants in Hz; errors [±]3Hz unless otherwise noted. Separate coupling to ²⁰³Tl and ²⁰⁵Tl was not resolved, except for ¹J(Tl-C) where the coupling given is to ²⁰⁵Tl. Chemical shifts (in parentheses) in ppm relative to internal TMS; errors [±] 0.2ppm unless otherwise noted. Results of relative sign determinations are indicated before the appropriate value of J(Tl-C). Preference for a positive sign for ¹J(Tl-C) (ref. 11) is indicated as ⁺ rather than ⁻. ^b Deuterated solvents were used. ^c In mol. dm.⁻³ ^d Data from ref. 277. ^e Data from ref. 253. ^f ⁵J(Tl-C) < 5Hz, $\delta(^{13}\text{C}) = 14.2 \pm 0.2\text{ppm}$. ^g ⁵J(Tl-C) < 5Hz, $\delta(^{13}\text{C}) = 22.8 \pm 0.2\text{ppm}$; ⁶J(Tl-C) < 5Hz $\delta(^{13}\text{C}) = 14.2 \pm 0.2\text{ppm}$.

Table 4.2. ^{13}C NMR Parameters for branched-chain bis(alkyl)thallium(III) compounds^a

Compound	Solvent ^b	Conc ^c	$^1\text{J}(\text{Tl}-\text{C})$ $\delta(^{13}\text{C})$	$^2\text{J}(\text{Tl}-\text{C})$ $\delta(^{13}\text{C})$	$^3\text{J}(\text{Tl}-\text{C})$ $\delta(^{13}\text{C})$	$^4\text{J}(\text{Tl}-\text{C})$ $\delta(^{13}\text{C})$
$[(\text{CH}_3)_2\text{CH}]_2\text{TlCl}$	py	0.35	$^+2225$ (55.1)	$^-63$ (23.7)		
$[(\text{CH}_3)_2\text{CH}]_2\text{TlCl}$	DMSO	0.24	2224 (55.2)	60 (22.5)		
$[(\text{CH}_3)_2\text{CHCH}_2]_2\text{TlCl}^d$	DMSO	0.40	$^+2357$ (60.6)	$^-71$ (27.4)	$^+370$ (26.7)	
$[(\text{CH}_3)_2\text{CHCH}_2\text{CH}_2]_2\text{TlNO}_3^d$	py	0.29	2472 (44.6)	143 (36.6)	518 (32.4)	< 5 (22.2)
$[(\text{CH}_3)_2\text{CHCH}_2\text{CH}_2]_2\text{TlNO}_3$	DMSO	0.25	$^+2431$ (46.0)	e (CH ₃) (CH ₂) 103 ^g < 5 (19.5) (29.0) 116 ^h (19.8)	524 (31.3)	< 5 (22.1)
$[\text{CH}_3\text{CF}_2(\text{CH}_3)\text{CH}]_2\text{TlCl}^f$	DMSO	0.25	$^+2175$ (64.1)		337 ^g (14.9) 324 ^h (14.1)	

TABLE 4.2 Continued

Compound	Solvent ^b	Conc. ^c	¹ J(Tl-C) δ(¹³ C)	² J(Tl-C) δ(¹³ C)	³ J(Tl-C) δ(¹³ C)	⁴ J(Tl-C) δ(¹³ C)
$[\text{CH}_3\text{CH}_2\text{CH}_2(\text{CH}_3)\text{CH}]_2\text{TlCl}^f$	py	0.16	2115 (62.0)	(CH ₃) (CH ₂) 145 ^g 12 ⁱ (20.6)(39.8) 122 ^h (21.1)	302 ^g (25.1) 325 ^h (24.5)	<5 (14.1)
$[\text{CH}_3\text{CH}_2\text{CH}_2(\text{CH}_3)\text{CH}]_2\text{TlCl}^i$	DMSO	0.20	2119 (62.2)	147 ^g j (19.0) 107 ^h (19.9)	291 ^g (24.0) 331 ^h (23.1)	<5 (13.9)
$[(\text{CH}_3)_3\text{CCH}_2]_2\text{TlCl}$	py	0.22	⁺ 2297 (67.5)	²⁶ (33.2)	³¹⁰ (34.4)	
$[(\text{CH}_3)_2\text{SiCH}_2]_2\text{TlCl}$	py	0.27	1847 (30.6)		168 (5.5)	
$[(\text{CH}_3)_3\text{SiCH}_2]_2\text{TlOCOR}^k$	py	0.27	1940 (28.7)		168 (1.8)	

TABLE 4.2 (Continued)

Compound	Solvent ^b	Conc. ^c	¹ J(Tl-C) δ(¹³ C)	² J(Tl-C) δ(¹³ C)	³ J(Tl-C) δ(¹³ C)	⁴ J(Tl-C) δ(¹³ C)
$ \begin{array}{c} \text{OCH}_3 \quad \text{CH}_3 \\ \quad \\ \text{CH}_3\text{CHCH}_2\text{TlOCOCH}_3^m \end{array} $	py		(CH ₃) 3160 (52.9)	158 (76.1)	309 (23.3)	7.0 (55.9)
			(CH ₂) 2754 (22.1)			

^aSpectra obtained at 22.63MHz and 30⁺ 2°C unless otherwise noted. Coupling constants in Hz; errors ⁺3Hz unless otherwise noted. One bond thallium-carbon coupling is for ¹J(²⁰⁵Tl-C) except for bis(iso-amyl)nitratotthallium(III) in DMSO solution. In the latter and other cases separate coupling to ²⁰³Tl and ²⁰⁵Tl was not resolved. Chemical shifts (in parentheses) in ppm relative to internal TMS; errors ⁺0.2ppm unless otherwise noted. Results of relative sign determinations are indicated before the appropriate value of J(Tl-C). Preference for a positive sign for ¹J(Tl-C) (ref.11) is indicated as ⁺ rather than ⁻. Deuterated solvents were used.

^c In mol dm⁻³. ^d Assignments confirmed by ¹³C-¹H off-resonance spectrum. ^e One component of signal overlapped by solvent peaks. ^f Assignments aided by ¹³C-¹H off-resonance spectra but results inconclusive. Two alternative assignments possible, (i) and (ii). ^g Alternative assignment(i). ^h Alternative assignment (ii). ⁱ Assignment by analogy with spectrum in pyridine solution. ^j Obscured

Table 4.2. Continued

by solvent. ^k R=CH(CH₃)₂. For OCOCH(CH₃)₂ δ(¹³C=O) = 184.3[±]0.2ppm, δ(¹³CH₃) = 20.4[±]0.2ppm, δ(¹³CH)=37.2[±]0.2ppm; ^mSpectra obtained at 20.1MHz. Assignments assisted by spectrum obtained at 45.28MHz. The sample contained a methyltin impurity which gave a signal coincident with TMS.

TABLE 4.3 ^{13}C NMR Parameters for bis(alicyclic)thallium(III) compounds^a

Compound	Solvent ^b	Conc. ^c	$^1\text{J}(\text{Tl}-\text{C})$ $\delta(^{13}\text{C})$	$^2\text{J}(\text{Tl}-\text{C})$ $\delta(^{13}\text{C})$	$^3\text{J}(\text{Tl}-\text{C})$ $\delta(^{13}\text{C})$	$^4\text{J}(\text{Tl}-\text{C})$ $\delta(^{13}\text{C})$
$[(\text{CH}_2)_2\text{CH}]_2\text{TlBr}$	DMSO	0.30	$^+4496$ (36.5)	$^-138$ (3.0)		
$[(\text{CH}_2)_2\text{CH}]_2\text{TlBr}$	py	0.32	$^+4552^{\text{d}}$ (35.0)	150 (4.2)		
$[(\text{CH}_2)_4\text{CH}]_2\text{TlBF}_4^{\text{e}}$	DMSO	0.20	$^+2380^{\text{d}}$ (64.5)	18 (30.1)	$^+394^{\text{e}}$ (25.5)	
$[(\text{CH}_2)_5\text{CH}]_2\text{TlBF}_4^{\text{f}}$	py	0.30	1880 (70.0)	66 (33.4)	452 (30.6)	53 (26.8)
$[(\text{CH}_2)_5\text{CH}]_2\text{TlBF}_4^{\text{g}}$	DMSO	0.24	$^+2047^{\text{d}}$ (68.8)	71 (31.9)	458 (29.8)	49 (26.5)
$[(\text{CH}_2)_6\text{CH}]_2\text{TlBr}^{\text{h}}$	DMSO	0.20	1863 (70.0)	30 (30.6)	538 (29.9)	< 5 (27.4)
$[(\text{CH}_2)_5\text{CHCH}_2]_2\text{TlBr}^{\text{i}}$	py	0.21	$^+2302^{\text{d}}$ (57.8)	$^-775$ (37.8)	366 (38.1)	< 5 (26.3)

TABLE 4.3 Continued

Compound	Solvent ^b	Conc ^c	¹ J(Tl-C) δ(¹³ C)	² J(Tl-C) δ(¹³ C)	³ J(Tl-C) δ(¹³ C)	⁴ J(Tl-C) δ(¹³ C)
$[(CH_2)_5CHCH_2]_2TlBr$	DMSO	0.22	2326 ^d (58.6)	78 (36.6)	j	j

^aSpectra obtained at 22.63 MHz and 30⁺2°C unless noted. Coupling constants in Hz; errors ⁺3 Hz unless otherwise noted. Separate coupling to ²⁰³Tl and ²⁰⁵Tl was not resolved unless otherwise noted. Chemical shifts (in parentheses) in ppm relative to internal TMS; errors ⁺0.2 ppm unless otherwise noted. Results of relative sign determinations are identified before the appropriate value of J(Tl-C). Preference for a positive sign for ¹J(Tl-C) (Ref. 11) is indicated as ⁺ rather than ⁻. ^b Deuterated solvents were used. ^c In mol dm⁻³: ^d_J(²⁰⁵Tl-C). ^e Assignments of ²J(Tl-C) and ³J(Tl-C) based on intensities of signals, by analogy with R₂TlBF₄ (R = cyclohexyl) in DMSO and by analogy with branched-chain alkylthallium(III) compounds. ^f Assignment of ²J(Tl-C) and ³J(Tl-C) by analogy with solution in DMSO. Errors on ¹J(Tl-C) ⁺ 10 Hz; δ(C₁) ± 0.5 ppm. Larger errors due to signal overlap. ^g Pairing and assignment of ²J(Tl-C) and ³J(Tl-C) based on differential perturbation of signals in ¹³C-{¹H} SFORD spectrum, based on the assumption that ³J(Tl-H) > ⁴J(Tl-H). The signs of ²J(Tl-C) and ³J(Tl-H) are opposite but the relative signs of ¹J(Tl-C) and ²J(Tl-C) are unknown.

Table 4.3 continued

^h Spectrum obtained at 20.1MHz. Assignments of ²J(Tl-C) and ³J(Tl-C) by analogy with R₂TlB⁴ (R = cyclohexyl) in DMSO. ⁱ Assignments based on intensity considerations and comparison of spectra obtained at 22.63 and 45.28MHz. Signals for C(δ) and C(ε) assigned by analogy with other cyclic and branched-chain compounds. ⁵J(Tl-C) = 41⁺3Hz; δ(C_ε) = 26.7⁺ - 0.2ppm.
^j Not assigned.

TABLE 4.4. ^{13}C NMR Parameters for bis(alkenyl)thallium(III) compounds^a.


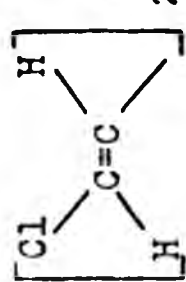
Compound	Solvent ^b	Conc. ^c	$^1\text{J}(\text{Tl}-\text{C})$ $\delta(^{13}\text{C})$	$^2\text{J}(\text{Tl}-\text{C})$ $\delta(^{13}\text{C})$
$(\text{H}_2\text{C}=\text{CH})_2\text{TlBF}_4^{\text{d}}$	DMSO	0.6	± 4874 (162.6)	± 55 (132.8)
$(\text{H}_2\text{C}=\text{CH})_2\text{TlOCOCH}_3^{\text{e}}$	py	0.5	5032 (160.6)	29 (133.2)
	DMSO	0.33	± 5828 (153.0)	730^{f} (130.2)
	CD_3OD	0.25	5435 (151.2)	669 (134.4)
$[\text{H}_2\text{C}=\text{C}(\text{CH}_3)]_2\text{TlBr}$	DMSO	0.2	4173 (174.8)	$(\text{CH}_2^{\text{h}})(\text{CH}_3^{\text{h,i}})$ 348 505 (124.4)(28.4)

TABLE 4.4 (Continued)

Compound	Solvent ^b	Conc ^c	¹ J(Tl-C) δ(¹³ C)	² J(Tl-C) δ(¹³ C)	³ J(Tl-C) δ(¹³ C)
$[H_2C=C(CH_3)]_2$ TlBr ^j	py	0.27	4232 ^k (173.4)	(CH ₂) (CH ₃) 370 445 (125.6)(28.6)	
$[CH_3C(H)=C(H)]_2$ TlNO ₃ ^m	py	0.3	4971 (151.8)	158 (139.2)	770 (22.2)
$[PhC(H)=C(H)]_2$ TlNO ₃ ⁿ	DMSO	0.28	5223 ^o (154.2)	175 (148.8)	759 ^p (137.3)

^a Spectra obtained at 22.63MHz and 30⁺2°C unless otherwise noted. Coupling constants in Hz; errors ⁺3Hz unless otherwise noted. Separate coupling to ²⁰³Tl and ²⁰⁵Tl was not resolved(except for ¹J(Tl-C) which is for coupling to ²⁰⁵Tl, unless otherwise noted. Chemical shifts (in parentheses) in ppm relative to internal TMS; error ⁺0.2ppm unless otherwise noted. Results of relative sign determinations are identified before

Table 4.4. Continued

the appropriate value of $J(\text{Tl-C})$. It is assumed that $^1J(\text{Tl-C})$ is positive (ref.11). ^b Deuterated solvents were used. ^c In mol dm⁻³. ^d Data from ref. 208. Assignments were confirmed by proton-coupled ¹³C spectrum. $^1J(\text{C-H})_{\text{gem}} = 157^{+7}\text{Hz}$; $^1J(\text{C-H})_{\text{trans}} = 157^{+7}\text{Hz}$. ^e Signals for O_2COCH_3 : $\delta(^{13}\text{C}=\text{O}) = 178.9 \pm 0.1\text{ppm}$. $\delta(^{13}\text{CH}_3) = 25.5^{+0.1}\text{ppm}$. ^f The signs of $^2J(\text{Tl-C})$ and $^3J(\text{Tl-H})$ are the same. ^g Spectrum obtained at 45.28MHz. ^h $^2J(\text{Tl-CH}_2)$ has the same sign as either $^3J(\text{Tl-H})$ trans or $^3J(\text{Tl-H})_{\text{cis}}$ or both. ⁱ Larger errors due to overlap of solvent signal and one component of $^{13}\text{CH}_3$ signal: $\pm 40\text{Hz}$; -2.21ppm . ^j Some decomposition occurred in solution. ^k Errors, ^{+13}Hz ; $^{-0.6}\text{ppm}$. ^m Mixture of cis and trans isomers. The proton-coupled ^{205}Tl spectrum indicates that the trans/trans-isomer is the dominant species present. The dominant component of the ^{13}C spectrum is reported here. The spectrum showed sufficient other signals to account for cis/cis and cis/trans compounds. ⁿ Signals for phenyl ortho-, meta- and para- carbons in the region 124 to 130ppm. The signals were broad but coupling to thallium was not resolved. ^o Larger errors due to overlap of solvent signal and one component of $\text{C}(\alpha)$. Errors; $\pm 37\text{Hz}$; $^{-1.64}\text{ppm}$. ^p Errors, ^{+19}Hz ; $^{-1.45}\text{ppm}$.


TABLE 4.5. ^{13}C NMR Parameters for monoorganothallium(III) compounds ^a				
Compound	Solvent ^b	Conc. ^c	$^1\text{J}(\text{Tl}-\text{C})$ $\delta(^{13}\text{C})$	$^2\text{J}(\text{Tl}-\text{C})$ $\delta(^{13}\text{C})$
$\text{CH}_3\text{Tl}(\text{OCOCH}_3)_2$ ^{d,e}	CD_3OD	ca. 1.0	5976 ^f (17.7)	$^3\text{J}(\text{Tl}-\text{C})$ $\delta(^{13}\text{C})$
$\text{CH}_3\text{Tl}(\text{OCOCH}_3)_2$ ^{d,e}	CDCl_3	ca. 0.5	5631 ^f (18.7)	
$\text{CH}_3(\text{CH}_2\text{Tl}(\text{OCOR}))_2$ ^h	DMSO	ca. 1.3	+6108 ^f (36.7)	281 ⁱ (7.5)
$(\text{CH}_3)_3\text{CCH}_2\text{TlX}_2$ ^j	py	0.1	5002 ^f (63.4)	313 (34.4)
$(\text{CH}_3)_3\text{SiCH}_2\text{Tl}(\text{OCOR})_2$ ^k	CD_2Cl_2 CH_2Cl_2	0.1	3540 ^m (27.2)	- 318 (-1.1)
$(\text{CH}_2)_2\text{CHTl}(\text{OCOR})_2$ ⁿ	DMSO	0.26	+9799 ^{f,i} (30.8)	318 ⁱ (2.6)
$\text{H}_2\text{C}=\text{CHTlCl}_2$	CD_3OD	p	8715 ^{f,q} (148.3)	100 ^q (134.8)
	CD_3OD	p	9185 ^{f,i} (141.8)	1069 ⁱ (133.6)

TABLE 4.5 Continued

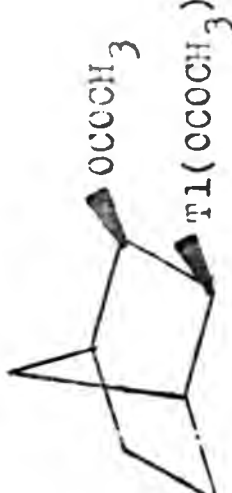
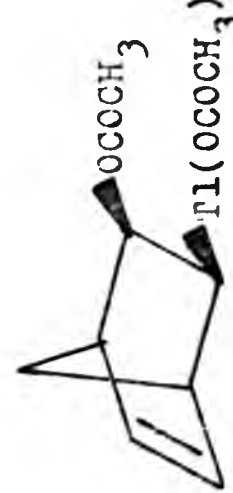
Compound	Solvent ^b	Conc ^c	¹ J(Tl-C) δ(13C)	² J(Tl-C) δ(13C) ($\bar{C}=$)	⁴ J(Tl-C) δ(13C) ($\bar{C}=$)
$ \begin{array}{c} \text{CH}_3 \\ \diagup \\ \text{C}=\text{C} \\ \diagdown \quad \diagup \\ \text{RCC} \quad \text{CH}_3 \\ \text{O} \end{array} \quad \text{Tl}(\text{OCOCH}_3)_2 $	DMSO	0.2	9556 ^f (139.6)	1626 ^s (147.9)	117 ^s (167.9)
	DMSO	0.2	6330 ^f (72.3)		
	DMSO	0.2	6464 ^f (67.6)		

Table 4.5 continued

^a Spectra obtained at 22.63MHz and 30-2°C unless otherwise noted. Coupling constants in Hz; error ⁺3Hz unless otherwise noted. Separate coupling to ²⁰³Tl and ²⁰⁵Tl was not resolved unless otherwise noted. Chemical shifts (in parentheses) in ppm relative to internal TMS; error ⁺0.2ppm unless otherwise noted. Results of relative sign determinations are identified before the appropriate value of J(Tl-C). It is assumed ¹J(Tl-C) is positive (ref.11). ^b Deuterated solvents were used. ^c In mol dm⁻³. ^d Data from ref. 12. ^e Signals for -OCOCH₃, $\delta(^{13}\text{C}=\text{O}) = 179.8^{+0.2}_{-0.2}$ ppm. ^f Coupling to ²⁰⁵Tl. ^g Signals for OCOCH₃, $\delta(^{13}\text{C}=\text{O}) = 179.1^{+0.2}_{-0.2}$ ppm. $\delta(^{13}\text{CH}_3) = 23.1^{+0.2}_{-0.2}$ ppm. ^h R = -CH(CH₃)₂. Data from ref. 253. Signals for OCOCH(CH₃)₂, $\delta(^{13}\text{C}=\text{O}) = 181.0^{+0.3}_{-0.3}$ ppm; $\delta(^{13}\text{CH}) = 35.6^{+0.3}_{-0.3}$ ppm; $\delta(^{13}\text{CH}_3) = 20.1^{+0.3}_{-0.3}$ ppm. ⁱ Errors, ⁺5Hz; ⁻0.3ppm. ^j X = Br or Cl. ^k Spectra obtained at 45.28MHz. Assignment by comparison with proton coupled spectrum. R = -CH(CH₃)₂. Signals for -OCOCH(CH₃)₂ $\delta(^{13}\text{C}=\text{O}) = 183.3^{+0.1}_{-0.1}$ ppm; $\delta(^{13}\text{CH}) = 34.8^{+0.1}_{-0.1}$ ppm; $\delta(^{13}\text{CH}_3) = 18.4^{+0.1}_{-0.1}$ ppm. ^m Errors, ⁺28Hz; ⁻0.45ppm. ⁿ R = CH(CH₃)₂. Signals for -OCOCH(CH₃)₂, $\delta(^{13}\text{C}=\text{O}) = 180.8^{+0.2}_{-0.2}$ ppm; $\delta(^{13}\text{CH}) = 35.3^{+0.2}_{-0.2}$ ppm; $\delta(^{13}\text{CH}_3) = 20.1^{+0.2}_{-0.2}$ ppm. ^p Compound made by reaction in NMR tube, not isolated. Concentration approx. 0.1 mol dm⁻³. ^q Errors, ⁺4Hz; ⁻0.3ppm. ^r R = CH₃. Other signals not assigned. ^s Assignment on basis of chemical shifts and comparison of spectra obtained at 22.63 and 45.28MHz. ^t Only ¹J(Tl-C) assigned. A number of detailed studies of the carbon spectra of these compounds (refs. 73-75) appeared during the course of this work and the spectra obtained here were not further assigned.

TABLE 4.6 ^{13}C NMR Parameters for arylthallium(III) compounds^a

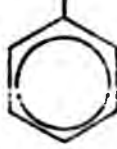




Compound	Solvent ^b	$^1\text{J}(\text{Tl}-\text{C})$ $\delta(^{13}\text{C})$	$^2\text{J}(\text{Tl}-\text{C})$ $\delta(^{13}\text{C})$	$^3\text{J}(\text{Tl}-\text{C})$ $\delta(^{13}\text{C})$	$^4\text{J}(\text{Tl}-\text{C})$ $\delta(^{13}\text{C})$
 $\text{C}_6\text{H}_5\text{OCOCF}_3$ ^c	DMSO	10718 ^d (153.6)	+500 (134.4)	+1010 (129.8)	+185 (130.1)
 $\text{CH}_3\text{CH}_2\text{C}_6\text{H}_4\text{OCOCF}_3$ ^{c,e}	DMSO	-	+556 (134.1)	+1066 (128.9)	+199 (145.9)
 $\text{C}_6\text{H}_4(\text{OC(=O)N})_2$ ^f	DMSO ^g	4496 (165.3)	319 (136.9)	453 (128.4)	83 (127.7)
 $\text{C}_6\text{H}_4(\text{OC(=O)N})_2$ ^h	DMSO ^h	5359 (165.6)	317 (136.2)	469 (128.3)	87 (127.9)
 $\text{C}_6\text{H}_4(\text{OCH}_3)_2$ ⁱ	DMSO ⁱ	5293 (165.9)	281 ^j (136.7)	433 ^j (127.9)	85 ^j (128.0)

Table 4.6 Continued

^aSpectra obtained at 22.63MHz and 30[±]2° unless otherwise noted. Coupling constants in Hz, error [±]3 unless otherwise noted. Separate coupling to ²⁰³Tl and ²⁰⁵Tl only resolved for ¹J(Tl-C) for which coupling to ²⁰⁵Tl is reported. Chemical shifts (in parentheses) in ppm relative to internal TMS, error [±]0.2ppm unless otherwise noted. Results of relative sign determinations are identified before the appropriate J(Tl-C). It was assumed ¹J(Tl-C) is positive (ref.11). ^bDeuterated solvents were used. ^cData from ref. 66. (Except ¹J(Tl-C)). Obtained at 25.16MHz and 36°. Errors, [±]15Hz. concentration not specified. ^dData from ref. 71, temperature concentration and errors not specified. ^e⁵J(Tl-CH₂) = 99Hz; $\delta(^{13}\text{CH}_2)$ = 28.1ppm. ⁶J(Tl-CH₃) = 48Hz; $\delta(^{13}\text{CH}_3)$ = 15.1ppm. ^fdata from ref. 143. ^gConcentration unknown. ^hConcentration 0.14 mol dm⁻³. ⁱConcentration 0.2 mol dm⁻³. ^jAssigned by analogy with Ph₂TlX (X = SSCN(C₂H₅)₂; tropolonato) derivatives. (Ref.143).

TABLE 4.7 ^1H NMR Parameters for straight-chain bis(alkyl)thallium(III) compounds^a

Compound	Solvent ^b	$^2J(\text{Tl-H})$ $\delta(^1\text{H})$	$^3J(\text{Tl-H})$ $\delta(^1\text{H})$	$^4J(\text{Tl-H})$ $\delta(^1\text{H})$
$(^{13}\text{CH}_3)_2\text{TlI}^c$	DMSO	$\mp 438^d$ (1.00)		
$(\text{CH}_3)_2\text{TlNO}_3^e$	DMSO	449 (0.70)		
$(\text{CH}_3\text{CH}_2)_2\text{TlX}^f$	D_2O	∓ 340.4	∓ 628.0	
$(\text{CH}_3\text{CH}_2\text{CH}_2)_2\text{TlX}^f$	D_2O	∓ 340.7	∓ 468.9	∓ 20.5
$(\text{CH}_3\text{CH}_2\text{CH}_2\text{CH}_2)_2\text{TlX}^f$	D_2O	391.6	451.8	-

^aSpectra were obtained at 60 MHz and $35^\circ\pm 1^\circ\text{C}$ unless otherwise noted. Coupling constants in Hz-Separate coupling to ^{203}Tl and ^{205}Tl was not resolved unless otherwise noted. Chemical shifts (in parentheses) in ppm relative to internal TMS. Results of relative sign determinations are identified before the appropriate $J(\text{Tl-H})$. It was assumed $^1J(\text{Tl-C})$ is positive (ref.11).

^bDeuterated solvents were used. ^cApprox. 60% ^{13}C enriched, $^1J(^{13}\text{C-H}) = 137^\pm 0.7\text{Hz}$. ^dError, $\pm 0.7\text{Hz}$; $\delta(^{12}\text{CH}_3) = 1.01^\pm 0.015\text{ppm}$; $\delta(^{13}\text{CH}_3) = 1.00^\pm 0.02\text{ppm}$. ^eData from ref.12. Concentration 0.2mol dm⁻³. ^fData from ref. 86; X = ClO_4^- or SO_4^{2-} .

TABLE 4.8. ^1H NMR Parameters for branched-chain bis(alkyl)thallium(III) compounds^a

Compound	Solvent ^b	Conc ^c	$2J(\text{Tl-H})$ $\delta(^1\text{H})$	$3J(\text{Tl-H})$ $\delta(^1\text{H})$	$3J(\text{Tl-CH}_2)_\text{A}$ $\delta(^1\text{H})$	$3J(\text{Tl-CH}_2)_\text{B}$ $\delta(^1\text{H})$	$4J(\text{Tl-H})$ $\delta(^1\text{H})$
$[(\text{CH}_3)_2\text{CH}]_2\text{TlCl}^\text{d}$	DMSO	0.35	+304 (2.07)	+587 ^e (1.55)			
$[(\text{CH}_3)_2\text{CH}]\text{TlCl}$	py	0.35	267 (2.51)	584 ^e (1.71)			
$[(\text{CH}_3)_2\text{CH}]_2\text{TlCOOCH}_3^\text{f}$	CD_3OD	0.13	270 (2.28)	577 (1.58)			
$[(\text{CH}_3)_2\text{CHCH}_2]_2\text{TlCl}$	DMSO	0.24	+404 (1.83)	+491 ^g (2.26)			+20 (0.96)
$[(\text{CH}_3)_2\text{CHCH}_2]_2\text{TlCl}$	py	0.15	+382 (2.26)	+519 (2.67)			+18 (1.02)
$[(\text{CH}_3)_2\text{CHCH}_2]_2\text{TlCl}$	C_6D_6	0.06	355 (2.51)				14 (0.95)
$[\text{CH}_3\text{CH}_2(\text{CH}_3)\text{CH}]_2\text{TlCl}$	DMSO	0.19	+323 (2.09)	+599 ^h (1.59)	+705 (2.05)	+513 ⁱ (2.01)	+20 (0.97)

TABLE 1.8. Continued

Compound	Solvent ^b	Conc. ^c	$^2J(\text{Tl-H})$ $\delta(^1\text{H})$	$^3J(\text{Tl-H})$ $\delta(^1\text{H})$	$^3J(\text{Tl-CH}_2)_\text{A}$ $\delta(^1\text{H})$	$^3J(\text{Tl-CH}_2)_\text{B}$ $\delta(^1\text{H})$	$^4J(\text{Tl-H})$ $\delta(^1\text{H})$
$[\text{CH}_3\text{CH}_2(\text{CH}_3)\text{CH}]_2\text{TlCl}$	py	0.10	293 (2.44)	548 ^h (1.74)	730 (2.16)	511 (2.05)	22 (1.09)
$[\text{CH}_3\text{CH}_2(\text{CH}_3)\text{CH}]_2\text{TlCl}$	C ₆ D ₆	0.01	k	582 (1.87)	k	k	25 (1.03)
$[(\text{CH}_3)_2\text{CHCH}_2\text{CH}_2]_2\text{TlOCCCH}_3$	DMSO	0.04	396 ⁿ (1.52)	418 ⁿ (1.70)			
$[(\text{CH}_3)_2\text{CHCH}_2\text{CH}_2]_2\text{TlOCCCH}_3$	py	0.28	†377 (1.93)	†423 (1.92)			
$[(\text{CH}_3)_2\text{CHCH}_2\text{CH}_2]_2\text{TlOCCCH}_3$	C ₆ D ₆	0.28	†377 ^g (1.91)	†465 ^g (1.92)			
$[(\text{CH}_3)_2\text{CHCH}_2\text{CH}_2]_2\text{TlNO}_3$	DMSO	0.25	†404 ⁿ (1.62)	†365 ⁿ (1.78)			
$[(\text{CH}_3)_2\text{CHCH}_2\text{CH}_2]_2\text{TlNO}_3$	py	0.19	†388 ⁿ (2.26)	†365 ⁿ (1.89)			
$[\text{CH}_3\text{CH}_2\text{CH}_2(\text{CH}_3)\text{CH}]_2\text{TlCl}$	DMSO	0.18	†307 ^s (2.19)	†563 ^{s,h} (1.64)	†716 ^s (2.02)	†474 (1.99)	

TABLE 4.8 Continued

Compound	Solvent ^b	Conc. ^c	$^2J(\text{Tl-H})$ $\delta(^1\text{H})$	$^3J(\text{Tl-H})$ $\delta(^1\text{H})$	$^3J(\text{Tl-CH}_2)_\text{A}$ $\delta(^1\text{H})$	$^3J(\text{Tl-CH}_2)_\text{B}$ $\delta(^1\text{H})$	$^4J(\text{Tl-H})$ $\delta(^1\text{H})$
$[\text{CH}_3\text{CH}_2\text{CH}_2(\text{CH}_3)\text{CH}]_2\text{TlCl}^\text{t}$	py	0.10	268 ^s (2.68)	553 ^{s,h} (1.79)	754 ^s (2.18)	465 ^s (2.12)	
$[\text{CH}_3\text{CH}_2\text{CH}_2(\text{CH}_3)\text{CH}]_2\text{TlCl}$	C ₆ D ₆	0.06	295 ^s (2.79)	584 ^h (1.93)	736 ^s (2.26)	538 ^u (2.26)	
$[(\text{CH}_3)_3\text{CCH}_2]_2\text{TlCl}$	py	0.21	415 (2.38)				31 (1.09)
$[(\text{CH}_3)_3\text{CCH}_2]_2\text{TlCl}$	C ₆ D ₆	0.02	394 ^q (2.61)				31 (1.03)
$[(\text{CH}_3)_3\text{CCH}_2]_2\text{TlCl}$	CDCl ₃	0.14	383 (2.47)				31 (1.11)
$[(\text{CH}_3)_3\text{CCH}_2]_2\text{TlOCOR}^\text{v,w}$	py	0.23	429 (2.19)				31 (1.10)
$[(\text{CH}_3)_3\text{CCH}_2]_2\text{TlOCOR}^\text{v,x}$	CDCl ₃	0.26	411 (2.07)				31 (1.08)

TABLE 4.8. Continued

Compound	Solvent ^b	Conc. ^c	$^2J(\text{Tl-H})$ $\delta(^1\text{H})$	$^4J(\text{Tl-H})$ $\delta(^1\text{H})$
$[(\text{CH}_3)_3\text{CCH}_2]_2\text{TlOCCOR}^{\text{v},\text{v}}$	C_6D_6	0.18	422 (2.23)	31 (1.09)
$[(\text{CH}_3)_3\text{SiCH}_2]_2\text{TlCl}$	py	0.22	556 (1.27)	18 (0.16)
$[(\text{CH}_3)_3\text{SiCH}_2]_2\text{TlCl}$	CDCl_3	0.04	545 (1.39)	17 (0.15)
$[(\text{CH}_3)_3\text{SiCH}_2]_2\text{TlCl}$	DMSO	0.05	592 (0.83)	18 (0.08)
$[(\text{CH}_3)_3\text{SiCH}_2]_2\text{TlOCCOR}^{\text{v},\text{z}}$	py	0.27	563 (1.09)	18 (0.17)
$[(\text{CH}_3)_3\text{SiCH}_2]_2\text{TlOCCOR}^{\text{v},\text{z}}$	CDCl_3	0.08	554 (1.09)	18 (0.11)
$[(\text{CH}_3)_3\text{SiCH}_2]_2\text{TlOCCOR}^{\text{v},\text{z}''}$	CD_3OD	0.03	571 (0.95)	18 (0.11)

Footnote to Table 4.3

Spectra obtained at 60MHz and 35[±]1°C unless otherwise noted. Coupling constants in Hz; error ^a7Hz unless otherwise noted. Separate coupling to 203Tl and 205Tl was not resolved unless otherwise noted. Chemical shifts (in parentheses) in ppm relative to internal TMS; error, ^b0.02ppm unless otherwise noted. Results of relative sign determinations are identified before the appropriate value of J(Tl-H). It is assumed that ¹J(Tl-C) is positive (ref. 11). ^b Deuterated solvents were used. ^c In mol dm.⁻³ ^d ³J(HH)=7.0[±]1Hz. ^e Coupling to 205Tl. ^f For OCOCH₃, $\delta(^1\text{H}) = 1.89 \pm 0.02\text{ppm}$. ^g Errors, [±]8Hz; [±]0.15ppm. ^h Coupling to CH₃. ⁱ Errors, [±]10Hz; [±]0.15ppm. ^j Errors, [±]1Hz; [±]0.20ppm. ^k Low solubility prevented determination. ^m Signals from CH(CH₃)₂ are in the range 0.7 to 2.1ppm (overlapping bands). Signal for OCOCH₃, $\delta(^1\text{H}) = 1.69 \pm 0.05\text{ppm}$. ⁿ Errors, [±]5Hz; [±]0.08ppm. ^p Signals from CH(CH₃)₂ are in the range 0.4 to 2.2 ppm (overlapping bands). Signal for OCOCH₃, $\delta(^1\text{H}) = 2.14 \pm 0.05\text{ppm}$. ^q Errors, [±]3Hz; [±]0.05ppm. ^r Signals from CH(CH₃)₂ are in the range 0.7 to 1.9ppm (overlapping bands). Signal for OCOCH₃, $\delta(^1\text{H}) = 1.92 \pm 0.05\text{ppm}$. ^s Errors, [±]7Hz; [±]0.15ppm. ^t ³J(HH)=7.4[±]0.5Hz for CH₃CH₂-. ^u Errors, [±]11Hz; [±]0.2ppm. ^v R = CH(CH₃)₂. ^w Signals for OCOCH(CH₃)₂, $\delta(^1\text{H}) = 2.64 \pm 0.02\text{ppm}$; $\delta(^1\text{H}_3) = 1.33 \pm 0.02\text{ppm}$. ^x Signals for OCOCH(CH₃)₂, $\delta(^1\text{H}) = 2.31 \pm 0.02\text{ppm}$; $\delta(^1\text{H}_3) = 1.14 \pm 0.02\text{ppm}$. ^y Signals for OCOCH(CH₃)₂, $\delta(^1\text{H}) = 2.46 \pm 0.02\text{ppm}$; $\delta(^1\text{H}_3) = 1.27 \pm 0.02\text{ppm}$. ^z Signals for OCOCH(CH₃)₂, $\delta(^1\text{H}) = 2.63 \pm 0.03\text{ppm}$; $\delta(^1\text{H}_3) = 1.28 \pm 0.03\text{ppm}$. ^{z'} For OCOCH(CH₃)₂, $\delta(^1\text{H}_3) = 1.10 \pm 0.03\text{ppm}$.

TABLE 6.9 ^1H NMR Parameters for bis(alicyclic)thallium(III) compounds^a

Compound	Solvent ^b	Conc ^c	$^2J(\text{Tl-H})$ $\delta(^1\text{H})$	$^3J(\text{Tl-H})$ $\delta(^1\text{H})$	$^3J(\text{Tl-H})$ $\delta(^1\text{H})$
$[(\text{CH}_2)_2\text{CH}]_2\text{TlBr}$	py	0.29	409 ^d	572 ^{cis} (1.48)	345 ^{trans} (0.93)
$[(\text{CH}_2)_2\text{CH}]_2\text{TlBr}$	DMSO	0.30	318 ^d	579 ^{cis} (1.08)	344 ^{trans} (0.75)
$[(\text{CH}_2)_2\text{CH}]_2\text{TlOCOR}^{\text{e,f}}$	py	0.30	(0.91) +405 ^g	(1.08) +563 ^g <u>cis</u>	(0.75) +340 ^g <u>trans</u>
$[(\text{CH}_2)_2\text{CH}]_2\text{TlOCOR}^{\text{e}}$	DMSO	0.25	(1.13) 343 ^d	(1.22) 571 ^{cis}	(0.86) 343 ^{trans}
$[(\text{CH}_2)_2\text{CH}]_2\text{TlOCOR}^{\text{e}}$	CD_3OD	0.20	(0.76) 338 ^d	(0.93) 568 ^{cis}	(0.76) 338 ^{trans}
$[(\text{CH}_2)_4\text{CH}]_2\text{TlBF}_4^{\text{h}}$	DMSO	0.20	(0.92) 268 ^d	(0.99) 496 ⁱ	(0.92) 268
$[(\text{CH}_2)_4\text{CH}]_2\text{TlBF}_4^{\text{j}}$	py	0.25	(2.05) 243 ^k	(2.00) 483 ⁱ	(2.05) 200 ^k
			(2.51)	(2.03)	(2.16)

Table 4.0 Continued

Compound	Solvent ^b	Conc ^c	$^2J_{(Tl-H)}\delta(^1H)$	$^3J_{(Tl-H)}\delta(^1H)$
$[(CH_2)_5CH]_2TlBF_4^m$	DMSO	0.27	346 ^d (2.17) 403 ^p	346 ^d (2.17) 598 ^p
$[(CH_2)_6CH]_2TlBF_4^n$	py	0.15	(2.78) +383 ^r	(2.55) +453
$[(CH_2)_5CHCH_2]_2TlBr^q$	py	0.11	(0.89)	(2.24)

^aSpectra obtained at 60MHz and 35⁺1⁰C unless otherwise noted. Coupling constants in Hz; error ⁺7% unless otherwise noted. Separate coupling to ²⁰³Tl and ²⁰⁵Tl was not resolved. Chemical shifts (in parentheses) in ppm relative to internal TMS error, ⁺0.12ppm unless otherwise noted. Results of relative sign determinations are identified before the appropriate values of J(Tl-H). It is assumed that ¹J(Tl-C) is positive (ref. 11). ^b Deuterated solvents were used. ^c In mol dm⁻³. ^d Errors, ⁺14Hz ⁺0.25ppm. ^eR = CH(CH₃)₂. ^f Signals for OCOCH(CH₃)₂; $\delta(C^1H)=1.32^{+0.02}$ ppm $\delta(C^1H_3)=2.64^{+0.02}$ ppm. ^g Values obtained using iterative NMR computer program (ref. 278). ^h Other signals in the range 1.0 to 2.4ppm (overlapping bands.) ⁱ Errors, ⁺4Hz ⁺0.07 ppm. ^j Other signals in the range 0.7 to 2.9ppm (overlapping bands). ^k Errors, ⁺11Hz; ⁺0.18ppm. ^m Other signals in the range 0.5 to 3.1ppm (overlapping bands). ⁿ Other signals in the range 0.7 to 2.8ppm (overlapping bands). ^p Errors, ⁺12Hz ⁺0.07ppm. ^q Other signals in the range 0.1

Table 4.2 Continued

to 2.4 ppm, (overlapping bands). r Errors, $\pm 1\text{Hz}$, $\pm 0.02\text{ppm}$. s Errors, $\pm 9\text{Hz}$; $\pm 0.15\text{ppm}$.

TABLE 4.10 ^1H NMR Parameters for bis(alkenyl)thallium(III) compounds^a

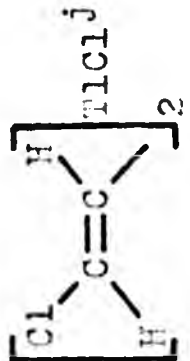
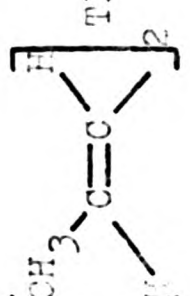
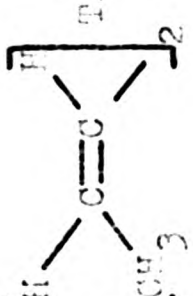
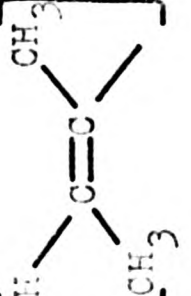
Compound	Solvent ^b	Conc ^c	$^2J(\text{TL-H})$ $\delta(^1\text{H})$	$^3J(\text{TL-H})$ $\delta(^1\text{H})$	$^3J(\text{TL-H})$ $\delta(^1\text{H})$
$(\text{H}_2\text{C}=\text{CH})_2\text{TLX}^{\text{d,e}}$	D_2O	f	$+842_{\text{gem}}$	$+805_{\text{cis}}$	$+1618_{\text{trans}}$
$(\text{H}_2\text{C}=\text{CH})_2\text{TLBr}_4^{\text{g,h}}$	DMSO	0.82	795_{gem} (6.80) $829^{\text{i}}_{\text{gem}}$ (6.76)	807_{cis} (5.84) $792^{\text{i}}_{\text{cis}}$ (5.75)	$1624^{\text{i}}_{\text{trans}}$ (6.07) $1590^{\text{i}}_{\text{trans}}$ (6.04)
$(\text{H}_2\text{C}=\text{CH})_2\text{TLCOCH}_3^{\text{h}}$	DMSO	0.5	$+456_{\text{gem}}^{\text{k}}$ (6.69) $+442^{\text{m}}_{\text{gem}}$ (6.55)	$+459_{\text{cis}}^{\text{k}}$ (6.43) $+474^{\text{m}}_{\text{cis}}$ (6.69)	
	DMSO	0.4		667_{cis} (5.59) (CH_3) 440 (2.36)	$1503^{\text{i}}_{\text{trans}}$ (5.88)
$[\text{H}_2\text{C}=\text{C}(\text{CH}_3)]_2\text{TLBr}$	py	0.27			

TABLE 4.10 Continued

Compound	Solvent ^b	Conc ^c	$^2J(\text{Tl-H})$ $\delta(^1\text{H})$	$^3J(\text{Tl-H})$ $\delta(^1\text{H})$	$^4J(\text{Tl-H})$ $\delta(^1\text{H})$
	D_2O	f	640 _{gem}	+809 _{cis}	-747
	D_2O	f	+637 _{gem}	+1485 _{trans}	-794
	D_2O	f		+1346 _{trans} (CH ₃) 398	+98

^a Spectra obtained at 60MHz and 35⁺1°C unless otherwise noted. Coupling constants in Hz; error⁺1Hz unless otherwise noted. Separate coupling to ²⁰³Tl and ²⁰⁵Tl was not resolved unless otherwise noted. Chemical shifts (in parentheses) in ppm relative to internal TMS, error ⁺0.02ppm unless otherwise noted. Results of relative sign determinations are identified before the appropriate value of J(Tl-H). It is assumed that ¹J(Tl-C) is positive (ref 11). ^b Deuterated solvents were used. ^c In mol dm⁻³. ^d Data from ref.86.

Table 4.10 Continued

e $X = SO_4^{2-}$ or ClO_4^- . f Concentration not specified in ref. 86.
g Data from ref. 208. h Assignments were based on the assumption (ref. 284) that $^3J(HH)_{trans} > ^3J(HH)_{cis} > ^2J(HH)_{gem}$. i Coupling to ^{205}Tl . j Two alternative assignments obtained by analysis of the spectrum. Assignment to gem and cis protons by analogy with bis(trans-chlorovinyl)mercury(II). (ref 297). k Alternative assignment (I). m Alternative assignment (II). n Assignments by analogy with $(H_2C=CH)_2TlBF_4$.

TABLE 4.11 ^1H NMR Parameters for monoorganothallium(III) compounds^a

Compound	Solvent ^b	Conc. ^c	$^2J(\text{Tl-H})$ $\delta(^1\text{H})$	$^3J(\text{Tl-H})$ $\delta(^1\text{H})$	$^4J(\text{Tl-H})$ $\delta(^1\text{H})$
$\text{CH}_3\text{Tl}(\text{OCOCH}_3)_2^{\text{d}}$	CD_3OD	1.0	939 ^{e,f} (1.72)		
$\text{CH}_3\text{CH}_2\text{Tl}(\text{OCOCH}(\text{CH}_3)_2)_2^{\text{d,g}}$	DMSO	1.2	7889 (2.29)	+1627 ^e (0.84)	
$(\text{CH}_3)_2\text{CHCH}_2\text{Tl}(\text{OCOR})_2^{\text{h}}$	CD_3OD	i	7335 (2.73)	+1722 (2.41)	
$(\text{CH}_3)_2\text{CHCH}_2\text{CH}_2\text{Tl}(\text{OCOR})_2^{\text{j}}$	CD_3OD	i	7898 ^{e,k} (2.68)	+1300 ^{e,k} (1.76)	
$(\text{CH}_3)_3\text{CCH}_2\text{TlX}_2^{\text{m}}$	py	n	665 (2.74)	-	68 (1.15)
$(\text{CH}_3)_3\text{CCH}_2\text{TlX}_2^{\text{m}}$	CDCl_3	n	666 ^p (2.92)	-	73 (1.17)
$(\text{CH}_3)_3\text{CCH}_2\text{Tl}(\text{OCOR})_2^{\text{h,q}}$	CDCl_3	n	772 ^p (2.90)	-	75 (1.14)

TABLE 4.11 Continued

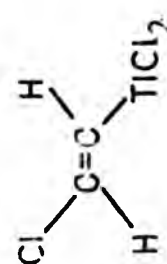
Compound	Solvent ^b	Conc. ^c	$^2J(\text{Tl-H})$ $\delta(^1\text{H})$	$^3J(\text{Tl-H})$ $\delta(^1\text{H})$	$^3J(\text{Tl-H})$ $\delta(^1\text{H})$	$^4J(\text{Tl-H})$ $\delta(^1\text{H})$
$(\text{CH}_3)_3\text{SiCH}_2\text{Tl}(\text{OCOR})_2^{\text{h,r}}$	py	0.10 ^s	1116 ^e (1.71)	-	-	33 (0.17)
$(\text{CH}_3)_3\text{SiCH}_2\text{Tl}(\text{OCOR})_2^{\text{h,t}}$	CDCl_3	0.10 ^s	1130 ^u (1.76)	-	-	31 ^u (0.20)
$(\text{CH}_2)_2\text{CHTl}(\text{OCOR})_2^{\text{h,v}}$	py	0.5	548 ^k (1.89)	1280 ^k _{cis} (1.20)	776 ^k _{trans} (0.84)	
$\text{H}_2\text{C}=\text{CHTlCl}_2^{\text{w}}$	CD_3OD	1	+1882 <u>gem</u> ^{e,k} (6.55)	+1707 <u>cis</u> ^{e,k} (5.82)	+3574 <u>trans</u> ^{e,x} (6.10)	
	CD_3OD	1	+807 ^e (6.77)	+1040 ^e (6.63)		

Table 4.11 Continued

Compound	Solvent ^b	Conc ^c	$^2J(\text{Tl-H})$ $\delta(^1\text{H})$	$^3J(\text{Tl-H})$ $\delta(^1\text{H})$	$^3J(\text{Tl-H})$ $\delta(^1\text{H})$	$^4J(\text{Tl-H})$ $\delta(^1\text{H})$
$\begin{array}{c} \text{CH}_3-\text{C}=\text{C}-\text{Tl}(\text{OCOR})_2 \\ \\ \text{R}-\text{C}-\text{O}-\text{CH}_3 \\ \\ \text{O} \end{array}$	DMSO	0.50	-	940 ^v (1.82)	-	139 (2.01)

^aSpectra obtained at 60MHz and 35 $^{\circ}\text{C}$ unless otherwise noted. Coupling constants in Hz; error \pm 1Hz unless otherwise noted.

Separate coupling to ^{203}Tl and ^{205}Tl was not resolved unless otherwise noted. Chemical shifts (in parentheses) in ppm relative to internal TMS, error, $\pm 0.02\text{ppm}$ unless otherwise noted.

Results of relative sign determinations are identified before the appropriate value of $J(\text{Tl-H})$. It is assumed $^1J(\text{Tl-C})$ is positive (ref. 11). ^b Deuterated solvents were used. ^c In mol dm^{-3} .

^d Data from ref. 253. Signal for OCOCH_3 , $\delta(^1\text{H}) = 1.95 \pm 0.01$ ppm. ^e Coupling to ^{205}Tl .

^f Errors, $\pm 0.4\text{Hz}$; $\pm 0.01\text{ppm}$. ^g Signals for $-\text{OCOCH}(\text{CH}_3)_2$, $\delta(\text{C}^1\text{H}) = 2.37 \pm 0.02\text{ppm}$; $\delta(\text{C}^1\text{H}_3) = 1.09 \pm 0.02\text{ppm}$.

^h R = $\text{CH}(\text{CH}_3)_2$. ⁱ Compound not isolated. Produced by reaction in NMR tube.

^j R = CH_3 . ^k Errors, $\pm 7\text{Hz}$; $\pm 0.12\text{ppm}$. ^m X = Br and/or Cl. ⁿ Reaction carried out in NMR tube and produced; not isolated. Concentration ca. 0.1 mol dm^{-1} . ^p Errors, $\pm 4\text{Hz}$, $\pm 0.07\text{ppm}$. ^q Signals for

$\text{OCOCH}(\text{CH}_3)_2$; $\delta(\text{C}^1\text{H}) = 2.50 \pm 0.02\text{ppm}$; $\delta(\text{C}^1\text{H}_3) = 1.16 \pm 0.02$ ppm. ^r Signals for $\text{OCOCH}(\text{CH}_3)_2$; $\delta(\text{C}^1\text{H}) = 2.61 \pm 0.03$ ppm; $\delta(\text{C}^1\text{H}_3) = 1.19 \pm 0.03\text{ppm}$. ^s Approximate concentration. ^t Signals for $\text{OCOCH}(\text{CH}_3)_2$;

Table 4.11 Continued

$\delta(\text{C}^1\text{H}) = 2.52 \pm 0.03$ ppm; $\delta(\text{C}^1\text{H}_3) = 1.16 \pm 0.03$ ppm. ^u Signals broad compared to solution in pyridine.
^v Signals for $\text{OCOCH}(\text{CH}_3)_2$, $\delta(\text{C}^1\text{H}) = 2.62 \pm 0.02$ ppm; $\delta(\text{C}^1\text{H}_3) = 1.13 \pm 0.02$ ppm. $^w J(\text{HH})_{\text{cis}} = 9.5 \pm 1$ Hz;
 $^x J(\text{HH})_{\text{trans}} = 18.0 \pm 1$ Hz; $^y J(\text{HH})_{\text{gem}} < 2$ Hz. ^xErrors, ± 17 Hz; ± 0.36 ppm. ^y Assignment by analogy with
 $[\text{H}_2\text{C}=\text{C}(\text{CH}_3)]_2\text{TiBr}$.

4.2.1. Determination of relative signs of coupling constants

A spin-spin coupling constant is a measure of the extent to which the nuclear magnetic moment of one nucleus can affect that of another. This interaction may be positive or negative in sign. A coupling constant is defined²⁸³ as positive if antiparallel nuclear spins are stabilised and if parallel spins are destabilised. The reverse holds for negative coupling constants. The absolute signs of coupling constants may be determined by studying molecules which have been partially oriented, eg. in liquid crystal systems,²⁸⁰ or by application of a strong electric field.²⁸¹ Determination of certain key²⁸² coupling constants by these methods, eg. $^1J(^{13}\text{C}-^1\text{H})$, allows other coupling constants to be related to them by double resonance methods.

The relative signs of the coupling constants between at least three non-equivalent nuclei can be obtained from NMR spectra only when the spectrum contains second order features. This procedure has been used in this work to obtain the relative signs of $^2J(\text{Tl-H})$ and $^3J(\text{Tl-H})$ in bis(trans-chlorovinyl)chlorothallium(III) and (trans-chlorovinyl)bischlorothallium(III) TABLES 4.10 and 4.11 respectively. The proton spectra for these compounds are shown in FIG 4.10.

Double resonance methods can be used to obtain the relative signs of coupling constants from first order spectra. As the signal of one nucleus is observed (field B_1), that from a second coupled nucleus is irradiated with a second radio-frequency field B_2 .

Observed transitions of the first nucleus which have a common energy level with the irradiated transition are perturbed to an extent depending on the strength of B_2 . In an AMX spin system if A is the directly observed nucleus and X is irradiated, (denoted A- { X }), then the relative signs of J_{AM} and J_{MX} can be obtained. (In fact it is the relative signs of K_{AM} and K_{MX} which are given by double resonance methods.²⁸³ However since the gyromagnetic ratios $\gamma^{205}\text{Tl}$, $\gamma^{13}\text{C}$ and $\gamma^1\text{H}$ are all positive, K and J will have the same sign for thallium-carbon and thallium-proton coupling constants. Therefore J will be used for convenience throughout the discussion).

The energy level diagram for the $\text{CH}_3\text{Tl}^{2+}$ system considered as an AMX_3 spin system (A,Tl;M,C; X,H) is shown in FIG 4.1. Transitions in the proton, carbon-13 and thallium-205 spectra (shown diagrammatically in FIG 4.2) can be assigned for all possible relative sign combinations of $J(\text{C-H})$, $J(\text{Tl-H})$ and $J(\text{Tl-C})$. For this system, and any other first order $\text{Tl}_a\text{C}_m\text{H}_x$ system, the experiments which give the relative signs of coupling constants are:-

- i) $^{205}\text{Tl}-\{^{13}\text{C}\}$ or $^{13}\text{C}-\{^{205}\text{Tl}\}$ for $J(\text{Tl-H})$ relative to $J(\text{C-H})$
- ii) $^{205}\text{Tl}-\{^1\text{H}\}$ or $^1\text{H}-\{^{205}\text{Tl}\}$ for $J(\text{Tl-C})$ relative to $J(\text{C-H})$
- iii) $^{13}\text{C}-\{^1\text{H}\}$ or $^1\text{H}-\{^{13}\text{C}\}$ for $J(\text{Tl-C})$ relative to $J(\text{Tl-H})$

Examination of the assignment diagram FIG 4.2. in conjunction with the energy-level diagram FIG 4.1 leads to the prediction that for $^{13}\text{C}-\{^1\text{H}\}$ experiments irradiation of the low frequency components of the proton spectrum will result in response(s) only in either the low or high frequency components of the carbon-13 spectrum.

This simple result facilitates the experimental procedure and interpretation of results. Detailed examination of other organothallium(III) systems reveals a similar situation.

FIG. 4.1

ENERGY LEVEL DIAGRAM FOR $\text{CH}_3\text{Ti}^{2+}$ AS AN AMX_3 SPIN SYSTEM

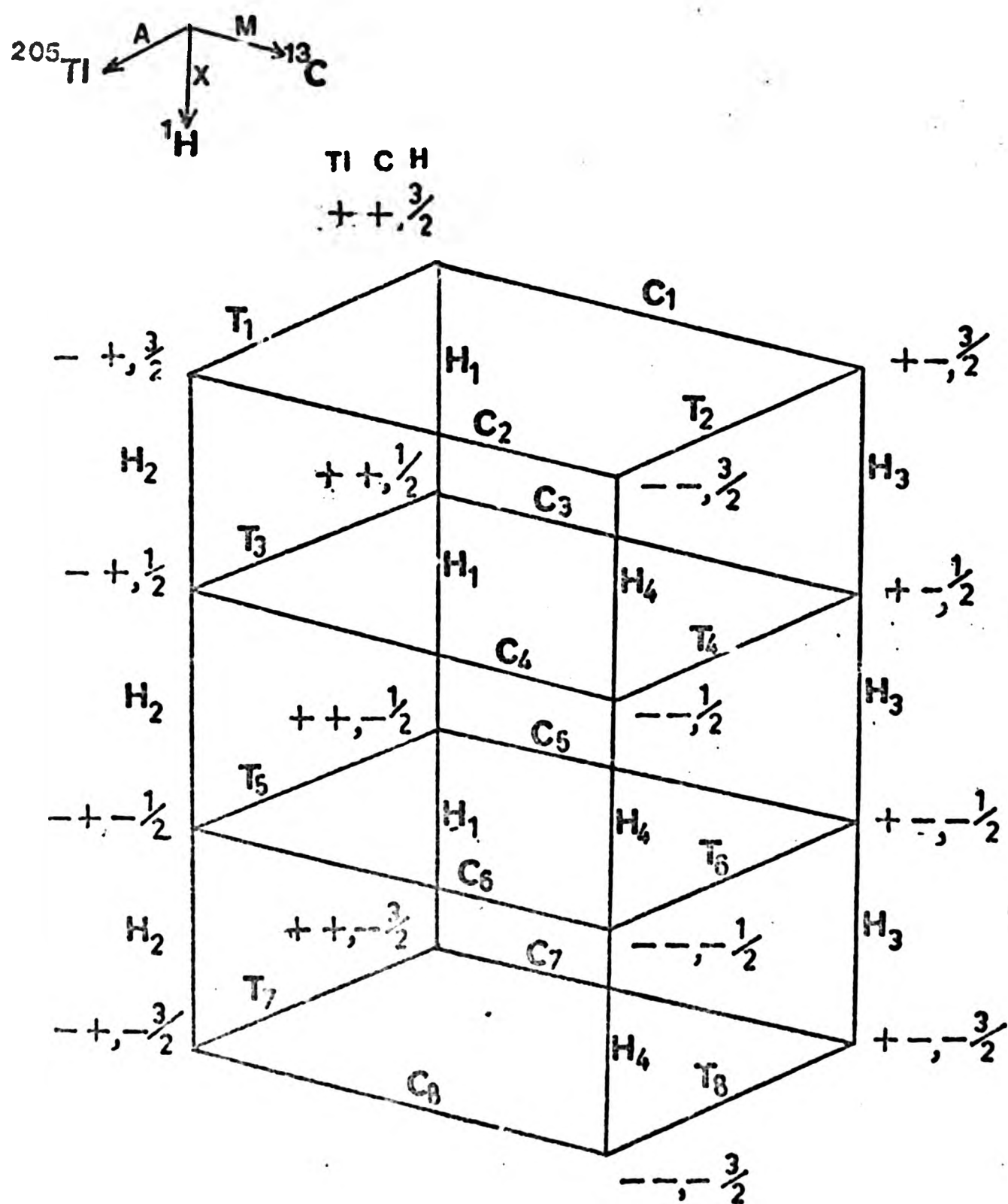


FIG. 4.2

ASSIGNMENT OF ^1H , ^{205}Ti , AND ^{13}C TRANSITIONS IN THE SPECTRA
OF $\text{CH}_3\text{Ti}^{2+}$ FOR ALL POSSIBLE RELATIVE SIGN COMBINATIONS

(SPECTRA NOT TO SCALE)

	^1H	^{205}Ti	^{13}C
J_{CH} J_{TiH} J_{TiC}			
+ + +	H_1H_3 H_2H_4	$\text{T}_1\text{T}_3\text{T}_5\text{T}_7$ $\text{T}_2\text{T}_4\text{T}_6\text{T}_8$	$\text{C}_1\text{C}_3\text{C}_5\text{C}_7$ $\text{C}_2\text{C}_4\text{C}_6\text{C}_8$
- - -	H_4H_2 H_3H_1	$\text{T}_8\text{T}_6\text{T}_4\text{T}_2$ $\text{T}_7\text{T}_5\text{T}_3\text{T}_1$	$\text{C}_8\text{C}_6\text{C}_4\text{C}_2$ $\text{C}_7\text{C}_5\text{C}_3\text{C}_1$
+ - +	H_2H_4 H_1H_3	$\text{T}_7\text{T}_5\text{T}_3\text{T}_1$ $\text{T}_8\text{T}_6\text{T}_4\text{T}_2$	$\text{C}_1\text{C}_3\text{C}_5\text{C}_7$ $\text{C}_2\text{C}_4\text{C}_6\text{C}_8$
+ + -	H_3H_1 H_4H_2	$\text{T}_2\text{T}_4\text{T}_6\text{T}_8$ $\text{T}_1\text{T}_3\text{T}_5\text{T}_7$	$\text{C}_8\text{C}_6\text{C}_4\text{C}_2$ $\text{C}_7\text{C}_5\text{C}_3\text{C}_1$
- + -	H_1H_3 H_2H_4	$\text{T}_2\text{T}_4\text{T}_6\text{T}_8$ $\text{T}_1\text{T}_3\text{T}_5\text{T}_7$	$\text{C}_2\text{C}_4\text{C}_6\text{C}_8$ $\text{C}_1\text{C}_3\text{C}_5\text{C}_7$
- - +	H_4H_2 H_3H_1	$\text{T}_7\text{T}_5\text{T}_3\text{T}_1$ $\text{T}_8\text{T}_6\text{T}_4\text{T}_2$	$\text{C}_7\text{C}_5\text{C}_3\text{C}_1$ $\text{C}_8\text{C}_6\text{C}_4\text{C}_2$
+ - -	H_2H_4 H_1H_3	$\text{T}_8\text{T}_6\text{T}_4\text{T}_2$ $\text{T}_7\text{T}_5\text{T}_3\text{T}_1$	$\text{C}_2\text{C}_4\text{C}_6\text{C}_8$ $\text{C}_1\text{C}_3\text{C}_5\text{C}_7$
- + +	H_3H_1 H_4H_2	$\text{T}_1\text{T}_3\text{T}_5\text{T}_7$ $\text{T}_2\text{T}_4\text{T}_6\text{T}_8$	$\text{C}_7\text{C}_5\text{C}_3\text{C}_1$ $\text{C}_8\text{C}_6\text{C}_4\text{C}_2$

Thus detailed assignment of transitions is generally unnecessary and the following 'rule' can be applied for systems where C and H are coupled to thallium. In $^{13}\text{C}-\{^1\text{H}\}$ experiments if the high frequency multiplet of the proton spectrum is irradiated, a response in the high frequency multiplet of the carbon spectrum indicates that the signs of $^n\text{J}(\text{Tl}-\text{C})$ and $n + 1\text{J}(\text{Tl}-\text{H})$ are the same (and vice versa). Use of this 'rule' is shown in FIG 4.4. for bis(cyclopropyl)bromothallium(III).

Similar arguments can be applied to situations where mutually coupled protons are also coupled to thallium and where the spin system can be approximated as first order (eg. $\text{CH}_3\text{CH}_2\text{Tl}^{2+}$; $\text{A}_3\text{M}_2\text{X}$). In these cases the sign of $^n\text{J}(\text{Tl}-\text{H})$ relative to $n+1\text{J}(\text{Tl}-\text{H})$ can be determined by $^1\text{H}-\{^1\text{H}\}$ experiments. An example of such a relative sign determination is shown in FIG 4.6. for bis(iso-butyl)chlorothallium(III). Maher and Evans⁸⁵ first used this method to determine the relative signs of thallium-proton coupling constants for R_2TlX derivatives (R = methylethyl, n-propyl, iso-butyl; phenyl; vinyl; X = anion) and RTlX_2 compounds (R = phenyl; vinyl).

The following assumptions have been made in reporting the relative signs of thallium-proton and thallium-carbon coupling constants. i) One-bond thallium-carbon coupling is positive,¹¹ relative to $^1\text{J}(\text{C}-\text{H})$, in all cases. ii) The thallium-proton coupling constants $^2\text{J}(\text{Tl}-\text{H})_{\text{gem}}$, $^3\text{J}(\text{Tl}-\text{H})_{\text{cis}}$, $^3\text{J}(\text{Tl}-\text{H})_{\text{trans}}$ in bis(vinyl)thallium(III) compounds all have the same sign, as reported by Maher³⁶ for the sulphate or perchlorate in D_2O solution, and this is not affected by change of anion or solvent.

Where relative signs have been determined, or are known from previous work, these will be indicated in the tables by an appropriate + or - sign. Where no sign is given this

implies that it has not been determined, not that it is positive. This is to avoid the use of $|J(Tl-X)|$ ($X = C, H, F$) for convenience.

4.2.2. Assignment of carbon-13 and proton spectra

Spectra were generally first-order, facilitating assignments. Assignment was based on multiplicity of fine structure, chemical shifts and by analogy with the spectra of key compounds which were assigned by more elaborate methods. Several of these methods will now be described. Assignment of the proton spectrum of bis(cyclopropyl)isobutyrate-thallium(III) was assisted by computer simulation and this will be described in detail.

4.2.2.1. Comparison of NMR spectra obtained at different magnetic fields

Comparison of carbon-13 spectra obtained at two different magnetic fields allowed identification of thallium-carbon coupling constants and carbon-13 chemical shifts. This is because the coupling constant is independent of operating field/frequency whereas the chemical shift is not. One-bond thallium-carbon couplings are generally so large ($>1800\text{Hz}$) that separate coupling to ^{203}Tl and ^{205}Tl is resolved. This results in a characteristic appearance for this coupling eg. see proton decoupled carbon-13 spectra of bis(cyclopropyl)-bromothallium(III) (FIG 4.4a) and bis(cyclohexylmethyl)-bromothallium(III) (FIG.4.7). One bond coupling is thus easily identified. However in one case, $\text{CH}_3\text{CH}(\text{OCH}_3)\text{CH}_2(\text{CH}_3)\text{TlOCOCH}_3$, (FIG 4.8) two $^1J(\text{Tl}-\text{C})$ couplings were present, (to CH_3 and CH_2 respectively). Comparison of spectra obtained at 201 MHz, 45.28MHz

(Continuous wave)

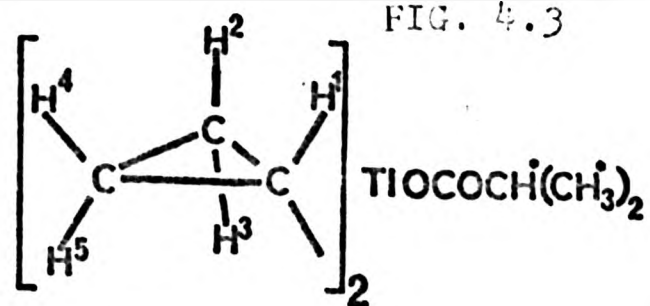
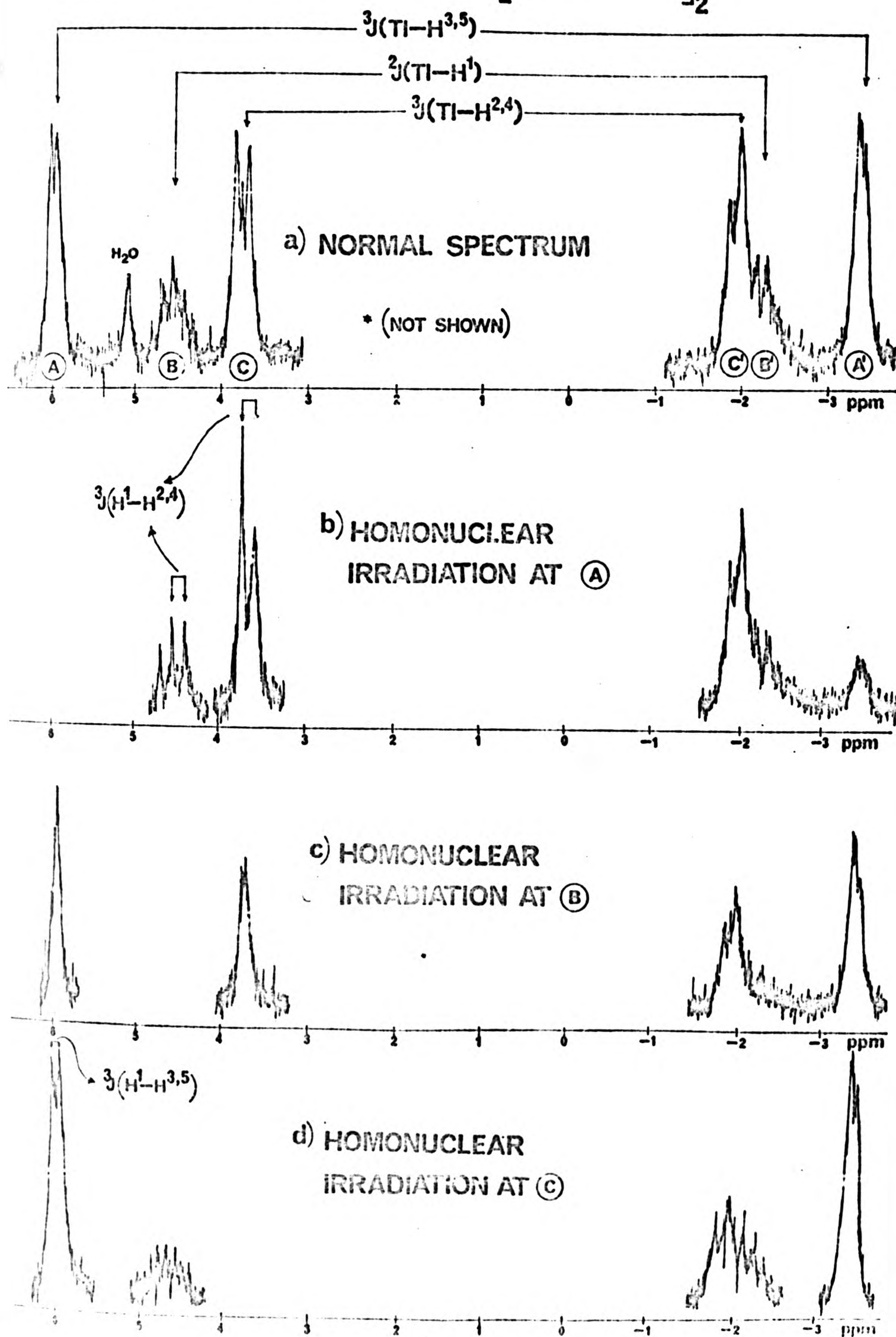


FIG. 4.3



^{13}C SPECTRA AT 22.63 MHz OF

FIG. 4.4.

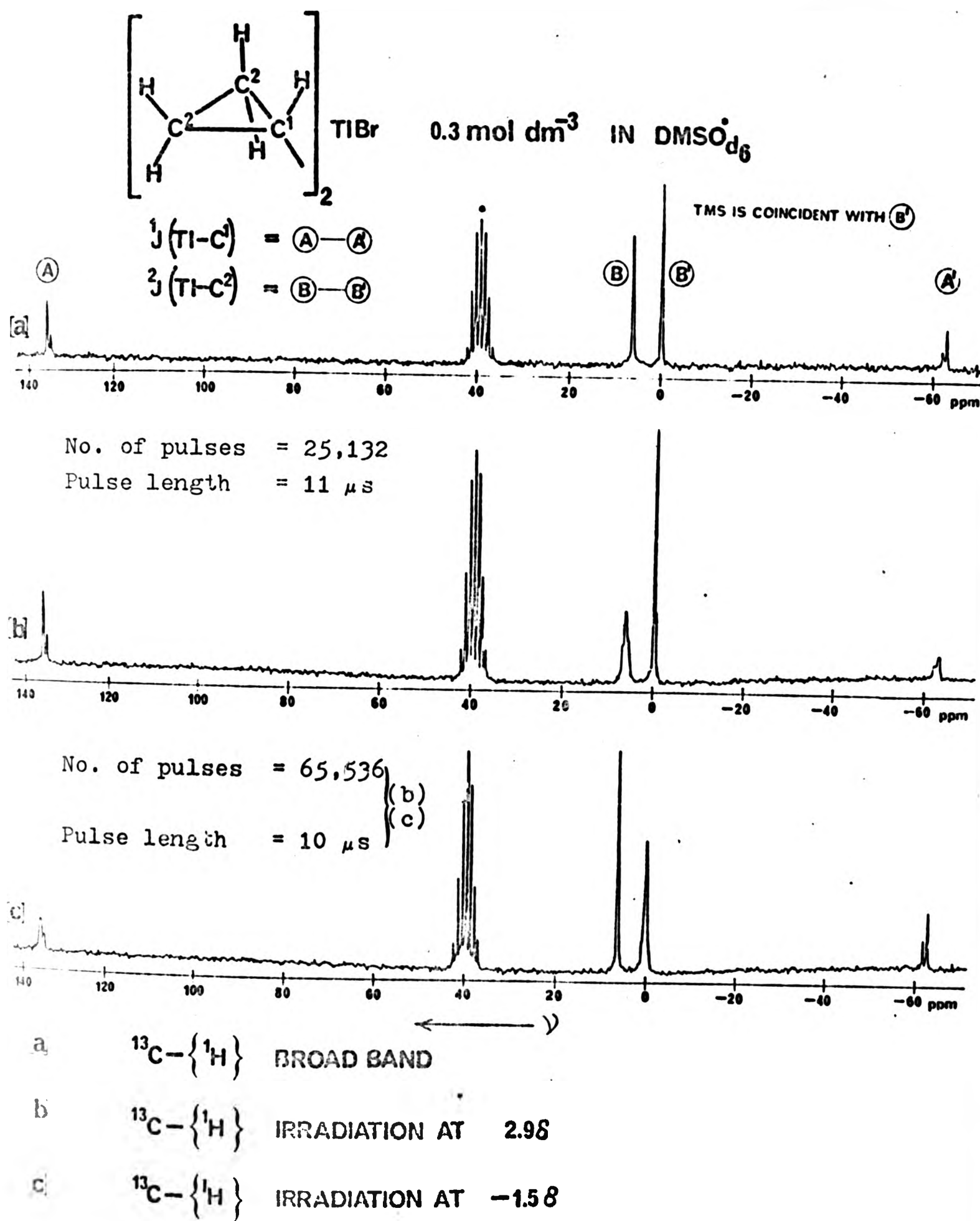
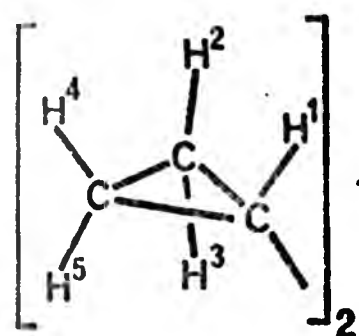


FIG 4.5

^1H SPECTRA AT 60MHz OF



$\text{TiOCOCH}(\text{CH}_3)_2$ 0.3 mol dm^{-3} IN PYRIDINE-d_5

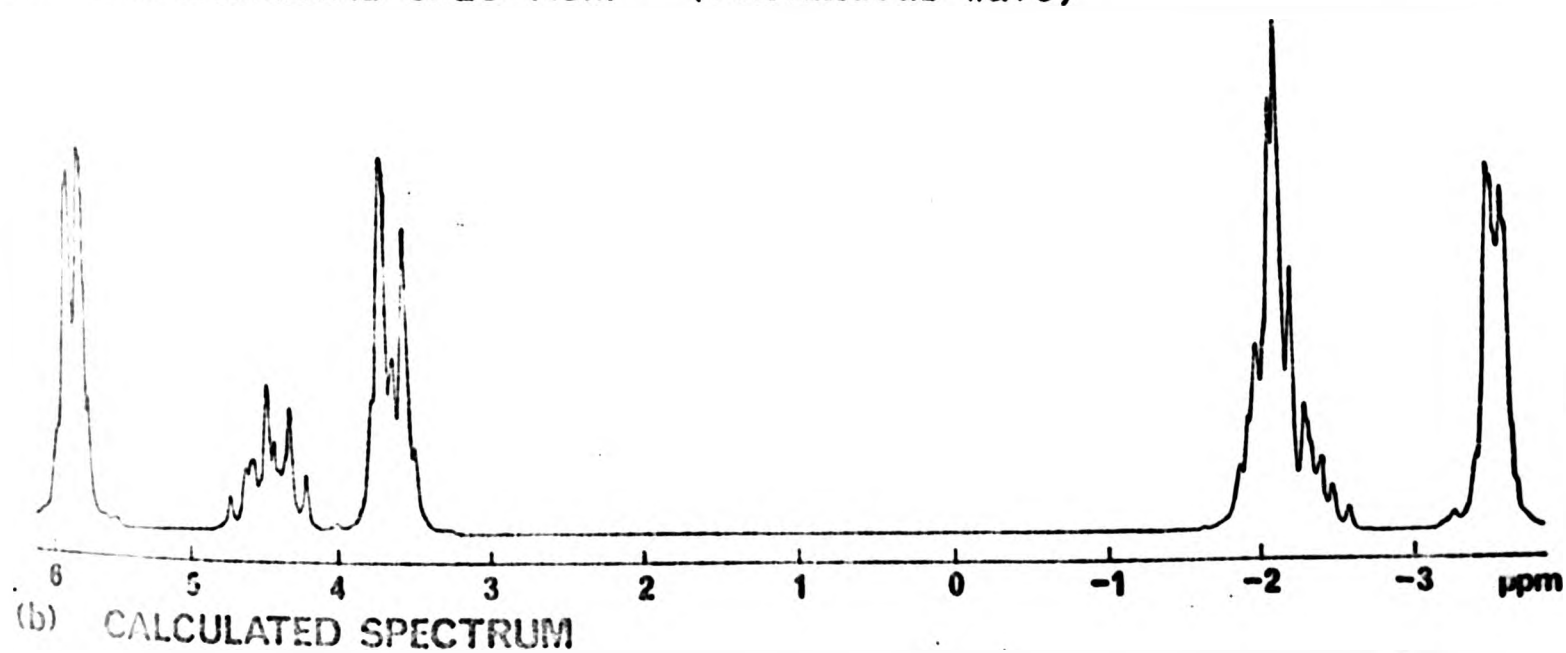
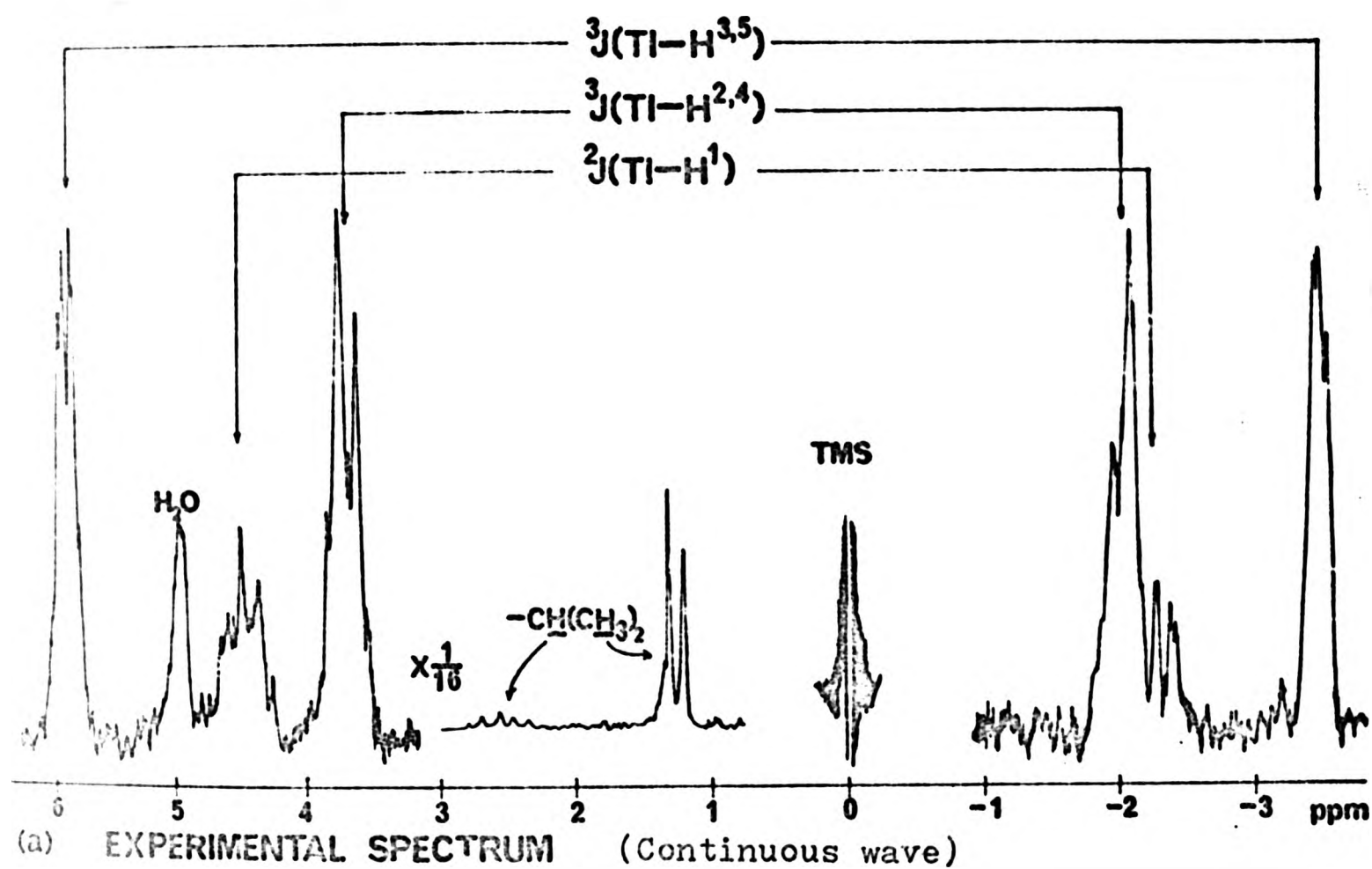
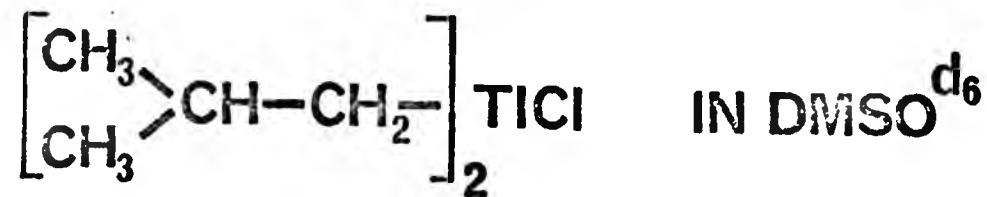


FIG 4.6.

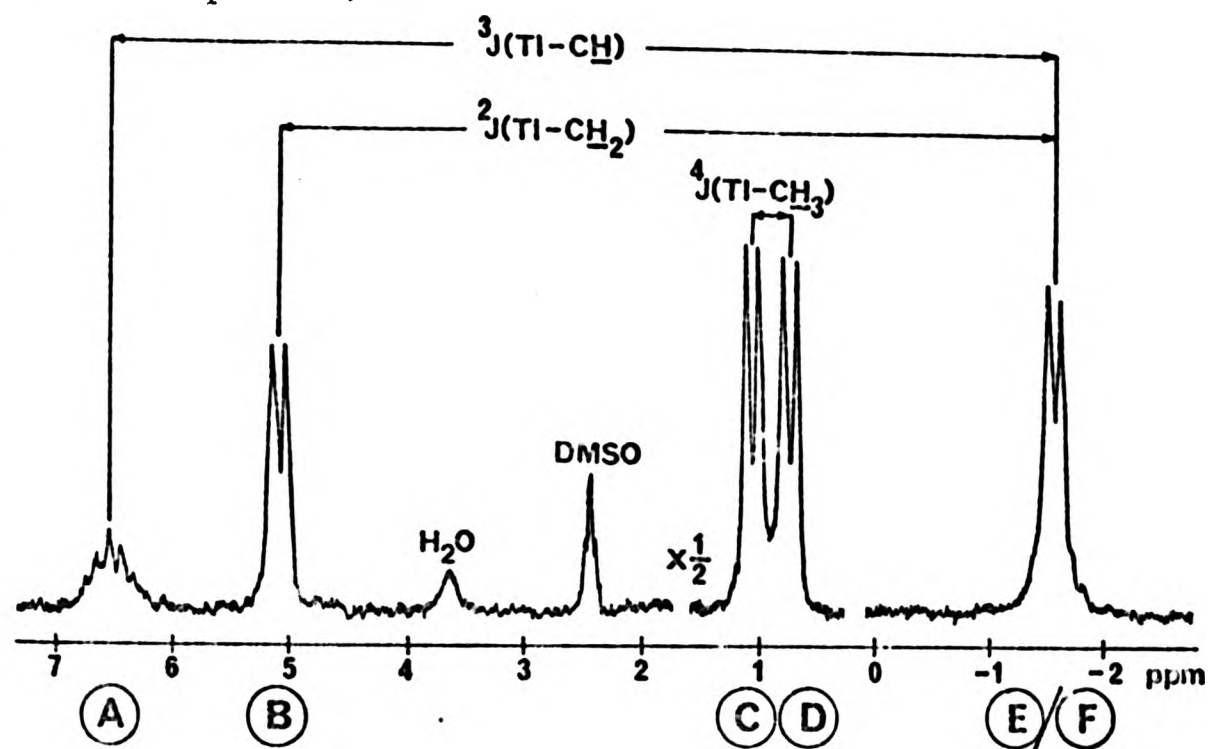
DETERMINATION OF RELATIVE SIGNS OF THALLIUM-PROTON COUPLING CONSTANTS

FOR

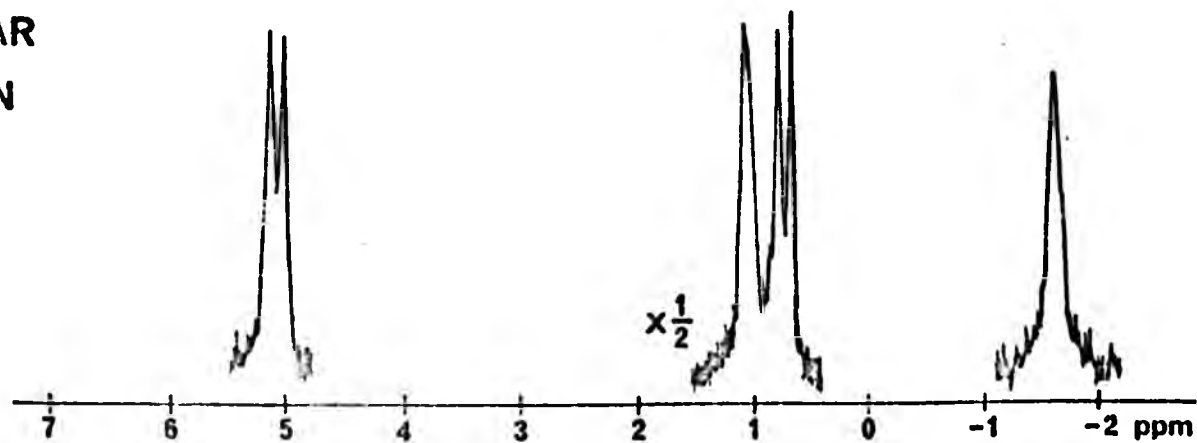


(Continuous wave spectra).

(a) NORMAL ^1H
SPECTRUM
AT 60 MHz



(b) HOMONUCLEAR
IRRADIATION
AT (A)



(c) HOMONUCLEAR
IRRADIATION
AT (E)/(F)

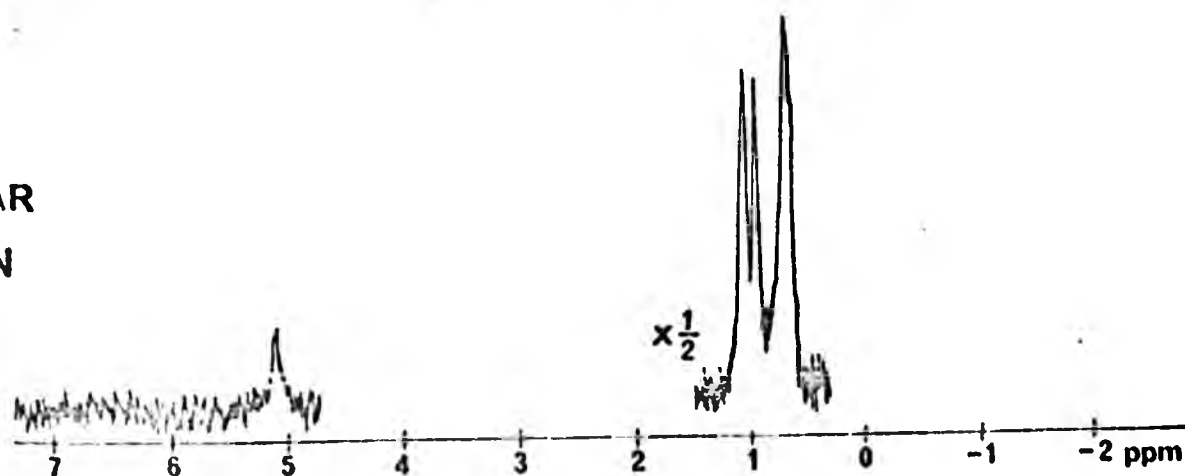
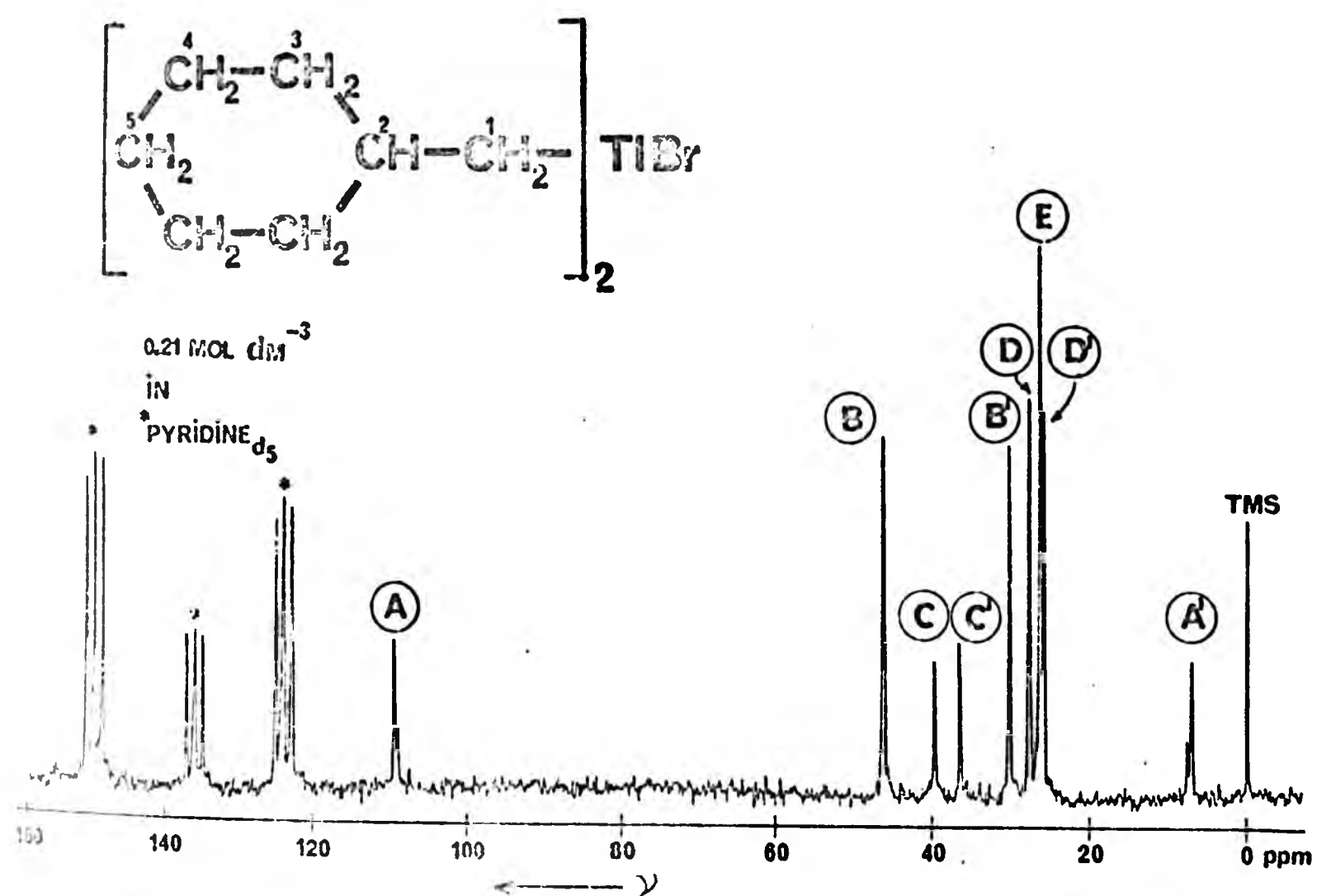


FIG. 4.7.

PROTON DECOUPLED ^{13}C SPECTRUM
AT 22.63 MHz OF :



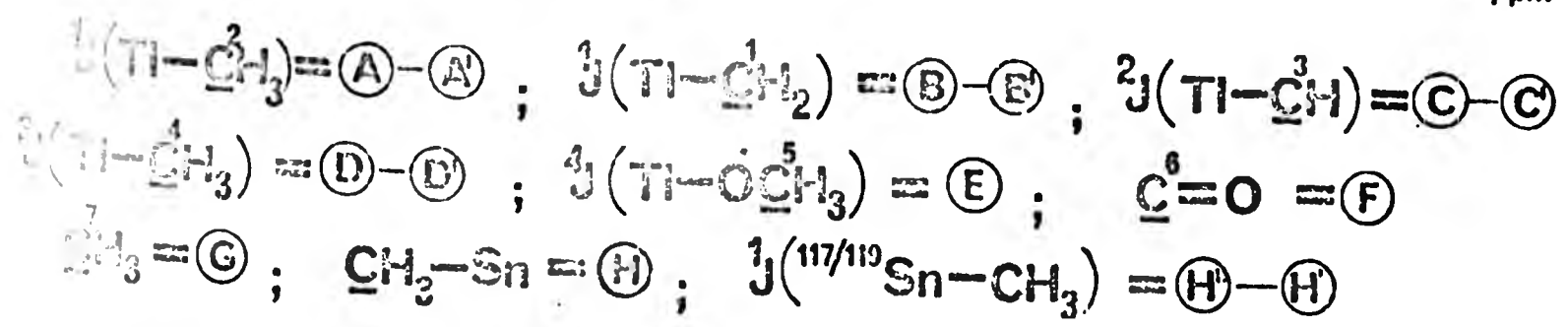
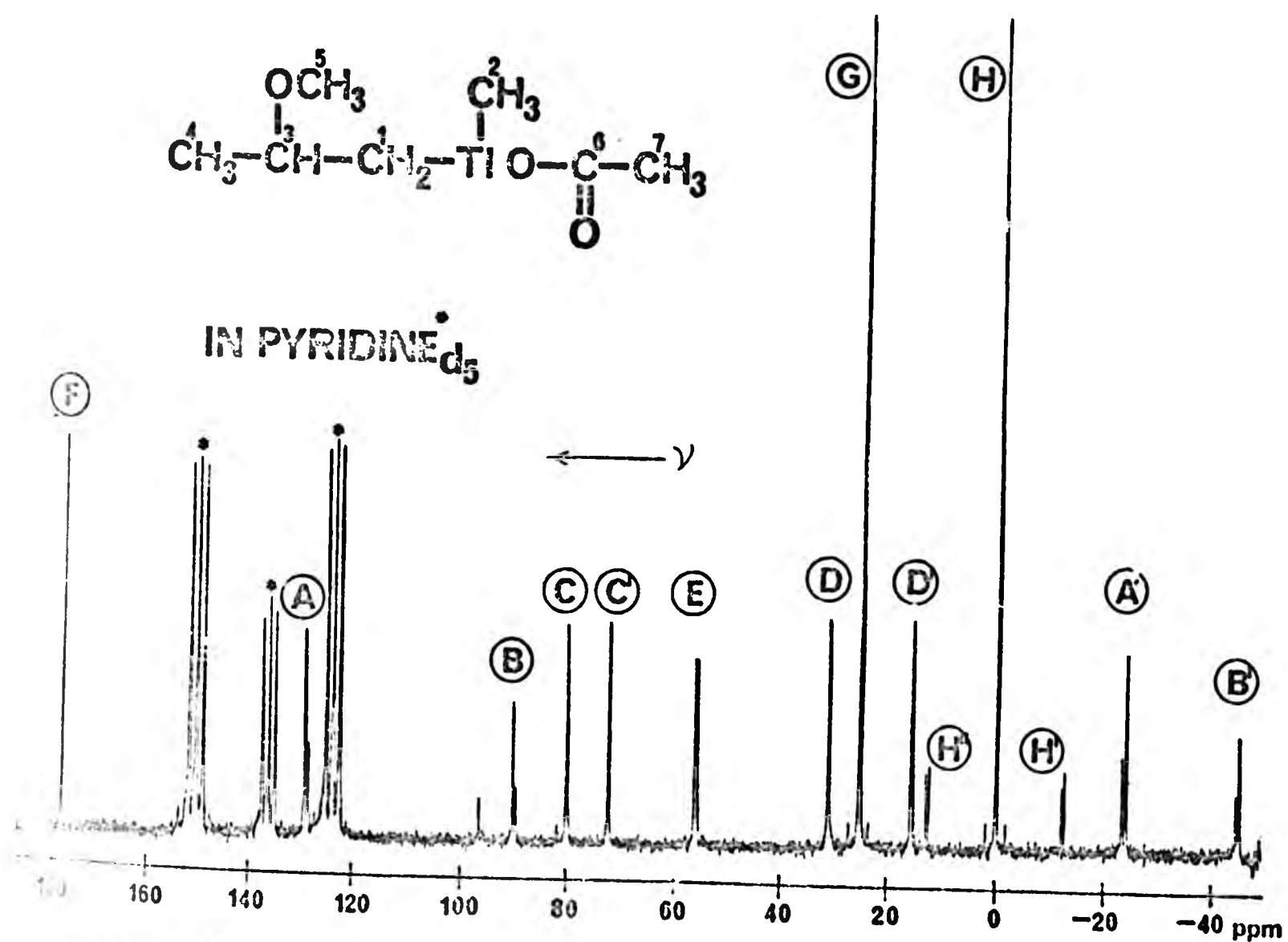
$$\begin{aligned} {}^1\text{J}(\text{Ti}-\text{C}_1) &= \text{A}-\text{A}' ; & {}^2\text{J}(\text{Ti}-\text{C}_2) &= \text{C}-\text{C}' ; & \text{C}_5 &= \text{E} \\ {}^3\text{J}(\text{Ti}-\text{C}_3) &= \text{B}-\text{B}' ; & {}^4\text{J}(\text{Ti}-\text{C}_4) &= \text{D}-\text{D}' ; \end{aligned}$$

Number of pulses = 12,222

Pulse length = 10 μs

FIG. 4.8.

PROTON DECOUPLED ^{13}C SPECTRUM AT 20.1 MHz OF



No. of pulses = 20,000

Pulse length = $3\mu\text{s}$

and $^{13}\text{C}-\{^1\text{H}\}$ off resonance spectra were used in the assignment (TABLE 4.2).

Proton spectra were obtained at 60MHz(1.4T) and the use of higher fields for assignment of these spectra was unfavourable due to relaxation effects at the coupled thallium nucleus. This will be discussed in detail in Chapter 5.

4.2.2.2. Use of the general nuclear Overhauser effect

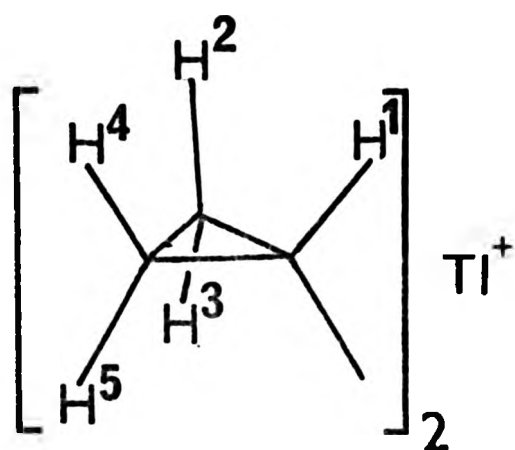
Thallium-proton coupling constants are generally very large eg. $^3\text{J}(\text{Tl-H})$ typically 600Hz. The component multiplets are often broad with a lack of detailed fine structure. This is due to overlap of components arising from ^1H coupled nuclei to both isotopes of thallium (^{203}Tl , ^{205}Tl) and broadening originating from relaxation processes at the thallium nucleus (See Chapter 5). As a result it is often difficult to pick out 'pairs' of signals arising from thallium-proton spin-spin coupling. The problem of this 'pairing' of signals is illustrated by the ^1H spectra of bis(sec-butyl)chlorothallium(III), (FIG 4.22),

and bis(cyclopropyl)isobutyrate thallium(III)(FIG 4.3). Anet⁹² has described the use of the general nuclear Overhauser effect²⁸⁵ in assignment of the proton spectra of norbornene- and norbornane-derivatives of thallium(III). This technique was used extensively in the present work and was extremely valuable in assisting 'pairing' of signals in the proton spectra of organothallium(III) compounds. In most cases it has obviated the need for comparison of spectra obtained at two different fields in order to assign thallium-proton couplings. This is especially important since higher fields generally give broader spectra. (see Chapter 5). Irradiation of one component of $^n\text{J}(\text{Tl-H})$ in an $^1\text{H}-\{^1\text{H}\}$ experiment causes collapse of any fine structure and eventual

disappearance of the other component as B_2 is increased. Other signals may be perturbed, but not eliminated if coupled to the irradiated signals. (See 4.2.1). The positions of other obscured components can often also be located by this method.

4.2.2.3. Assignment of the proton spectrum of bis(cyclopropyl)-isobutyrateothallium(III)

The proton spectrum of bis(cyclopropyl)isobutyrateothallium(III) is rather complex and shows second order features. (FIG 4.3). An attempt was made to carry out a detailed analysis. It was necessary to use double resonance techniques in the assignment and the derived parameters were used in a computer simulation of the spectrum. The system is characterised by the following ^1H coupling constants and chemical shifts:



$$^2J(\text{Tl}-\text{H}^1)$$

$$^3J(\text{Tl}-\text{H}^2) = ^3J(\text{Tl}-\text{H}^4)$$

$$^3J(\text{Tl}-\text{H}^3) = ^3J(\text{Tl}-\text{H}^5)$$

$$^3J(\text{H}^1-\text{H}^2) = ^3J(\text{H}^1-\text{H}^4)$$

$$^3J(\text{H}^1-\text{H}^3) = ^3J(\text{H}^1-\text{H}^5)$$

$$^2J(\text{H}^2-\text{H}^3) = ^2J(\text{H}^4-\text{H}^5)$$

$$^3J(\text{H}^2-\text{H}^5) = ^3J(\text{H}^3-\text{H}^4)$$

$$\delta_{\text{H}^1}$$

$$\delta_{\text{H}^2} = \delta_{\text{H}^4}$$

$$\delta_{\text{H}^3} = \delta_{\text{H}^5}$$

$$^3J(\text{H}^2-\text{H}^4)$$

$$^3J(\text{H}^3-\text{H}^5)$$

Results of integration and ^1H - $\{^1\text{H}\}$ experiments allows pairing of signals as shown in FIG 4.3(a). The assignments are made assuming that $^3J(\text{Tl-H})_{\text{cis}}$ i.e. $^3J(\text{Tl-H}^{3,5})$ is greater than $^3J(\text{Tl-H})_{\text{trans}}$ i.e. $^3J(\text{Tl-H}^{2,4})$ by analogy with the corresponding couplings in the systems:- (cyclopropyl) $_n^{\text{M}}$ (M = Sn, Pb, Hg, F; n = 1-4).²⁸⁶

^1H - $\{^1\text{H}\}$ experiments indicate that $^2J(\text{Tl-H}^1)$ and $^3J(\text{Tl-H}^{3,5})_{\text{cis}}$ and $^3J(\text{Tl-H}^{2,4})_{\text{trans}}$ have the same signs (See FIG 4.3.)

^{13}C - $\{^1\text{H}\}$ experiments show that $^1J(\text{Tl-C})$ (see FIG 4.4) and $^2J(\text{Tl-H}^1)$ have the same signs. On the assumption that one-bond Tl-C coupling has a positive sign,¹¹ this yields positive signs for all three $J(\text{Tl-H})$ couplings, and shows that $^2J(\text{Tl-C})$ has opposite signs to both

$^3J(\text{Tl-H}^{3,5})_{\text{cis}}$ and $^3J(\text{Tl-H}^{2,4})_{\text{trans}}$. Irradiation of signal A in FIG 4.3(b) the lowfield component of $^3J(\text{Tl-H}^{3,5})_{\text{cis}}$, removes coupling of H^3H^5 with the remaining protons. This reveals the lowfield component of H^1 as a triplet due to coupling to H^2 and H^4 and the lowfield component of $^3J(\text{Tl-H}^{2,4})_{\text{trans}}$ as a doublet due to its coupling to H^1 . The appropriate roofing is apparent. Thus a value for $^3J(\text{H}^1-\text{H}^2) = ^3J(\text{H}^1-\text{H}^4)$ can be estimated.

Irradiation of signal C in FIG 4.3 (d) (the lowfield component of $^3J(\text{Tl-H}^{2,4})_{\text{trans}}$), removes coupling between H^2H^4 and the remaining protons. The remaining doublet A yields a value for $^3J(\text{H}^1-\text{H}^3) = ^3J(\text{H}^1-\text{H}^5)$. The values obtained for $^3J(\text{H}^1-\text{H}^{2,4})$ and $^3J(\text{H}^1-\text{H}^{3,5})$ are similar to reported values for analogous coupling in other metal-cyclopropyl systems.²⁸⁶ The signs of all $^3J(\text{H-H})$ vicinal couplings are assumed to be positive.²⁸⁸

Using a first-order analysis, direct measurements were made of the following parameters:-

$$\begin{array}{ll}
{}^2J(\text{Tl-H}^1) & \delta_{\text{H}^1} \\
{}^3J(\text{Tl-H}^2) = {}^3J(\text{Tl-H}^4) & \delta_{\text{H}^2} = \delta_{\text{H}^4} \\
{}^3J(\text{Tl-H}^3) = {}^3J(\text{Tl-H}^5) & \delta_{\text{H}^3} = \delta_{\text{H}^5} \\
{}^3J(\text{H}^1\text{-H}^2) = {}^3J(\text{H}^1\text{-H}^4) & \\
{}^3J(\text{H}^1\text{-H}^3) = {}^3J(\text{H}^1\text{-H}^5) &
\end{array}$$

The four remaining J(H-H) coupling constants were taken from those reported for bis(cyclopropyl)mercury(II).²⁸⁹ It has been reported that J(H-H) coupling constants in cyclopropyl-X systems depends on the electronegativity of X (X = Sn, Pb, Hg, Li).²⁸⁹ The values for the mercury compound were chosen because the electronegativity of thallium is close to that of mercury. Reported values of J(H-H) coupling constants for Hg, Pb, Sn cyclopropyl derivatives show only slight variation as the metal is changed.²⁸⁹ The geminal couplings ${}^2J(\text{H}^4\text{H}^5) = {}^2J(\text{H}^2\text{H}^3)$ are assumed to be negative.²⁸⁸

The following determined and assumed (* indicated thus) parameters were used as input to the LAGCOON 1968²⁷⁸ spectral simulation computer programme. The best values (in Hz) obtained as output, by iterating on selected input parameters are given in parentheses.

$$\begin{array}{llll}
{}^2J(\text{Tl-H}^1) & & = & 405.13(405.13) \\
{}^3J(\text{Tl-H}^2) = {}^3J(\text{Tl-H}^4) & & = & 340.06(340.06) \\
{}^3J(\text{Tl-H}^3) = {}^3J(\text{Tl-H}^5) & & = & 7.86(7.86) \\
{}^3J(\text{H}^1\text{-H}^2) = {}^3J(\text{H}^1\text{-H}^4) & & = & 9.36(9.36) \\
{}^3J(\text{H}^1\text{-H}^3) = {}^3J(\text{H}^1\text{-H}^5) & & = & 6.32(6.32) \\
{}^2J(\text{H}^2\text{-H}^3) = {}^2J(\text{H}^4\text{-H}^5) & & = & -3.80*(-3.80) \\
{}^3J(\text{H}^2\text{-H}^5) = {}^3J(\text{H}^3\text{-H}^4) & & = & 4.90*(4.90) \\
{}^3J(\text{H}^2\text{-H}^4) & & = & 8.47*(8.47) \\
{}^3J(\text{H}^3\text{-H}^5) & & = & 7.86*(7.86) \\
\delta_{\text{H}^1} & & = & 67.96(66.70)
\end{array}$$

$$\delta H^2 = \delta H^4 = 51.74 (50.90)$$

$$\delta H^3 = \delta H^5 = 73.10 (72.53)$$

The calculated spectrum consists of 141 transitions.

It was only possible to use eighteen experimental line positions in the iterative programme because of broadness of lines in the experimental spectrum. The broadness arising from overlap of spectra due to separate coupling to ^{203}Tl and ^{205}Tl and relaxation processes at the thallium nucleus makes assignment of all but the most intense transitions dubious.

The experimental and calculated spectra are compared in FIG 4.5. Moderate agreement has been achieved. The computer output from the iterative programme showing experimental and calculated line positions is shown in Appendix II.

4.3. Discussion

4.3.1. The origin of nuclear spin-spin coupling

Nuclear spin-spin coupling arises from the interaction of nuclear moments and is transmitted indirectly through the valence electrons in the molecule. Ramsey²⁹⁰ showed that the indirect coupling between two nuclei, A and B is the sum of three distinct contributions:

$$J_{AB} = J_{AB}(1) + J_{AB}(2) + J_{AB}(3) \quad (4.1)$$

$J_{AB}(1)$ is an orbital contribution which arises from the interaction of orbital electronic currents with nuclear magnetic moments. Each nuclear magnetic moment induces currents in the molecule setting up secondary magnetic fields which will be experienced by other nuclei.

$J_{AB}(2)$ represents the dipole-dipole interactions between the nuclear magnetic moments and the electronic magnetic moments. This interaction polarises electron spins in parts of the molecule near the first nucleus and the magnetic fields associated with the electron spins then act directly on the second nucleus.

$J_{AB}(3)$ represents the Fermi contact contribution and arises from interaction of the nuclear magnetic moment and electrons at the nucleus. Only electrons in s-orbitals have wave functions which are non-zero at the nucleus and so only these will contribute

All of the preceding terms are proportional to the product of the gyromagnetic ratios of the coupled nuclei. This has led to the introduction of a 'reduced' coupling constant K_{AB} , defined as:-²⁹¹

$$K_{AB} = J_{AB} \cdot \frac{2}{\hbar \gamma_A \gamma_B} \quad (4.2)$$

K_{AB} is independent of individual nuclear properties and depends only on the electronic interactions between A and B.

Its units are $\text{N} \text{Å}^2 \text{m}^{-3}$.

Ramsey²⁹⁰ gave detailed expressions for each of these contributions to the coupling constant. McConnell²⁹² used molecular orbital theory to derive approximate but more useful modifications of Ramsey's equations. Pople and Santry²⁹¹ further developed this approach and showed that for coupling involving elements of the first row of the periodic table the contact contribution was dominant. The orbital and dipolar terms were shown to be zero for coupling involving hydrogen nuclei and the orbital contribution to be zero in the absence of multiple bonding between the elements. Pople and Santry²⁹¹ gave the following expression for the contact contribution to coupling between directly bonded nuclei.

$$^1K_{AB} = \frac{64\pi^2}{9} \beta^2 \left| \psi_{ns}(A)(0) \right|^2 \cdot \left| \psi_{ns}(B)(0) \right|^2 \cdot \pi_{AB} \quad (4.3)$$

where β is the Bohr magneton, $\left| \psi_{ns}(0) \right|^2$ is the valence s electron density at the nucleus and π_{AB} is the mutual polarisability of atoms A and B; a measure of the change in electron density in the s-orbital of one atom which arises when the energy of the other s-orbital changes. It is defined as:-

$$\pi_{AB} = \sum_i^{\text{occ.}} \sum_j^{\text{unocc.}} ({}^3\Delta E_{i-j})^{-1} \cdot C_i^s A C_j^s A C_j^s B C_i^s B \quad (4.4)$$

where $({}^3\Delta E_{i-j})$ is the triplet excitation energy between occupied and unoccupied molecular orbitals ψ_i and ψ_j respectively. C is the coefficient of the valence s-electrons of the atom in the molecular orbital. π_{AB} depends on the relative energies of the various electronic excited states. The sign of $^1K_{AB}$ resides in π_{AB} .²⁹³ If $({}^3\Delta E_{i-j})$ is replaced by an average

excitation energy, ΔE , the expression (4.4.) may be written -

$$^1K_{AB} = \frac{64\pi^2}{9} \beta^2 \left| \psi_{ns(A)}^{(0)} \right|^2 \left| \psi_{ns(B)}^{(0)} \right|^2 \alpha^2(A) \cdot \alpha^2(B) \cdot \Delta E^{-1} \quad (4.5)$$

where $\alpha^2(A)$ represents the s-character of the hybrid orbital on A used to form the A-B bond.

Jameson and Gutowsky²⁹⁴ assessed the relative importance of the orbital, dipolar and contact contributions to couplings between carbon, fluorine, protons and other nuclei. They concluded that periodic trends in coupling could be attributed to changes in the contact term. They estimated that the spin-dipolar term would make a contribution of ca.20Hz to $^1J(Tl-C)$ in an isolated carbon-thallium bond. Theoretical studies^{291,294} indicate that the coupling constant K_{AB} between directly bonded elements of group IV of the periodic table should be large and positive when $A=B=^{13}C, ^{29}Si, ^{119}Sn, ^{207}Pb$. Experimental results confirm this and suggest that expression (4.5) may be used to describe the couplings.²⁹⁵

Equation (4.5) can be modified by assuming that

$$\left| \psi_{ns(A)} \right|^2 \propto \frac{Z_A^*}{n_A^3} \quad \text{where } Z_A^*$$

is the effective nuclear charge

of the s-orbital used by the metal atom A in forming the A-B bond and n_A is the principal quantum number of that orbital.

Using such an approach Dalling and Gutowsky²⁹⁶ and Weigert²⁷² calculated $^1K(M-C)$ for $(CH_3)_4M$, ($M = ^{29}Si, ^{63}Ge, ^{119}Sn, ^{207}Pb$) and found good agreement with experiment. Similarly, Mann²⁹⁷ has calculated calculated and experimental one bond metal-carbon coupling constants for $(CH_3)_2M$: ($M = ^{113}Cd, ^{199}Hg$); $(CH_3)_4M$: ($M = ^{119}Sn, ^{207}Pb$) and $(CH_3)_3Tl$. The calculated value of

$^1J(\text{Ti-C})$; 2410Hz, must be compared to the reported value; 1930Hz.¹¹ The agreement between calculated and experimental coupling constants is surprising considering the approximations made in equation (4.5) and modifications of it.

The use of equation (4.5) to describe coupling constants has been criticised in studies of coupling between Pb, Sn and other directly bonded elements,^{267,312} on the basis that it fails to account for cases of K_{AB} which are negative in sign. Mitchell²⁵⁷ has also suggested that the average energy approximation may not be valid for tin-carbon coupling in organotin compounds where the carbon bonded to tin is sp^2 or sp hybridised. In these cases it was suggested that the Pople and Santry²⁹¹ expression (4.3) can be used with the mutual polarisability playing an important role. Then the couplings depend on β_{PbX} and β_{SnX} . Where β is the s overlap integral between lead or tin and X, (X = Sn, Pb, H, B, C, N, P, Se).²⁶⁷ Iwayanagai²⁹⁸ has calculated the mutual polarisabilities of the valence s-electron for $^1K(\text{Hg-C})$, $^2K(\text{Hg-C})$ and $^2K(\text{Hg-H})$ in alkylmercurials using extended Hückel molecular orbital methods. Using equation (4.3) the magnitudes and signs of the couplings were calculated and found to be in agreement with experimental results. Henneike²⁹⁹ carried out similar calculations for one- and two-bond mercury-proton couplings in RHgX (R = CH_3 ; CH_2CH_3) and Barbieri³⁰⁰ has used the method to calculate $^2J(\text{Sn-H})$ in methyltin derivatives.

4.3.2. Effects of solvent and anion on the NMR parameters

As a prelude to discussions of the dependence of the NMR parameters on the number and nature of the organic groups bonded to thallium, it is important to establish the magnitude of anion(X) and solvent induced changes. This investigation was not extensive in respect of solvent, being limited mainly to DMSO and pyridine by solubility considerations. Benzene, methanol and chloroform were used in some cases where suitable. Solubility requirements also limited the number of cases where the effects of anion changes could be measured, particularly for carbon-13 spectra. The anions studied in the case of R_2TlX derivatives were mainly chloride or bromide. In some cases carboxylates, nitrates or tetrafluoroborates were employed as a means of enhancing and extending solubility. The available results confirm that the effects of solvent and anion are generally insufficient to interfere with the discussion of other dependencies. Studies of $RTlX_2$ derivatives were limited mainly to the more stable carboxylate compounds. The solvent and anion dependence of NMR parameters for R_2TlX derivatives are summarised as follows.

Variation of $^nJ(Tl-C)$, ($n = 1-4$), with solvent is $<1\%$ (with the exception of $^1J(Tl-C)$ for bis(ethyl) bromothallium- (III), (TABLE 4.1) where a 19% change between DMSO and pyridine was observed). This is less than the maximum change (25%) reported for $(CH_3)_2TlX$ compounds.¹⁶ The variation of $^nJ(Tl-C)$ with anion (for the same solvent) for $[(CH_3)_3SiCH_2]_2TlX$ ($X = Cl; OCOCH(CH_3)_2$) in pyridine (5%), (TABLE 4.2), and for $(C_6H_5)_2TlX$ ($X = SSCN(C_2H_5)_2; OCOCH_3$) in DMSO ($<18\%$), (TABLE 4.6) are within the ranges previously noted for methyl- ($<4\%$),¹⁶ and aryl- ($<20\%$)¹⁴³ R_2TlX derivatives. Solvent

induced variations in $^nJ(\text{Tl-H})$ ($n = 2-4$) for R_2TlX compounds are $<15\%$ (with the exceptions of $^2J(\text{Tl-H})$ for $[(\text{CH}_2)_2\text{CH}]_2\text{TlBr}$ (20%) and $[(\text{CH}_2)_2\text{CH}]_2\text{TlOCOCH}(\text{CH}_3)_2$ (29%), (TABLE 4.9)); $^3J(\text{Tl-H})$ for $(\text{C}_5\text{H}_9)_2\text{TlBr}$ (34%) (TABLE 4.9) and $^4J(\text{Tl-H})$ for $[\text{CH}_3\text{CH}_2(\text{CH}_3)\text{CH}]_2\text{TlCl}$ (25%) (TABLE 4.8)). This variation is within the range found for $(\text{CH}_3)_2\text{TlX}$ derivatives ($<16\%$),^{12,16} where $^2J(\text{Tl-H})$ was found to increase in the order: non-polar solvent $<$ pyridine $<$ DMSO. Such a trend was also observed here although there are exceptions, ($[(\text{CH}_2)_2\text{CH}]_2\text{TlX}$; $\text{X} = \text{Br}$; $\text{OCOCH}(\text{CH}_3)_2$, TABLE 4.9) where the order for pyridine and DMSO is reversed. Anion changes were found to have only slight ($<8\%$) effects on $^nJ(\text{Tl-H})$, ($n = 2-4$), close to the variation previously reported for $(\text{CH}_3)_2\text{TlX}$ ¹⁶ and $(\text{C}_6\text{H}_5)_2\text{TlX}$ ¹⁴³ (with the exception of $^3J(\text{Tl-H})$ for $[(\text{CH}_3)_2\text{CHCH}_2\text{CH}_2]_2\text{TlX}$ ($<16\%$); TABLE 4.8). Solvent and anion effects on chemical shifts are small and within the ranges previously reported ($<6\text{ppm}$ for $\delta(^{13}\text{C})$ and $<0.9\text{ppm}$ for $\delta(^1\text{H})$)^{12,16,143} There is insufficient data to permit reliable assessment of the solvent anion and concentration dependence of carbon-13 and proton NMR parameters for RTlX_2 derivatives. The few available results suggest that changes are likely to be similar to those summarised for R_2TlX derivatives.

The variation of spin-spin coupling constants and chemical shifts with concentration were not investigated because these parameters were previously¹⁶ shown to have negligible concentration dependence in $(\text{CH}_3)_2\text{TlX}$ derivatives.

4.3.3. Effect of orbital hybridisation on spin-spin coupling constants involving thallium

Coupling constant results will be discussed in terms of the Fermi contact contribution because the dominance of this term has now been generally accepted for one-bond metal-carbon and geminal metal-proton coupling constants involving heavy metal nuclei of $l = \frac{1}{2}$. The relative importance of the different terms in equation (4.5), ie. ΔE , $|\psi_{ns}(C)|^2$, α^2 , and Z_{eff} , on the magnitude of one-bond metal-carbon and geminal metal-proton coupling constants has been widely discussed for organo-derivatives of Sn^{234,249,257,293,301-304}, Pb^{230,266-269,305,306}, and Hg^{229,264,298,299,304,307-309}.

The approximate expression for the contact contribution to coupling, (4.5) may be written as:-

$$^1J(Tl-X) \propto |\psi_{ns}(Tl)^{(0)}|^2 |\psi_{ns}(X)^{(0)}|^2 \alpha^2(X) \cdot \alpha^2(Tl); \Delta E^{-1} \quad (4.6)$$

Under certain circumstances some terms in expression (4.6) can be assumed to be constant. If the organo group R is fixed for the series $R_3Tl, R_2TlX, RTlX_2$ (R = organo group; X = anion) then the terms $|\psi_{ns}(X)^{(0)}|^2$; $\alpha^2(X)$ and ΔE can be assumed to be constant for this series. Thus variation in $J(Tl-X)$ for this series may be ascribed to changes in $|\psi_{ns}(Tl)^{(0)}|^2$ and $\alpha^2(Tl)$. Equating $\alpha^2(Tl)$ with the square of the coefficient of the thallium 6s orbital in the thallium hybrid orbitals and using the proportionality of $|\psi_{6s}(Tl)^{(0)}|^2$ and $(Z_{eff})^3$ (where Z_{eff} is the effective nuclear charge on the thallium atom and is approximated by $(Z_0 Z)^{\frac{1}{2}}$; Z_0 = Slater screened nuclear charge and Z = nuclear charge), the product $(Z_{eff})^3 \cdot \alpha^2(Tl)$ may be calculated for the series $R_3Tl, R_2TlX, RTlX_2$. In this series the hybridisation of thallium

is considered to be sp^2 , sp and $'s'$ respectively.⁸⁶ The values of the product $(Z_{eff})^3 \times \alpha^2(Tl)$ for the same series are 1.0; 1.7; 3.37 respectively. Since $J(Tl-X)$ will be proportional to $(Z_{eff})^3 \times \alpha^2(Tl)$ then we might expect the ratio of coupling constants for the series to be in the same ratio as the values of this product.

Only R_2TlX and $RTlX_2$ compounds were examined in this study and the ratio of coupling constants in these two series could be predicted to be 1.0:2.2. Great caution must be used in comparing observed and calculated ratios in view of the approximations involved, especially that only the thallium $6s$ orbital is used in bonding⁸⁶ and concerning the hybridisation of thallium. The essentially linear C-Tl-C unit found in R_2TlX derivatives,^{62,127-131,134-136} where thallium is sp hybridised,⁸⁶ is paralleled in the near-linear (168°) C-Tl-O unit found in cyclopropyl bis(isobutyrate)thallium(III) (Chapter 6). The short Tl-O bond length (2.125\AA) found in this unit compared to other Tl-O bonds ($2.568-2.718\text{\AA}$) in the same compound (Fig. 6.3) reflects the strength of this bond and the preference of thallium for this linear configuration. Such a configuration suggests an sp hybridised thallium and the proposed $'s'$ hybridisation for RTl^{2+} compounds⁸⁶ may be misleading.

The ratios of the coupling constants $^1J(Tl-C)$ and $^nJ(Tl-H)$ ($n = 1-3$) for the series $RTlX_2$ and R_2TlX ($R = \text{alkyl, branched alkyl, alicyclic, alkenyl, aryl; } X = \text{anion}$) are presented in TABLE 4.12. An attempt was made to keep the anion and solvent the same when comparing $RTlX_2$ and R_2TlX . However this was not always possible and details are given in TABLE 4.12.

Continuation of the ratios for $^1J(Tl-C)$ in TABLE 4.12 for the

Table 4.12 Observed ratios of $J(\text{TL-C})$ and $J(\text{TL-H})$ respectively in RLX_2 and R_2PLM derivatives a

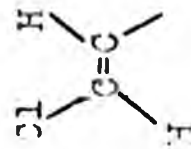
R	$\frac{1}{2}J(\text{TL-C})$	$\frac{2}{3}J(\text{TL-C})$	$\frac{3}{4}J(\text{TL-C})$	$\frac{2}{3}J(\text{TL-H})$	$\frac{3}{4}J(\text{TL-H})$	$\frac{4}{5}J(\text{TL-H})$
CH_3	2.38-2.24 ^b			2.23 ^c		
CH_3CH_2	2.31 ^d	1.55 ^d		2.69 ^e	2.66 ^e	
$(\text{CH}_3)_2\text{CHCH}_2$ ^f				2.07-2.35 ^g	3.22-3.51 ^g	
$(\text{CH}_3)_2\text{CHCH}_2\text{CH}_2$ ^f				2.27-2.38 ^h	2.80-3.11 ^h	
$(\text{CH}_3)_3\text{CCH}_2$	2.18 ⁱ	12.04 ⁱ	2.06 ⁱ	1.60 ⁱ	-	2.19 ⁱ
$(\text{CH}_3)_3\text{SiCH}_2$	1.82 ^j		1.89 ^j	2.04 ^k	-	1.72 ^k
$(\text{CH}_2)_2\text{CH}$	2.18 ^m	2.30 ^m		1.35 ⁿ	$\left\{ \begin{array}{l} 2.27\text{cis}^n \\ 2.28\text{trans}^n \end{array} \right.$	
$\text{H}_2\text{C=CH}$	1.73-1.79 ^p	1.82-3.45 ^p		2.27-2.37 ¹	$\left\{ \begin{array}{l} 2.15-2.16\text{cis}^q \\ 2.20-2.25\text{trans}^q \end{array} \right.$	
	1.69 ^r	1.60 ^r		1.77 ^s	2.27 ^s	
C_6H_5	2.00-2.38 ^t	1.57-1.58 ^u	2.15-2.23 ^u		2.10 ^v	2.63 ^v

Table 4.12 Continued

^aRatio is for R_1X_2/R_2X . R = organo group; X = anion. ^bFor $CH_3Tl(OCOCH_3)_2$ in methanol and chloroform (Table 4.5) compared to $(CH_3)_2TlOCOCH_3$ in D_2O . All data from ref. 12. ^cFor $CH_3Tl(OCOCH_3)_2$ in methanol (Table 4.11) compared to $(CH_3)_2TlOCOCH_3$ in methanol. All data from ref. 12. ^dFor $CH_3CH_2TlOCOCH(CH_3)_2$ in DMSO (Ref. 253), (Table 4.5); compared to $(CH_3CH_2)_2TlOCOCH_3$ in DMSO (Ref. 310). ^eFor $CH_3CH_2TlOCOCH(CH_3)_2$ compared to $(CH_3CH_2)_2TlOCOCH(CH_3)_2$ in chloroform. All data from ref. 89. ^fNo carbon-13 data available. ^gFor $(CH_3)_2CHCH_2Tl[OCOCH(CH_3)_2]_2$ in methanol (Table 4.11) compared to $[(CH_3)_2CHCH_2]_2TlCl$ in the solvents DMSO, pyridine and benzene respectively. (Table 4.8). ^hFor $(CH_3)_2CHCH_2Tl(OCOCH_3)_2$ in methanol. (Table 4.11) compared to $[(CH_3)_2CHCH_2]_2TlOCOCH_3$ in the solvents DMSO, pyridine, benzene respectively (Table 4.8). ⁱFor $(CH_3)_3CCH_2TlX$; (X = Cl and/or Br) in pyridine (Table 4.5) compared to $[(CH_3)_3CCH_2]_2TlCl$ in pyridine (Table 4.2). ^jFor $(CH_3)_3SiCH_2Tl[OCOCH(CH_3)_2]_2$ in CD_2Cl_2/CH_2Cl_2 (Table 4.5) compared to $[(CH_3)_3SiCH_2]_2TlOCOCH(CH_3)_2$ in pyridine (Table 4.2). ^kFor $(CH_3)_3SiCH_2Tl[OCOCH(CH_3)_2]_2$ in chloroform (Table 4.11) compared to $[(CH_3)_3SiCH_2]_2TlOCOCH(CH_3)_2$ in chloroform (Table 4.8). ^mFor $(CH_2)_2CHTl[OCOCH(CH_3)_2]_2$ in DMSO (Table 4.5) compared to $[(CH_2)_2CH]_2TlOCOCH(CH_3)_2$ in pyridine (Table 4.3). ⁿFor $(CH_3)_2CHTl[OCOCH(CH_3)_2]_2$ in pyridine (Table 4.11) compared to $[(CH_2)_2CH]_2TlOCOCH(CH_3)_2$ in pyridine (Table 4.9). ^pFor $CH=CHTlCl_2$ in methanol (Table 4.5) compared to $(H_2C=CH)_2TlOCOCH_3$ in pyridine and $(H_2C=CH)_2TlBF_4$ in DMSO (Table 4.4). ^qFor $CH_2=CHTlCl_2$ in methanol (Table 4.11) compared to $(H_2C=CH)_2TlOCOCH_3$ and $(H_2C=CH)_2TlBF_4$ respectively in DMSO (Table 4.10). ^rFor trans- $ClCH=CHTlCl_2$ in methanol (Table 4.5) compared to (trans- $ClCH=CH$) $_2TlCl$ in methanol (Table 4.4). ^sFor trans- $ClCH=CHTlCl_2$ in methanol (Table 4.11) compared to (trans- $ClC=CH$) $_2TlCl$ in DMSO (Table 4.10). ^tFor $C_6H_5Tl(OCOCH_3)_2$ in DMSO (ref. 71), (Table 4.6), compared to $(C_6H_5)_2TlX$; (X = SSCN(C_2H_5) $_2$; tropolonato) in DMSO (ref. 143). (Table 4.6). ^uFor $C_6H_5Tl(OCOCH_3)_2$ in DMSO (ref. 66), compared to $(C_6H_5)_2TlX$; (X = SSCN(C_2H_5) $_2$; tropolonato) in DMSO (ref. 143). (Table 4.6). ^vFor $C_6H_5TlCl_2$ in DMSO compared to $[(C_6H_5)_2Tl]_2SO_4$ in D_2O . All data from ref. 86.

series $RTlX_2$ and R_2TlX (R = alkyl, branched alkyl, alicyclic, alkenyl, aryl) shows that in most cases the ratio between couplings is close to the theoretical ratio of coupling constants between $RTlX_2$ and R_2TlX of 2.2:1.0. Although these would seem to be no justification in expecting the same ratio to be found for coupling over more than one-bond it is interesting to note that in the majority of cases the ratio is close to the theoretical value of 2.2 for couplings $^nJ(Tl-C)$ and $^{n+1}J(Tl-H)$, ($n=1-3$).

Using the proportionality of $J(Tl-X)$ and $(Z_{eff})^3 \alpha^2(Tl)$ previously discussed, Maher and Evans predicted the ratio of $^2J(Tl-H)$ in the series: $R_3Tl, R_2TlX, RTlX_2$ (R =alkyl, vinyl, phenyl). Hoad et al.¹² recalculated these ratios and the values of 1.0; 1.3; 2.1 were found to be in better agreement with experimental values of $^1J(Tl-C)$ and $^2J(Tl-H)$ for the above series where $R = CH_3$; $X = COOCH_3$. Wiebel and Oliver²⁸⁷ rationalised changes of $^2J(Tl-H)$ in the series $Li[(Me_3Sn)_nTlMe_{4-n}]$ ($n = 0$ to 4) solely in terms of changes of s-character of thallium. This also gave good agreement with experiment since changes in $(Z_{eff})^3$ were relatively small.

Hybridisation of the carbon atom bonded to thallium is also important in determining the magnitude of thallium-carbon coupling constants. Evidence for this comes from the relative magnitudes of $^1J(Tl-C)$ for R_2TlX derivatives. $^1J(Tl-C)$ is larger for alkenyl- (TABLES 4.4; 4.5) (4173-5828Hz) and aryl-(TABLE 4.6) (4496-5359Hz) derivatives than in n -alkyl (TABLE 4.1) (2416-2991Hz), branched-chain alkyls (TABLE 4.2) (1947-3160Hz) or alicyclic (excluding cyclopropyl) (TABLE 4.3), (1113-2380Hz) compounds. The same relative order of $^1J(Tl-C)$ also may be observed in $RTlX_2$ compounds (TABLE 4.5) for alkenyl-

(8715-9556Hz), aryl- (10718Hz) compared to alkyl- and alicyclic- (excluding cyclopropyl), (3540-6464Hz). The carbon atom bonded to thallium in alkenyl and aryl derivatives is sp^2 hybridised whereas in the alkyl and alicyclics (except cyclopropyl) it is sp^3 hybridised. Carbon atoms in alkenyl and aryl derivatives thus have greater 's' character than those in alkyl and alicyclic (excluding cyclopropyl) compounds. The increased s character at the carbons would be expected to cause an increase in both $\alpha^2(C)$ and $|\psi_{ns}(X)|^2$, ($X = C$), in equation (4.6) leading to larger values of $^1J(Tl-C)$ as observed. The carbon atoms of the cyclopropyl ring are known to exhibit some olefinic character with the hybridisation state of the carbon orbital involved in bonding to substituents between sp^3 and sp^2 but probably closer to sp^2 .³¹¹ The increased s-character of these carbons compared to those in other cycloalkyl and alkyl compounds may be a reason for the larger values for $^1J(Tl-C)$ found in cyclopropyl compounds: R_2TlX (TABLE 4.3) (4496-4552Hz) ; $RTlX_2$ (TABLE 4.5) (9899Hz). One bond tin-carbon coupling in a cyclopropyltin derivative was also found to be larger than in other alicyclotin compounds.³⁹⁹ This was attributed to the greater s-character of the carbon atoms in the cyclopropyl ring compared to the other compounds.

Comparison of $^1J(Tl-C)$ in alkenyl- and aryl-compounds may only be made directly for bis(vinyl)acetatothallium(III) (TABLE 4.4), (5032Hz) and bis(phenyl)acetatothallium(III) (TABLE 4.6), (5295Hz) in DMSO solution. The difference in $^1J(Tl-C)$ indicates that other factors besides hybridisation (sp^2 for carbon and sp for thallium in both cases) are involved. However the difference in $^1J(Tl-C)$ between these

vinyl and phenyl compounds is relatively small compared to the difference between $^1J(\text{Tl-C})$ in these and in alkyl derivatives. No linear correlation between $^1J(\text{Tl-C})$ and $^2J(\text{Tl-H})$ was found here over the whole range of R_2TlX and RTlX_2 ($\text{R} = \text{n-alkyl, branched-chain alkyl, alicyclic, alkenyl}$) derivatives studied. Hoad et al.¹² reported a linear relationship between $^1J(\text{Tl-C})$ and $^2J(\text{Tl-H})$ for the series: $\text{R}_3\text{Tl}, \text{R}_2\text{TlX}, \text{RTlX}_2$ ($\text{R} = \text{CH}_3$; $\text{X} = \text{OOCCH}_3$). The results were discussed in terms of the Fermi contact interaction and the close approach of the line to the origin suggested that common factors dominated the coupling to both carbon and hydrogen. However it has been pointed out by deBoer²⁵³ that such a linear relationship is unnecessary to allow for the dominance of the Fermi contact term in both these couplings.

4.3.4. Relative signs of coupling constants involving thallium

Little is known about the signs, or factors influencing the signs, of heavy metal coupling to carbon or protons associated with different chemical and stereochemical situations. The relative signs of thallium-carbon and thallium-proton coupling constants have been determined here for a variety of alkyl, alicyclic and alkenylthallium(III) derivatives in an attempt to identify some of the factors influencing these signs.

The sign of $^nJ(\text{Tl-C})$ alternates along the carbon chain for straight-chain alkylthallium(III) derivatives R_2TlX , for $\text{R} = \text{CH}_3\text{CH}_2\text{CH}_2$ (TABLE 4.1). $^1J(\text{Tl-C})$ is positive, $^2J(\text{Tl-C})$ negative and $^3J(\text{Tl-C})$ positive. Branching at various positions in the alkyl chain does not alter this sequence, since for $[\text{CH}_3)_2\text{CHCH}_2]_2\text{TlCl}$ (Table 4.2) $^1J(\text{Tl-C})$ is positive, $^2J(\text{Tl-C})$

negative and $^3J(\text{Tl-C})$ positive. Similarly in $[(\text{CH}_3)_2\text{CH}]_2\text{TlCl}$ (Table 4.2) $^1J(\text{Tl-C})$ is positive and $^2J(\text{Tl-C})$ negative. There is evidence that the same sequence is present in alicyclic derivatives (Table 4.3) with $^1J(\text{Tl-C})$ positive and $^2J(\text{Tl-C})$ negative in $[(\text{CH}_2)_2\text{CH}]_2\text{TlBr}$. The same sequence for $^1J(\text{Tl-C})$ and $^2J(\text{Tl-C})$ is found in $[\text{cyclo-C}_6\text{H}_{13}\text{CH}_2]_2\text{TlBr}$. (Table 4.3). During the course of the present work McFarlane⁴⁰⁰ noted the alternation in sign of $^nJ(\text{Sn-C})$ ($n = 1$ to 3) in several alkyl and alicyclic tin derivatives, where $^1K(\text{Sn-C})$ was positive, $^2K(\text{Sn-C})$ negative and $^3K(\text{Sn-C})$ positive.

This alternation of the sign of thallium-carbon coupling along the chain in alkyl systems is in contrast to the situation for alkenyls where, for $(\text{H}_2\text{C}=\text{CH})_2\text{TlPF}_4$, (Table 4.4), both $^1J(\text{Tl-C})$ and $^2J(\text{Tl-C})$ are positive. The sequence in alkylthallium(II) derivatives R_2TlX is analogous to that reported by Ernst⁶⁶ for $\text{PhTl}(\text{OCOCF}_3)_2$ where $^2J(\text{Tl-C})$ is also positive. Additionally, in contrast to alkyl derivatives, $^3J(\text{Tl-C})$ is positive in $\text{PhTl}(\text{OCOCOCF}_3)_2$ while $^4J(\text{Tl-C})$ is negative.

Thallium-proton coupling in alkyl derivatives R_2TlX appears to follow the same pattern as thallium-carbon coupling in these compounds over three bonds. $^2J(\text{Tl-H})$ is negative (for $\text{R} = \text{CH}_3; \text{CH}_3\text{CH}_2; \text{CH}_3\text{CH}_2\text{CH}_2$) while $^3J(\text{Tl-H})$ is positive (for $\text{R} = \text{CH}_3\text{CH}_2; \text{CH}_3\text{CH}_2\text{CH}_2$) (Table 4.7). The presence and position of branching in the alkyl group again does not affect the sequence of signs. $^2J(\text{Tl-H})$ is negative and $^3J(\text{Tl-H})$ positive for R_2TlX ($\text{R} = (\text{CH}_3)_2\text{CH}; (\text{CH}_3)_2\text{CHCH}_2; \text{CH}_3\text{CH}_2(\text{CH}_3)\text{CH}; \text{CH}_3\text{CH}_2\text{CH}_2(\text{CH}_3)\text{CH}; \text{cyclo-C}_6\text{H}_{13}\text{CH}_2$) (Table 4.8). A difference in the sign of $^4J(\text{Tl-H})$ is noted between $[(\text{CH}_3)_2\text{CHCH}_2]_2\text{TlCl}$

where it is positive and $[\text{CH}_3\text{CH}_2(\text{CH}_3)\text{CH}]_2\text{Tl}^+$ where it has a negative sign (Table 4.8).

This change of sign may reflect the stereochemical dependence of coupling in the latter type of system discussed in (4.3.7.2.) The signs of thallium-proton coupling constants determined here for $[(\text{CH}_3)_2\text{CHCH}_2]_2\text{TlCl}$ (Table 4.8) in DMSO solutions are in agreement with those determined by Maher and Evans⁸⁶ for the corresponding sulphates or perchlorates in D_2O .

Thallium-proton couplings in the rigid cyclopropyl system, $[(\text{CH}_2)_2\text{CH}]_2\text{TlOCCCH}(\text{CH}_3)_2$, are different from those in alkyl derivatives in that $^2J(\text{Tl-H})_{\text{gem}}$, $^3J(\text{Tl-H})_{\text{cis}}$ and $^3J(\text{Tl-H})_{\text{trans}}$ in the former compound all have positive signs. The carbon atoms of the cyclopropyl ring are considered to possess a certain degree of olefinic character³¹¹ and it is interesting to compare the positive signs of the thallium-proton couplings in $[(\text{CH}_2)_2\text{CH}]_2\text{TlOCCCH}(\text{CH}_3)_2$ with those signs reported by Maher and Evans⁸⁶ for R_2TlClO_4 and $\text{RTl}(\text{ClO}_4)_2$ ($\text{R} = \text{H}_2\text{C}=\text{CH}$) in D_2O , where $^2J(\text{Tl-H})_{\text{gem}}$, $^3J(\text{Tl-H})_{\text{cis}}$ and $^3J(\text{Tl-H})_{\text{trans}}$ are all positive. However it should be pointed out that the dihedral angles in the vinyl system, $^3J(\text{Tl-H})_{\text{trans}}$ ($\phi = \text{ca. } 180^\circ$), $^3J(\text{Tl-H})_{\text{cis}}$ ($\phi = \text{ca. } 0^\circ$) are close to those expected in the rigid cyclopropyl system: $^3J(\text{Tl-H})_{\text{cis}}$ ($\phi = \text{ca. } 0^\circ$), $^3J(\text{Tl-H})_{\text{trans}}$ ($\phi = \text{ca. } 150^\circ$). This is in contrast to the situation in alkyl groups where we expect the presence of freely rotating alkyl groups.

It appears that the number of organo groups bonded to thallium (and hence the hybridisation of thallium) does not influence the signs of thallium-proton couplings. This is apparent when the signs for the same coupling are compared in

R_2TlX and $RTlX_2$ derivatives. $^2J(Tl-H)$ is negative and $^3J(Tl-H)$ positive in both R_2TlX (Tables 4.7 and 4.8) and $RTlX_2$ (Table 4.11) for $R = CH_3CH_2; (CH_3)_2CHCH_2; (CH_3)_2CHCH_2CH_2$. Further support for this is found in the series R_3Tl, R_2Tl^+, RTl^{2+} ($R = C_6H_5$) where Maher and Evans⁸⁶ report that $^3J(Tl-H)$ ortho, $^4J(Tl-H)$ meta and $^5J(Tl-H)$ para are positive in all cases. A similar situation is found for R_2Tl^+, RTl^{2+} ($R = H_2C=CH$) where thallium-proton couplings are all positive in both cases.⁸⁶

Substitution of chlorine in $(H_2C=CH)_2TlCl$ to give $(trans-ClCH=CH)_2TlCl$ (Table 4.10) does not change the signs of thallium-proton couplings although the magnitudes of the couplings are greatly reduced. An analogous situation is found for the $RTlX_2$ compounds ($R = H_2C=CH; trans-ClCH=CH$). (Table 4.11) (see Fig 4.10 for spectra)

4.3.5. The influence of the organo group on spin-spin coupling constants involving thallium

Consideration of variations in thallium-carbon and thallium-proton coupling constants in organothallium(III) compounds reveals some common patterns.

4.3.5.1. Alkyl derivatives

Coupling, $^nJ(Tl-C)$ ($n=1-4$), in straight-chain alkyl thallium(III) compounds (Table 4.1) follows the pattern:-

$$|^1J(Tl-C)| \gg |^3J(Tl-C)| > |^2J(Tl-C)| > |^4J(Tl-C)|$$

These couplings appear to follow the same pattern in branched-chain alkyl derivatives (Table 4.2) and the position of branching in the alkyl group does not affect the order. A typical $^{13}C\{-^1H\}$ broadband spectrum illustrating this pattern of

thallium-carbon coupling is shown in FIG 4.7 for bis(cyclohexylmethyl)bromothallium(III). Similar coupling patterns for metal-carbon coupling over three bonds have been observed in alkyl derivatives of $\text{Sn}^{242,255,302}$, $\text{Hg}^{261,262}$ and $\text{Pb}^{230,266}$. Thallium-carbon coupling over more than four bonds was not observed here, but Ernst⁶⁶ has noted ${}^6J(\text{Tl}-\text{C})$ in compounds of the type $\text{RC}_6\text{H}_4\text{TlX}_2$ ($\text{R} = \text{alkyl}$; $\text{X} = \text{OCOCF}_3$).

Replacement of a proton by CH_3 in going from $(\text{CH}_3)_2\text{TlNO}_3$ to $(\text{C}_2\text{H}_5)_2\text{TlBr}$ (Table 4.1) results in a decrease of 472Hz in ${}^1J(\text{Tl}-\text{C})$ (for solutions in pyridine). Further substitution by another CH_3 to give $[(\text{CH}_3)_2\text{CH}]_2\text{TlCl}$ (Table 4.2) causes a further decrease of 294Hz in ${}^1J(\text{Tl}-\text{C})$ (for solutions in pyridine). Similar changes in ${}^1J(\text{Tl}-\text{C})$ can be observed in going from $(\text{CH}_3\text{CH}_2\text{CH}_2)_2\text{TlBr}$ (in pyridine) (Table 4.1) to $[\text{CH}_3\text{CH}_2(\text{CH}_3)\text{CH}]_2\text{TlCl}$ (in DMSO) (Table 4.2). In this case ${}^1J(\text{Tl}-\text{C})$ is reduced by 261 Hz. On going from $(\text{CH}_3\text{CH}_2\text{CH}_2\text{CH}_2)_2\text{TlBr}$ (in pyridine) (Table 4.1) to $[\text{CH}_3\text{CH}_2\text{CH}_2(\text{CH}_3)\text{CH}]_2\text{TlCl}$ (in pyridine) (Table 4.2) a reduction of 310 Hz in ${}^1J(\text{Tl}-\text{C})$ is observed. The difference in ${}^1J(\text{Tl}-\text{C})$ coupling to a directly bonded CH_3 group compared to that for a directly bonded CH_2 group can be clearly seen in the ${}^{13}\text{C}\{-{}^1\text{H}\}$ broadband spectrum of $\text{CH}_3(\text{OCH}_3)\text{CHCH}_2(\text{CH}_3)\text{TlOCCCH}_3$ (FIG. 4.8) where both groups are simultaneously bonded to thallium and ${}^1J(\text{Tl}-\text{CH}_3) = 3160 \text{ Hz}$; ${}^1J(\text{Tl}-\text{CH}_2) = 2754 \text{ Hz}$. Reductions in thallium-carbon couplings to carbon atoms more than one bond away from thallium may also be observed on substituting CH_3 for protons. For the change $(\text{CH}_3\text{CH}_2\text{CH}_2)_2\text{TlBr}$ (in pyridine) (Table 4.1) to $[(\text{CH}_3)_2\text{CHCH}_2]_2\text{TlCl}$ (in DMSO) (Table 4.2); ${}^2J(\text{Tl}-\text{C})$ is reduced by 56 Hz. Further substitution to give $[(\text{CH}_3)_2\text{CCH}_2]_2\text{TlCl}$ (in pyridine) (Table 4.2) causes a further reduction in ${}^2J(\text{Tl}-\text{C})$ of 30 Hz. Simultaneously

$^1J(\text{Tl-C})$ is reduced, successively by 79Hz and 60Hz respectively, on going from the n-propyl to the neo-pentyl derivative. Variation of thallium-carbon couplings to the alkyl group of the carboxylate ligands in $\text{Pd-Tl}(\text{OCOR})_5$ ($\text{R} = \text{CH}_3; \text{CH}_3\text{CH}_2; (\text{CH}_3)_2\text{CH}$)⁸⁴ appears to follow the same pattern to that observed here for alkylthallium(III) derivatives. Reductions in $^3J(\text{Tl-C})$ (ca. 13% for terminal carboxylate ligands and ca. 10% for bridging carboxylate ligands) are observed in going from $\text{R} = \text{CH}_3$ to CH_3CH_2 .⁸⁴ Further substitution to give $\text{R} = (\text{CH}_3)_2\text{CH}$ leads to a further reduction in $^3J(\text{Tl-C})$ (ca. 10% for terminal and ca. 11% for bridging ligands).⁸⁴ However for this series $^2J(\text{Tl-C})$ increases for $\text{R} = \text{CH}_3 \rightarrow \text{CH}_3\text{CH}_2 (+17\%) \rightarrow (\text{CH}_3)_2\text{CH} (+15.1\%)$ for coupling to the carbonyl carbon in bridging ligands but remains constant for terminal ligands.⁸⁴

Changes in one-bond thallium-carbon coupling constants in alkyl derivatives on substituting carbon for protons may be rationalised within the framework of the Fermi contact equation. (Equation 4.5) on the following basis. Replacement of protons by methyl groups results in an increased electron donating +I effect for the alkyl group as a whole. This will result in a decrease in the effective nuclear charge at thallium to which the group is bonded and a decrease in the s-character of the C-Tl bond, thus leading to a reduction in the magnitude of $^1J(\text{Tl-C})$. If indeed the effective nuclear charge at thallium is altered by the electron releasing ability of the organo group bonded to it, we might expect to find some correlation between electron releasing ability of this group and $^1J(\text{Tl-C})$. Taft's σ^* constant is a useful measure of the electron releasing ability of an organo group.²³³ A positive value for σ^* indicates a -I effect while a negative value indicates a +I effect for the group. The methyl group has $\sigma^* = 0$. A plot of σ^* , for organo

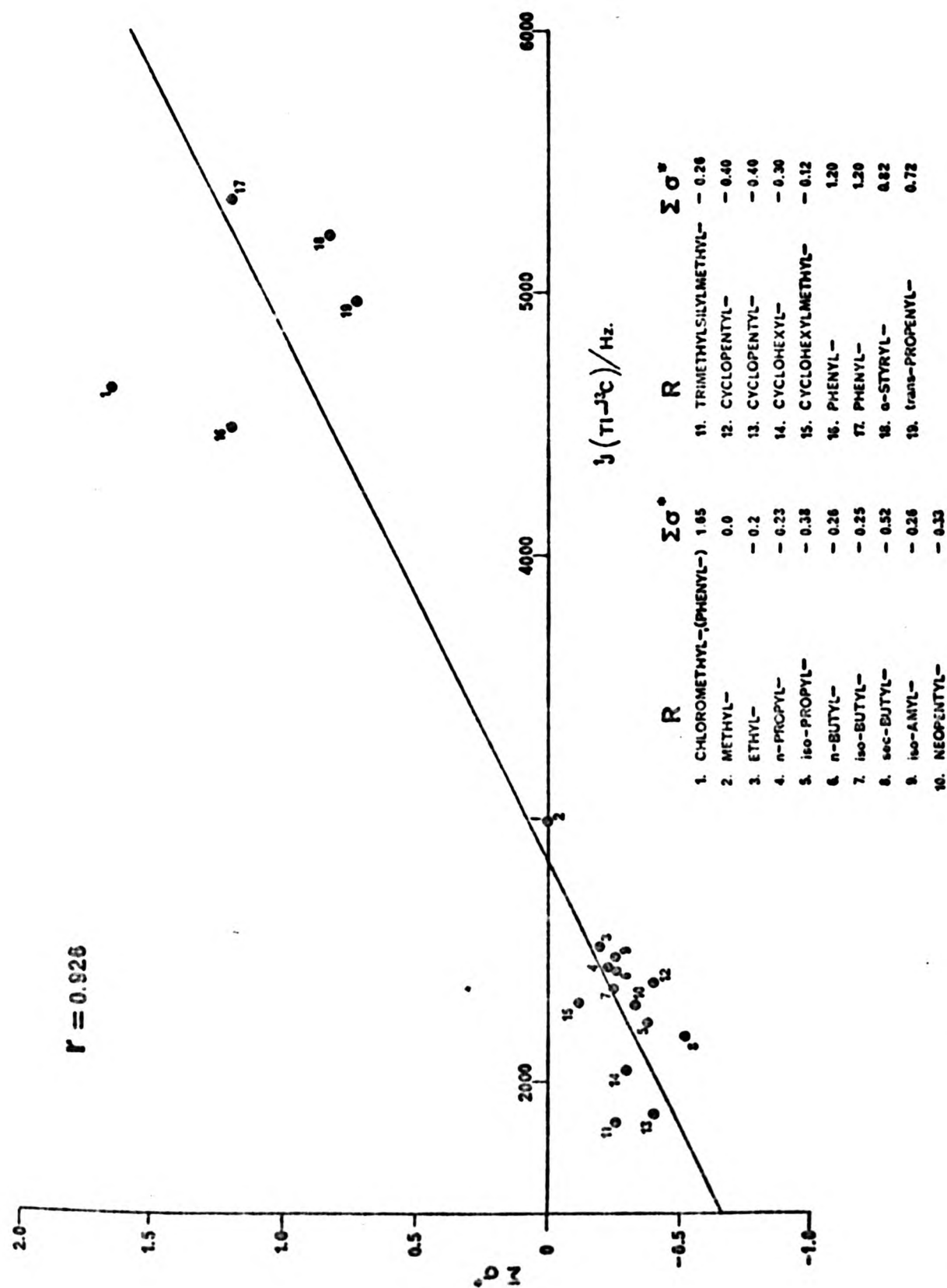
groups bonded to thallium, against $^1J(\text{Tl-C})$ for R_2TlX compounds is shown in FIG 4.9. While there appears to be no detailed correlation between σ^* and $^1J(\text{Tl-C})$ there appears to be a trend of increasing $^1J(\text{Tl-C})$ with increasing electron withdrawing ability of the organo group involved. Mitchell has proposed that in organo derivatives of Sn^{302} and Pb^{230} an increasing +I effect of the organic group bonded to the metal causes a reduction in the effective nuclear charge at the metal and that this is largely responsible for the reduction in metal-carbon couplings observed. For a series of hexaorganoditins³⁰¹ Mitchell has correlated $\sum \sigma^*$ for the organo groups with $^1J(\text{Sn-Sn})$ although Kennedy et al²⁹³ have criticised this on the basis that the changes in $^1J(\text{Sn-Sn})$ are too large to be accounted for on this basis alone. This serves to emphasise the difficulty in separating the effects responsible for variations in coupling in these compounds.

Thallium-proton coupling $^nJ(\text{Tl-H})$ ($n=2$ to 4) follows the order:-

$$|^3J(\text{Tl-H})| > |^2J(\text{Tl-H})| > |^4J(\text{Tl-H})|$$

in both straight-chain (Table 4.7) and branched-chain (Table 4.8) alkyl derivatives R_2TlX . A similar situation is found for RTlX_2 compounds (Table 4.11). The position of branching does not appear to affect the above sequence. The order is different in only one case, $[(\text{CH}_3)_2\text{CHCH}_2\text{CH}_2]_2\text{TlNO}_3$ (Table 4.8) where $|^2J(\text{Tl-H})| > |^3J(\text{Tl-H})|$. Because of the different anions and solvents involved it is difficult to quantify changes in thallium-proton couplings resulting from substitution of carbon for protons in these compounds. However some patterns may be discerned. Substitution of CH_3 for H at the carbon bonded to thallium causes $^2J(\text{Tl-H})$ to become less negative. This can be seen for R_2TlX on going from $\text{R} = \text{CH}_3$ to CH_3CH_2 (Table 4.7)

FIG. 4.9.



Plot of $1J(Tl-C)$ against $\Sigma\sigma^*$ for R_2TlX Derivatives.

to $(\text{CH}_3)_2\text{CH}$ (Table 4.8) and for RtlX_2 on going from $\text{R} = \text{CH}_3$ to CH_3CH_2 . Changes induced by substitution at the β carbon appear to be less regular, with a decrease in $^3\text{J}(\text{Tl-H})$ observed for R_2tlX in going from $\text{R} = \text{CH}_3\text{CH}_2$ to $\text{CH}_3\text{CH}_2\text{CH}_2$ (Table 4.7) followed by an increase in going to $\text{R} = (\text{CH}_3)_2\text{CHCH}_2$ (Table 4.8). $^2\text{J}(\text{tl-H})$ is unaffected by the former change (ethyl to n-propyl) but shows an increase for the latter change (n-propyl to iso-butyl).

4.3.5.2. Alkenyl derivatives

Thallium-carbon coupling $^n\text{J}(\text{Tl-C})$ ($n = 1$ to 3) in alkenylthallium(III) derivatives R_2tlX (Table 4.4) and RtlX_2 (Table 4.5) appear to follow the same pattern as in alkylthallium(III) compounds:

$$|{}^1\text{J}(\text{Tl-C})| \gg |{}^3\text{J}(\text{Tl-C})| > |{}^2\text{J}(\text{Tl-C})|$$

However the magnitude of thallium-carbon couplings in alkenyl and alkyl derivatives are different. $^1\text{J}(\text{Tl-C})$ in alkenyls is approximately twice as large as in alkyl derivatives while $|{}^2\text{J}(\text{Tl-C})|$ in alkenyls is generally smaller than in alkyls though of opposite sign. Interestingly two-bond metal-carbon coupling was not observed in several studies of vinyl derivatives of Sn ,³¹⁰ and Pb ²⁶⁶ although values of $^2\text{J}(\text{Hg-C})$ of ca. 40Hz have been noted in various solvents for $(\text{H}_2\text{C}=\text{CH})_2\text{Hg}$.^{262, 313} Mitchell²⁴⁹ has also noted that two-bond tin-carbon coupling could not be observed in propenyltin compounds. Two-bond metal-carbon couplings are observable in alkenyl derivatives of thallium and mercury because coupling of carbon with these metals is generally larger than in the analogous tin or lead compounds.

Substitution of a CH_3 group for a proton on the α -carbon of $(\text{H}_2\text{C}=\text{CH})_2\text{tl}^+$ to give $[\text{H}_2\text{C}=\text{C}(\text{CH}_3)]_2\text{tl}^+$ (Table 4.4) results in decreases of $^1\text{J}(\text{tl-C})$ of 701-859Hz. $^2\text{J}(\text{tl-C})$ simultaneously

increases by 293-341 Hz for the same systems.

Thallium-proton couplings in alkenyl systems are generally larger than those found in alkyl compounds, both for R_2TlX (Table 4.10) and RtX_2 (Table 4.11) alkenyl derivatives. The order of coupling is generally $^3J(Tl-H) > ^2J(Tl-H)$ as for alkyl systems. Maher and Evans⁸⁶ previously reported thallium-proton coupling constants R_2TlX and RtX_2 ($R = H_2C=CH$; $X = ClO_4^-$) in D_2O and for $(trans-ClCH=CH)_2Tl^+$ (anion not specified) in D_2O . The values reported here for these systems (Table 4.10 and 4.11) involving different anions and/or solvents are of the same order of magnitude as those reported by Maher and Evans above.

It has been established that proton-proton couplings in $H_2C=CHX$ derivatives depend largely on the electronegativity of X .³¹⁴ The proton-proton couplings in such systems decrease in the series: $|^3J(H-H)_{trans}| > |^3J(H-H)_{cis}| > |^3J(H-H)_{gem}|$. This relationship has been rationalised by a valence-bond calculation of vinyl coupling constants by Karplus.²⁸⁴ Assignment of the proton spectra of R_2TlX and RtX_2 ($R = H_2C=CH$) derivatives in this study were partly based on this assumption. The same order for thallium-proton couplings was found for $(H_2C=CH)_2TlBF_4$ in DMSO (Table 4.10) and has previously been noted in bis(vinyl)mercury²⁶⁰. However for $(H_2C=CH)_2TlOCOCH_3$ in DMSO (Table 4.10) and $H_2C=CHTlCl_2$ in CD_3OD (Table 4.11), the order of cis and gem thallium-proton couplings is reversed giving: $|^3J(Tl-H)_{trans}| > |^2J(Tl-H)_{gem}| > |^3J(Tl-H)_{cis}|$, although the differences between the cis and gem couplings are relatively small, (37Hz in R_2TlX and 75Hz in RtX_2). Maher and Evans⁸⁶ also found this order of thallium-proton coupling for R_2TlClO_4 and $Rt(ClO_4)_2$ ($R = H_2C=CH$) in D_2O . A similar order has been observed for metal-proton coupling in $(H_2C=CH)_4Sn$

to $(\text{CH}_3)_2\text{CH}$ (Table 4.8) and for RTLX_2 on going from $\text{R} = \text{CH}_3$ to CH_3CH_2 . Changes induced by substitution at the β carbon appear to be less regular, with a decrease in $^3\text{J}(\text{Tl-H})$ observed for R_2TLX in going from $\text{R} = \text{CH}_3\text{CH}_2$ to $\text{CH}_3\text{CH}_2\text{CH}_2$ (Table 4.7) followed by an increase in going to $\text{R} = (\text{CH}_3)_2\text{CHCH}_2$ (Table 4.8). $^2\text{J}(\text{Tl-H})$ is unaffected by the former change (ethyl to n-propyl) but shows an increase for the latter change (n-propyl to iso-butyl).

4.3.5.2. Alkenyl derivatives

Thallium-carbon coupling $^n\text{J}(\text{Tl-C})$ ($n = 1$ to 3) in alkenylthallium(III) derivatives R_2TLX (Table 4.4) and RTLX_2 (Table 4.5) appear to follow the same pattern as in alkylthallium(III) compounds:

$$|{}^1\text{J}(\text{Tl-C})| \gg |{}^3\text{J}(\text{Tl-C})| > |{}^2\text{J}(\text{Tl-C})|$$

However the magnitude of thallium-carbon couplings in alkenyl and alkyl derivatives are different. $^1\text{J}(\text{Tl-C})$ in alkenyls is approximately twice as large as in alkyl derivatives while $|{}^2\text{J}(\text{Tl-C})|$ in alkenyls is generally smaller than in alkyls though of opposite sign. Interestingly two-bond metal-carbon coupling was not observed in several studies of vinyl derivatives of Sn,³¹⁰ and Pb²⁶⁶ although values of $^2\text{J}(\text{Hg-C})$ of 22.4 kHz have been noted in various solvents for $(\text{H}_2\text{C}=\text{CH})_2\text{Hg}$.^{262, 313} Mitchell²⁴⁹ has also noted that two-bond tin-carbon coupling could not be observed in propenyltin compounds. Two-bond metal-carbon couplings are observable in alkenyl derivatives of thallium and mercury because coupling of carbon with these metals is generally larger than in the analogous tin or lead compounds.

Substitution of a CH_3 group for a proton on the α -carbon of $(\text{H}_2\text{C}=\text{CH})_2\text{Tl}^+$ to give $[\text{H}_2\text{C}=\text{C}(\text{CH}_3)]_2\text{Tl}^+$ (Table 4.4) results in decreases of $^1\text{J}(\text{Tl-C})$ of 701-849 Hz. $^3\text{J}(\text{Tl-C})$ simultaneously

increases by 293-341 Hz for the same systems.

Thallium-proton couplings in alkenyl systems are generally larger than those found in alkyl compounds, both for R_2TlX (Table 4.10) and RtX_2 (Table 4.11) alkenyl derivatives. The order of coupling is generally $^3J(Tl-H) > ^2J(Tl-H)$ as for alkyl systems. Maher and Evans⁸⁶ previously reported thallium-proton coupling constants R_2TlX and RtX_2 ($R = H_2C=CH$; $X = ClO_4^-$) in D_2O and for (trans- $ClCH=CH$) Tl^+ (see

Page 191 Missing from ORC.

derivatives in this study were partly based on this assumption.

The same order for thallium-proton couplings was found for $(H_2C=CH)_2TlBF_4$ in DMSO (Table 4.10) and has previously been noted in bis(vinyl)mercury²⁶⁰. However for $(H_2C=CH)_2TlOCOCH_3$ in DMSO (Table 4.10) and $H_2C=CHTlCl_2$ in CD_3OD (Table 4.11), the order of cis and gem thallium-proton couplings is reversed giving: $|^3J(Tl-H)_{trans}| > |^2J(Tl-H)_{gem}| > |^3J(Tl-H)_{cis}|$, although the differences between the cis and gem couplings are relatively small, (37Hz in R_2TlX and 75Hz in RtX_2). Maher and Evans⁸⁶ also found this order of thallium-proton coupling for R_2TlClO_4 and $Rt(ClO_4)_2$ ($R = H_2C=CH$) in D_2O . A similar order has been observed for metal-proton coupling in $(H_2C=CH)_4Sn$

where it has been proposed that through-space contributions play a role in heavy metal-proton geminal coupling.³¹⁵

Coupling in alkenylthallium(III) systems will be further discussed later. (4.3.6.2. and 4.3.7.3.)

4.3.5.3. Aryl derivatives

Thallium-carbon coupling $^nJ(\text{Tl-C})$ ($n = 1$ to 4) in $(\text{C}_6\text{H}_5)_2\text{TlOCCCH}_3$ (Table 4.6) follows the same pattern found for other R_2TlX and RTlX_2 ($\text{R} = \text{C}_6\text{H}_5$) derivatives previously reported (Table 4.6): $|^1J(\text{Tl-C})| > |^3J(\text{Tl-C})| > |^2J(\text{Tl-C})| > |^4J(\text{Tl-C})|$. This parallels the order found for alkyl and alkenylthallium(III) derivatives. $|^1J(\text{Tl-C})|$ is larger (ca. $\times 2$) than in alkyl systems but of the same order of magnitude as in alkenyl derivatives.

$^2J(\text{Tl-C})$ is larger (ca. $\times 10$ for R_2TlX and ca. $\times 5$ for RTlX_2) than in alkenyls; or alkyls (ca. $\times 2$).

Maher and Evans⁸⁶ reported thallium-proton coupling constants for arylthallium(III) systems R_3Tl , R_2Tl^+ and RTl^{2+} and the order of coupling was: $J(\text{Tl-H})_{\text{ortho}} > J(\text{Tl-H})_{\text{meta}} > J(\text{Tl-H})_{\text{para}}$ in all cases.

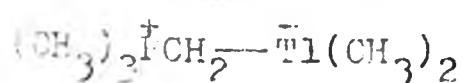
4.3.6. The effect of heteroatom substitution on spin-spin coupling constants involving thallium

4.3.6.1. Alkyl derivatives

Carbon-13 (Tables 4.2; 4.5) and proton (Tables 4.8; 4.11) spectra of the neo-pentylthallium(III) derivatives $[(\text{CH}_3)_3\text{CCH}_2]_n\text{TlX}_{3-n}$ and trimethylsilylmethylthallium(III) derivatives $[(\text{CH}_3)_3\text{SiCH}_2]_n\text{TlX}_{3-n}$, ($n = 1, 2$; $\text{X} = \text{anion}$) can be used to examine the effects of heteroatom substitution in the alkyl chain on J parameters.

The previously reported proton NMR parameters for bis(neo-pentyl)chlorothallium(III) and neo-pentyldihalothallium(III) in pyridine solution⁸⁷ are in good agreement with those reported here, with the exception of $^2J(Tl-H)$ for $(CH_3)_3CCH_2TlBr_2$, for which the value of 712Hz was given.⁸⁷ Previous⁸⁸ values of $^2J(Tl-H)$ for R_2TlCl and $R_nTl[OCCH(CH_3)_2]_{3-n}$ in $CHCl_3$ ($R = (CH_3)_3SiCH_2$; $n = 1, 2$) also agree closely with the values reported here.

Substitution of Si for C in these otherwise similar compounds causes considerable decreases in $^1J(Tl-C)$: 450 and 1462 Hz for bisalkyl (Table 4.2) and monoalkyl (Table 4.5) compounds respectively. Large reductions in $^1J(Hg-C)$ on silicon substitution have also been noted for neo-pentyl^{261, 316} and trimethylsilylmethyl^{317, 318} derivatives of the types R_2Hg and $RHgCl$. These changes may be rationalised within the framework of the Fermi contact term on the basis of Bent's³²¹ postulate that the s-character of an atom tends to concentrate in orbitals directed towards the more electropositive substituents. $^1J(Tl-C)$ in the neo-pentyl and trimethylsilylmethyl derivatives are proportional to the $\alpha^2(C)$ term in equation 4.6. This $\alpha^2(C)$ term will be decreased by substitution of Si for the β -carbon in the neo-pentyl group. $^3J(Tl-C)$ and $^4J(Tl-H)$ are also reduced by about half by silicon substitution. In contrast $^2J(Tl-H)$ is increased by 134-207Hz for R_2TlX compounds and by 358Hz for $R_2Tl[OCCH(CH_3)_2]_2$ compounds. Broadly similar results were observed for the analogous mercury compounds.^{304, 317-320} It is interesting here to note the relatively small value of $^1J(Tl-CH_2) = 352Hz$ reported in the compound $(CH_3)_3PCH_2Tl(CH_3)_2$.⁶⁴ This has been attributed to strong polarisation of the Tl-C bond in the sense:



^{13}C - $\{^1\text{H}\}$ experiments for $[(\text{CH}_3)_3\text{CCH}_2]_2\text{TlCl}$ in pyridine solution show that the signs of $^1\text{J}(\text{Tl-C})$ and $^2\text{J}(\text{Tl-H})$ are opposite, and it is reasonable to suppose that similar sign combinations are present in the other neo-pentyl and trimethylsilylmethyl compounds studied. Thus a negative sign for $^2\text{J}(\text{Tl-H})$ could be considered to imply a decrease in thallium-proton coupling on Si substitution.

The dependence of the coupling constants on anion and solvent are small compared to the effect of Si substitution and changing the number of organo groups on thallium. The effect of Si substitution on thallium shielding is discussed in Chapter 3.

In contrast to the reduction in thallium-carbon coupling observed on silicon substitution, the presence of more electro-negative atoms appears to cause an increase in coupling. The methoxy substituted β -carbon in the compound $\text{CH}_3\text{CH}(\text{OCH}_3)\text{CH}_2\text{TlXY}$ ($\text{X} = \text{CH}_3$, $\text{Y} = \text{OCOCH}_3$) (Table 4.2) gives rise to a larger value for $^2\text{J}(\text{Tl-C})$ (158Hz) than in either bis(iso-butyl)thallium(III) (Table 4.2) or bis(n-propyl)thallium(III) (Table 4.1) where it is 71 Hz and 127 Hz respectively. Replacement of a proton in methylbis(acetato)thallium(III) by chlorine to give chloromethylbis(acetato)thallium(III) causes $^1\text{J}(\text{Tl-C})$ to increase by 2900Hz.²⁵³ It is suggested that the effective nuclear charge at the substituted carbon is increased by an electro-negative substituent such as O or Cl. Such substitution would result in an increase in the electron withdrawing ability of the organo group and consequently an increase in the effective nuclear charge at thallium. These increases in Z_{eff} would lead to increased thallium-carbon coupling. Increases in metal-carbon coupling have previously been observed for methoxy substituted cyclohexyl and norbornylmercury systems²⁴⁸ where it was assumed that changes in the 'effective nuclear charge term' (at which atom(s) not specified) were responsible for the increased mercury-carbon coupling observed on oxygen substitution.

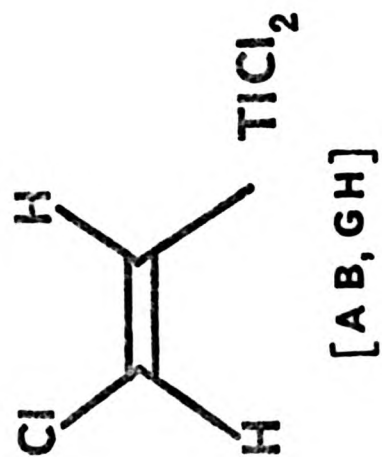
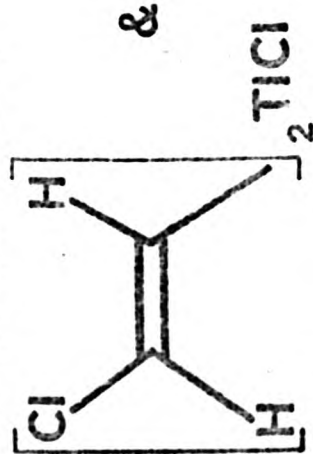
4.3.6.2. Alkenyl derivatives

Substitution of chlorine in the trans position at the β carbon of vinylthallium(III) derivatives results in a large increase in $^2\text{J}(\text{Tl-C})$; eg. $^2\text{J}(\text{Tl-C})$ in R_2TlX ($\text{R} = \text{H}_2\text{C}=\text{CH}$) (29-55Hz) derivatives increases to 730Hz on chlorine substitution (Table 4.4). An analogous increase in $^2\text{J}(\text{Tl-C})$ is observed:

for $RTlX_2$ compounds (Table 4.5) on chlorine substitution. Large increases in $^1J(Tl-C)$ of 403-954 Hz were simultaneously observed for R_2TlX derivatives and 470 Hz for $RTlX_2$. Increases in mercury-carbon couplings have been reported, in alkenylmercury(II) compounds,³¹³ where $^1J(Hg-C)$ increases by ca.10% and $^2J(Hg-C)$ increases by ca.400% on substituting chlorine in the trans position in bis(vinyl) mercury(II). The magnitude of $^2J(Tl-C)$ to the acetoxy substituted β -vinyl carbon in the trans(2-acetoxy)but-2-enylthallium(III) system is also large (1626Hz) compared to the analogous two-bond coupling (100 Hz) in the unsubstituted vinyl compound $RTlX_2$. (Table 4.5). $^1J(Tl-C)$ is also larger, by 841Hz, in the acetoxy substituted compound. It appears likely that the observed increases in thallium-carbon coupling are largely due to increases in the effective nuclear charge term, both at the β -vinyl carbon where substitution occurs and at thallium as a result of the increased electronegativity of the organo group, as was suggested for alkyl derivatives. Substitution of ethylenic systems with chlorine, oxygen containing substituents and alkyl groups causes absorption in the ultraviolet spectra to shift to longer wave lengths.³²² However the observed reductions in ΔE are relatively small³²² and would not therefore be expected to make a major contribution to the increased couplings observed here. However Mitchell³⁰¹ in a study of tin-carbon coupling in a series of unsaturated organotins warns that it may not be valid to make the average energy approximation when the metal is bonded to an sp^2 or sp hybridised carbon. Chlorine substitution at the β -carbon in vinylthallium(III) compounds causes a reduction in $^2J(Tl-H)$ and $^3J(Tl-H)$ in R_2TlX (Table 4.10) as was previously noted by Maher.⁹⁷ A similar effect is observed for $RTlX_2$, (Table 4.11) where $^2J(Tl-H)_{gem}$ is reduced by 1075Hz and

¹H SPECTRUM at 60 MHz of

(Continuous wave)



in METHANOL-d₄
[·*]

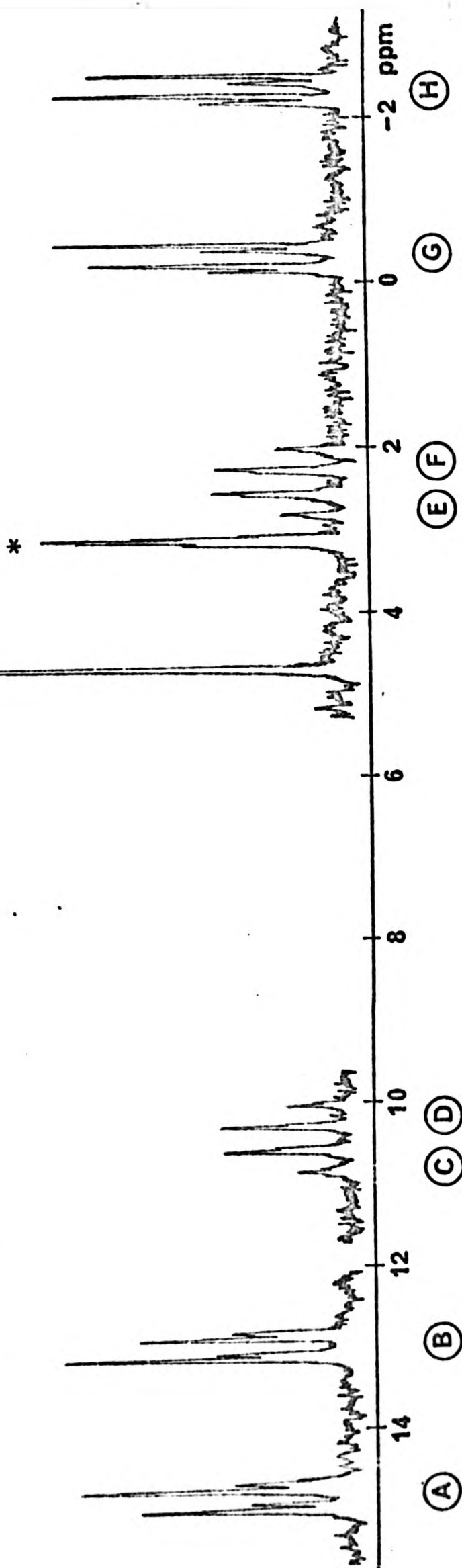


FIG. 4.10

$^3J(\text{Tl-H})_{\text{cis}}$ by 667Hz on substitution of chlorine at the trans position on the β -carbon in vinylthallium.²⁺ Smaller reductions in the magnitudes of all thallium-proton couplings can be observed in substituting a methyl group in various positions in $(\text{H}_2\text{C}=\text{CH})_2\text{Tl}^+$ to give cis, trans and iso-propenyl derivatives. (Table 4.10). It seems likely that thallium-proton couplings in these systems depend upon the electronegativity of substituents, in a similar way to proton-proton couplings in $\text{H}_2\text{C}=\text{CHX}$, as was suggested by Maher.⁹⁷

4.3.7. Influence of stereochemistry on spin-spin coupling constants involving thallium

A number of compounds were investigated with the objects of examining the influence of stereochemistry on thallium-carbon and thallium-proton spin-spin coupling constants.

4.3.7.1. Alicyclic derivatives

Alicyclic derivatives of thallium present the potential for examination of the stereochemical dependence of vicinal thallium-carbon and thallium-proton coupling constants. The proton spectra of R_2TlX (R = cyclopentyl, cyclohexyl, cycloheptyl) allowed determination of $^nJ(\text{Tl-H})$ up to $n = 3$, but the spectra were broad and lacked detailed fine structure. The proton spectrum of the rigid cyclopropyl derivative on the other hand showed detailed fine structure. (Fig 4.3). The proton-decoupled thallium-205 spectra of a number of cyclopentyl, cyclohexyl and cycloheptyl R_2TlX compounds were generally broader ($\nu_{\frac{1}{2}} = 300\text{-}600\text{Hz}$; Table 3.3) than other alkyl derivatives ($\nu_{\frac{1}{2}}$ typically 50Hz), whereas the spectra of cyclopropyl compounds exhibited linewidths similar to those of other alkyl

derivatives. The broadness observed in the spectra of the larger ring compounds may well be due to the rings flipping between different conformations.

Carbon-13 and proton NMR results for alicyclic derivatives of thallium will be discussed separately. Solubility considerations precluded low temperature studies of alicyclic derivatives.

a) Carbon-13 NMR results

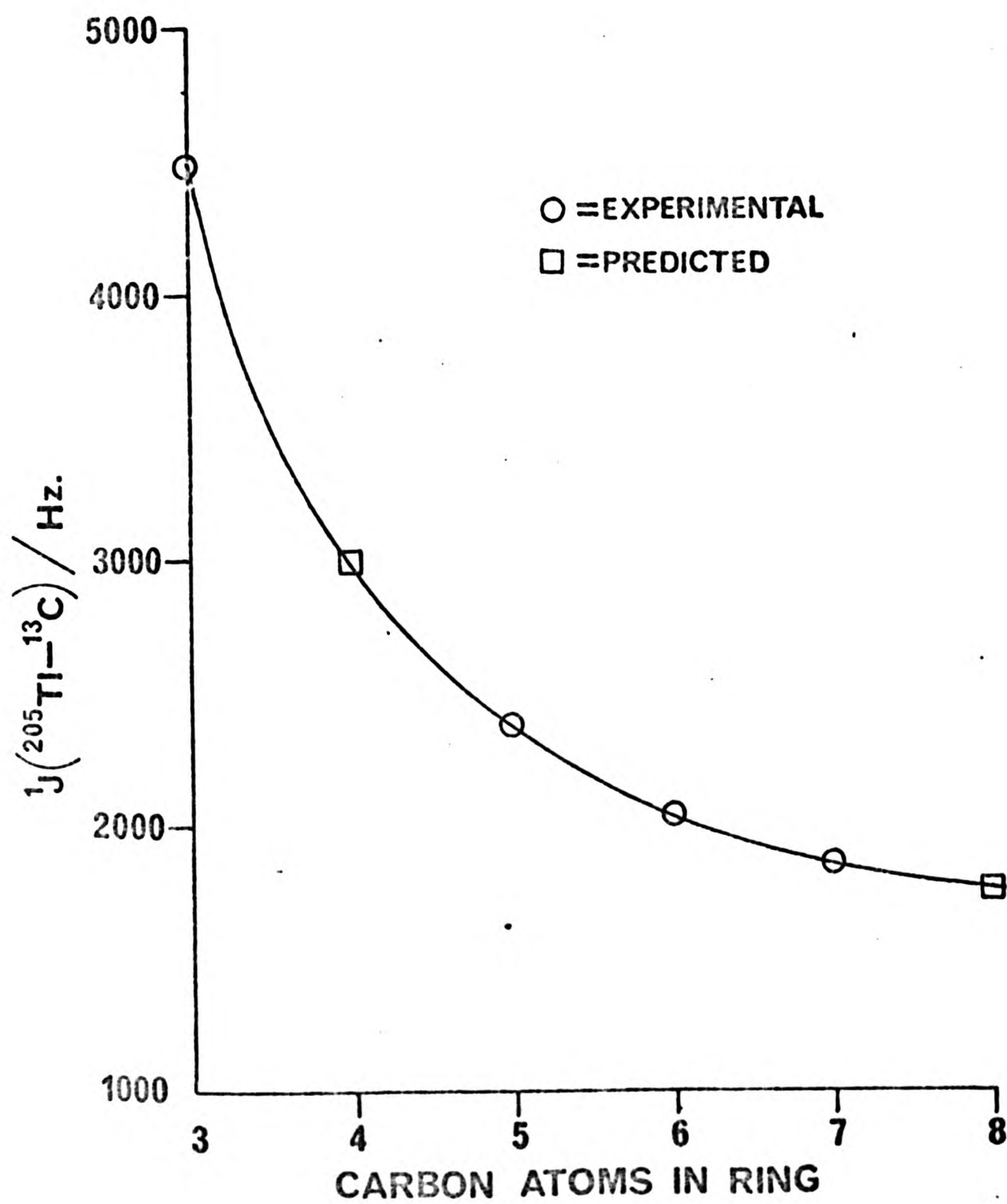
Coupling $^nJ(Tl-C)$, ($n = 1-4$), (Table 4.3) in R_2TlX ($R =$ alicyclic) follows the same pattern as for alkyls with $|^1J(Tl-C)| > |^3J(Tl-C)| > |^2J(Tl-C)| > |^4J(Tl-C)|$

$^1J(Tl-C)$ is generally less in alicyclic systems than in alkyls (with the exception of cyclopropyl compounds which have a larger $^1J(Tl-C)$ than in alkyls due to hybridisation of the π -carbon (see 4.3.3.)). A trend of increasing $^1J(Tl-C)$ with decreasing ring size is observed (Fig 4.11) which may reflect changes in hybridisation at the carbon bonded to thallium. A similar trend for $^1J(CH)$ can be seen on plotting the data observed for $H_2C(CH_2)_n$ ($n = 2-5$).³²³ A linear relationship between $^1J(CH)$ and ring strain energy was found for these cycloalkanes.³²³ The plot of $^1J(Tl-C)$ against ring size for R_2TlX (Fig 4.11) leads to prediction of values of $^1J(Tl-C)$ for four (ca. 3000Hz) and eight (ca. 1700 Hz) membered alicyclic derivatives R_2TlX . However caution must be used since in alicyclic tin compounds, $^1J(Sn-C)$ was shown to be smaller in the cyclobutyl compound than in either cyclopentyl or cyclohexyl derivatives.³¹⁰

Cyclopropyl, cyclohexyl, cyclopentyl and cycloheptyl derivatives of thallium will now be discussed separately and in that order.

FIG. 4.11.

PLOT OF $^1J(^{205}\text{Ti}-^{13}\text{C})$ AGAINST RING SIZE
FOR R_2TiX ($\text{R} = \text{ALICYCLIC}$; $\text{X} = \text{ANION}$)
IN DMSO_{d_6}



(i) Cyclopropylthallium(III)

Cyclopropylthallium derivatives are interesting because of the possibility of multipath coupling $^nJ(\text{Tl-C})$, ($n = 1-4$), in these small rigid systems. Multipath coupling is unlikely to be important in the larger ring systems since $J(\text{Tl-C})$ over more than four bonds was not observed in alkyl derivatives. The observed $^2J(\text{Tl-C})$ in cyclopropyl derivatives R_2TlX (150Hz for $\text{R} = (\text{CH}_2)_2\text{CH}$; $\text{X} = \text{Br}$ in pyridine; Table 4.3) is larger than $^2J(\text{Tl-C})$ in other alicyclics (18-78Hz) studied. It is also larger than $^2J(\text{Tl-C})$ in $[(\text{CH}_3)_2\text{CH}]_2\text{TlCl}$ (63Hz in pyridine, Table 4.2) but close to that in $(\text{CH}_3\text{CH}_2\text{CH}_2)_2\text{TlBr}$ (127Hz in pyridine; Table 4.1). Coupling to the carbon in the cyclopropyl system may involve two independent paths, the observed coupling being the algebraic sum of $^2J(\text{Tl-C})$ and $^3J(\text{Tl-C})$. Interestingly the observed $^2J(\text{Tl-C})$ in cyclopropylthallium R_2TlX has a negative sign as in alkyl derivatives while $^2J(\text{Tl-H})$ and both $^3J(\text{Tl-H})$ couplings are positive as found for alkenyl derivatives.

The observed coupling to the α carbon in cyclopropylthallium-(III) compounds might be expected to have a contribution to coupling from $^4J(\text{Tl-C})$, although by analogy with other $^4J(\text{Tl-C})$ couplings this would be expected to be relatively small.

Multipath coupling has been proposed for $J(\text{Pt-C})$ in a number of small ring systems in which Pt is incorporated in the ring.³²⁴

(ii) Cyclohexylthallium(III)

The observed $^3J(\text{Tl-C})$ for R_2TlBF_4 ($\text{R} = \text{cyclohexyl}$) is in the range 452-458Hz at ambient temperature (Table 4.3). This could represent the value for $^3J(\text{Tl-C})$ in either I(ee), II(aa) or III(ae), (Fig 4.12), since thallium can be either

equatorial(e) or axial(a). The observed $^3J(\text{Tl-C})$ could be also an 'average' value of (ee + ae + aa); (ee + ae); (aa + ae) or (ae + ee).

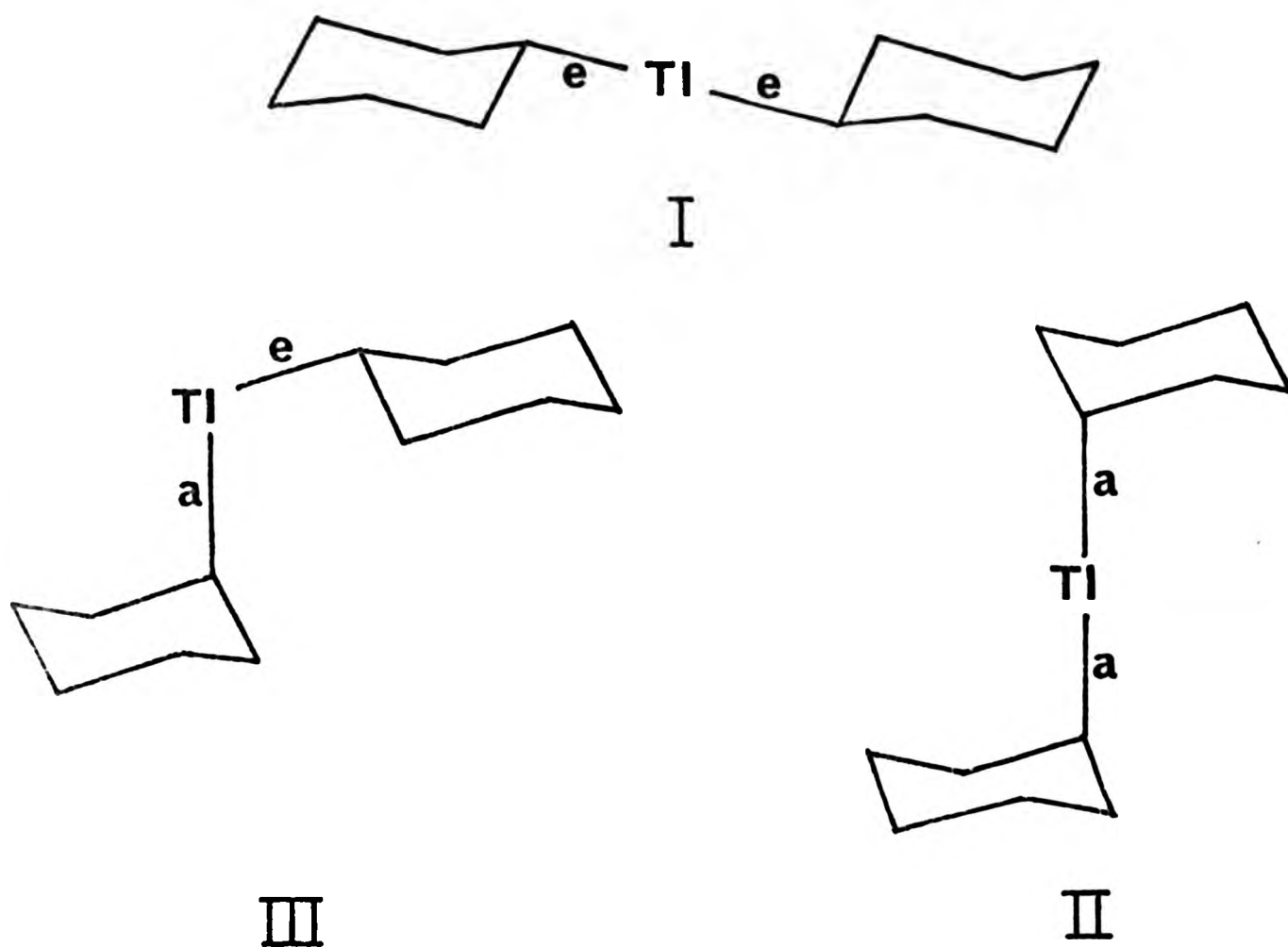


FIG 4.12 Conformations of bis(cyclohexyl)thallium.

Barron et al²⁴⁷ showed that in the analogous bis(cyclohexyl)-mercury, for an equatorial mercury, $^3J(\text{Hg-C})_e$ in ee was approximately equal to $^3J(\text{Hg-C})_e$ in ae. Assuming that this is also true for R_2Tl^+ derivatives, then in the most complicated situation, when all three conformers (ee, ae, aa) are present there will only be two observable $^3J(\text{Tl-C})$ values: $^3J(\text{Tl-C})$ with Tl equatorial (from ee and ea) and $^3J(\text{Tl-C})$ with Tl axial (from aa and ae). Therefore only two conformations need be considered. These are shown in FIG 4.13, with the associated dihedral angles for $^3J(\text{Tl-C})$.

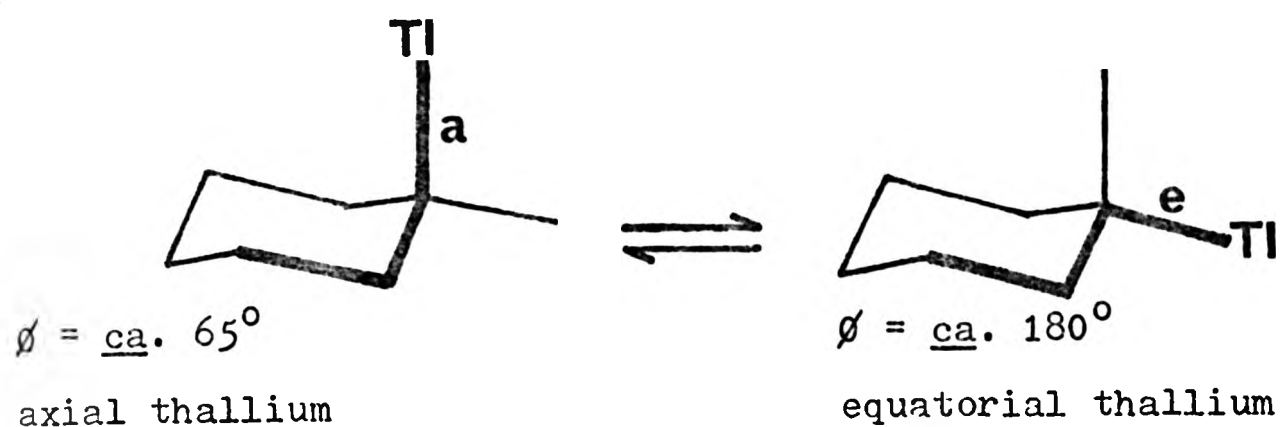


Fig. 4.13. Dihedral angles for $^3J(\text{Tl}-\text{C})$ for axial and equatorial thallium in cyclohexylthallium

Previous work on norbornane derivatives of thallium, RTlX_2 ,⁷³⁻⁷⁵ has identified a stereochemical dependence of $^3J(\text{Tl}-\text{C})$ which depends on dihedral angle ϕ as shown in Table 4.13.

TABLE 4.13

Dependence of $^3J(\text{Tl}-\text{C})$ on dihedral angle ϕ in norbornane derivatives RTlX_2

Range of $^3J(\text{Tl}-\text{C})^a$	Dihedral Angle ϕ^b	Coupling through molecular unit c
3 - 169	80°	$\begin{array}{c} \text{C} \quad \text{C} \quad \text{C} \\ \quad \quad \\ \text{Tl}-\text{C}-\text{C}-\text{C} \end{array}$
0 - 119	$115 - 120^\circ$	$\begin{array}{c} \text{C} \quad \text{O} \quad \text{C} \\ \quad \quad \\ \text{Tl}-\text{C}-\text{C}-\text{C} \end{array}$
1057 - 1303	170°	$\begin{array}{c} \text{C} \quad \text{C} \quad \text{C} \\ \quad \quad \\ \text{Tl}-\text{C}-\text{C}-\text{C} \end{array}$

^aIn Hz. Data from refs. 73-75. ^bEstimated from molecular models. ^cOnly the 80° and 170° data will be considered because these pathways do not have the complication of an O atom on the carbon. The presence of an electronegative atom has been shown to affect thallium-carbon coupling(4.3.6.)

Using the dependence of $^3J(\text{Tl-C})$ on dihedral angle (Table 4.13) then the predicted values of $^3J(\text{Tl-C})$ for a hypothetical RTlX_2 ($\text{R} = \text{cyclohexyl}$) would be ca. 1000-1300 Hz for Tl equatorial and ca. 0-200 Hz for Tl axial. Based on the empirical relationship that the ratio of $^3J(\text{Tl-C})$ in RTlX_2 and R_2TlX is ca. 2:1 (Table 4.12), then the predicted values of $^3J(\text{Tl-C})$ in R_2TlX are 500-650Hz for Tl equatorial and 0-100Hz for Tl axial. It is concluded from the observed values of $^3J(\text{Tl-C})$, 452-458Hz, that in $(\text{C}_6\text{H}_{11})_2\text{TlBF}_4$ thallium shows a distinct preference for equatorial substitution. Both axial and equatorial conformations probably exist in solution but the equilibrium is heavily in favour of the equatorial conformer.

Much effort has been devoted to the study of the equatorial-axial equilibrium in monosubstituted cyclohexanes and tabulations of A values ($A = \text{RTln}K = -\Delta G^\circ$; a positive A value indicates an equatorial preference) for the equilibria are available for many substituents.^{325,326} Almost all substituents examined had a definite equatorial preference.³²⁵⁻³²⁷

Jensen et al.³²⁸ showed that in RHgX , ($\text{R} = 4\text{-methylcyclohexyl}$; $\text{X} = \text{benzoxy}$), Hg had a small equatorial preference. However it was important when the same authors subsequently determined, by direct equilibration using benzoyl peroxide, that at 95° in pyridine RHgBr ($\text{R} = \text{cyclohexyl}$) had no conformational preference ($A = 0$), but there were some indications of a slight axial preference.³²⁹ Jensen et al.³²⁷ later used ^1H NMR (100 MHz) to show that for RHgOCOCH_3 ($\text{R} = \text{cyclohexyl}$) at -79°C $A = 0 \pm 0.09$. However Anet et al.³³⁰ used high field NMR, ^{13}C (63.1 MHz) and ^1H (250 MHz) to show that RHgOCOCH_3 (in CDCl_3 and $\text{CS}_2/\text{pyridine}$) and RHgCl (in CDCl_3) ($\text{R} = \text{cyclohexyl}$) exist preferentially in the axial forms at -90°C . This was the first demonstration

that a monosubstituted cyclohexane could prefer the axial form. Further investigation of RHgX by Barron et al²⁴⁷ ($\text{R} = \text{cyclohexyl}$; $\text{X} = \text{OCOCH}_3, \text{CN}, \text{C}_6\text{H}_5, \text{cyclohexyl}$ in $\text{CD}_2\text{Cl}_2/\text{pyridine}$ and $\text{X} = \text{OCOCH}_3, \text{CN}$ in CD_2Cl_2) using ^{199}Hg and ^{13}C NMR indicated a preference for axial conformation at low temperatures. Similarly Gibbard and Hall⁷² conclude that Tl is axial in the thallation adduct of D-galactal triacetate, although details of assignment are not given. In contrast to these cases where the metal has an axial preference, Kitching et al³³¹ report that for $\text{RM}(\text{CH}_3)_3$ ($\text{R} = \text{cyclohexyl}$) there is an equatorial preference at -69°C with $\text{M} = \text{Pb}$ ($A = 0.67 \pm 0.06$) and $\text{M} = \text{Sn}$ ($A = 1.06 \pm 0.14$).

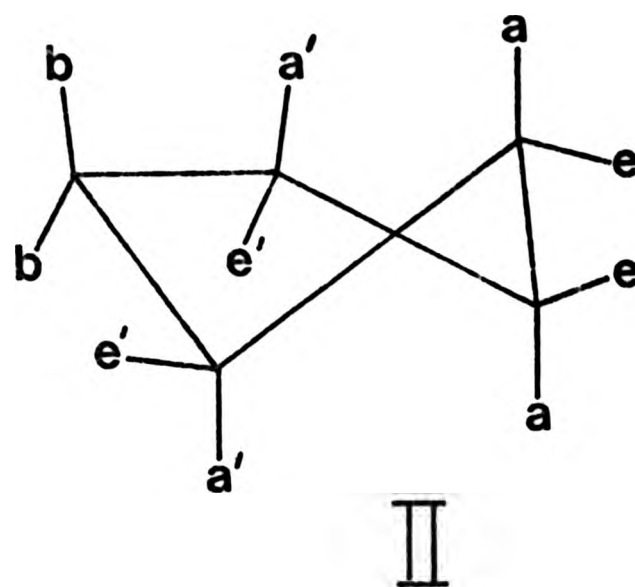
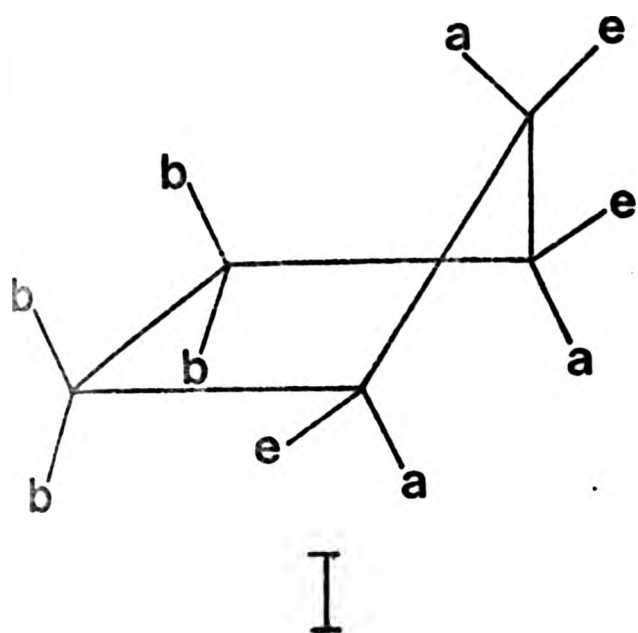
Other thallium-carbon couplings.

By analogy with R_2Hg ($\text{R} = \text{cyclohexyl}$)²⁴⁷ $^1\text{J}(\text{Tl}-\text{C})$ will be different in axial and equatorial conformation, therefore in an equilibrium an 'average' value will be observed. Barron et al²⁴⁷ found $^1\text{J}(\text{Hg}-\text{C})$ equatorial $>$ $^1\text{J}(\text{Hg}-\text{C})$ axial. The same authors also found differences in $^2\text{J}(\text{Hg}-\text{C})$ for axial and equatorial Hg , although these were not as great as for $^3\text{J}(\text{Hg}-\text{C})$. Therefore $^2\text{J}(\text{Tl}-\text{C})$ observed will by analogy also be an average value.

(iii) Cyclopentylthallium(III)

$^3\text{J}(\text{Tl}-\text{C})$ in R_2TlBF_4 (394Hz) (Table 4.3) is smaller than in $\text{R} = \text{cyclohexyl}$.

Two puckered conformations of cyclopentane, the envelope (I) and half-chair forms (II) have been recognised as probably representing energy minima³³² (FIG. 4.14)



a = axial

e = equatorial

a' = quasi axial

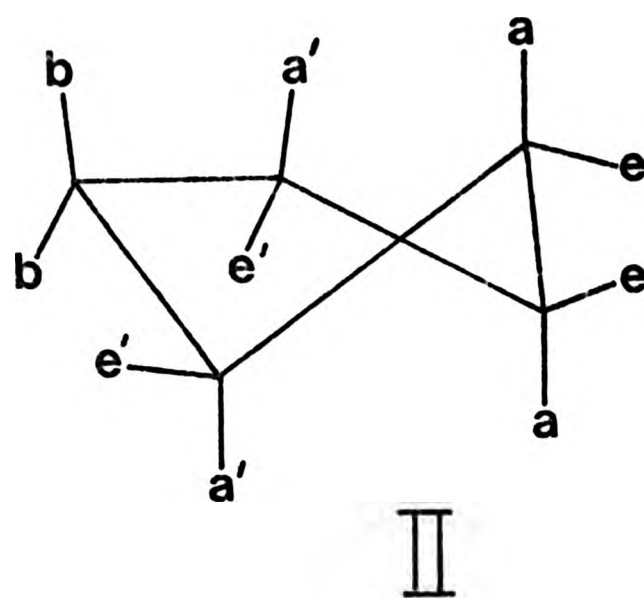
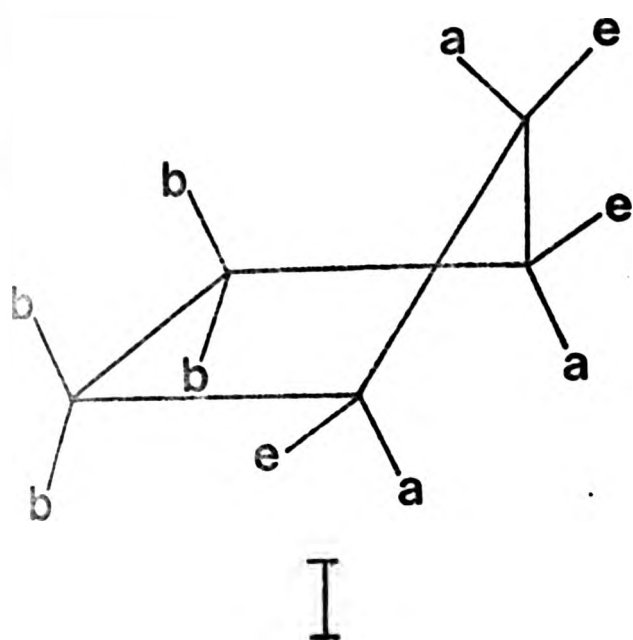
e' = quasiequatorial

b = bisectional bonds

FIG.4.14 Conformations of cyclopentane.

Substitution of thallium in axial or equatorial positions would minimise interaction with adjacent CH_2 groups (shown by molecular models,) compared with substitution in quasi-axial, quasi-equatorial or bisectional positions³³².

The dihedral angles associated with axial (a) and equatorial (e) thallium are shown in FIG.4.15.



a = axial

a' = quasi axial

b = bisectional bonds

e = equatorial

e' = quasiequatorial

FIG.4.14 Conformations of cyclopentane.

Substitution of thallium in axial or equatorial positions would minimise interaction with adjacent CH_2 groups (shown by molecular models,) compared with substitution in quasi-axial, quasi-equatorial or bisectional positions³³².

The dihedral angles associated with axial (a) and equatorial (e) thallium are shown in FIG.4.15.

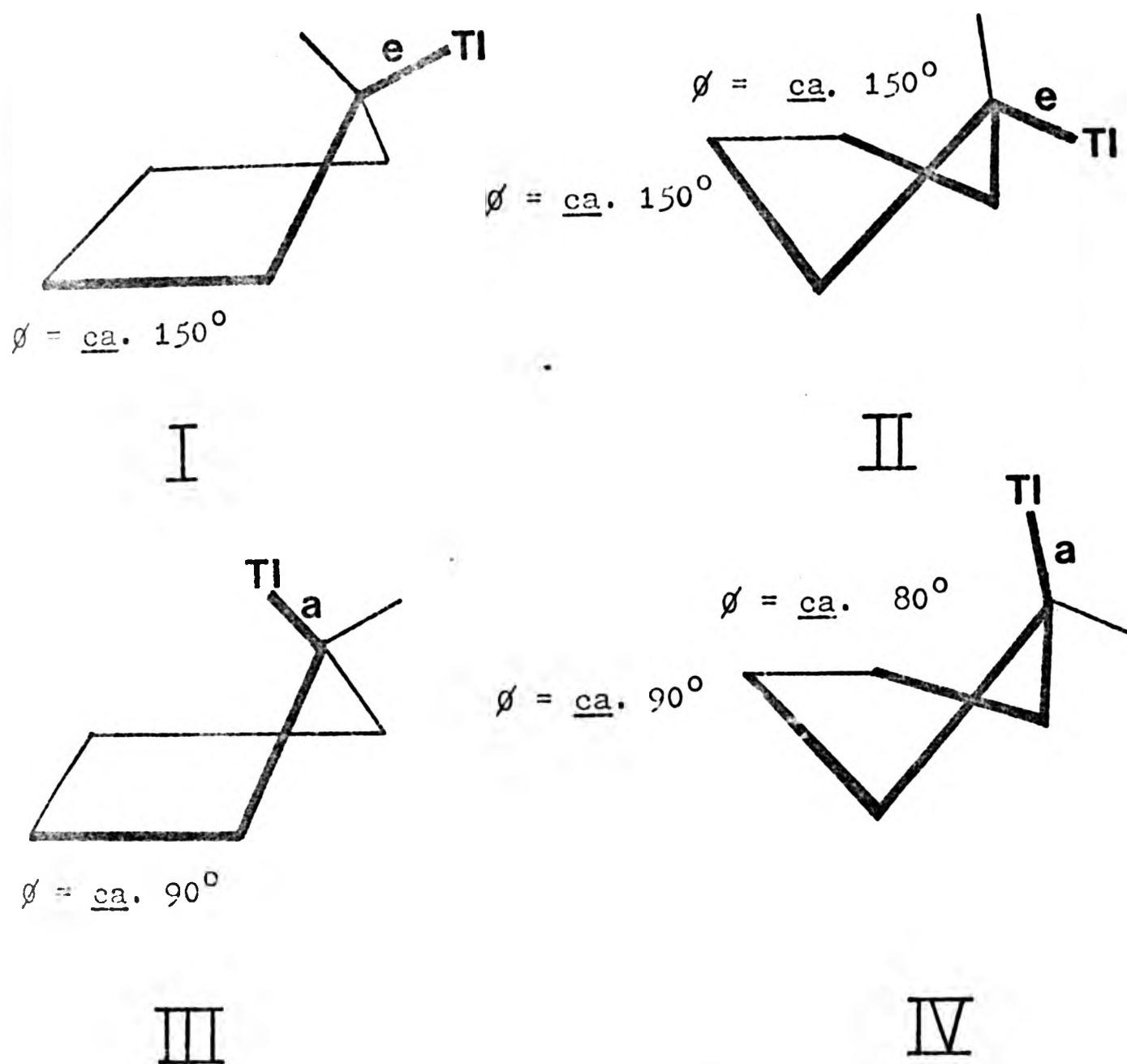


FIG 4.15. Dihedral angles for $^3J(\text{Tl}-\text{C})$ in cyclopentylthallium.

(For Tl_e in the envelope form $\phi = 140-150^\circ$ and $120-150^\circ$ in the half-chair form.

Tl_a in the envelope form $\phi = 90-100^\circ$ and $85-115^\circ$ in the half-chair form).

Therefore axial or equatorial substitution of Tl yields dihedral angles for $^3J(\text{Tl}-\text{C})$ in the ranges $80-100^\circ$ (Tl_{axial}) and $140-150^\circ$ ($\text{Tl}_{\text{equatorial}}$). By comparison with the data for norbornane derivatives (Table 4.13) and the predicted ratio of $^3J(\text{Tl}-\text{C})$ in RTlX_2 and R_2TlX systems (Table 4.12),

the observed value of $^3J(\text{Tl}-\text{C}) = 358\text{Hz}$ may be used to suggest an equatorial preference for thallium in the cyclopentyl derivative R_2TlBF_4 .

The smaller $^3J(\text{Tl}-\text{C})$ value observed in cyclopentyl compared to cyclohexyl R_2TlBF_4 may be rationalised on the basis of the smaller dihedral angle ($140-150^\circ$) expected in the cyclopentyl compound compared to that in cyclohexyl(180°).

(iv) Cycloheptylthallium(III)

The value of $^3J(\text{Tl}-\text{C}) = 538\text{Hz}$ in R_2TlBr (Table 4.3) is larger than in either the cyclohexyl or cyclopentyl analogues.

A monosubstituted cycloheptane would preferentially assume the twist-chair conformation (FIG.4.16 I) with the substituent quasi-equatorial(e').³³²

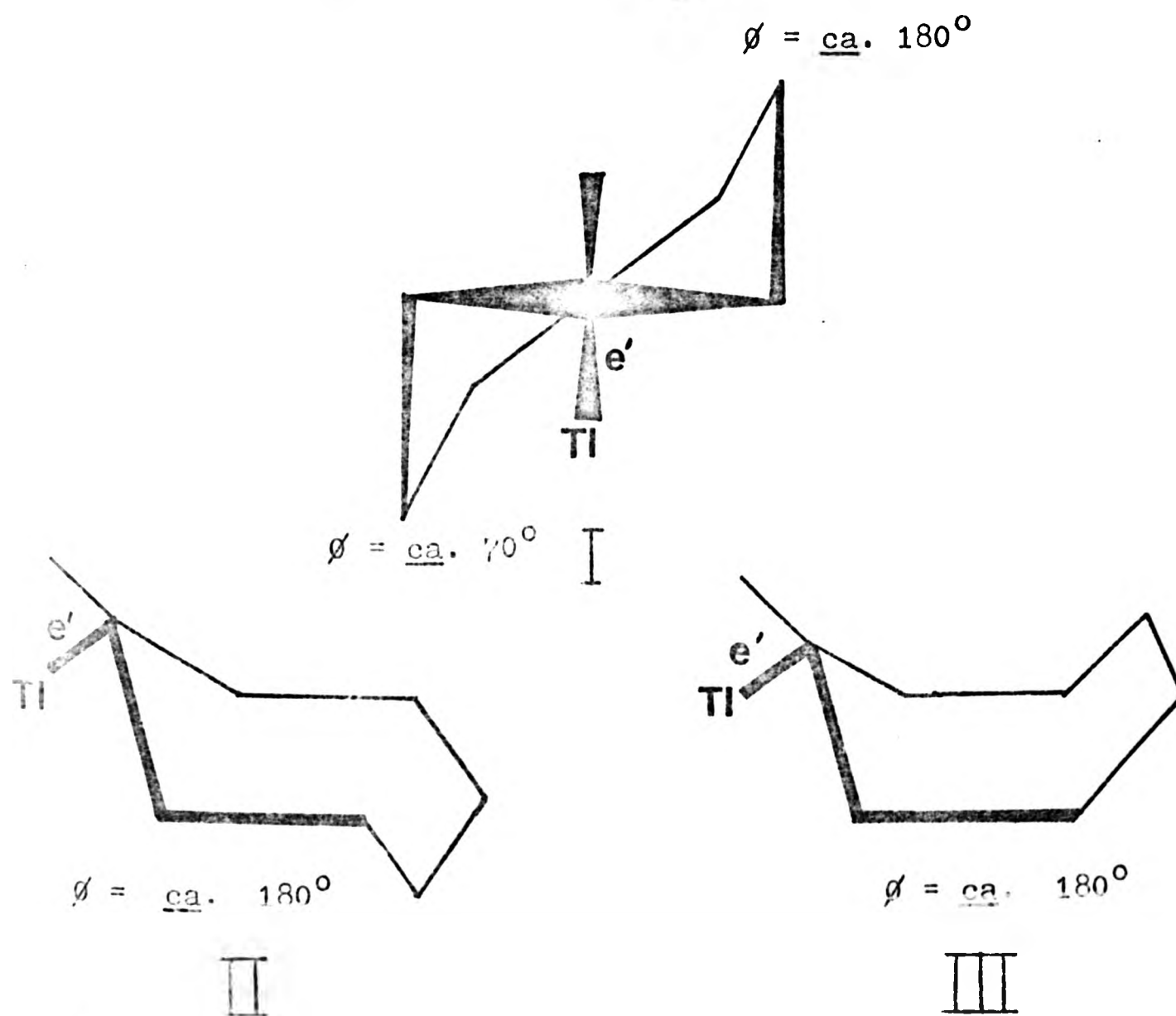


FIG. 4.16 Conformations and dihedral angles for $^3J(\text{Tl}-\text{C})$ in cycloheptylthallium.

A given substituent moves through all possible quasi-equatorial positions as a result of pseudo-rotation, trans-
versing the twist-chair, chair and boat conformations.³³²
The large value of $^3J(\text{Tl}-\text{C})$ (538Hz) compared to the cyclopentyl
and cyclohexyl analogues may be rationalised on the basis that
conformers where $\phi = 180^\circ$ (thallium equatorial) make the dominant
contribution to $^3J(\text{Tl}-\text{C})$ in the cycloheptyl system (FIG 4.16).
It is interesting that the value of $^3J(\text{Tl}-\text{C})$ observed is close
to that predicted (assuming the ratio of $^3J(\text{Tl}-\text{C})$ in RTlX_2
and R_2TlX is ca.2:1) from the data for nobornane systems
(Table 4.13) (539-651Hz for $\phi = 165^\circ$).

b) Proton NMR results

All the alicyclic systems studied exhibited two separate
 $^3J(\text{Tl}-\text{H})$ couplings to the $\beta\text{-CH}_2$ group. These were different to
each other and different for each compound. Each system will
be discussed separately.

(i) Cyclopropylthallium(III)

The rigid cyclopropyl ring provides an ideal opportunity
to examine the dihedral angle dependence of $^3J(\text{Tl}-\text{H})$. The
dihedral angles associated with $^3J(\text{Tl}-\text{H})$ for this system are
shown in FIG 4.17

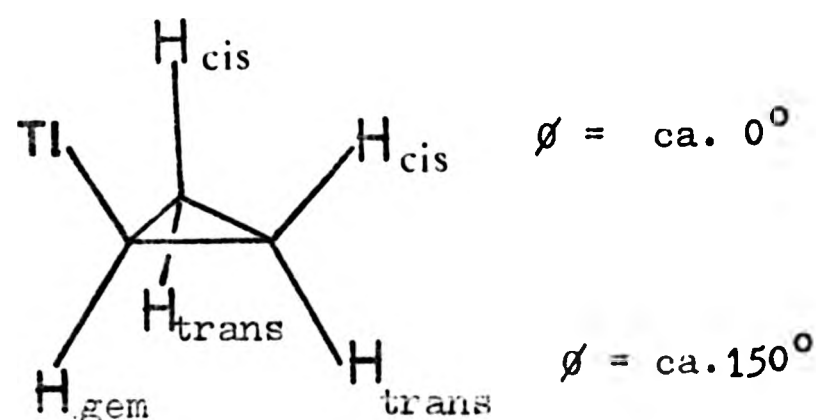


FIG. 4.17. Dihedral angles for $^3J(\text{Tl}-\text{H})$ in cyclopropylthallium.

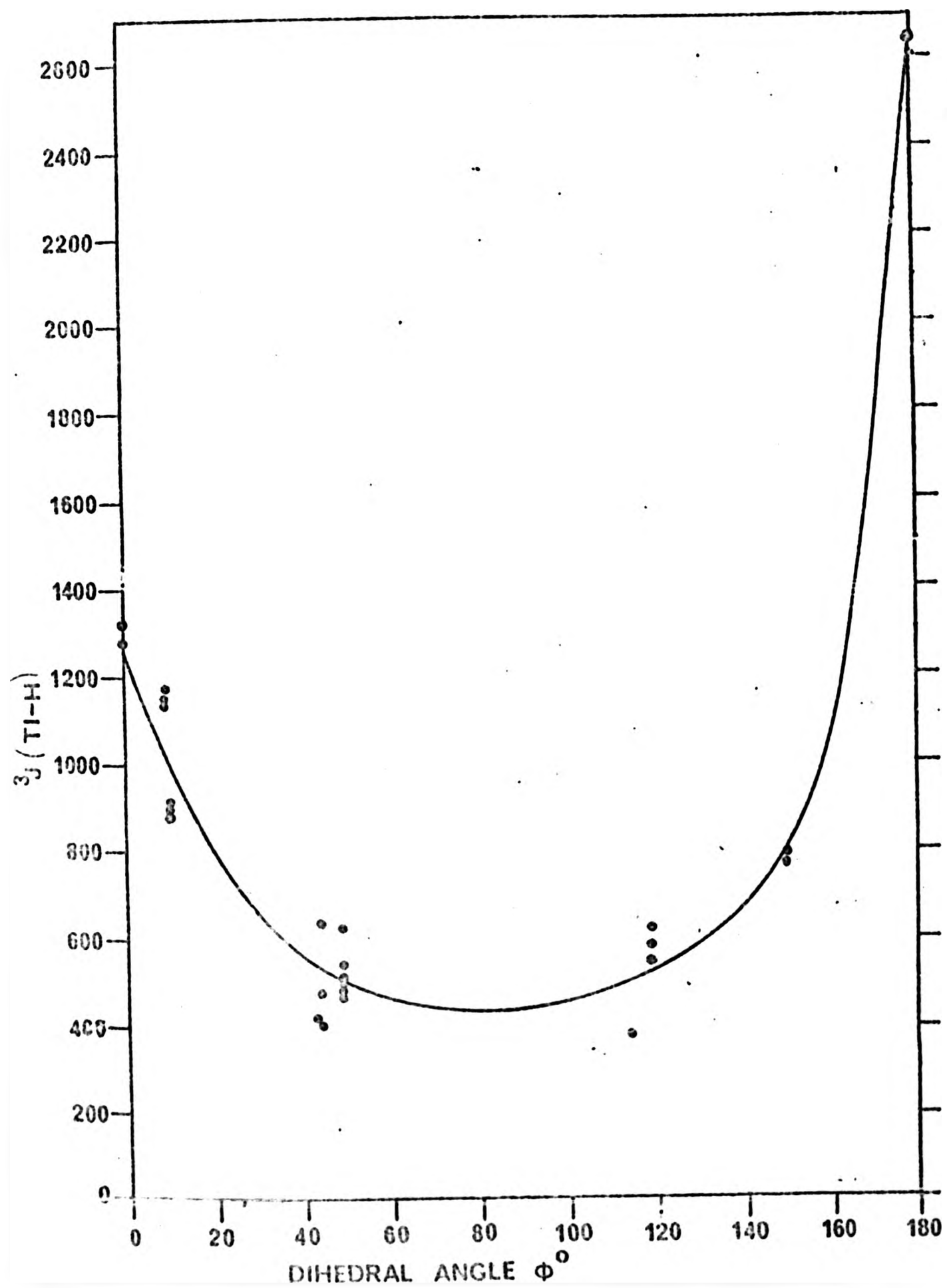
The ^1H spectrum of $[(\text{CH}_2)_2\text{CH}]_2\text{TlOCOCH}(\text{CH}_3)_2$ is shown in FIG 4.3. Differences of 223-235 Hz were found between the cis and trans $^3\text{J}(\text{Tl-H})$ couplings in R_2TlX compounds (Table 4.9) while differences of 504Hz (Table 4.11) and 530Hz (sec 3.2.6.2.) were noted for RTlX_2 . The $^3\text{J}(\text{Tl-H})_{\text{cis}}$ coupling has been assigned as the larger coupling and the trans as the smaller. The $^3\text{J}(\text{M-H})_{\text{cis}}$ coupling has also been reported as the larger coupling in other cyclopropyl-M derivatives (M = Pb, Hg, Sn)²⁸⁹.

An empirical means of predicting the magnitude of $^3\text{J}(\text{Tl-H})_{\text{cis}}$ in $[(\text{CH}_2)_2\text{CH}]_2\text{Tl}^+$ exists. It has been reported that regularities were found by analysing the M-H couplings (M= metal) in ethyl, cyclopropyl, and vinyl derivatives of Sn, Pb, Hg and Tl (not cyclopropyl). The increments in $^3\text{J}(\text{M-H})$ on going from ethyl to cyclopropyl were equal in magnitude to those observed on going from cyclopropyl to vinyl derivatives. This leads to a simple empirical relationship of the form $\text{J}(\text{XH}) = \text{A J}(\text{YH}) + \text{B}$ (where A and B are empirical constants) which can be used to predict $\text{J}(\text{MH})$ in ethyl, vinyl and cyclopropyl derivatives of Sn, Pb, Hg and Tl. Using this method a value of $^3\text{J}(\text{Tl-H})_{\text{cis}}$ for $[(\text{CH}_2)_2\text{CH}]_2\text{Tl}^+$ was calculated.* This compares with observed values of 563-579Hz for this coupling. (Table 4.9)

Using values of $^3\text{J}(\text{Tl-H})$ for cyclopropyl systems RTlX_2 (Table 4.11) and those obtained from the ^{205}Tl proton coupled spectrum (3.2.6.2.) in conjunction with data for rigid norbornane derivatives of thallium,^{73,92,333} and the thallation adduct of D-galactal acetate⁷², with dihedral angles for $^3\text{J}(\text{Tl-H})$ estimated from molecular models, it was possible to determine the approximate form of the dihedral angle dependence of $^3\text{J}(\text{Tl-H})$. This is shown in Fig. 4.18.

FIG 4.18

PLOT OF $^3J(\text{Ti-H})$ AGAINST DIHEDRAL ANGLE ϕ° FOR
RTIX₂ DERIVATIVES



(ii) Cyclohexylthallium(III)

Two different $^3J(\text{Tl-H})$ couplings were observed for $(\text{C}_6\text{H}_5)_2\text{TlBPh}_4$ in DMSO (Table 4.9) of 346 and 207 Hz respectively. The dihedral angles for $^3J(\text{Tl-H})$ in the cyclohexyl system are shown in FIG 4.19.

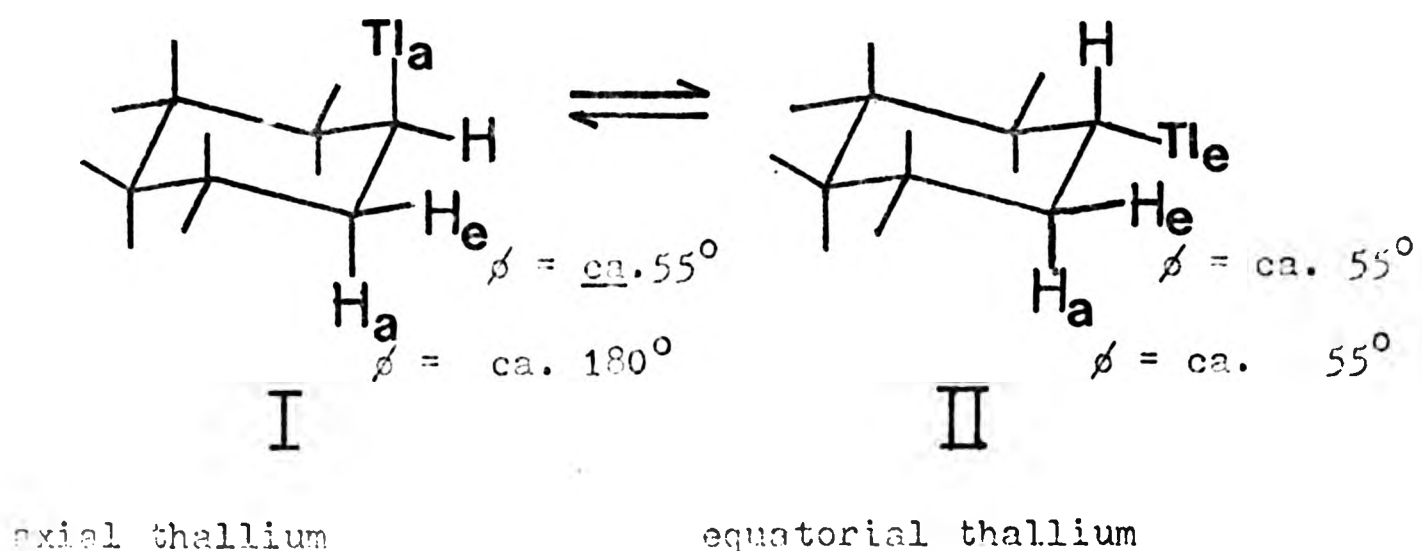


FIG.4.19 Dihedral angles for $^3J(\text{Tl-H})$ in cyclohexylthallium.

'Trans' coupling (ie. $Tl\text{a}\underline{H}a$ in I and $Tl\text{e}\underline{H}e$ in II) will be an average value because the dihedral angle ϕ differs. Values observed will depend on the equilibrium constant. 'Cis' coupling (ie. $Tl\text{a}\underline{H}e$ in I and $Tl\text{e}\underline{H}a$ in II) will differ slightly because although ϕ is the same (55°) in both cases, Tl is in different environments. Therefore coupling will also be an average although the difference between the two will probably not be as large as for the 'trans' coupling.

By examining the dihedral angle dependence of $^3J(Tl-H)$ (FIG 4.18) and assuming that the ratio of $^3J(Tl-H)$ in $RTlX_2$ and R_2TlX is ca. 2:1 (Table 4.12) then it is possible to exclude a major contribution from I, where the dihedral angle

(180°) would be expected to produce a much larger coupling than that observed. It is proposed that the form with Tl equatorial makes the dominant contribution and the larger coupling can be assigned to $^3J(\text{Tl-H})_{\text{trans}}$, however this is an average value which depends on the populations of I and II. (FIG.4.19)

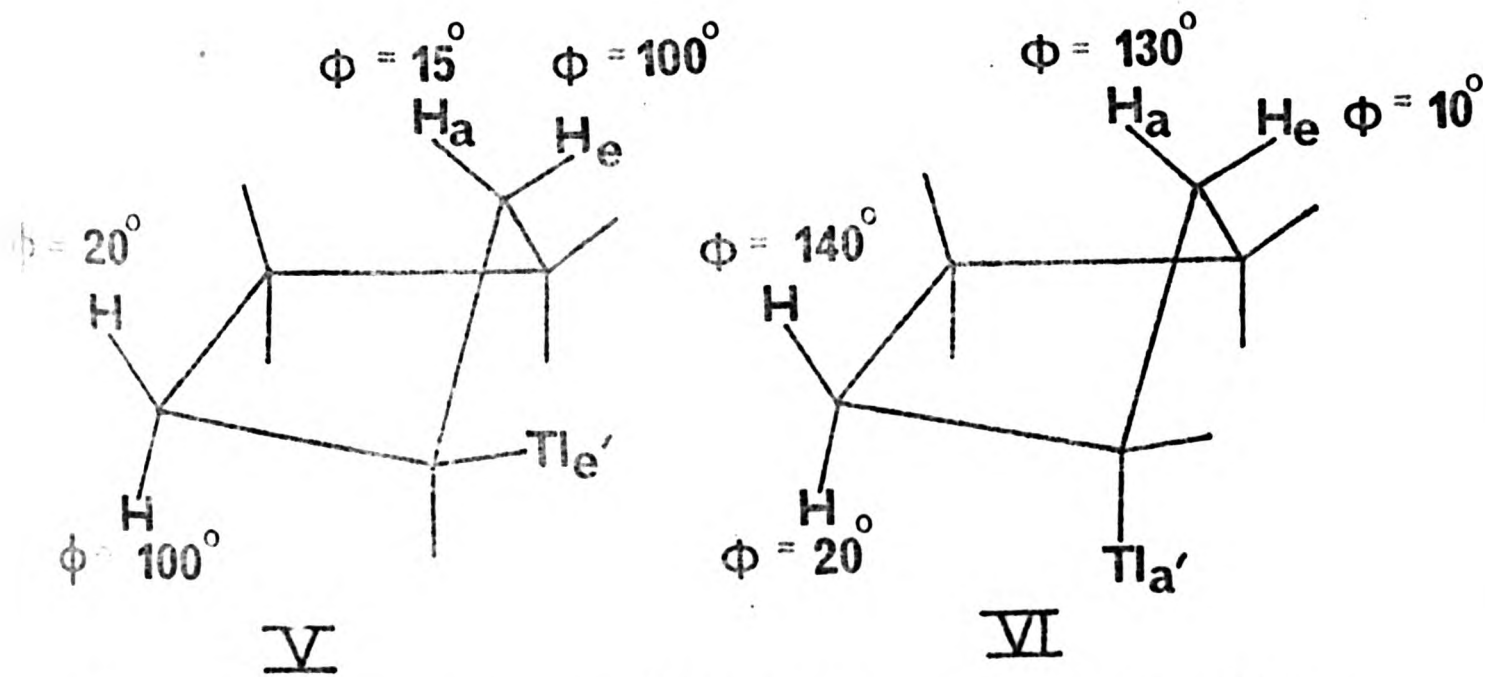
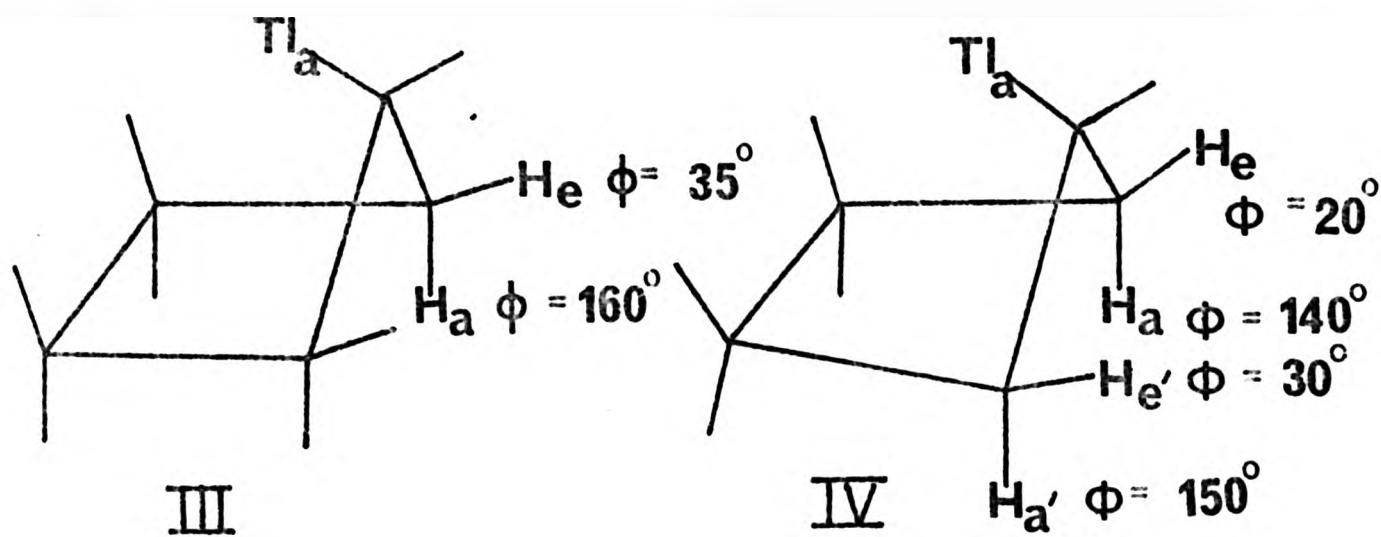
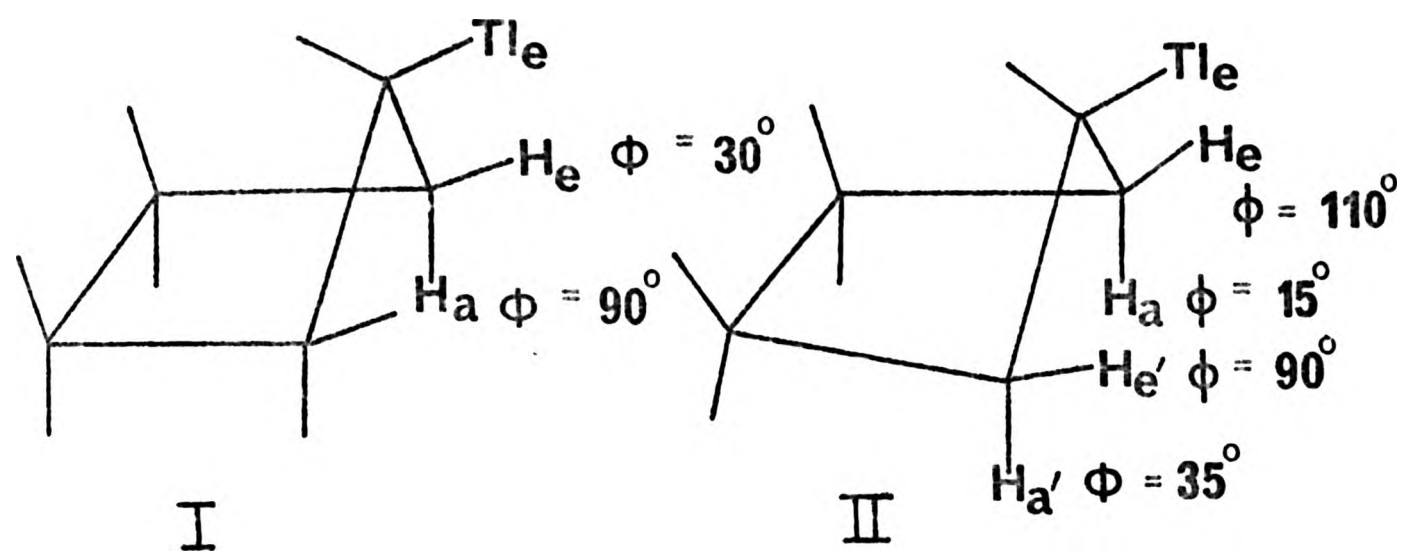
(iii) Cyclopentylthallium(III)

Differences in $^3J(\text{Tl-H})$ of 228 Hz in DMSO and 283Hz in pyridine were observed for $(\text{C}_5\text{H}_9)_2\text{TlBF}_4$ (Table 4.9). The dihedral angles for $^3J(\text{Tl-H})$ are shown in FIG.4.20.

The differences in dihedral angles in all cases would give rise to differences in $^3J(\text{Tl-H})$ and although the data cannot be used to propose that Tl is equatorial (as was suggested by ^{13}C data) it is not inconsistent with it.

(iv) Cycloheptylthallium(III)

A large difference of 384Hz is observed for the $^3J(\text{Tl-H})$ couplings in $(\text{C}_7\text{H}_{13})_2\text{TlBF}_4$ (Table 4.9) in pyridine. The dihedral angles associated with $^3J(\text{Tl-H})$ in the cycloheptyl system are shown in FIG.4.21.



4.20. Dihedral angles for $^3J(\text{Tl-H})$ in cyclopentylthallium.

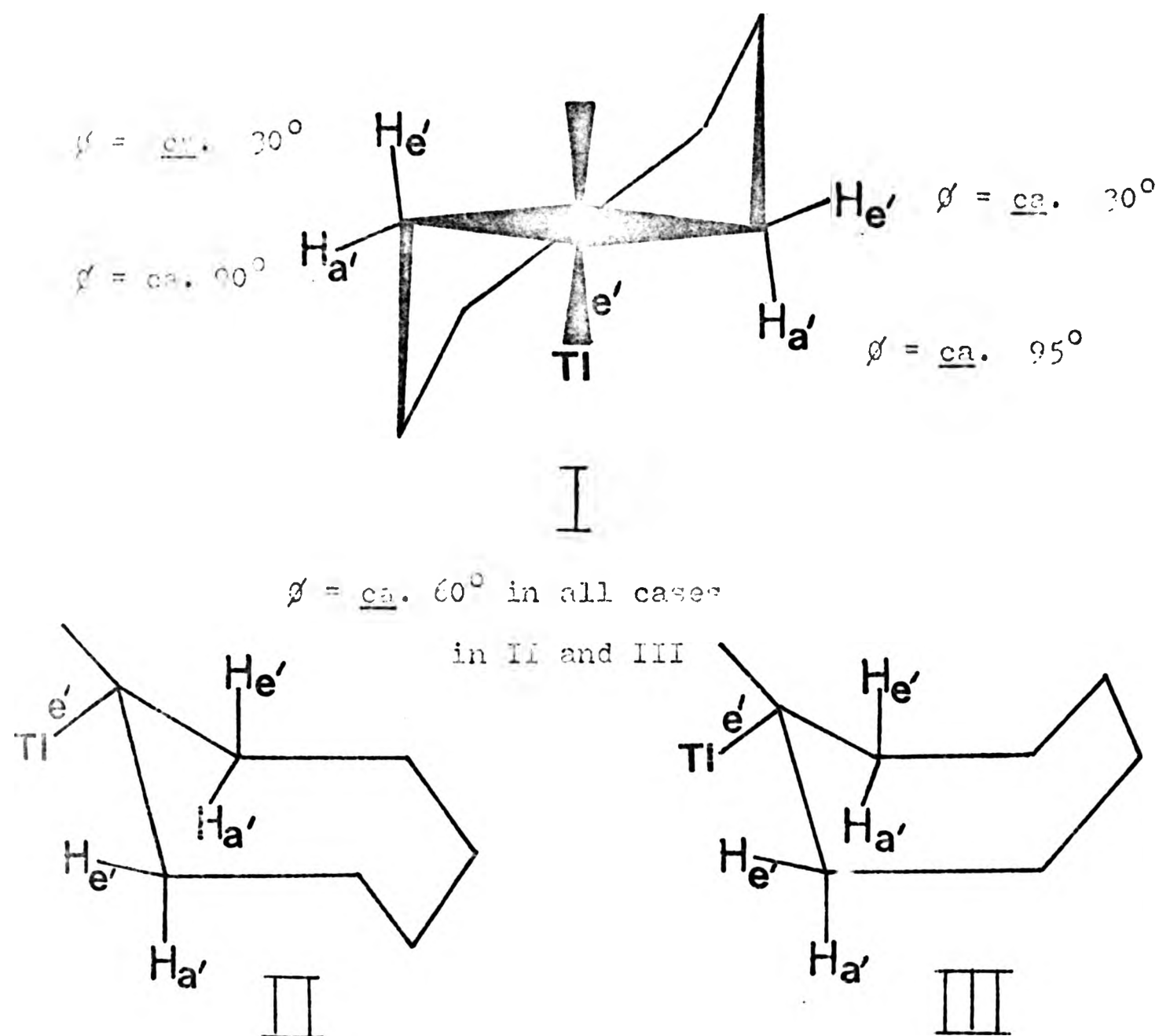
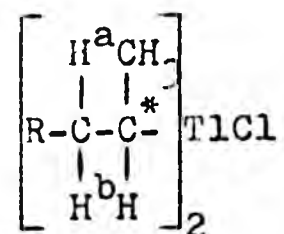


FIG. 4.21. Dihedral angles for $^3J(\text{Tl}-\text{H})$ in cycloheptylthallium (quasi-equatorial thallium).

The proposal that Tl is equatorial in a twist boat form(I) is not inconsistent with the proton data. In both the chair(II) and boat(III) forms the dihedral angle $\phi = \text{ca. } 60^\circ$ for $^3J(\text{Tl}-\text{H})$ for coupling to both a' and e' protons. In the twist-boat conformation with Tl quasi-equatorial large differences in ϕ are observed (I). Similar differences in ϕ can be observed in other twist chair conformations with thallium quasi-equatorial.

4.3.7.2. Alkyl derivatives

Large differences were noted in thallium-proton couplings to the methylene protons $H^{a,b}$ in compounds of the type:



($R = CH_3; CH_3CH_2$) where the CH_2 group is adjacent to a chiral centre (*) (Table 4.8). The difference is 242Hz for $[CH_3CH_2CH_2(CH_3)-CH]_2TlCl$ in DMSO, 290Hz in pyridine and 198Hz in benzene solutions. For $[CH_3CH_2(CH_3)CH]_2TlCl$ in DMSO the difference is 192Hz in DMSO and 182Hz in pyridine. The difference is probably sensitive to the nature of R for steric reasons. The 1H NMR spectrum of $[CH_3CH_2(CH_3)CH]_2TlCl$ is shown in FIG 4.22. $^1H-\{^1H\}$ experiments show that $^3J(Tl-H^{a,b})$ both have the same relative signs in sec-butyl and in sec-amyl compounds R_2TlCl (Table 4.8). These experiments also allowed 'pairing' of the signals using the nuclear Overhauser effect previously described. (4.2.2.2.). The magnetic non-equivalence of H^a and H^b may be appreciated using the Newman projections (FIG 4.23) showing the extreme cases of the gauche rotamers.

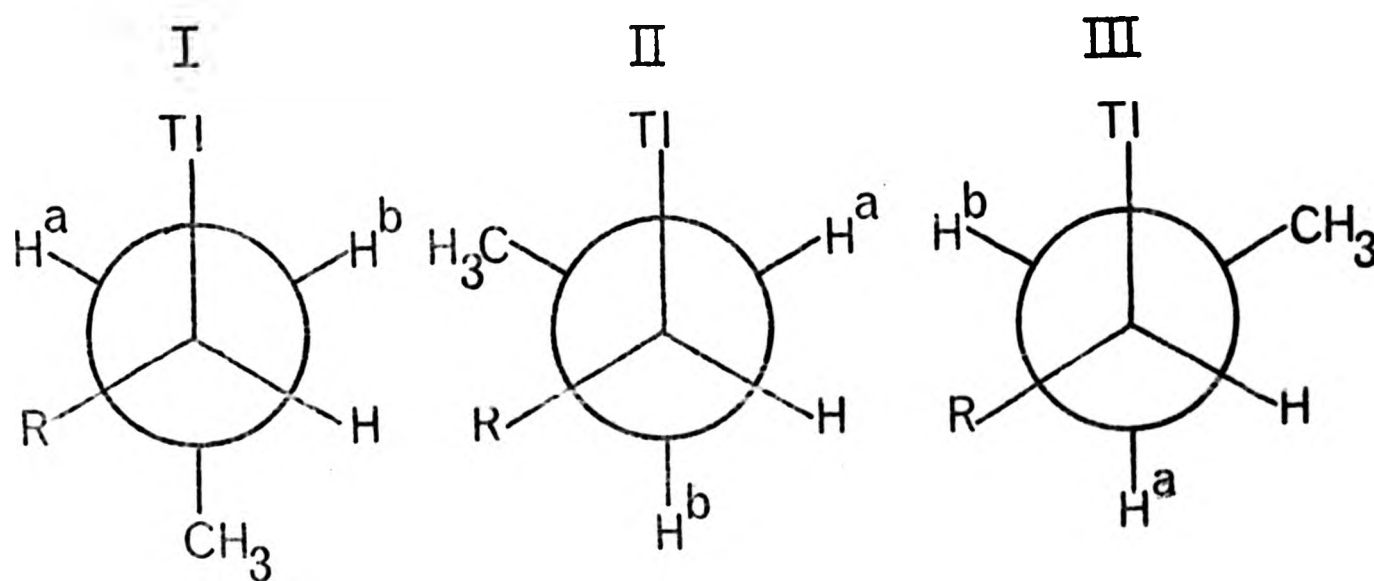
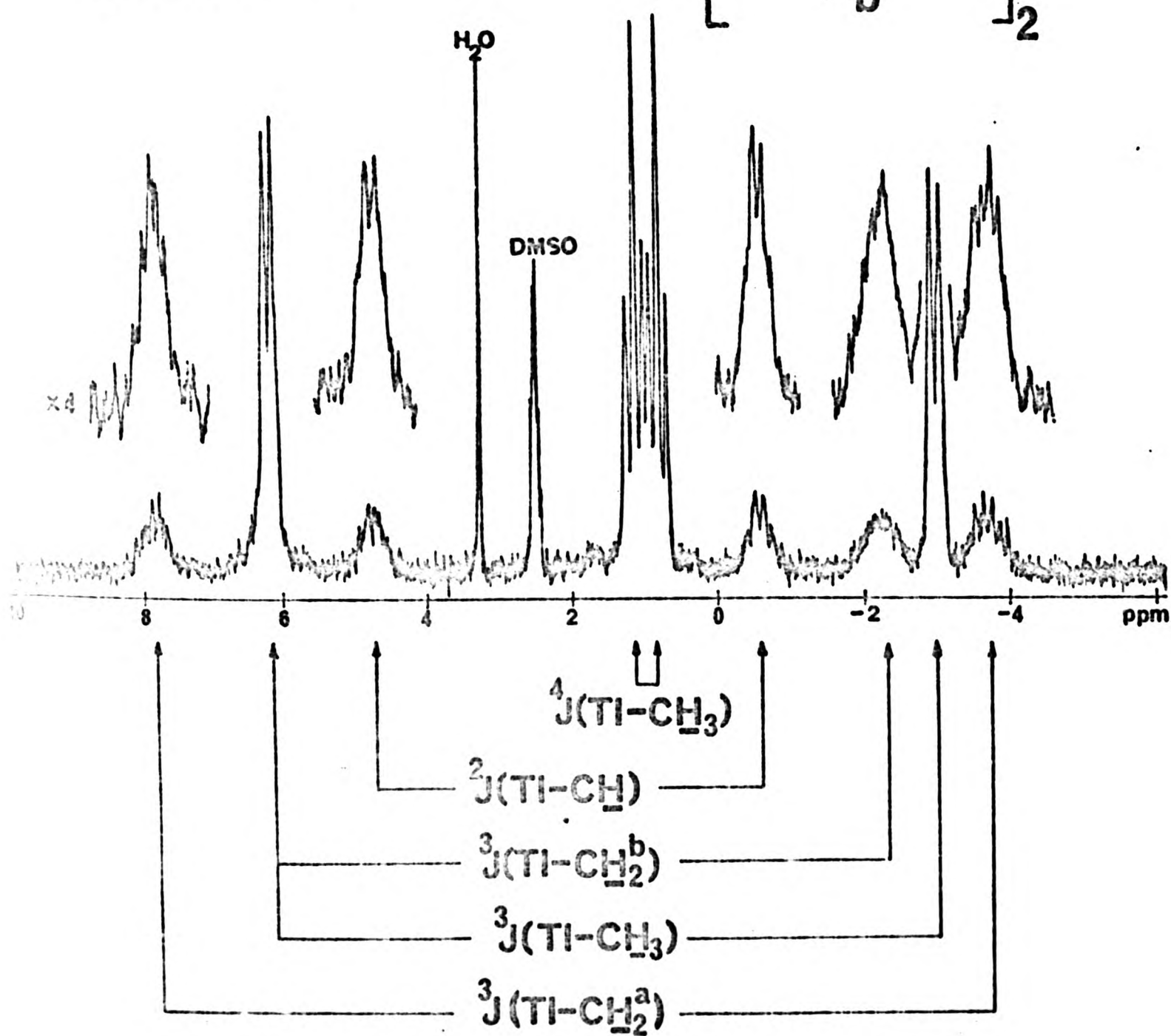
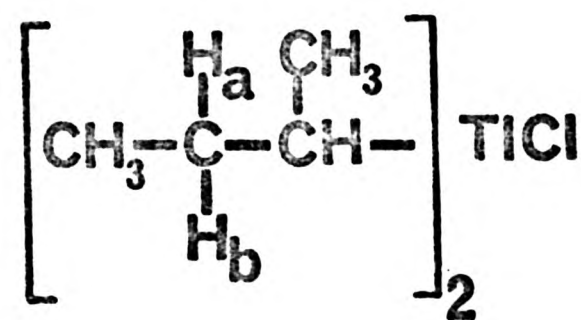


FIG. 4.23 . Newman projection of a sec-alkylthallium(III) derivative

FIG. 4.22.

60 MHz ^1H SPECTRUM OF
IN DMSO-d_6
(Continuous wave)



It is seen that for fast rotation even if I, II and III are equally populated there will be an intrinsic non-equivalence between H^a and H^b , leading to a chemical shift difference.³³⁴ Although small 1H chemical shift differences were observed here for H^a and H^b in $[CH_3CH_2(CH_3)CH]_2TlCl$ and $[CH_3CH_2CH_2(CH_3)CH]_2TlCl$ (Table 4.8) these differences were within the experimental errors as a result of the broadness of the resonances and cannot be considered further. In addition to the intrinsic non-equivalence of H^a and H^b the possibility of unequal residence in any conformer, due to restricted rotation or other factors, may augment their non-equivalence. Assuming a Karplus³³⁵ type dependence of $^3J(Tl-H)$, (See FIG. 4.18) either II or III might be expected to predominate and on steric grounds III would be favoured.

Many examples of magnetically non-equivalent methylene protons have been reported for cases where the CH_2 group is adjacent to a chiral centre. Abraham³³⁶ and Busby³³⁷ have reported differences in thallium-proton couplings to the anisochronous methylene protons in the alkyl side chains of $Tl(III)$ porphyrins. Uemura et al³³⁸ noted a difference in the values of $^2J(Tl-CH_2^{a,b})$ for the two non-equivalent α -protons of $PhCH(OR)CH_2Tl(OCOR')_2$ and Kurosawa^{93,276} gave an explanation of this non-equivalence in terms of unequal population of rotamers in these compounds due to restricted rotation. The anisochronous methylene protons in these latter compounds are on the carbon atom which is directly bonded to thallium and the chiral centre is two bonds removed. This situation is reversed here with the chiral centre bonded to thallium and the CH_2 group two bonds removed. In the former case the difference in $^3J(Tl-H^{a,b})$ is in the range 30-185Hz⁹³. While here it is in the range 182-290Hz at comparable temperatures.

4.3.7.3. Alkenyl derivatives

Thallium-carbon coupling $^3J(\text{Tl-C})$ to the CH_3 in $[\text{trans}-(\text{CH}_3)\text{CH}=\text{CH}]_2\text{TlNO}_3$ is larger than in the cis isomer. (TABLE 4.4). $[(\text{CH}_3)_2\text{CH}=\text{CH}]_2\text{TlNO}_3$ could only be prepared as a mixture of cis and trans isomers. The major component of this mixture was identified as the trans/trans isomer from the proton coupled thallium-205NMR spectrum (see 3.2.6.3) and (FIG 3.9). The major component in the carbon-13 spectrum is reported in Table 4.4 as the trans/trans isomer. The ^{13}C spectrum of the mixture showed sufficient other signals to account for cis/cis and cis/trans isomers but these were not readily assignable. All the couplings involved were less than in the trans/trans isomer. A similar value of $^3J(\text{Tl-C})$ -trans was observed in $[\text{trans}-(\text{C}_6\text{H}_5)\text{CH}=\text{CH}]_2\text{TlNO}_3$ (Table 4.4) (759Hz) to that found for $[\text{trans}(\text{CH}_3)\text{CH}=\text{CH}]_2\text{TlNO}_3$ (770Hz). Mitchell²⁴⁹ also reports that $^3J(\text{Sn-C})$ trans in propenyltin compounds is greater than the cis coupling.

It is interesting to note that coupling over more than three bonds to the aryl carbon atoms was not observed in $[\text{trans}-(\text{C}_6\text{H}_5)\text{CH}=\text{CH}]_2\text{TlNO}_3$, although Ernst⁶⁶ has reported thallium-carbon coupling over six bonds to the alkyl groups R in $\text{RC}_6\text{H}_4\text{TlX}_2$ compounds

Large differences in $^3J(\text{Tl-H})$ between the larger trans and smaller cis couplings of 817Hz for $(\text{H}_2\text{C}=\text{CH})_2\text{TlBF}_4$ in DMSO and 798Hz for $(\text{H}_2\text{C}=\text{CH})_2\text{TlOOCCH}_3$ in DMSO were observed. (Table 4.10). Maher found a difference of 813Hz for $(\text{H}_2\text{C}=\text{CH})_2\text{TlClO}_4$ in D_2O .⁸⁶ A difference in $^3J(\text{Tl-H})$ cis and trans of 1867Hz was found for $\text{H}_2\text{C}=\text{CHTlCl}_2$ in CD_3OD (Table 4.11). Maher noted a difference of 1944Hz for $\text{H}_2\text{C}=\text{CHTl}(\text{ClO}_4)_2$ in D_2O .⁸⁶

Thallium-proton coupling $^4J(\text{Tl-CH}_3)$ in propenylthallium(III) compounds, reported by Maher⁸⁶ and shown in Table 4.10 is seen to depend on the geometry of the system. $^4J(\text{Tl-H})$ in $[\text{trans}-(\text{CH}_3)-$

$\text{CH=CH}]_2\text{Tl}^+$ is -47Hz whereas in $[\text{cis}-(\text{CH}_3)\text{CH=CH}]_2\text{Tl}^+$ it is -94Hz.

Karplus³³⁵ has shown that $^3\text{J}(\text{H-H})$ couplings in alkenyl systems are very sensitive to the $\text{C}=\hat{\text{C}}-\text{H}$ bond angles. The larger values of $^3\text{J}(\text{Tl-C})_{\text{trans}}$ and $^3\text{J}(\text{Tl-H})_{\text{trans}}$ and $^4\text{J}(\text{Tl-H})_{\text{trans}}$ observed here might be rationalised on the basis of the dihedral angles; $^3\text{J}_{\text{trans}}$ ($\phi = \text{ca. } 180^\circ$); $^3\text{J}_{\text{cis}}$ ($\phi = \text{ca. } 0^\circ$).

At first sight the large values of $^3\text{J}(\text{Tl-H})$ couplings (especially the trans) in alkenylthallium(III) systems might be attributed to the increased s-character at the sp^2 hybridised vinyl carbon atoms. However on closer examination it would appear that this is largely as a result of the stereochemical dependence of the vicinal coupling. Values of $^3\text{J}(\text{Tl-H})$ for the freely rotating ethyl group in $(\text{C}_2\text{H}_5)_2\text{Tl}^+$ (628Hz) (Table 4.7) and $\text{C}_2\text{H}_5\text{Tl}^{2+}$ (1627Hz) (Table 4.11) are comparable to $^3\text{J}(\text{Tl-H})_{\text{cis}}$ in $(\text{H}_2\text{C=CH})_2\text{Tl}^+$ (792-805Hz) (Table 4.10) and $\text{H}_2\text{C=CHTl}^{2+}$ (1707Hz) (Table 4.11). Only the $^3\text{J}(\text{Tl-H})_{\text{trans}}$ coupling is larger than in the alkyl compound with $(\text{H}_2\text{C=CH})_2\text{Tl}^+$ (1590-1618Hz) and $\text{H}_2\text{C=CHTl}^{2+}$ (3574Hz). However the trans coupling in the vinyl system has an associated dihedral angle of ca. 180° in this rigid system and would therefore be expected to exhibit the largest coupling, whereas the $^3\text{J}(\text{Tl-H})$ observed for the ethyl system is an 'average' value for the various rotamers present.

A large value of $|^3\text{J}(\text{Tl-H})| = 2646\text{Hz}$ ($\phi = \text{ca. } 180^\circ$) has been noted in the rigid oxythallation adduct (RTlX_2) of D-galactaltriacetate, where the carbon atom to which the proton is bonded also has an $-\text{OCOCH}_3$ group attached through the oxygen atom.⁷² It is also of interest to note the smaller values of $^3\text{J}(\text{Tl-H})_{\text{ortho}}$ in arylthallium(III) derivatives

Ph_2Tl^+ (451Hz), PhTl^{2+} (948Hz)⁸⁶ where the carbon atoms to which the protons are bonded are sp^2 hybridised and $\delta = \underline{\text{ca}} 0^\circ$.

CHAPTER FIVE

THALLIUM-205 SPIN LATTICE RELAXATION IN
ORGANOTHALLIUM(III) COMPOUNDS

5.1 Introduction

Carbon-13 spin-lattice relaxation studies have been widely used to elucidate structural problems in organic compounds.³³⁹ However studies of heavy metal relaxation in organo-metallic derivatives have been relatively few: eg. ^{113}Cd ^{275,340}, ^{119}Sn ³⁴¹⁻³⁴³, ^{199}Hg ^{228,344,345}, ^{207}Pb ³⁴⁶. While thallium-205 relaxation has been used to some extent for structural studies of Tl(I) compounds in solution^{51,52,54-58} only one investigation of Tl(III), (for $(\text{CH}_3)_2\text{TlNO}_3$ ¹⁹) has been reported.

In order to determine the feasibility of utilising thallium-205 spin lattice relaxation as a probe of the structure of organothallium(III) derivatives in solution, a diverse range of compounds have been examined. The factors influencing thallium-205 relaxation are largely unknown and it was also hoped to gain some understanding of these.

No attempt will be made here to restate the background theory of nuclear magnetic relaxation and the reader is referred to several of the texts^{5,6,347} available on the subject. However the mechanisms of relaxation will be discussed in some detail in order to facilitate discussion of the results.

5.2. Results

Thallium-205 spin lattice relaxation times for RTlX_2 derivatives, R = chloromethyl; cyclopropyl; norbornene; over temperature ranges are reported in TABLE 5.1. The associated energies of activation, E_{act}, for the relaxation process are also reported.

Thallium-205 spin lattice relaxation times, for a number of R_2TlX derivatives; R = methyl, ethyl, n-alkyl, neo-pentyl,


cyclopropyl, phenyl are given in Table 5.2. The temperature dependence of T_1 has been reported for cases where $R = CH_3$; $(CH_2)_2CH$; C_6H_5 , and associated energies of activation and reorientational correlation times, τ_c , given.

Values for $M_z(\tau)$ and τ for the relaxation studies are listed in appendix III.

Proton spectra of $(CH_3)_2TiOCOCH_3$ and $[(CH_3)_3CCH_2]_2TiCl$ were obtained at spectrometer operating frequencies in the range 60 to 400 MHz and details are given in the text and in Tables 5.3 -5.5. Experimental details are given in Chapter 2.

Table 5.1

^{205}Tl Spin-lattice relaxation times (T_1) and activation energies (Eact) for RTlX_2 derivatives at 34.7 MHz

Compound	Solvent	Conc. ^a	Temp ^b	T_1^c	Eact. ^d
$\text{ClCH}_2\text{Tl}(\text{OCOR})_2^e$	CD_3OD	0.40	30.5	0.062	- 42.5 ^g
			42.7	0.061	
			46.8	0.059	
			51.9	0.054	
			56.2	0.045	
			61.0	0.042	
$(\text{CH}_2)_2\text{CHTl}(\text{OCOR}')_2^f$	DMSO-d6	0.39	26.5	0.112	13.4
			36.5	0.139	
			50.7	0.178	
			62.8	0.199	
 $\text{Tl}(\text{OCOCH}_3)_2$	DMSO d6	0.56	16.3	0.097	17.9
			30.3	0.137	
			45.6	0.192	

a. In mol dm^{-3} b. In degrees C. ($\pm 1^\circ\text{C}$). c. T_1 (Total) in seconds. Error $\pm 10\%$. d. In kJ mol^{-1} . Error $\pm 1 \text{ kJ mol}^{-1}$ unless otherwise noted. e. $\text{R} = \text{CH}_3$. f. $\text{R}' = \text{CH}(\text{CH}_3)_2$. g. Error $\pm 3 \text{ kJ mol}^{-1}$

Table 5.2

^{205}Tl Spin-lattice relaxation times (T_1), activation energies and correlation times (τ_c) for R_2TlX derivatives at 34.7 MHz

Compound	Solvent	Conc. ^a	Temp. ^b	T_1^c	Eact. ^d	τ_c^k
$(\text{CH}_3)_2\text{TlNO}_3^e$	H_2O	0.7	25.5	0.096		9.5×10^{-11}
$(\text{CH}_3)_2\text{TlNO}_3^f$	H_2O	0.8	26.0	0.556		
$(\text{CH}_3)_2\text{TlOCOR}^i$	D_2O	0.2	25.7	0.103		
			40.7	0.136		
			51.2	0.149		
			56.0	0.158		
			70.0	0.166		
$(\text{CH}_3)_2\text{TlNO}_3^h$	DMSO	0.30	25.5	0.081	8.4	7.0×10^{-11}
$(\text{C}_2\text{H}_5)_2\text{TlNO}_3^h$	"	"	"	0.057	15.6	1.0×10^{-10}
$(n\text{-C}_3\text{H}_7)_2\text{TlNO}_3^h$	"	"	"	0.052	13.7	1.1×10^{-10}
$(n\text{-C}_4\text{H}_9)_2\text{TlNO}_3^h$	"	"	"	0.042	13.6	1.3×10^{-10}
$(n\text{-C}_6\text{H}_{13})_2\text{TlNO}_3^h$	"	"	"	0.024	16.6	2.4×10^{-10}
$[(\text{CH}_3)_3\text{CCH}_2]_2\text{TlCl}^g$	py- d_5	0.18	39.9	0.192		2.97×10^{-11}
$[(\text{CH}_2)_2\text{CH}]_2\text{TlOCOR}^j$	py- d_5	0.25	45.5	0.165	6.4	3.4×10^{-11}
"	"	"	58.0	0.185		3.1×10^{-11}
"	"	"	64.5	0.188		3.0×10^{-11}
"	"	"	81.5	0.213		2.7×10^{-11}
$(\text{C}_6\text{H}_5)_2\text{TlCl}$	DMSO- d_6	0.20	23.5	0.066	16.1	8.6×10^{-11}
"	"	"	34.5	0.083		6.8×10^{-11}
"	"	"	50.7	0.125		4.6×10^{-11}
"	"	"	62.8	0.161		3.5×10^{-11}
"	"	"	80.7	0.199		2.9×10^{-11}

a. In mol dm^{-3} b. In degrees C ($\pm 1^\circ\text{C}$). c. T_1 (TOTAL) in seconds. Error $\pm 10\%$. d. In kJmol^{-1} . Error ± 1 .

Table 5.2(continued)

- e. Data from ref. 361. At 34.7 MHz. f. Data from ref. 19
at 15.1 MHz. g. Data from ref 372. h. Data from ref. 370 .
i. $R = CH_3$ Data from ref. 133. j. $R' = CH(CH_3)_2$.
k. Reorientational correlation time in seconds. See p258
for method of calculation.

Table 5.3

Variation of Linewidth^a, in the proton spectra of R₂TlX derivatives with spectrometer operating frequency.

Operating frequency (MHz)	Temp ^b . (°C)	(CH ₃) ₂ TlOCOCH ₃ ^c	V _{1/2} ^a [(CH ₃) ₃ CCH ₂] ₂ TlCl ^d
60	33	4.0 ± 0.5	3.5 ± 0.5
150	27	9.08 ± 0.03 ^e	8.39 ± 0.18 ^e
220	25	19.4 ± 0.7	-
300	27	29.7 ± 0.5	29.3 ± 1.0
360	27	46.4 ± 0.5 ^e	29.53 ± 0.19 ^e
400	27	49.5 ± 1.0	-

a. In Hz taken as half-height width of the components of ²J(Tl-H). ^bError ± 1°C. c. In D₂O, 0.2 mol dm⁻³

d. In pyridine-d₅ 0.3 mol dm⁻³. e. From a Lorentzian fit. Otherwise measured from the spectrum.

Table 5.4

Variation of linewidth^a in the proton spectra of (CH₃)₂TlOCOCH₃^b with temperature at 80, 220 and 360 MHz.

80 MHz		220 MHz		360 MHz	
Temperature ^c	V _{1/2} ^a	Temperature ^c	V _{1/2} ^a	Temperature ^c	V _{1/2} ^a
7	6.50	10	29.7	27	46.42 ^{d,e}
17	4.88	25	19.44	47	30.35 ^{e,f}
27	3.95	32	15.83	67	19.85 ^{e,g}
37	3.63	45	14.44		
47	3.55	65	7.78 ^d		
57	3.30	75	6.67 ^d		
67	3.05				
77	3.00				

a. In Hz. Error ± 1 Hz unless otherwise noted. Taken as the half height width of the components of ²J(Tl-H). b. In D₂O, 0.2 mol dm⁻³. c. In degrees C. Error ± 1°C. d. Error ± 0.50 Hz. e. From a Lorentzian fit. Otherwise measured from the spectrum. f. Error ± 0.26 Hz. g. Error ± 0.21 Hz.

Table 5.5

Variation of linewidth^a in the proton spectra of $[(CH_3)_3CCH_2]_2TlCl^b$ with temperature at 360MHz.

<u>Temperature^c</u>	<u>$v_{1/2}^d$</u>
27	29.53 ± 0.19
67	15.42 ± 0.07

- a. In Hz. taken as half-height linewidth of the components of $^2J(Tl-H)$. b. In pyridine 0.3 mol dm⁻³ c. In °C ± 1 .
d. From a Lorentzian fit.

5.2.1. Measurement of T_1

^{205}Tl T_1 measurements were obtained by the inversion recovery method using the 180° - τ - 90° pulse sequence. The basis of this method is shown in FIG 5.1. A 180° pulse inverts the bulk magnetisation vector along the z' axis (coordinates for the rotating frame of reference shown). Spin lattice relaxation now occurs and causes M_z' to recover towards its equilibrium value of M_0 . A 90° pulse, applied at some time τ after the 180° pulse, then rotates the magnetisation onto the y' axis. This can then be observed as an FID (free induction decay) which can be Fourier transformed to give a spectrum as usual. The experiment is repeated using different values of τ allowing a delay $>5T_1$ in each case to enable the magnetisation to return to its equilibrium position. Recovery of the magnetisation is described by equation (5.1);

$$M_\tau = M_0 \left\{ 1 - 2 \exp(-\tau/T_1) \right\} \quad (5.1)$$

A plot of $\ln\left(\frac{M_0 - M_\tau}{M_0}\right)$ against τ allows T_1 to be calculated from the gradient. The results of a typical ^{205}Tl T_1 experiment are shown in FIG.5.2. For short τ ($<0.69T_1$) values the magnetisation is still inverted. As τ is increased it becomes positive until it reaches its equilibrium value M_0 .

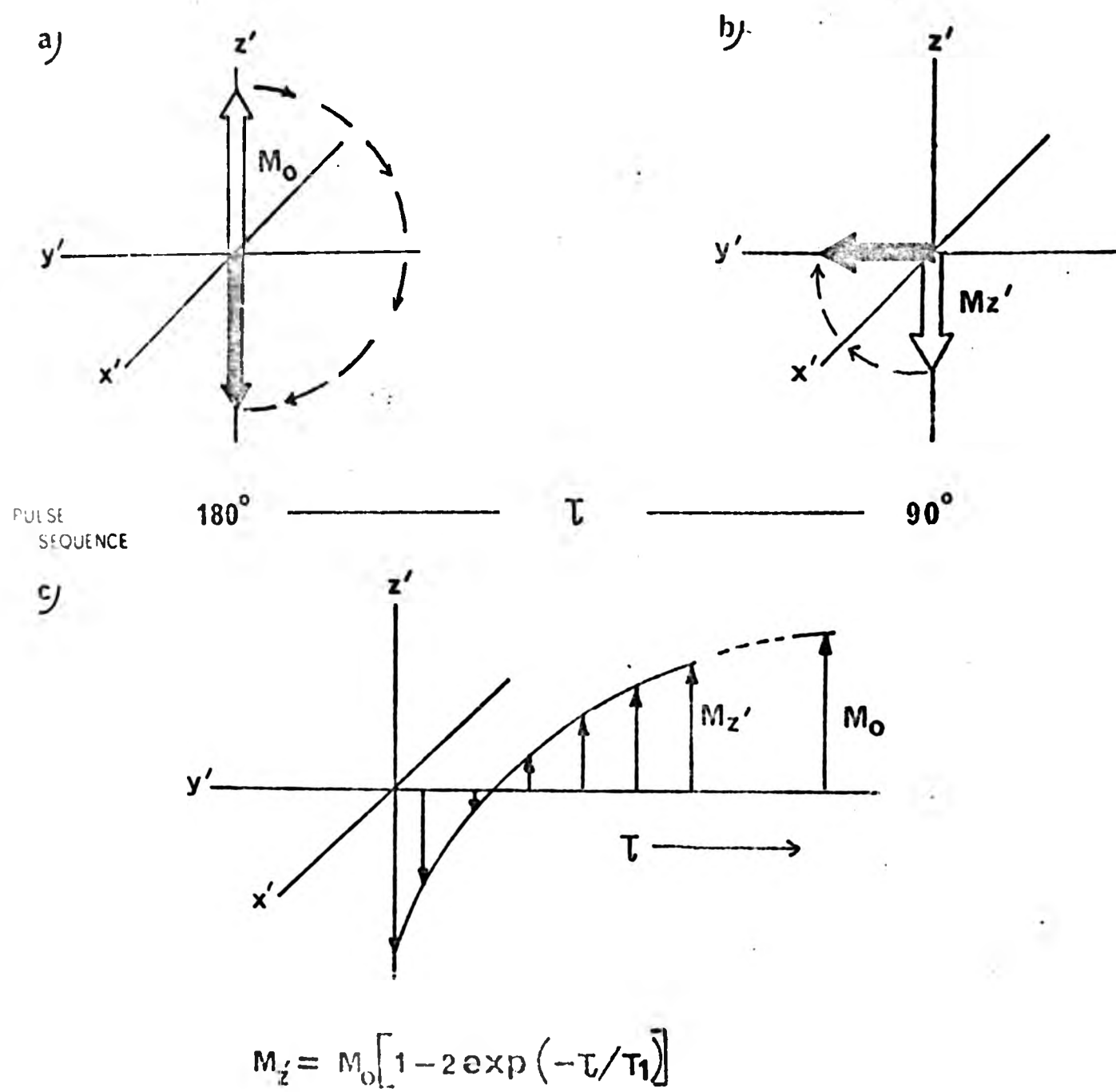
5.2.2. Energy of Activation

Measurement of a rate constant over a temperature range allows calculation of an energy of activation for the process using the Arrhenius relationship shown in equation (5.2)

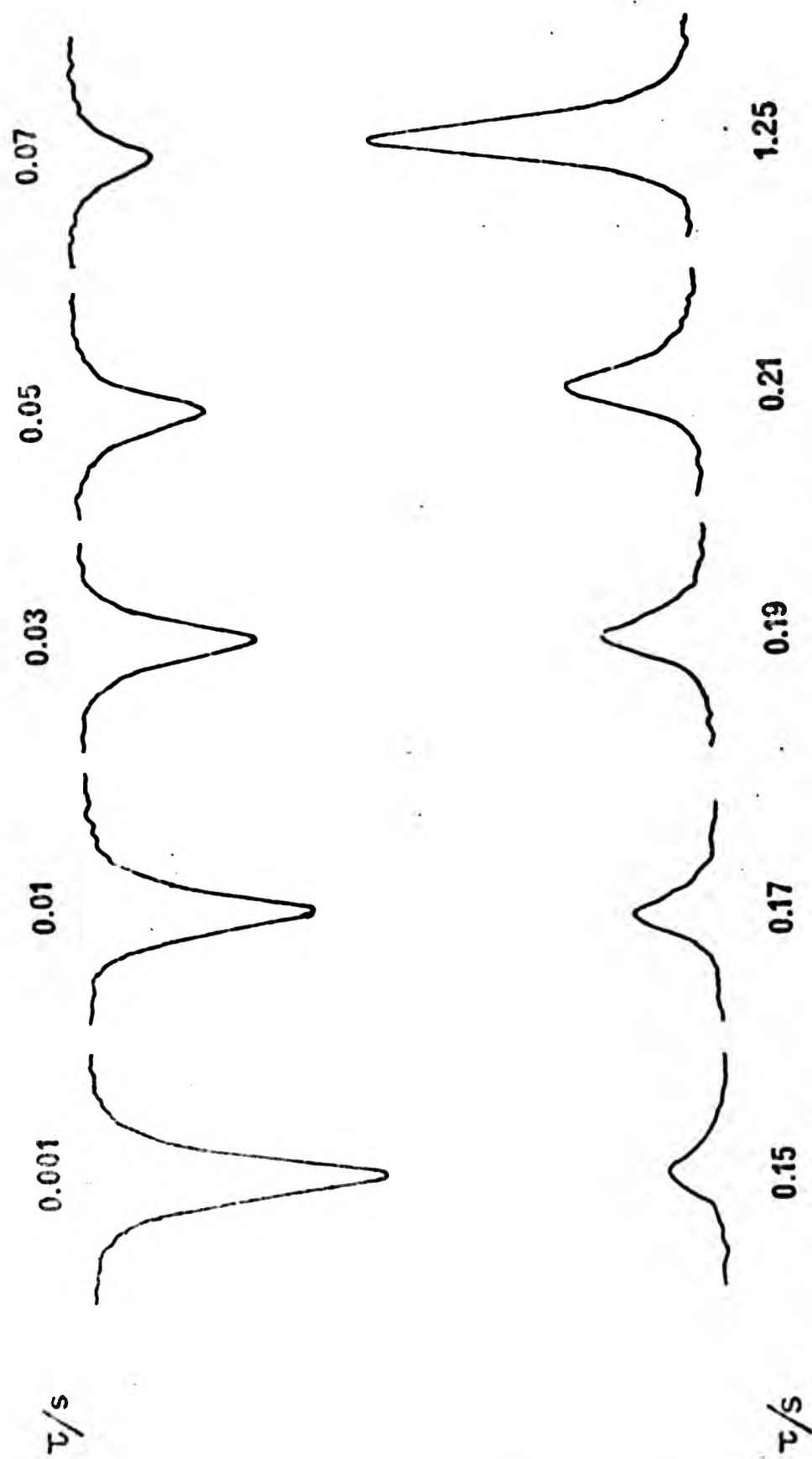
$$\ln R_1 = \ln A - E_a/RT \quad (5.2)$$

FIG. 5.1.

DETERMINATION OF T_1 BY THE INVERSION RECOVERY METHOD
USING THE $(180^\circ - \tau - 90^\circ)$ PULSE SEQUENCE



TYPICAL RESULTS OF A ^{205}Tl T_1 DETERMINATION AT 34.7 MHz USING THE $(180^\circ\text{-}\tau\text{-}90^\circ)$ PULSE SEQUENCE



THESE RESULTS ARE FOR DICYCLOPROPYLTALLIUM(I)ISOBUTYRATE 0.25mol dm^{-3} IN PYRIDINE- d_5 AT 58°C USING 400 TRANSIENTS. $T_1 = 0.185\text{s}$

FIG. 5.2.

where A = a constant. Since the spin lattice relaxation time is the inverse of the relaxation rate R_1 a plot of $\ln R_1$ against $1/T$ yields the energy of activation from the gradient. The spin lattice relaxation time is directly proportional to an appropriate correlation time and the Arrhenius plot yields an energy of activation for the reorientational correlation time τ_c or the angular momentum correlation time τ_j , depending on the mechanism involved.

5.3. Relaxation mechanisms

5.3.1. Dipole-Dipole Relaxation

This is generally the most important relaxation mechanism for nuclei with $I = \frac{1}{2}$ in the liquid state. Consider the relaxation of a nucleus I by a second nucleus S in the same molecule. The magnetic field B_{local} experienced by I depends on the energy of interaction of the two magnetic moments μ_I, μ_S . The magnitude of this interaction depends upon the separation r of I and S and their relative orientations to the applied magnetic field B_0 ³⁴⁷. Since the two nuclei are in motion in solution this term depends on the frequency components of this motion. For intramolecular dipole-dipole interaction we need only consider rotational motion. For isotropic motion in mobile liquids where molecular reorientation is fast

$$(T_1)^{-1} = (T_2)^{-1} = \hbar^2 \cdot \gamma_I^2 \gamma_S^2 \cdot \sum_N r_{IS}^{-6} \cdot \tau_c \quad (5.3)$$

where γ is the gyromagnetic ratio of the nucleus, N is the number of nuclei of type S , r is the separation between I and S and τ_c is a rotational correlation time. This situation is referred to as the extreme narrowing condition and $(T_1)^{-1}$ and

and $(T_2)^{-1}$ are frequency independent. In the case of inter-molecular dipole-dipole interaction τ_c is a translational correlation time.

When the overall motion is not isotropic quantitative description of this mechanism becomes complex and cannot be described by a single correlation time.

The dependence of dipole-dipole relaxation on the inverse sixth power of the separation of the nuclei indicates that it is only effective over very short distances. This also results in the intramolecular mechanism being dominant especially when I and S both have $I = \frac{1}{2}$ and are directly bonded.

Apart from the importance of dipole-dipole relaxation for carbon in organic compounds³³⁹ it has also been shown to make considerable contribution to the relaxation of ^{119}Sn in some alkyltin compounds,³⁴³ eg. $(n\text{-propyl})_3\text{SnCl}$, $n\text{-Butyl}_3\text{SnCl}$, $n\text{-butyl}_3\text{SnH}$, to ^{77}Se in $\text{C}_6\text{H}_5\text{SeH}$ ³⁴⁸ and is the dominant relaxation mechanism for ^{29}Si in some alkylsilanes R_3SiH ³⁴⁹ (R = $n\text{-propyl}$, $n\text{-butyl}$, $n\text{-hexyl}$).

5.3.2. Spin Rotation

This is the only relaxation mechanism for which the relaxation rate increases with increasing temperature, allowing it to be easily distinguished. The fluctuating fields associated with this mechanism are generated by the motion of the molecular magnetic moment arising from the electronic distribution within the molecule. For a rotating molecule whose moment of inertia is I, in the Jth rotational state, its rotational frequency will be given by:-

$$V = h J / 2\pi I$$

Any electron in the molecule undergoing such rotation will generate a local magnetic field at the nucleus. Molecular collisions altering this rotation will modulate the local field and so provide a relaxation mechanism. For molecules undergoing isotropic reorientation the relaxation rate is given by

$$(T_1)_{SR}^{-1} = (2IkT^0/3h^2) (2C_{\perp}^2 + C_{\parallel}^2) \tau_j \quad (5.4)$$

where τ_j is the angular momentum correlation time, C is the appropriate spin-rotation constant and k is the Boltzmann constant. In the liquid state τ_j is inversely related to the molecular reorientation correlation time, τ_c , used in the dipole-dipole mechanism by^{350,351}

$$\tau_c \tau_j = 1/6kT \quad (5.5)$$

where T is the absolute temperature, for temperatures well below the liquid's boiling point.

The spin rotation mechanism is most efficient for small symmetrical molecules at high temperatures. At low temperatures it is inefficient. It is especially important for nuclei with large chemical shift ranges (eg. ^{13}C , ^{15}N , ^{19}F , ^{31}P)^{5,352} in small symmetric molecules. This relationship between chemical shift range and $(T_1)^{-1}_{SR}$ is because both depend on the electronic distribution within the molecule.³⁵³

Spin rotation has been shown to be an important relaxation mechanism for ^{29}Si in $(\text{CH}_3)_3\text{SiX}$ ($X = \text{anion}$)¹⁹⁶; for ^{119}Sn in $(\text{CH}_3)_6\text{Sn}_2$ ³⁴³. It has also been reported to make significant contributions to the relaxation of ^{113}Cd for $\text{Cd}(\text{ClO}_4)_2$ in H_2O ³⁵⁵ and for ^{195}Pt in $\text{Na}_2[\text{PtCl}_4]$ and $\text{Na}_2[\text{PtCl}_6]$ in aqueous

solution,³⁵⁴ also for ^{199}Hg in $(\text{CH}_3)_2\text{Hg}$.^{228,344}

5.3.3. Chemical Shift Anisotropy

The field experienced by a nucleus, B_{local} , in an applied magnetic field B_0 , is given by

$$B_{\text{loc}} = B_0(1 - \sigma)$$

where σ is the screening tensor. In mobile liquids the average value of the tensor is observed as

$$\sigma = \frac{1}{3}(\sigma_{xx} + \sigma_{yy} + \sigma_{zz})$$

If the components of σ are not equal the chemical shift is anisotropic and molecular motion provides a fluctuating magnetic field at the nucleus which provides a relaxation pathway. The contributions from the screening anisotropy in the case of molecules possessing axial symmetry are given by:

$$(T_1)^{-1} \text{CSA} = \frac{1}{15} \gamma^2 B_0^2 (\sigma_{||} - \sigma_{\perp})^2 \left\{ \frac{2\tau_c}{1 + \omega^2 \tau_c^2} \right\} \quad (5.6)$$

$$(T_2)^{-1} \text{CSA} = \frac{1}{90} \gamma^2 B_0^2 (\sigma_{||} - \sigma_{\perp})^2 \left\{ \frac{6\tau_c}{1 + \omega^2 \tau_c^2} + 8\tau_c \right\} \quad (5.7)$$

where $\sigma_{||}$ and σ_{\perp} are the screening constants parallel to and perpendicular to the symmetry axes respectively. τ_c is the rotational correlation time and ω is the resonance frequency in radians s^{-1} . In the absence of axial symmetry the equations become much more complex.³⁴⁷

In the extreme narrowing limit, the usual situation in non-viscous liquids, the frequency dependence vanishes and we obtain:-

$$(T_1)_{\text{CSA}}^{-1} = \frac{2}{15} \gamma^2 B_0^2 (\sigma_{\parallel} - \sigma_{\perp})^2 \tau_c \quad (5.8)$$

$$(T_2)_{\text{CSA}}^{-1} = \frac{7}{45} \gamma^2 B_0^2 (\sigma_{\parallel} - \sigma_{\perp})^2 \tau_c \quad (5.9)$$

It can be seen that $(T_1)^{-1}/(T_2)^{-1} = 6/7$ and the mechanism depends on the square of the applied field.

Few authenticated examples of this mechanism have been reported. It has been shown to contribute to ^{19}F relaxation in CH_2Cl_2 at -142° .³⁵⁶ It has also been shown to be effective for ^{13}C in $\text{Ph-C}\equiv^{13}\text{C-C}\equiv\text{C-Ph}$ ³⁵⁷ and $\text{CH}_3^{13}\text{CO}_2\text{H}$.⁶ It has been proposed as the dominant relaxation mechanism for ^{77}Se in $\text{Zn}[\text{Se}_2\text{CN}(\text{C}_2\text{H}_5)_2]_2$ and $\text{Pd}[\text{Se}_2\text{CN}(\text{iso-C}_4\text{H}_9)_2]_2$ ³⁵⁸ and also in $\text{C}_6\text{H}_5\text{SeOH}$ ³⁵⁹ as a result of the temperature dependence of T_1 and negligible NOE. Other cases where CSA has been proposed as contributing are for ^{113}Cd in R_2Cd ($\text{R} = \text{CH}_3, n\text{-Bu}$)^{275,340} at lower temperatures, and for ^{199}Hg in $(\text{CH}_3)_2\text{Hg}$.²²⁸ although this has been questioned.³⁴⁴

A theoretical study by Schwartz³⁶⁰ suggested that a transient chemical shift anisotropy mechanism may be important in relaxation of spin $\frac{1}{2}$ heavy metal nuclei in electrolyte solution. Gillies has found it to be dominant at 2.35T for ^{199}Hg in $(\text{C}_6\text{H}_5)_2\text{Hg}$.³⁶¹

5.3.4. Scalar Relaxation

A nucleus S which is spin-spin coupled to another nucleus I can provide fluctuating magnetic fields via scalar interactions involving the bonding electrons. Relaxation by nucleus S alters the magnetic field experienced by nucleus I through spin-spin coupling and thus provides a relaxation mechanism for nucleus I. For spin-lattice relaxation fluctuations may arise in two ways:-

(i) As a result of any time dependence of the spin coupling constant between nuclei I and S, resulting for example from chemical exchange. Then the local field at I (or S) will fluctuate as a function of the exchange rate. This is known as scalar relaxation of the first kind.

(ii) As a result of the time dependence of the excited state of spin S, i.e. when the T_1 value of S is short compared to the inverse of the coupling constant A_{IS} , ($A = 2 \pi J$), then the local field at I fluctuates. This is scalar relaxation of the second kind.

In order that this mechanism may be efficient the exchange rate in (i) and the relaxation rate in (ii) must be large, in fact comparable to the difference in resonance frequencies of I and S.

For scalar relaxation the expression for T_1 is:

$$(T_1)_I^{-1} = \frac{2A^2}{3} S(S+1) \left\{ \frac{\tau_S}{1 + (\omega_I - \omega_S)^2 \tau_S^2} \right\} \quad (5.10)$$

The contribution to T_2 is given by :-

$$(T_2)_I^{-1} = \frac{A^2}{3} S(S+1) \left\{ \tau_S + \frac{\tau_S}{1 + (\omega_I - \omega_S)^2 \tau_S^2} \right\} \quad (5.11)$$

where τ_S , the correlation time for this process, is the spin-lattice relaxation time of S, A is the coupling constant in rad sec⁻¹, ω is the resonance frequency.

Scalar relaxation is most commonly found when S is a quadrupolar nucleus that relaxes rapidly. Even in this case however it is rare that scalar relaxation has much effect on $(T_1)_I$ unless the resonance frequencies ω_S and ω_I are nearly equal. $(T_2)_I$ however is commonly affected; line broadening (ie. increase in $(R_2)_I$) in the ¹H spectrum of nuclei coupled to ¹⁴N is commonly observed for example.³⁵² $(T_2)_I$ may also be affected in cases where T_1 relaxation of S is much greater than 1/A; eg. in molecules with ¹³C coupled to ¹H, the ¹H

T_1 is normally long enough so that spin-spin coupling is observed, but T_2 (¹³C) is nonetheless shortened by scalar coupling to the proton.³⁶²

5.3.5. Quadrupolar Relaxation

Nuclei of spin $I = \frac{1}{2}$ have a spherical nuclear charge distribution whereas nuclei with $I \neq \frac{1}{2}$ have a non-spherical distribution and a quadrupole moment Q. Such quadrupolar nuclei do not have an electric dipole moment hence their energy is independent of orientation in a uniform electric field. Where an electric field gradient exists the nuclei precess about the net electric field providing an efficient relaxation pathway via molecular rotation. In the extreme narrowing limit it can be shown that:

$$(T_1)_Q^{-1} = (T_2)_Q^{-1} = \frac{3}{40} \left\{ \frac{2I+3}{I^2(2I-1)} \right\} \cdot \left\{ \frac{1+\eta^2}{3} \right\} \cdot \left\{ \frac{e^2 q Q}{\hbar} \right\} \cdot \tau_c \quad (5.12)$$

where η is an asymmetry parameter, q is the electric field gradient at the nucleus and $(e^2 q Q / \hbar)$ is the quadrupolar coupling constant.

Quadrupolar relaxation is the dominant relaxation mechanism for nuclei with $I > \frac{1}{2}$ eg. ^{23}Na , ^{364}Mg , ^{25}Mg , ^{363}Al , ^{366}Al , ^{75}As , ^{365}As , also for ^{45}Sc and other transition metals ²³⁸.

5.3.6. Electron-Nuclear Relaxation

The electron is a magnetic dipole and an unpaired electron moving in solution will generate fluctuating magnetic fields which can provide a relaxation mechanism. The magnetic moment of the electron is ca. 10^3 times larger than that of the proton which itself has the largest nuclear moment. Electron-nuclear dipolar relaxation is thus 10^6 times more efficient than nuclear-nuclear dipolar relaxation.

Thus even small amounts of paramagnetic materials present in solution may significantly affect relaxation times. Oxygen is the most common paramagnetic species. Dissolved oxygen must be removed from solutions by degassing before relaxation measurements are carried out. The electron-nuclear mechanism was shown to dominate the spin lattice relaxation rate of thallium-205 for solutions of Tl(I) containing the radical 4-hydroxy-2,2,6,6-tetramethylpiperidine-1-oxyl ('TANOL')¹²⁵

5.3.7. Separation of relaxation mechanisms

Theoretically any measured spin-lattice relaxation rate can have contributions from each of these mechanisms. However, in practice, contributions from all mechanisms to the relaxation of a given nucleus will rarely be found. Inspection of the

equations governing each mechanism can often indicate whether a particular mechanism is likely to contribute. Examination of the temperature dependence of the relaxation rate can also assist in elucidating the contributing mechanisms. The spin-rotation mechanism has an opposite temperature dependence to all others, FIG.5.3.,and thus may be easily distinguished. The dipole-dipole mechanism can be separated from all others (irrespective of temperature dependence) by using the nuclear Overhauser effect³⁶⁷(NOE) and the relationship in equation(5.13)

$$\left\{ \frac{1}{T_1} \right\}_{DD} = \frac{\eta}{\eta_{\max}} \cdot \left\{ \frac{1}{T_1} \right\}_{TOT} \quad (5.13)$$

where η/η_{\max} is the NOE factor.

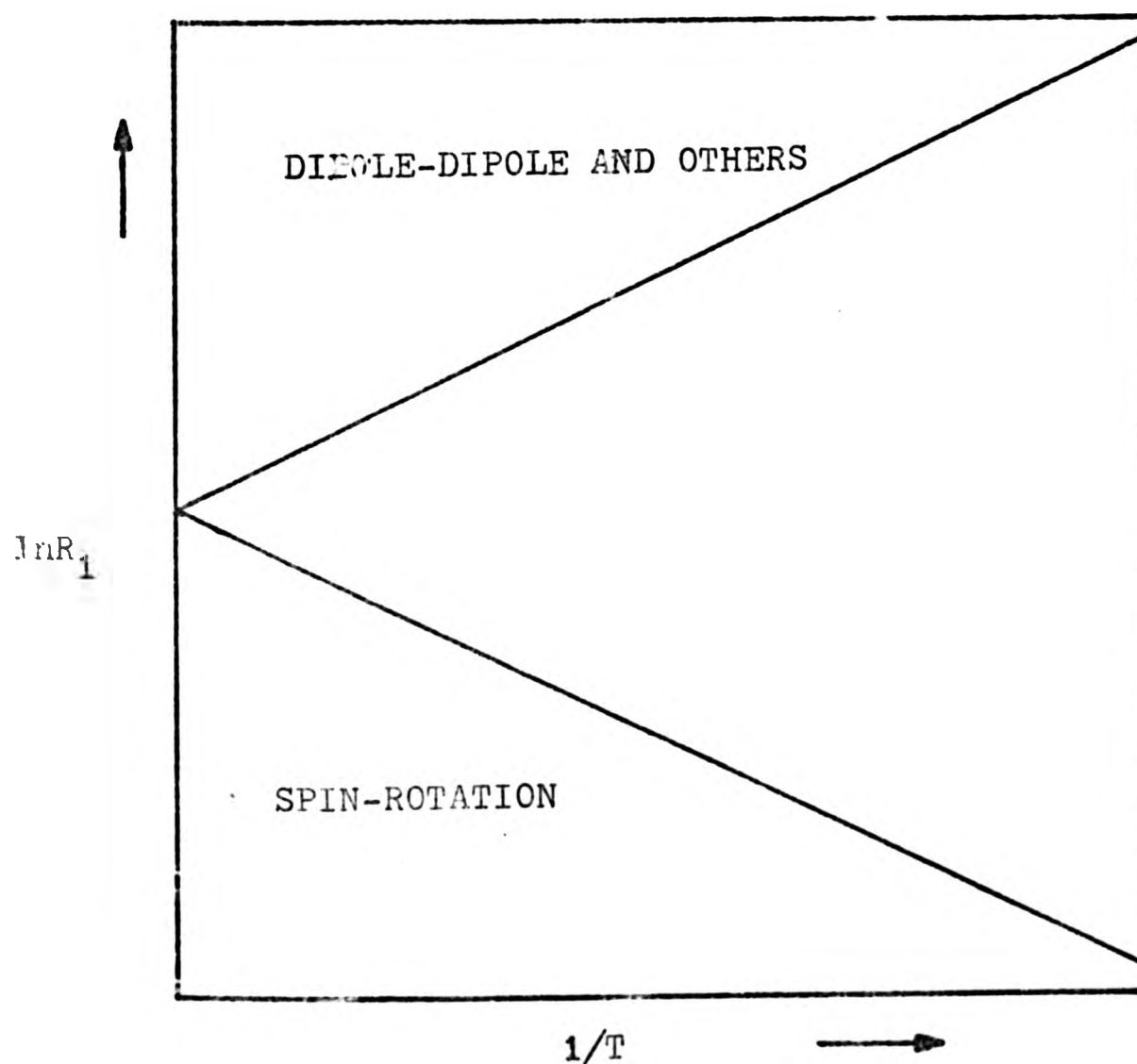


FIG. 5.3. Temperature dependence of spin-lattice relaxation.

The chemical shift anisotropy mechanism can be readily distinguished by its dependence on the square of the applied field. Of the remaining mechanisms quadrupolar relaxation requires the presence of quadrupolar nuclei and electron-nuclear relaxation requires paramagnetic species. Scalar relaxation requires stringent matching of time scales usually only occurring with rapid chemical exchange or in the presence of a rapidly relaxing nucleus.

5.4. Discussion

For the organothallium(III) compounds $RTlX_2$ (R = cyclopropyl, norbornene, X^- - anion) (TABLE 5.1) and R_2TlX , (R = methyl, ethyl, *n*-propyl, *n*-butyl, *n*-hexyl, *neo*-pentyl, cyclopropyl, phenyl) (TABLE 5.2), thallium-205 spin lattice relaxation times were found to increase with temperature implying a lower relaxation rate at higher temperatures. This is reflected in the reorientational correlation times τ_c for R_2TlX , (R = cyclopropyl, phenyl) (TABLE 5.2) which become shorter as the temperature increases. (See p.258 for method of calculation of τ_c).

The relaxation rates for the straight chain alkylthallium(III) compounds R_2TlX decrease with increasing chain length. The accompanying increase in τ_c can be interpreted in terms of rotation of the molecules becoming slower as the chain length increases because more 'solvent' molecules have to be swept out of the way. The increasing energy of activation for the reorientational process as the chain becomes longer reflects this.

A surprising feature of the T_1 results is that molecules R_2TlX where R is a bulky group such as $(CH_3)_3CCH_2C_6H_5$, appear to undergo reorientation and relaxation at rates comparable to molecules where $R = CH_3$. It might reasonably be expected that such processes would be more rapid in the smaller molecule, especially since the activation energies for the *neo*pentyl and phenyl derivatives are approximately twice as large as those for $(CH_3)_2TlNO_3$ in DMSO. Caution must however be exercised in making these comparisons since a number of different solvents and anions are involved and the influence of these factors is largely unknown here. Several tentative explanations can be offered, however.

a). The dimethylthallium(III) ion exists in solution ^{103,368,369} as a linear moiety $\text{CH}_3\text{-Tl}^+\text{-CH}_3$: it can be seen that thallium could easily be surrounded by an equatorial 'bracelet' of solvent molecules (in this case DMSO). This would result in a rather bulky species which would undergo slower reorientation. The presence of the bulky groups on the larger molecules on the other hand might hinder solvation of thallium.

b). As discussed in Chapter 6(6.3.2.), compounds R_2TlX where R is a bulky group and X a relatively small anion are likely to exist as dimers. Any oligomeric behaviour in solution would result in loss of axial symmetry. The correlation times are calculated assuming such symmetry and in its absence would become meaningless.

c). Correlation times have been calculated assuming that the chemical shift anisotropy mechanism makes the dominant contribution to thallium relaxation (see later). Contributions from other mechanisms are unknown and have been neglected. Such a gross assumption may not be valid especially where bulky groups having a large number of protons may have a significant dipole-dipole contribution. (This is further discussed later). However in the case of the phenyl derivative where the protons are further away from thallium this latter mechanism would not be expected to be important. Gillies has found a very small dipole-dipole contribution to ^{199}Hg relaxation in $(\text{C}_6\text{H}_5)_2\text{Hg}$.³⁶¹

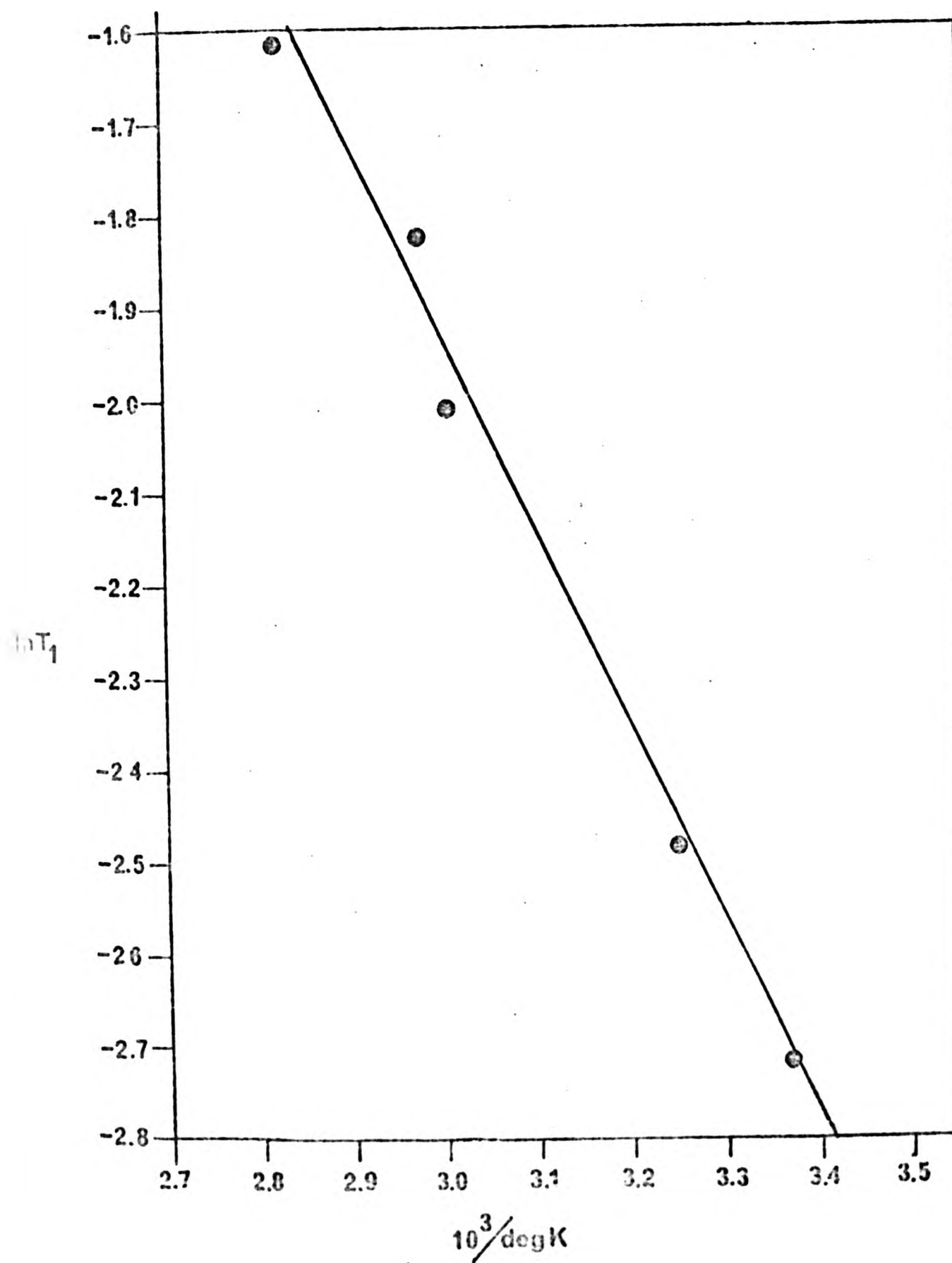
The spin lattice relaxation rates for RTlX_2 derivatives are, unexpectedly, not significantly different from those for R_2TlX compounds. In the one case where direct comparison can be made, $\text{R} = (\text{CH}_2)_2\text{CH}$, the T_1 values are almost the same for

both mono- and diorgano derivatives, although different solvents are involved. The increased bulk of the norbornene derivative compared to the cyclopropyl appears to have no significant effect on T_1 although the energy of activation is greater for the reorientational process involving the larger norbornene group. Correlation times are not reported for $RTlX_2$ derivatives as they are not expected to possess axial symmetry.

For all the compounds studied (except $ClCH_2Tl(OCOCH_3)_2$ and $(CH_3)_2TlOCOCH_3$ in D_2O which will be discussed separately) the ^{205}Tl spin lattice relaxation time T_1 , showed a linear increase with temperature. The plot of $\ln T_1$, against $1/T$ for $(C_6H_5)_2TlCl$ in DMSO shown in FIG 5.4. is typical. The direction of this temperature dependence implies that spin-rotation is not a major contributing factor for ^{205}Tl spin-lattice relaxation in these compounds in the temperature ranges studied. Since no quadrupolar nuclei are involved the possible contributing mechanisms are dipole-dipole, chemical shift anisotropy and scalar relaxation. Preliminary measurements of nuclear Overhauser effects for $(CH_3)_2TlNO_3^{361}$ suggests these are negligible. Since no data is available for any of the other compounds studied the dipole-dipole contribution is unknown. The gross assumption that this contribution may be small in some cases, since there is an r^{-6} dependence on $Tl-H$ distance, may not be valid in such cases as the $[(CH_3)_3CCH_2]_2TlCl$ or $[(CH_2)_2CH]_2TlX$ where there are larger numbers of protons involved. Scalar relaxation of thallium would appear unlikely since in organothallium derivatives R_2TlX and $RTlX_2$ the organo groups are generally not labile.¹⁴⁸ This is in contrast with R_3Tl derivatives where rapid exchange of the

FIG. 5.4.

PLOT OF $\ln T_1$ AGAINST $10^3/\text{deg K}$ FOR $(\text{C}_6\text{H}_5)_2\text{TiCl}$ 0.2 mol dm^{-3} IN DMSO-d_6



organo groups does occur. Scalar relaxation of the second kind is ruled out since there are no rapidly relaxing nuclei involved under the conditions used.

This leaves the chemical shift anisotropy mechanism as being the dominant contributing relaxation mechanism. In theory this mechanism is easily distinguishable since it depends upon the square of the operating field, becoming more efficient with increasing field. Unfortunately no definitive experiments could be carried out since spectrometers operating at different fields for ^{205}Tl were not accessible. However several pieces of evidence are available to support the importance of the CSA mechanism in this study. These will be discussed in the following section (5.4.1.)

5.4.1. Evidence for the CSA mechanism in organothallium(III) compounds

1. The ^{205}Tl spin-lattice relaxation time T_1 has previously been reported for $(\text{CH}_3)_2\text{TlNO}_3$ in H_2O^{19} (see TABLE 5.1) at a different operating frequency of 15.1MHz compared to the 34.73MHz used in this study. Measurement of ^{205}Tl T_1 for the same solution under almost the same conditions gave $T_1 = 0.096$ seconds at 34.73MHz compared to the reported value $T_1 = 0.556$ seconds at 15.1MHz. The relaxation is clearly seen to be field dependent and if this was a square dependence we would predict a value of $T_1 = 0.096 \times (34.73/15.1)^2 = 0.51$ seconds at 15.1MHz which is close to the reported value of 0.56 seconds.

2. It was observed that proton spectra of R_2TlX derivatives ($\text{R} = \text{isopropyl, sec-butyl, sec-amyl, iso-butyl, cyclohexyl}$) obtained at 220MHz gave broad signals, with loss of fine structure compared to spectra obtained at 60MHz. It was also found that increasing the temperature at the higher frequency eventually resulted in the signals sharpening again with reappearance of fine structure. To investigate this phenomenon the proton spectra of $(\text{CH}_3)_2\text{TlOCOCH}_3$ and $[(\text{CH}_3)_3\text{COCH}_2]_2\text{TlCl}$ were obtained at various operating frequencies in the range 60 to 400 MHz. Some of the spectra for $(\text{CH}_3)_2\text{TlOCOCH}_3$ are shown in FIG 5.5. It can be seen that the component linewidths increase with increasing field with an approximately linear dependence of $V_{1/2}$ (width at half height) on the square of the operating frequency. A plot of $V_{1/2}$ against the square of the operating frequency is shown in FIG 5.6. Linear regression analysis gave $r = 0.99$. A similar linear relationship was

FIG. 5.5.

PROTON SPECTRA OF $(\text{CH}_3)_2\text{TiOCOCH}_3$ IN D_2O AT DIFFERENT
FREQUENCIES (not to scale)

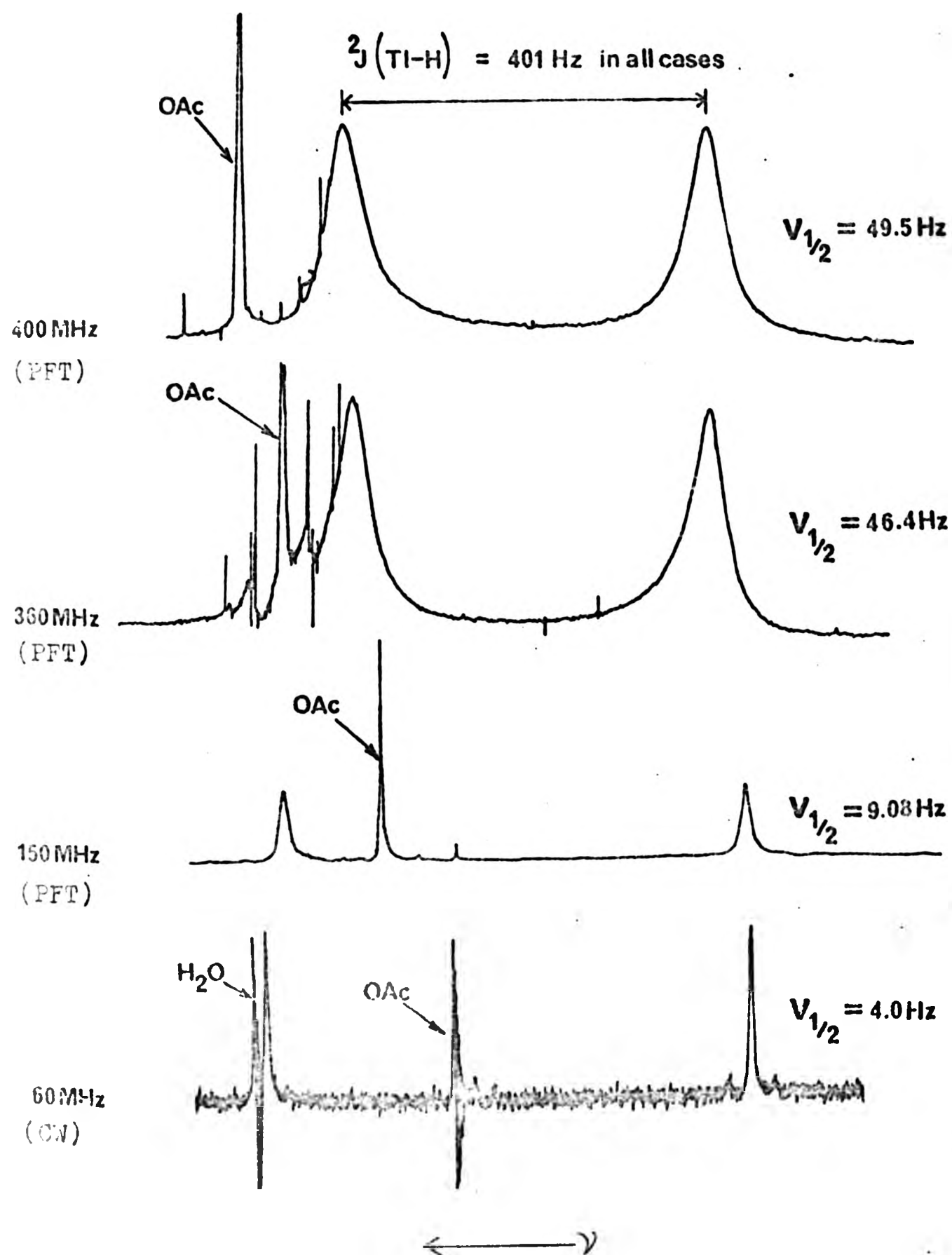
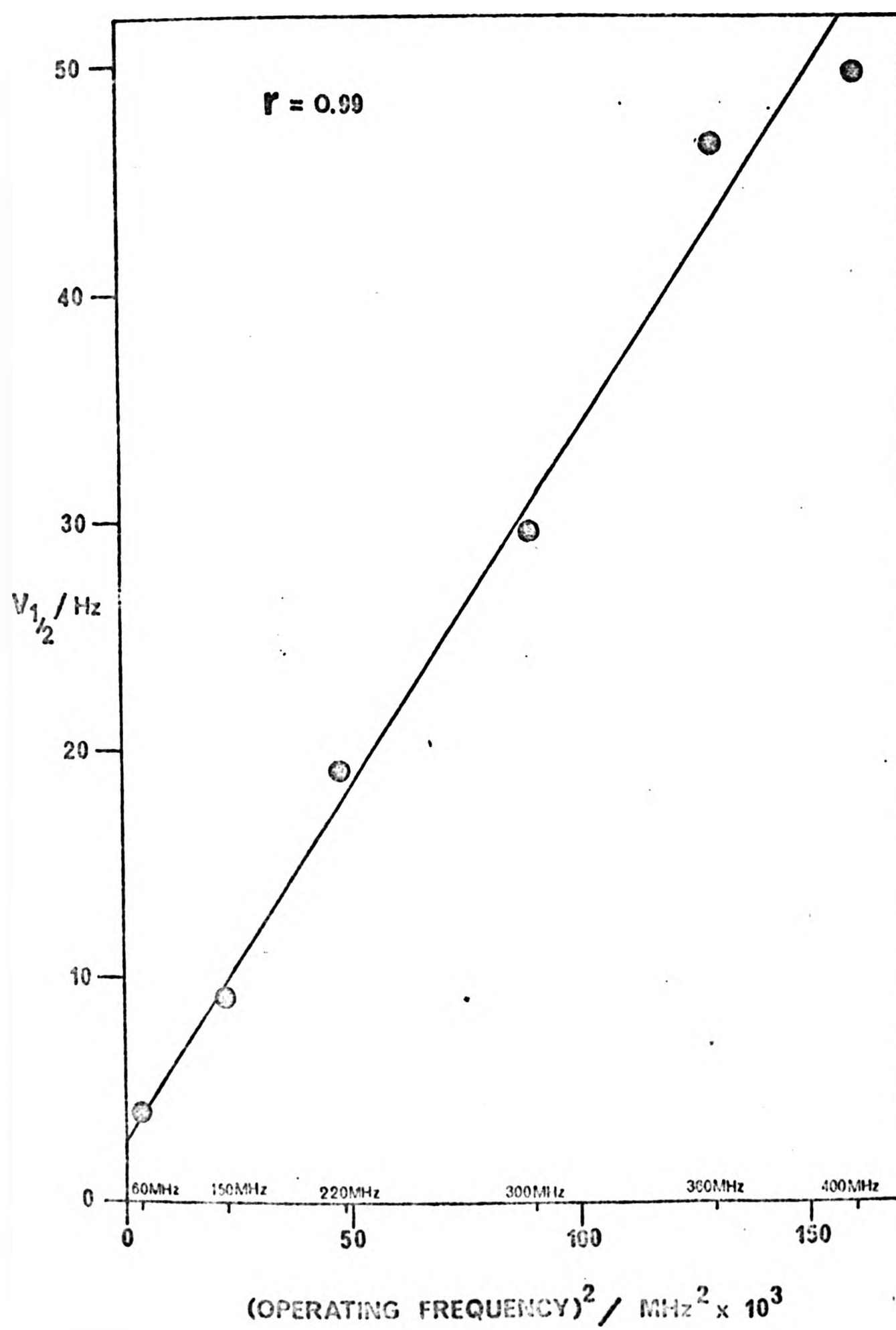


FIG. 5.6.
DEPENDENCE OF $\nu_{1/2}$ ON OPERATING FREQUENCY FOR
PROTON SPECTRA OF $(\text{CH}_3)_2\text{TiOCOCH}_3$ IN D_2O 0.24 mol dm^{-3}
AT 27°C



found for bis(neopentyl)chlorothallium(III) in pyridine ($r = 0.96$). The relationship can be attributed to domination of the proton linewidths by a field dependent relaxation process at the coupled thallium nuclei, and it is suggested that this is as a result of domination of thallium relaxation by the chemical shift anisotropy mechanism.

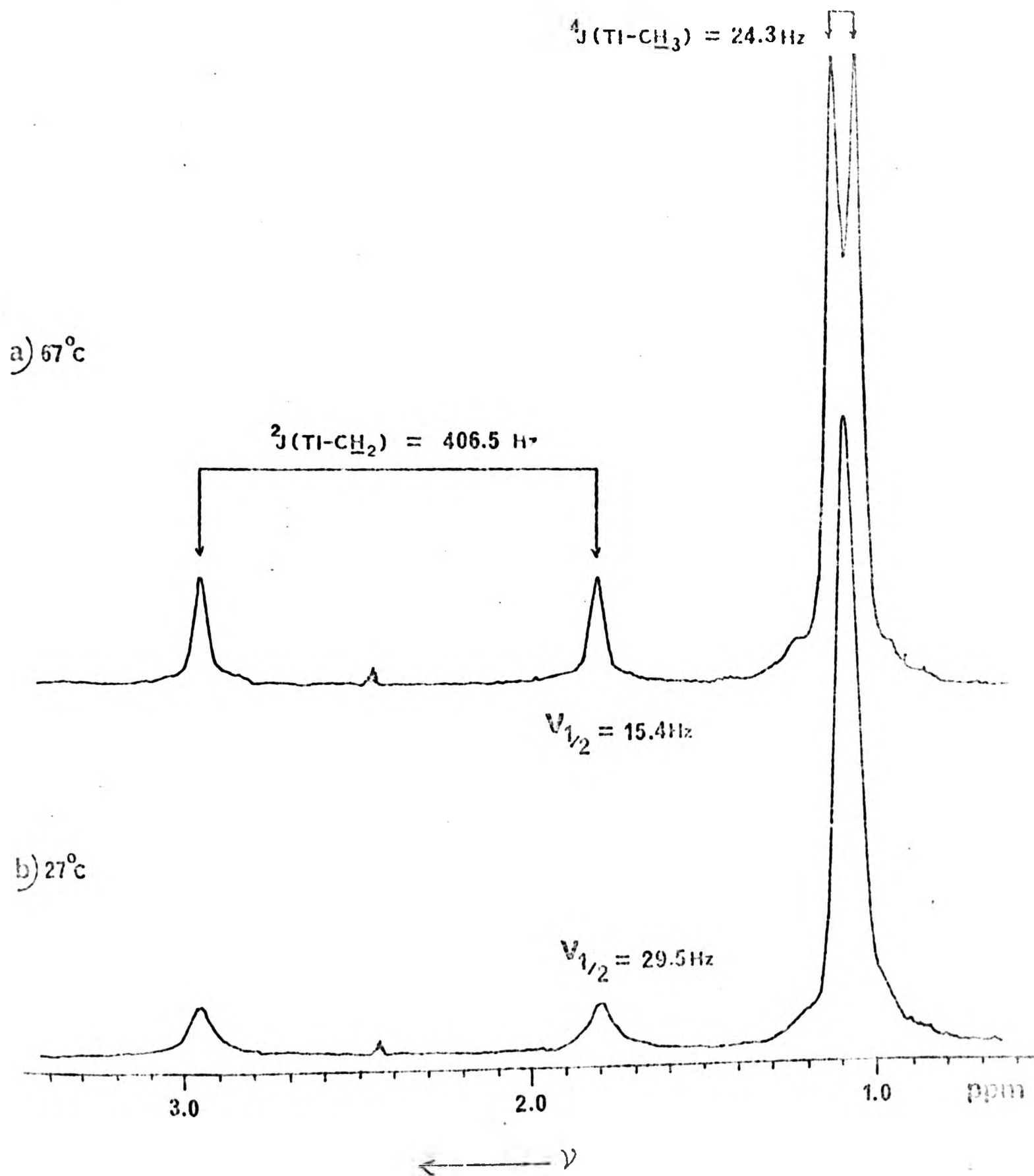
It is proposed that the shortening lifetimes of the thallium spin states with increasing field strength ($\propto B_0^2$) causes linewidth changes in the spectra of nuclei coupled to thallium (protons in this case) by scalar relaxation of the second kind. In this situation a nucleus S causes relaxation of a nucleus I to which it is spin-spin coupled. If $(T_1)_S$ is short compared to $1/\Delta_{IS}$ then multiplet structure from coupling between I and S collapses and we see only an average value. At the coalescence point we may apply the expression (5.11) for T_2 of spin I (protons in this case)

$$(T_2)_I^{-1} = \frac{A^2}{3} S(S+1) \left\{ \tau_S + \frac{\tau_S}{1 + (\omega_I - \omega_S)^2 \tau_S^2} \right\} \quad (5.11)$$

the second term in parentheses is negligible in the case of thallium/protons, especially at higher operating frequencies. If we examine the proton spectra of bis(neo-pentyl)chlorothallium (III) in pyridine (FIG. 5.7) at 360 MHz it can be seen that the doublet due to $^1J(\text{Tl}-\text{CH}_3)$ apparent at 67°C, has clearly coalesced at 27°C. Although the exact coalescence temperature is unknown it is probably about 60°C. The measured ^{205}Tl spin lattice relaxation time at 60.9°C = 0.228s for $[\text{CH}_3)_3\text{CCH}_2]_2\text{TlCl}$ at 34.73 MHz.³⁷² Assuming the thallium relaxation is dominated by the CSA mechanism, at 360 MHz this

PROTON SPECTRA AT 350MHz OF $\left[\left(\text{CH}_3\right)_3\text{CCH}_2\right]_2\text{TiCl}_2$ 0.13 mol dm⁻³
IN Pyridine-d₅

(FFT spectra)



would be $0.228(34.73/360)^2 = 0.00212\text{s}$. Substituting $\tau_s = 0.00212$ and $A = 2\pi J$ in equation 5.11, a value of $T_2(^1\text{H})$ may be calculated and was found to be 0.08s . This is compared to a value of $T_2(^1\text{H}) = 0.021\text{s}$ derived from the measured linewidth (15.4Hz), of the components of the doublet arising from $^2\text{J}(\text{Tl}-\text{CH}_2)$ at 67°C , using the relationship (5.12).

$$T_2^* = \frac{1}{\pi \nu_{\frac{1}{2}}} \quad (5.12).$$

From the point of view of the proton it is irrelevant what mechanism is limiting the lifetime of the nucleus it is coupled to. It could be chemical exchange or rapid relaxation. The fact that in this case the rapid relaxation is as a result of the greater efficiency of the CSA mechanism at higher fields is irrelevant to the proton and this could have been as a result of rapid relaxation of a quadrupolar nucleus, had one been present.

Three factors militate against observation of an exact square law dependence of linewidth on operating field.

(i) Although it is suggested that the CSA mechanism dominates thallium relaxation at higher fields there is some evidence that at lower fields and higher temperatures other relaxation mechanisms become important.

Proton spectra of $(\text{CH}_3)_2\text{TlOCOCH}_3$ in D_2O solution were obtained at 80, 220 and 360 MHz, over a temperature range (Table 5.4). If the component linewidths of the thallium-coupled signals are taken as a direct measure of R_1 for ^{205}Tl , i.e. $R_1(^{205}\text{Tl}) \propto \nu_{\frac{1}{2}}(^1\text{H})$, a temperature dependence in the same sense as for thallium-205 spin lattice relaxation rates is obtained. A plot of $\ln R_1(^{205}\text{Tl}) \propto \nu_{\frac{1}{2}}(^1\text{H})$ against

temperature is shown in FIG. 5.8.

At 220 and 360MHz the relaxation rate shows a linear increase with decreasing temperature and activation energies are calculated as $18.1 \pm 0.5 \text{ kJ mol}^{-1}$ (220MHz) and 17.9 kJ mol^{-1} (360MHz). At 360MHz if the measured linewidth is taken as $(V_{\frac{1}{2}}^{\text{CH}_3}) - (V_{\frac{1}{2}}^{\text{OCOCH}_3})$, where the linewidth of the acetate signal is essentially constant (0.5Hz), then an activation energy of 19.8 kJ mol^{-1} is obtained. However at 80MHz the plot shows a distinct curvature suggesting the presence of competing mechanisms. Thallium-205 spin lattice relaxation times were measured for this solution over a range of temperatures at 34.7MHz (TABLE 5.2) and the Arrhenius plot is shown in FIG 5.9. where the curvature is also evident. (The field strength of 1.41T used for observation of ^{205}Tl at 34.7MHz is close to that, (1.88.T) used for observation of ^1H at 80MHz). An activation energy of $20 \pm 3 \text{ kJ mol}^{-1}$ was obtained for the low temperature region where the CSA mechanism would be expected to be more efficient. Further work in progress on this solution at the time of writing confirms that the competing mechanism is spin rotation at the higher temperatures.

(ii) In the proton spectra, the component thallium coupled signals consist of two overlapping signals arising from coupling to ^{205}Tl ($I = \frac{1}{2}$, natural abundance 70%), and ^{203}Tl ($I = \frac{1}{2}$, natural abundance 30%). The gyromagnetic ratios of the two isotopes are similar $\left[\gamma(^{205}\text{Tl}) / \gamma(^{203}\text{Tl}) = 1.0072 \right]$. The separation of signals due to coupling to the two isotopes depends on the magnitude of $J(\text{Tl-H})$. Although not clearly resolved for $^2J(\text{Tl-H})$ in R_2TlX ($\text{R} = \text{CH}_3; (\text{CH}_3)_3\text{CCH}_2$), at 60MHz the ^{203}Tl coupled signal component may be seen as a 'hump' on the inner side of the ^{205}Tl coupled signals. This makes accurate

FIG. 5.3.

PLOT OF $\ln R_1^{205\text{Ti}} (\propto \nu_{1/2} [^1\text{H}])$ AGAINST $10^3/\text{degK}$ FOR
 $(\text{CH}_3)_2\text{TiOCCOCH}_3$ 0.2 mol dm^{-3} IN D_2O AT 80, 220 AND 360 MHz

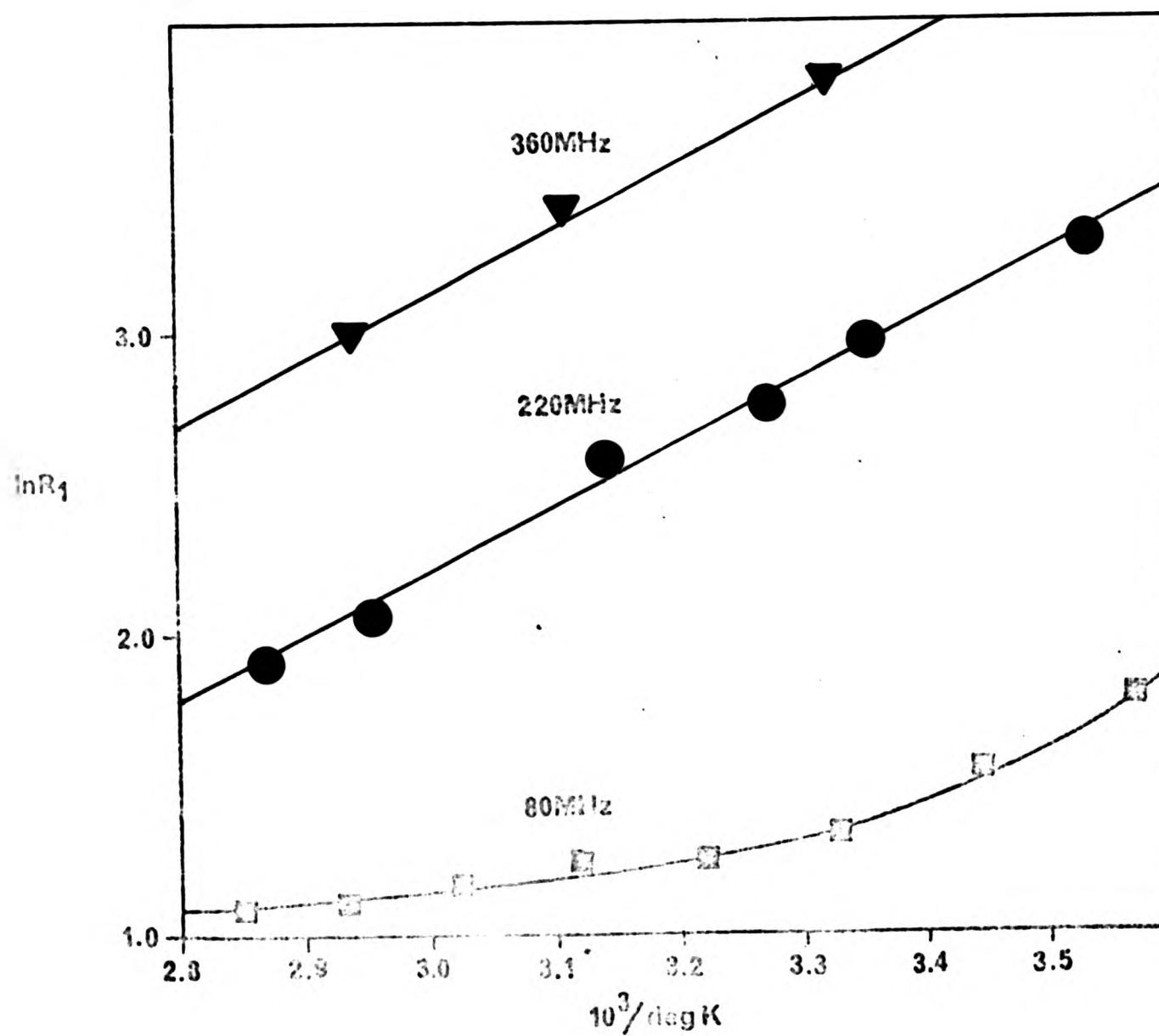
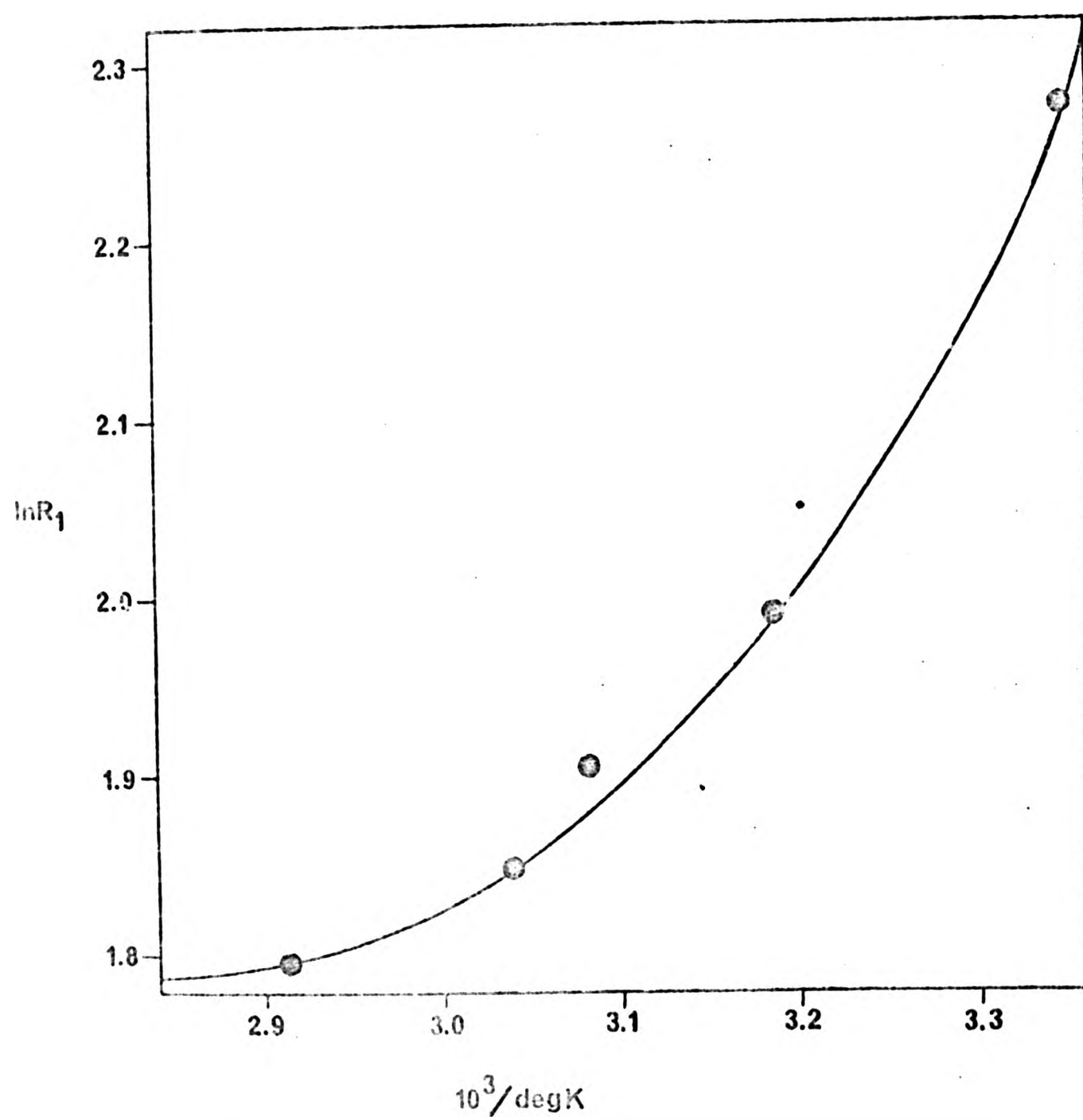


FIG. 5.9.

PLOT OF $\ln R_1(^{205}\text{Ti})$ AGAINST $10^3/\text{degK}$ FOR
 $(\text{CH}_3)_2\text{TiOCOCH}_3$ 0.2mol dm^{-3} IN D_2O AT 34.7MHz



determination of linewidths difficult. However at high fields this diminishes in importance.

(iii) The 'intrinsic' linewidths of the proton signals in the absence of broadening arising from coupling to thallium are unknown. They are clearly less than the linewidth of signals at 60MHz and in theory would not be expected to broaden with increasing field. The linewidth of the OCOCH_3 resonance in $(\text{CH}_3)_2\text{TlOCOCH}_3$ remains approximately constant as the field increases. The effect of intrinsic linewidths on the spectra in FIG.5.5. will be greatest at low fields.

3. Reorientational correlation times calculated for these compounds are reasonable values for this relaxation mechanism.

From a study of $(\text{CH}_3)_2\text{TlNO}_3$ oriented in a lyotropic phase Gillies³⁶¹ obtained a value of $\Delta\sigma = 5263 \pm 68\text{ppm}$ for ^{205}Tl in this linear molecule. Assuming that other R_2TlX derivatives are linear^{103,148,368,369} and possess axial symmetry, the value for $\Delta\sigma$ may be used in conjunction with measured ^{205}Tl T_1 values to calculate a reorientation correlation time τ_c using equation (5.14)

$$\frac{1}{T_1}_{\text{CSA}} = \frac{2}{15} \cdot \left\{ \omega_0^2 \Delta\sigma^2 \tau_c \right\} \quad (5.14)$$

where ω_0^2 = the thallium resonance frequency in radians $2\pi \nu_0$. Calculated correlation times are listed in TABLE 5.2.

For a typical ^{205}Tl T_1 of 0.1sec calculated $\tau_c = 5.69 \times 10^{-11}$ seconds. Assuming the Hubbard relationship,^{350,351} equation (5.5)

$$\tau_c \cdot \tau_j = \frac{I}{6kT} \quad (5.5)$$

where τ_j is the angular momentum correlation time ; I is the moment of inertia and k is the Boltzmann constant, a value of $\tau_j = 9.72 \times 10^{-16}$ seconds may be calculated. Substituting this value in the expression for spin-rotation relaxation, equation (5.15):

$$(\tau_1)_{SR}^{-1} = \frac{2I}{kT/3h^2} (C^2) \tau_j \quad (5.15)$$

where C^2 the average square of the spin-rotation tensor is estimated from σ_p data ³⁶¹ a spin rotation contribution of ca. 46s can be calculated. This is too long to be important here. However this calculation assumes the Hubbard relationship is valid and the calculated value for I may be an underestimate for solvated species.

(4) Even in the spherically symmetric solvated Tl^+ ion, for solutions of $TlNO_3$ and $TlClO_4$ in DMSO, Hinton and Ladner¹²⁴ have suggested the importance of a transient chemical shift anisotropy relaxation mechanism arising from transient anion penetration of the Tl^+ solvation sphere. Hinton and Briggs report that CSA makes the dominant (90%) contribution to the ²⁰⁵Tl relaxation for the Tl^+ /valinomycin complex at 2.114T⁵⁷ based on the temperature dependence of ²⁰⁵Tl relaxation times.

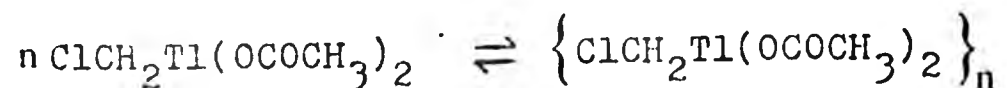
Schwartz³⁶⁰ has proposed that the transient chemical shift anisotropy mechanism will be important for heavy metal nuclei such as ²⁰⁵Tl and ²⁰⁷Pb, where chemical shielding anisotropies resulting from ion pair formation will be of similar magnitude to those for covalently bonded organo derivatives.

5.4.2. Chloromethylbis(acetato)thallium(III)

The thallium-205 spin-lattice relaxation times for this compound are given in TABLE 5.1. The relaxation time is seen to decrease with increasing temperature. The temperature dependence is illustrated in FIG 5.10. This indicates that spin-rotation is the dominant relaxation mechanism over the higher temperature range and an associated activation energy of -43 kJmol^{-1} can be calculated. The curved nature of the plot in FIG 5.10. suggests that another relaxation mechanism is contributing and becomes more important at the lower temperatures. The curve reaches a maximum and there is a suggestion that the relaxation time then begins to increase again. This may be due to the chemical shift anisotropy mechanism and/or the dipole-dipole mechanism becoming important at the lower temperatures. The high value of the activation energy is unexpected. Spin-rotation is usually an important relaxation mechanism for small symmetric molecules e.g. $(\text{CH}_3)_4\text{Sn}; (\text{C}_2\text{H}_5)_4\text{Sn}^{343}$ and becomes more efficient at higher temperatures. The high value for activation energy found would appear inconsistent with a small freely rotating species in solution.

Unfortunately no structural data is available for $\text{ClCH}_2\text{Tl}(\text{OCOCH}_3)_2$, either in the solid state or in solution. In methanol solution several situations must be considered.

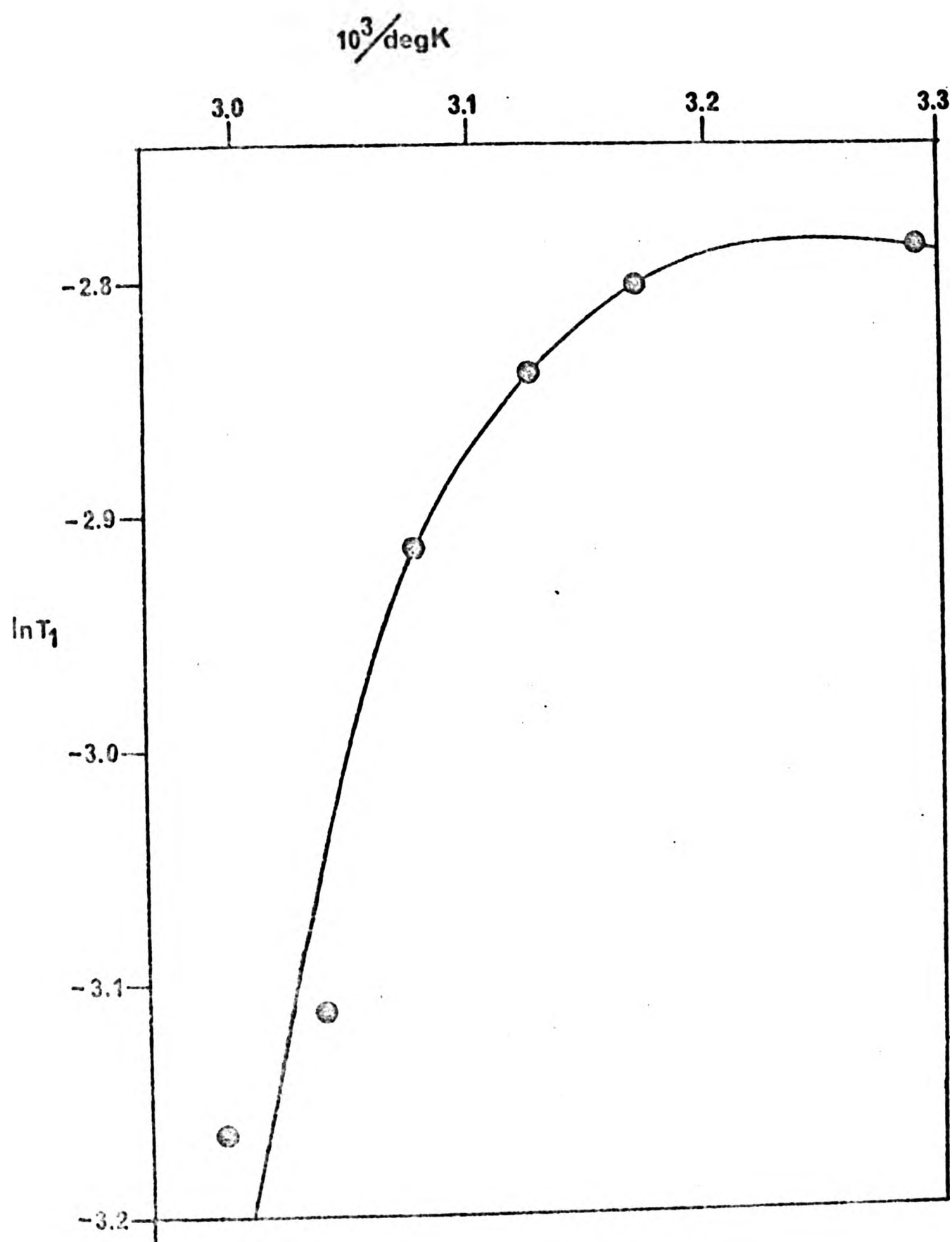
a) An equilibrium situation exists in which



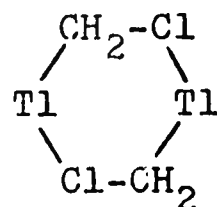
association may be achieved in a number of ways.

FIG. 5.10

PLOT OF $\ln T_1$ AGAINST $10^3/\text{degK}$ FOR $\text{ClCH}_2\text{Ti}(\text{OCOCH}_3)_2$
 0.19 mol dnT^3 IN CD_3OD



(i) There is a well known tendency for metal derivatives of the type $\text{Cl-CH}_2\text{-M}$ ($\text{M}=\text{metal}$) to associate forming six-membered rings in which the chlorine is coordinated to the metal.³⁷¹ Thus the structural unit:



might be present, at least in the solid state.

(ii) By bridging of adjacent thallium atoms through the oxygens of the carboxylate group as was found for cyclopropylbis(isobutyrate)thallium(III). (Chapter 6).

(iii) A combination of (i) and (ii).

Such an equilibrium would be temperature dependent and the measured spin-lattice relaxation times would then be 'weighted averages' depending on the species present. A feasible explanation might be due to the presence of a transient spin-rotation mechanism resulting from the carboxylate groups and/or the chlorine of the $\text{ClCH}_2\text{-}$ group rapidly forming and breaking bonds with thallium (as suggested in situations (i) to (iii)). It might then be reasonably suggested that thallium would experience a 'pseudo-rotation' resulting in the transient spin-rotation mechanism.

b). A 'free' $\text{ClCH}_2\text{Tl}^{2+}$ species is present. Such a relatively small species might be expected to have a spin-rotation contribution to the thallium relaxation rate. However the presence of such a small 'free' species is inconsistent with the high activation energy found. It is possible that hindered rotation of such a species might result from hydrogen bonding between the chlorine atom on the alkyl group and the solvent.

CHAPTER SIX

CRYSTAL AND MOLECULAR STRUCTURES OF
CYCLOPROPYLBIS(ISOBUTYRATO)THALLIUM(III)

AND

BIS(TRIMETHYLSILYLMETHYL)CHLOROTHALLIUM(III)

AND

INFRA-RED SPECTROSCOPIC STUDIES OF
ORGANOTHALLIUM(III) CARBOXYLATES.

6.1. Crystal structure Determination

The procedure and underlying theories for determining crystal structures by single crystal X-ray diffraction are well documented in several texts.^{373,374} A brief outline only is given here.

The magnitude and phase of X-rays diffracted by the hkl set of planes in a crystal depends on the nature and arrangement of atoms within the unit cell.

The intensity of the experimentally observed reflection I_{hkl} is directly related to the square of the structure factor F_{hkl} for that reflection by:

$$F_{hkl} = \frac{K I_{hkl}^{\frac{1}{2}}}{L_p} \quad (6.1)$$

p is a polarisation factor to account for the reduction in intensity of the diffracted beam which occurs as a result of polarisation; it is defined as:

$$p = \frac{1}{2}(1 + \cos^2 \theta) \quad (6.2)$$

L is the Lorentz factor which depends on the measurement technique used and for diffractometer data is:

$$L = \frac{1}{\sin^2 \theta} \quad (6.3)$$

K is a scale factor correction depending on crystal dimension, intensity of incident beam and other constants.

An electron density map may be calculated from hkl and F_{hkl} values for the reflections from a crystal using the

expression for centrosymmetric systems

$$\rho(x,y,z) = \frac{1}{V} \sum_h \sum_k \sum_l F_{hkl} \cos 2\pi (hx+ky+lz) \quad (6.4)$$

where $\rho(x,y,z)$ is the electron density at a point xyz in the unit cell of volume V. F_{hkl} is the structure factor for a reflection having Miller indices h,k and l. Points of maximum electron density correspond to the positions of atoms. In the non-centrosymmetric case the phase angle α is introduced giving

$$\rho(x,y,z) = \frac{1}{V} \sum_h \sum_k \sum_l \begin{matrix} +\infty \\ -\infty \end{matrix} |F_{hkl}| \cos \{2\pi(hx+ky+lz) - \alpha_{hkl}\} \quad (6.5)$$

Where α is the phase angle whose Miller index is hkl.

The electron density cannot be calculated directly using these expressions because the phase of F_{hkl} is not known.

6.1.1. Patterson Synthesis

Patterson ³⁷⁵ showed that values of F_{hkl}^2 could be used in a Fourier synthesis to provide a three-dimensional vector map of the unit cell of the crystal.

$$P(UVW) = \frac{1}{V} \sum_h \sum_k \sum_l |F_{hkl}|^2 \cos 2\pi(hU+kV+lW) \quad (6.6)$$

$P(UVW)$ is the vector density at the point defined by the fractional coordinates U,V and W. The value of $P(UVW)$ will be zero everywhere except where the values of UVW represent a vector between atoms. Vectors between atoms A and A' at positions x,y,z and x',y',z' respectively, give rise to

peaks in the Patterson map at positions $(x_A - x_{A'}, y_A - y_{A'}, z_A - z_{A'})$. The peak heights will be proportional to the atomic numbers $Z_A \cdot Z_{A'}$.

The Patterson synthesis allows assignment of the coordinates of heavy atom(s). Phases can be allocated to every structure factor from a Fourier synthesis. The assumption is that the scattered rays will be dominated by the effect of the heavy atom and so each reflection will have the same phase as the heavy atom contribution to that reflection.

6.1.2. Fourier Synthesis Program

Unlike the Patterson synthesis, a Fourier synthesis uses the magnitudes and phases of the structure factors. A three dimensional electron density contour map can be calculated using equation (6.4). Thus the positions of 'new' atoms can be found. Using these new positions structure factors can be calculated using the expression:-

$$F_{hkl} = \sum_{j=1}^n f_j \exp \{ 2\pi i (hx_j + ky_j + lz_j) \} \quad (6.7)$$

summed over j atoms where x_j, y_j, z_j are the known positions of the n atoms in the unit cell. The scattering factor of the j th atom at a Bragg angle θ_{hkl} is f_j . The 'new' signs obtained from (6.7) are combined with the observed intensities in a second Fourier synthesis giving a second electron density map and a more complete structure. This cycle is repeated until all the signs are correct.

6.1.3. Difference Fourier Synthesis

A Fourier synthesis is now performed on the difference between $F(\text{observed})$ and $F(\text{calculated})$. This gives a measure of the correctness of the crystal structure since the calculated structure factors F_c are based on the crystal structure model. The difference in electron density between the postulated and observed structures is given by

$$\Delta\rho(xyz) = \frac{1}{V} \sum_h \sum_k \sum_l (|F_o| - |F_c|) \exp(i a) \exp \left\{ -2\pi i (hx + ky + lz) \right\} \quad (6.8)$$

Where a is the calculated phase of F_c . F_o is the observed structure factor. The difference map will show up any additional atoms which have not been found and also indicate errors in the intensities, positions and motions of atoms.

6.1.4. Temperature factors

To allow for the thermal vibrations of atoms the scattering factor f_j in equation (6.7) must be multiplied by a temperature factor.

$$f_j = f(0)_j \exp \left\{ \frac{B \sin^2 \theta}{\lambda^2} \right\} \quad (6.9)$$

where $f(0)_j$ is the scattering factor if there was no thermal motion. B is the temperature coefficient which is related to the root mean square displacement of the atoms from their mean position, \bar{U}^2 , by the expression

$$B = 8\pi^2 \bar{U}^2 \quad (6.10)$$

The isotropic (ie.spherical) temperature factor assumes the atom is vibrating equally in all directions. When this is not the case each atom is assigned six anisotropic (ie. ellipsoidal) temperature factors $U_{11}, U_{22}, U_{33}, U_{12}, U_{13}, U_{23}$.

6.1.5. Structure Refinement

When the coordinates of atoms in the unit cell are known an iterative least squares program is used to slightly alter the atomic coordinates to give the best agreement between the observed structure factors and those calculated for the postulated structure. Additionally the program also refines either one isotropic or six anisotropic vibration parameters for each atom and an overall scale factor.

The measure of agreement between observed and calculated structure factors is related to the correctness of the final structure. A calculated agreement index R should become progressively smaller as the refinement continues.

$$R = \sum w (|F_o| - |F_c|)^2 / \sum |F_o| \quad (6.11)$$

w = a weighting factor = $\frac{1}{\sigma^2}$ where σ^2 = the variance.

6.2. Crystallography

6.2.1. Cyclopropylbis(isobutyrate)thallium(III), I.

Weissenberg photographs of cyclopropylbis(isobutyrate)-thallium(III), I, indicated orthorhombic symmetry. The systematically absent reflections were those required for either the space group $Pna2_1$ or $Pnma$. The non-centrosymmetric space group, $Pna2_1$, was found to be the correct one.

Unit cell calibration was carried out by a least squares fit of the angular parameters for 25 reflections with 2θ ca. 20° on a Phillips PW1100 automatic four-circle diffractometer using graphite monochromatised Mo- K_α radiation ($\lambda 0.7107\text{\AA}$). A θ - 2θ scan mode was used for data collection and reflections with $3.0 \leq \theta \leq 26.0^\circ$ were examined. Weak reflections which gave $I_t - 2(I_t)^{\frac{1}{2}} < I_b$ on the first scan were not further examined. (I_t is the intensity at the top of the reflection peak and I_b is the mean of two preliminary 5s background measurements on either side of the peak). Of the remaining reflections, those for which the total intensity recorded in the first scan of the peak (I_i) was < 500 counts were scanned twice to increase their accuracy. A constant scan speed of 0.05°s^{-1} and a variable scan width of $(0.70 + 0.05 \tan \theta)^\circ$ was used, with a background measuring time proportional to I_b/I_i . Three standard reflections were measured every 6h. These showed a decrease of ca. 21% during data collection and were used to scale the data to a common level. Pertinent crystal information and details of data collection are given in TABLE 6.1.

Reflections in an octant (761) were measured after the preliminary test (see above). The reflection intensities were calculated from the peak and background measurements using a program written for the PW1100 diffractometer.³⁷⁶

The variance of the intensity, I , was calculated as the sum of the variance due to counting statistics and $(0.04I)^2$, where the term in I^2 was introduced to allow for other sources of error.³⁷⁷ I and $\sigma(I)$ were corrected for Lorentz and polarisation factors and reflections for which $I \leq 3\sigma(I)$ were rejected. The transmission factors estimated for the crystal along the non-equivalent edge lengths were (0.336) and (0.065). No absorption corrections were applied. Equivalents were averaged to give 749 unique reflections of which 54 were considered to be unobserved. The structure was solved by the heavy atom method and refined by full matrix least-squares.

The Patterson function and an initial difference map were solved in the centrosymmetric space group $Pnma$ and showed peaks corresponding to an isobutyrate ligand lying on a mirror plane and a second isobutyrate ligand oblique to the mirror plane, inconsistent with the space group symmetry elements. Subsequent difference maps with the non-centrosymmetric space group $Pna2_1$ revealed all the non-hydrogen atoms and the presence of disorder in both the methyl groups of the isobutyrate ligands and in one atom of the cyclopropyl ring. See FIG 6.2 for the atomic labelling scheme. Two positions for C(2) [C2(a), C(2b)] and for C7 [C7(a), C7(b)] were found together with a three-fold disorder for the atoms C(10) and C(11) [C(10a), C(10b), C(10c)]. It was necessary to constrain isotropic thermal parameters to be equal for the disordered sets of atoms. Based on these restrictions $R = \sum ||F_o| - |F_c|| / \sum |F_o|$ was 0.045. However, the bond lengths obtained from this model were not chemically reasonable within the disordered parts of the molecule with chemically equivalent bonds showing a long/short pattern with average values at the expected values.

The chemically equivalent distances in the disordered parts of the molecule were then constrained to be equal within an e.s.d. of 0.005 Å by the addition of extra observational equations to the least squares matrix.³⁷⁸ The bond lengths were initially set at the average values obtained from the previous model and acceptable values were then obtained at the completion of the refinement. In the final cycle of refinement the mean and maximum shift/σ were (0.33) and (1.58) respectively. The final R was 0.045 and $R_w = 0.050$ where:

$$R_w = \left[\sum w(|F_o| - |F_c|)^2 / \sum w |F_o|^2 \right]^{1/2}; \text{ with } w = 0.8247$$

$$(\sigma^2 |F_o| + 2.045 \times 10^{-3} |F_o|^2)^{-1}.$$

Neutral atom scattering factors were used,³⁷⁹ and those for thallium were corrected for anomalous dispersion effects. ($\Delta f'$, $\Delta f''$)³⁸⁰. Computation was carried out using the 'SHELX'³⁷⁸ system and ORTEP2.³⁸¹ The final atomic positions and thermal parameters are listed in TABLE 6.2. The observed and calculated structure factors are given in APPENDIX IV.

6.2.2. Bis(trimethylsilylmethyl)chlorothallium(III), II

Data collection was essentially similar to that for I. 1963 reflections ($3.0 \leq \theta \leq 25.0^\circ$) were recorded using a θ - 2θ scan mode. TABLE 6.1 summarises the crystal data and details of intensity collection. Three standard reflections were measured every 6h. These showed a decrease of ca13% during data collection and were used to scale the data to a common level. Lp corrections and semi-empirical absorption corrections based on a pseudo-ellipsoid model and 449 azimuthal scans from 33 independent reflections were applied. The merging R factor equalled 0.1963 before and 0.0932 after absorption corrections. Transmission factors ranged from 0.998 to 0.678 for the full data set. Equivalent reflections were averaged to give 1703 unique observed reflections [$F > 6\sigma(F)$]. Cell dimensions were derived from the angular measurements of 25 strong reflections ($10.0 < \theta < 15.0^\circ$).

The Tl, Cl and Si(1) atoms were located by a conventional Patterson synthesis and the other non-hydrogen atoms from subsequent difference maps. The molecular structure and atom labelling scheme is shown in FIG 6.7. The structure displayed disorder in one of the trimethylsilylmethyl groups. (FIG 6.6) Two equal positions for each Si(2) and C(8) atom were found, but the remaining two methyl positions, C(6) and C(7) were not disordered. A model involving geometric constraints to the disordered Si atom to fix these positions as tetrahedra was used in the refinement. This gave an R factor of 0.0824. The model free of constraints gave an R factor of 0.0786 with $R_w = \sum w^{\frac{1}{2}} \Delta / \sum w^{\frac{1}{2}} |F_o| = 0.0874$.

The structure was refined by full-matrix least squares with complex neutral-atom scattering factors and the weighting scheme $w = 2.8137/(\sigma^2(F) + 0.000381 F^2)$.

The refined parameters included anisotropic thermal parameters for Tl, Cl, Si(1); common isotropic temperature factors for Si(2A), Si(2B), C(8A) and C(8B). The final atomic coordinates and thermal parameters for the atoms are listed in TABLE 6.7. Hydrogen atom positions were not found. Interatomic distances and angles for the monomer unit and the dimer are listed in TABLE 6.8. Tables of observed and calculated structure factors are given in APPENDIX IV.

TABLE 6.1

Summary of crystal data and intensity collection

Compound	$(\text{CH}_2)_2\text{CHTi}[\text{OCOCH}(\text{CH}_3)_2]_2$ (I)	$[(\text{CH}_3)_3\text{SiCH}_2]_2\text{TiCl}$ (II)
Formula weight	419.4	414
Crystal system	Orthorhombic	Monoclinic
Space group	$\text{Pna}2_1$	$\text{P}2_1/\text{n}$
Unit cell dimensions ^a		
$a(\text{\AA})$	7.316 (3)	10.618 (3)
$b(\text{\AA})$	12.079 (3)	24.492 (5)
$c(\text{\AA})$	16.119 (4)	6.017 (2)
$\beta(^{\circ})$	(2)	99.76 (3)
Volume (\AA^3)	1424.43	1542.11
Z	4	4
$F(000)$	792	784
Crystal dimensions ^b	0.1 x 0.1 x 0.25(mm)	0.29 x 0.16 x 0.13(mm)
μ (cm^{-1})	108.90	103.42
Final no. of variables	82	71
Unique data used	695	1703
$I > 3\sigma(I)$		

^aThe estimated standard deviation in the last significant figure is given in parentheses.

^bIn mm.

TABLE 6.2

Final fractional coordinates ($\text{Tl} \times 10^5$; $\text{C}, \text{O} \times 10^4$) and isotropic thermal parameters ($\times 10^3$) for $(\text{CH}_2)_2\text{CHTl}[\text{OCOCH}(\text{CH}_3)_2]_2$

Atom	x	y	z	$U/\text{\AA}^2$	s.o.f. ^b
Tl	-1130	-6260	25000	c	1
O(1)	591(25)	674(11)	1061(40)	86(10)	1
O(2)	234(19)	740(9)	4004(37)	65(7)	1
O(3)	-1994(16)	-1549(14)	2333(68)	95(8)	1
O(4)	-1744(15)	-145(12)	2754(128)	89(5)	1
C(1)	1447(23)	-1275(22)	2707(102)	107(10)	1
C(3)	2411(28)	-822(20)	2269(75)	117(15)	1
C(4)	513(21)	1113(16)	2522(44)	74(6)	1
C(5)	763(23)	2047(17)	2230(92)	100(11)	1
C(6)	2023(26)	2123(26)	2301(137)	145(18)	1
C(8)	2308(28)	839(21)	2257(220)	93(14)	1
C(9)	-3670(27)	-660(19)	2412(53)	151(14)	1
C(2a)	2258(56)	-1128(45)	4056(86)	72(15)	1/2
C(2b)	2117(55)	-1525(38)	1226(102)	72(15)	1/2
C(7a)	270(59)	2499(65)	3885(105)	110(20)	1/2
C(7b)	341(60)	2459(67)	485(101)	110(20)	1/2
C(10a)	-4211(46)	-1290(23)	3451(56)	102(10)	2/3
C(10b)	3986(47)	-723(24)	548(52)	102(10)	2/3
C(10c)	3988(40)	129(22)	3097(63)	102(10)	2/3

^a Values of e.s.d.'s in parentheses. ^b Site occupation factor.

^c Anisotropic thermal parameters ($\times 10^3$) for Tl: $U_{11}, 67(0)$;

$U_{22}, 84(0)$; $U_{33}, 57(0)$; $U_{12}, 0(0)$; $U_{13}, 9(1)$; $U_{23}, -1(5)$.

TABLE 6.3

Final fractional coordinates ($\times 10^4$)^a and isotropic thermal parameters ($\times 10^4$)^a for $\{[(CH_3)_3SiCH_2]_2TlCl\}_2$

Atom	x	y	z	U(\AA^2)
Tl	464(1)	591(1)	2615(2)	b
C(1)	-1442(36)	976(15)	2172(61)	791(97)
C(2)	-3011(57)	2032(25)	1777(99)	1569(215)
C(3)	-157(75)	1989(31)	266(129)	2149(306)
C(4)	-2608(96)	1491(40)	-2002(169)	2970(459)
C(5)	2477(32)	382(13)	3201(55)	700(89)
C(6)	3281(42)	1389(19)	5236(76)	1139(142)
C(7)	5283(53)	791(22)	3044(90)	1388(180)
C(8A)	4654(80)	612(34)	7080(130)	1238(192)
C(8B)	3093(83)	1565(38)	1324(141)	1238(192)
Si(1)	-1544(11)	1680(4)	1167(17)	b
Si(2A)	3769(22)	722(9)	4161(39)	920(44)
Si(2B)	3530(23)	919(10)	2899(41)	920(44)
Cl	-382(11)	-477(3)	2362(12)	b

^aValues of e.s.d.'s in parentheses.

^bAnisotropic thermal parameters ($\times 10^4$) for:

Atom	U ₁₁	U ₂₂	U ₃₃	U ₁₂	U ₁₃	U ₂₃
Tl	455(5)	407(5)	459(6)	19(6)	60(4)	38(6)
Si(1)	977(78)	743(68)	742(64)	382(60)	179(58)	315(55)
Cl	1509(81)	526(46)	366(33)	-298(54)	198(41)	-8(37)

TABLE 6.4

Interatomic distances and angles for $(\text{CH}_2)_2\text{CHTi}[\text{OCOCH}(\text{CH}_3)_2]_2$ Distances^b

O(1)-C(4)	1.285(16)	C(5)-C(6)	1.527(28)
O(2)-C(4)	1.285(16)	C(5)-C(7a)	1.533(27) ^c
O(3)-C(8)	1.207(32)	C(5)-C(7b)	1.527(30) ^c
O(4)-C(8)	1.359(61)	C(8)-C(9)	1.675(45)
C(1)-C(3)	1.411(30) ^c	C(9)-C(10a)	1.419(28) ^c
C(1)-C(2a)	1.410(30) ^c	C(9)-C(10b)	1.420(28) ^c
C(1)-C(2b)	1.410(30) ^c	C(9)-C(10c)	1.419(28) ^c
C(4)-C(5)	1.550(35)		

Angles^d

C(1)-C(3)-C(2a)	60.0(3)	Tl-C(1)-C(2a)	125.0(49)
C(1)-C(3)-C(2b)	60.0(3)	Tl-C(1)-C(2b)	125.8(49)
C(1)-C(2a)-C(3)	60.0(3)	O(1)-Tl-O(2)	52.2(6)
C(1)-C(2b)-C(3)	60.0(4)	O(4)-Tl-O(3)	55.2(7)
C(3)-C(1)-C(2a)	60.0(3)	C(1)-Tl-O(1)	98.0(13)
C(3)-C(1)-C(2b)	60.0(3)	C(1)-Tl-O(4)	168.3(26)
C(4)-C(5)-C(6)	105.5(27)	C(1)-Tl-O(3)	117.9(10)
C(4)-C(5)-C(7a)	106.1(56)	C(1)-Tl-O(2)	104.4(13)
C(4)-C(5)-C(7b)	118.2(55)	O(1)-Tl-O(3)	136.5(11)
C(8)-C(9)-C(10a)	111.4(43)	O(2)-Tl-O(4)	78.2(13)
C(8)-C(9)-C(10b)	100.7(63)	O(1)-Tl-O(4)	92.6(13)
C(8)-C(9)-C(10c)	116.4(36)	O(2)-Tl-O(3)	130.0(9)
C(10a)-C(9)-C(10b)	109.2(13) ^e	O(1 ⁱⁱ)-Tl-O(1)	120.6(6)
C(10a)-C(9)-C(10c)	109.3(13) ^e	O(1 ⁱⁱ)-Tl-O(2)	68.4
C(10b)-C(9)-C(10c)	109.3(13) ^e	O(1 ⁱⁱ)-Tl-O(3)	81.2(11)
O(1)-C(4)-O(2)	117.6(22)	O(1 ⁱⁱ)-Tl-O(4)	74.0(13)
O(1)-C(4)-C(5)	114.0(32)	O(1 ⁱⁱ)-Tl-C(1)	96.1(13)
O(2)-C(4)-C(5)	128.5(33)	O(1 ⁱⁱ)-Tl-O(2 ⁱ)	163.3(6)
O(3)-C(8)-O(4)	127.7(58)	O(2 ⁱ)-Tl-O(1)	70.1(6)
O(3)-C(8)-C(9)	117.9(31)	O(2 ⁱ)-Tl-O(2)	120.7(6)
O(4)-C(8)-C(9)	109.4(41)	O(2 ⁱ)-Tl-O(3)	82.5(9)
C(6)-C(5)-C(7a)	108.8(11) ^e	O(2 ⁱ)-Tl-O(4)	93.5(13)
C(6)-C(5)-C(7b)	109.0(12) ^e	O(2 ⁱ)-Tl-C(1)	94.9(13)
Tl-C(1)-C(3)	117.0(29)		

Table 6.4 Continued

^a The superscripts i and ii refer to the symmetry transformations $-x, -y, -1/2+z$ and $-x, -y, 1/2+z$ respectively.

^b In Å ; e.s.d.'s in parentheses. ^c Constrained bond lengths.

^d In degrees; e.s.d.'s in parentheses. ^e Constrained angles.

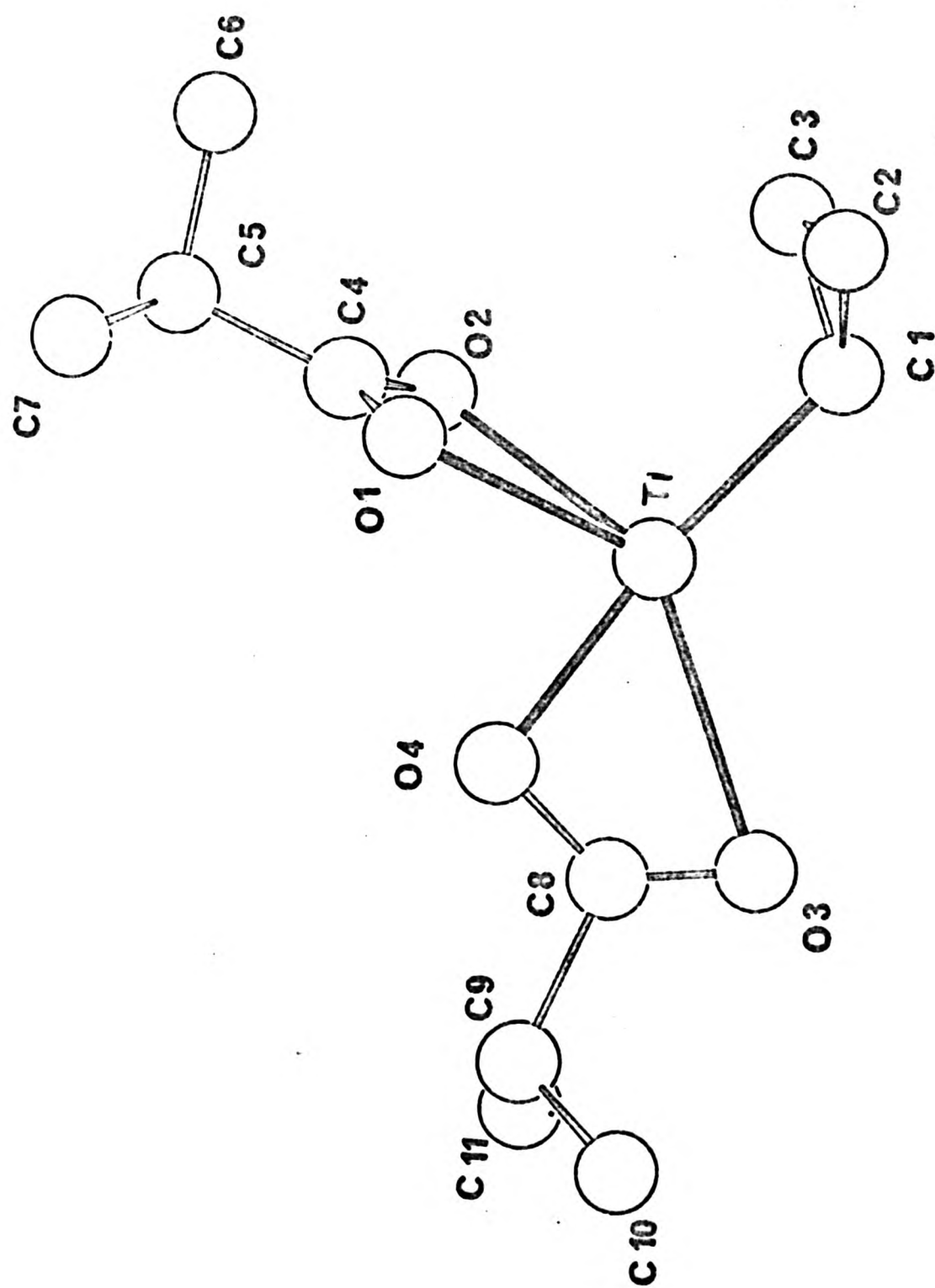
6.3. DISCUSSION OF THE STRUCTURES

6.3.1. Cyclopropylbis(isobutyrate)thallium(III)

Cyclopropylbis(isobutyrate)thallium(III), I, was obtained as colourless crystals from biscyclopropylisobutyrate-thallium(III) by an exchange reaction with bis(isobutyrate)-mercury(II) in a manner similar to that described for the preparation of other monoalkylthallium(II) carboxylates^{89,189}. The crystals were suitable for single crystal X-ray crystal structure determination and the results obtained represent the first available for a monoorganothallium(III) derivative with a simple anionic ligand. Structural details of only one other cyclopropyl-metal derivative, $\text{Al}_2(\text{C}_3\text{H}_5)_6$, appear to have been reported.³⁸²

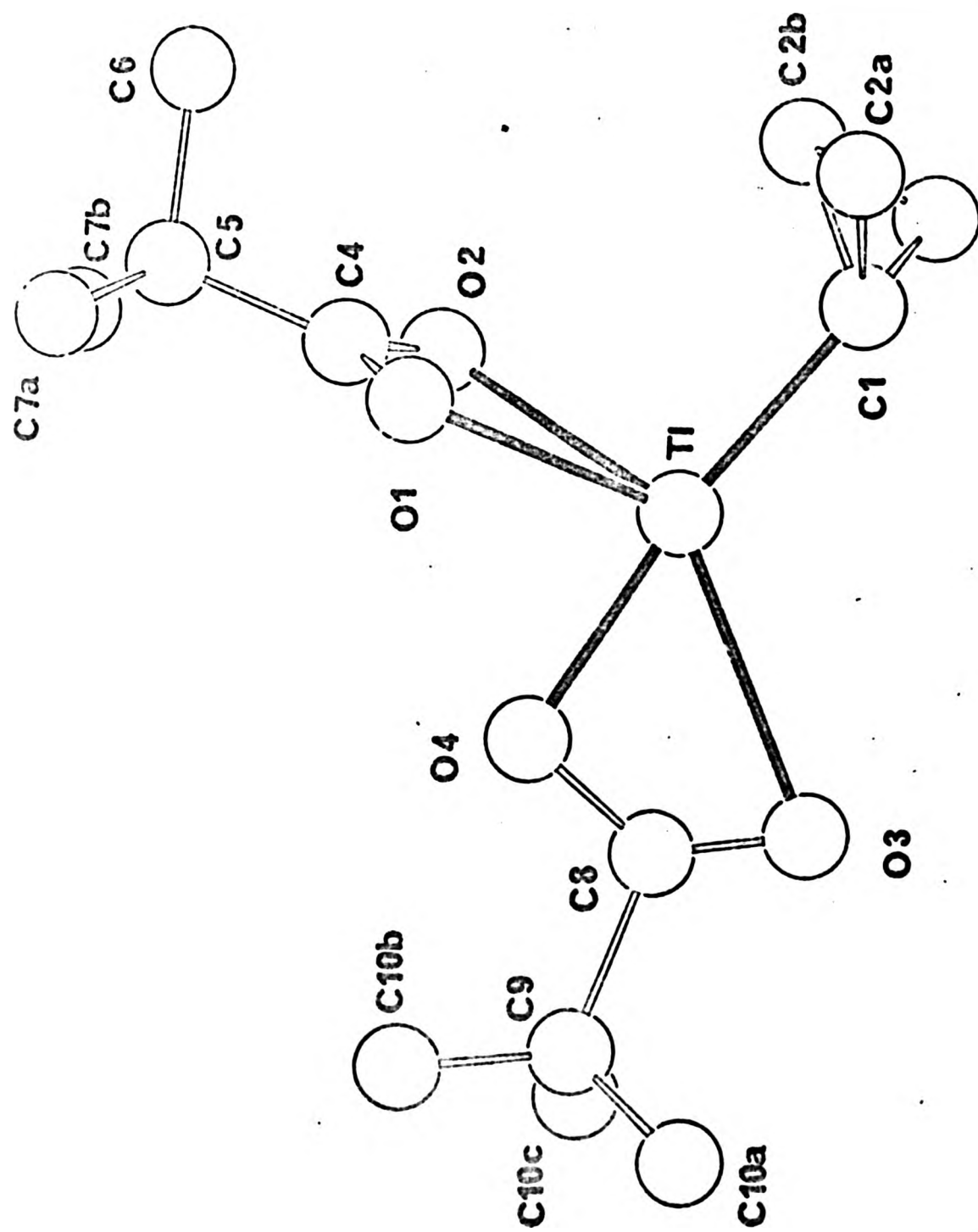
A view of I illustrating the disorder observed and the atomic numbering scheme is shown in FIG 6.2. The same view is shown without disorder in FIG. 6.1. The principal bond lengths and angles are listed in TABLE 6.4. and the coordination geometry around thallium is shown in FIG 6.3.

FIG. 6.1.



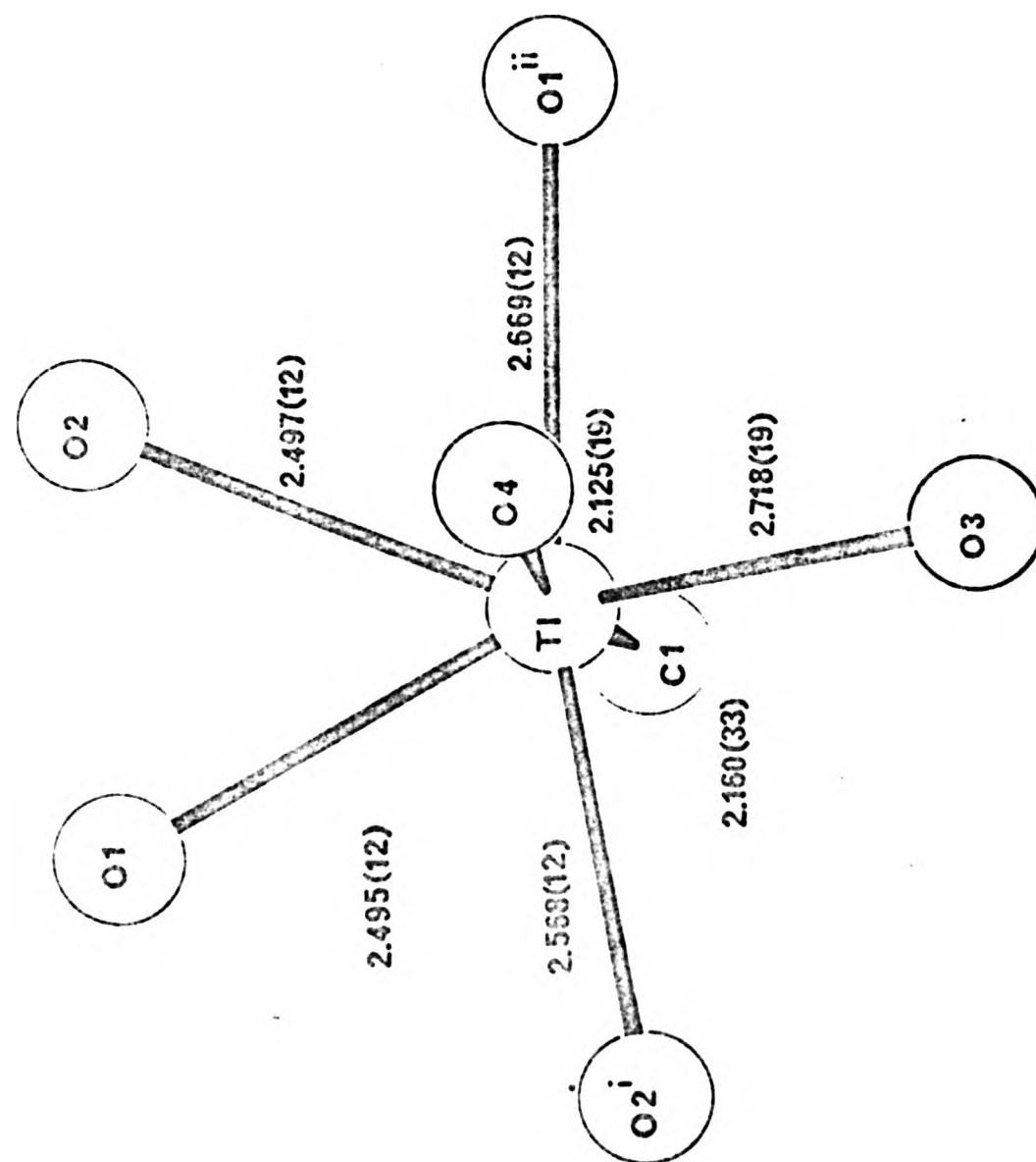
The structure of a monomer unit of $(\text{CH}_2)_2\text{CHTl}[\text{OCOCH}(\text{CH}_3)_2]_2$.

FIG. 6.2.



The structure of a monomer unit of $(\text{CH}_2)_2\text{CHTl}[\text{OCOCH}(\text{CH}_3)_2]_2$ showing disorder in atoms C(2), C(7) and C(10).

FIG. 6.3.



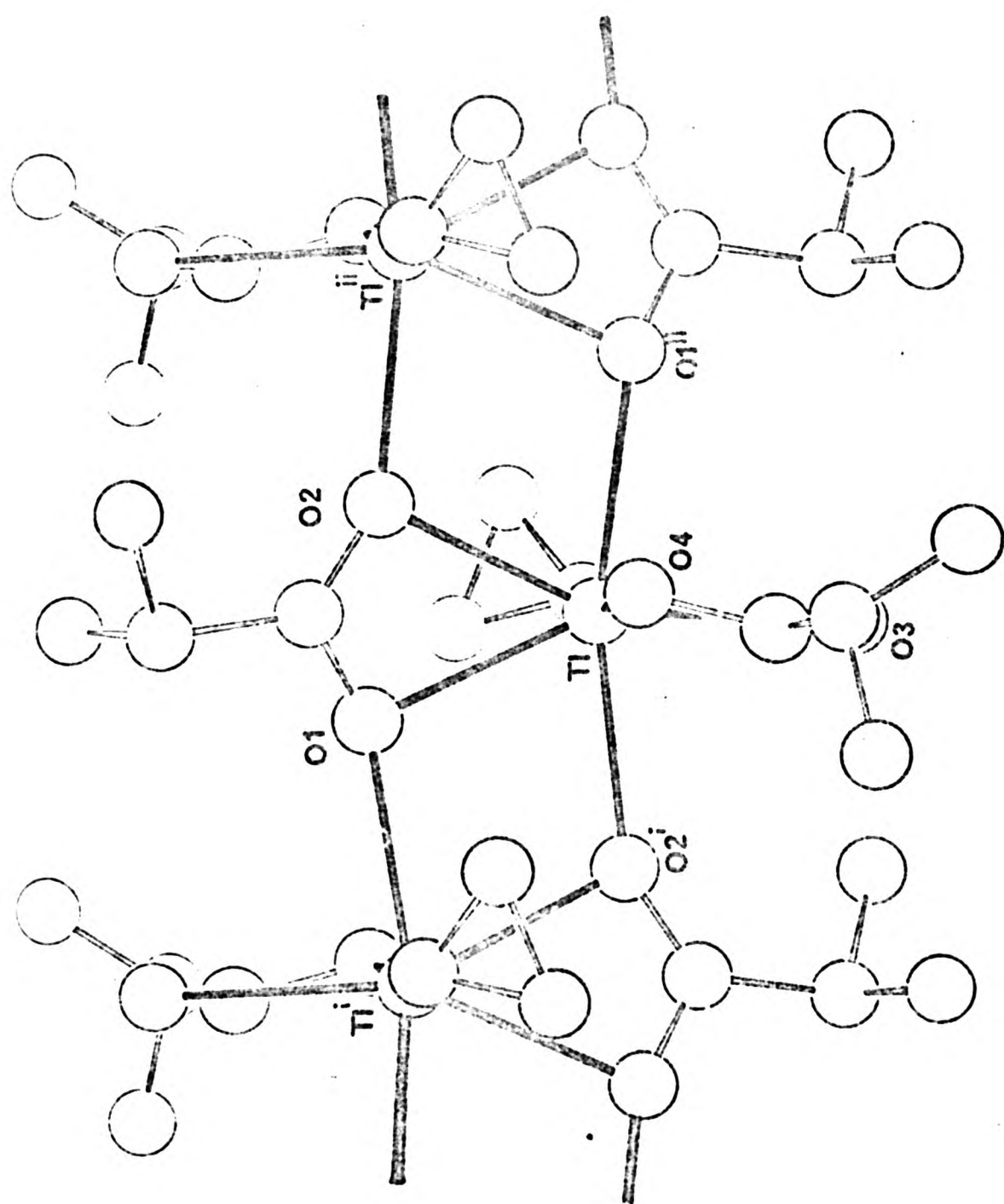
Coordination geometry around thallium in $(\text{CH})_2\text{CHTl}[\text{OCOCH}(\text{CH}_3)_2]_2$.

The $C_3H_5Tl(O_2C_4H_7)_2$ units exist in the crystal as infinite linear polymers in which one of the isobutyrate groups, while chelating the Tl atom, also forms oxygen bridges to the Tl atoms of adjacent units. A section of the polymer chain is shown in FIG 6.4.

In the $C_3H_5Tl(O_2C_4H_7)_2$ unit (FIG 6.1) the thallium atom is five coordinate. Polymerisation via the bridging oxygen atoms, however, increases the coordination to seven (FIG. 6.4). The coordination geometry of the Tl atom is irregular but may be derived from a pentagonal bipyramid by bending the equatorial atom O(3) towards the O(4) axial position. Seven coordinate thallium is unusual but has been reported previously in bis-methylxanthenatothallium(III)¹³¹ although bridging S-Tl distances of 3.19 and 3.35 Å were found compared to S-Tl distances of 2.96 Å within the planar TlS_2C unit. In the case of $C_3H_5Tl(O_2C_4H_7)_2$ the bridging O-Tl distances are not overly long (2.57 to 2.67 Å) compared to the chelating O-Tl distances of 2.5 Å within the same isobutyrate group. The Tl-Tl distance between adjacent monomer units is 4.187 Å.

The non-bridging isobutyrate ligand acts as a weak chelate to the thallium atom, showing considerable ester-type character with two very different O-Tl distances of 2.12 and 2.71 Å to oxygen atoms O(4) and O(3) respectively. The shorter of these two bonds makes an angle of 168° with the Tl-C bond to the cyclopropyl ring and strikingly demonstrates that the dominant characteristic of dialkylthallium(III) compounds whereby thallium tends to form a near linear arrangement with two strongly bonded groups persists into monoalkylthallium(III) systems. Indeed the polymeric pattern of I is very similar to that found for dimethylacetatothallium(III), $(CH_3)_2TlO_2CCH_3$

129



A section of the polymer chain in $(\text{CH}_2)_2\text{CHTi}[\text{OCOCH}(\text{CH}_3)_2]_2$

and the structural arrangement of I can be considered to be derived from the latter by replacing one of the alkyl groups with the non-bridging isobutyrate group. The C-Tl-C angle in $(\text{CH}_3)_2\text{TlO}_2\text{CCH}_3$ is $172(2)^\circ$,¹²⁹ (compared to C(1)-Tl-O(4) in I $168(3)^\circ$). The least squares plane through O(1), O(4), C(8), C(9), Tl of the bridging ligand and that through O(3), O(4), C(8), C(9), Tl of the non-bridging ligand intersect at an angle of 78° (see TABLE 6.5). This is close to the angle (86°) made between the Tl-CH₃ bond and the TlC₂O₂ plane of the chelating and bridging acetate ligand in dimethylacetatothallium(III).

The C-Tl bond length of 2.160\AA is similar to that found in the two other reported structures of monoalkylthallium(III) compounds (Tl-C = 2.147\AA in methyl-5,10,15,20-tetraphenylporphinatothallium(III);⁶¹ Tl-C = 2.073\AA in a methylthallium(III) complex of 2,6-bis(2-methyl-2-benzothiazolyl)pyridine.¹⁴⁶ The Tl-C distance in I is also in the range (2.01 - 2.20\AA) found for Tl-C bonds in neutral dialkylthallium(III) species.

The short C-C distances found in the cyclopropyl group (1.41\AA) are a result of the crystallographic treatment of the disorder and are not comparable to the values found in other monosubstituted cyclopropyl derivatives (1.497 - 1.506\AA).^{383,384}

6.3.1.1. Infra-red spectroscopic studies

The role of the carboxylate anions (bridging and/or chelating) in organothallium(III) carboxylates has previously been suggested, from assignments of their IR spectra.^{89,182,189,385-387} Consideration of the structure of cyclopropylbis(isobutyrate)-thallium(III), I, together with that of $(\text{CH}_3)_2\text{TlO}_2\text{CCH}_3$ ¹²⁹ allows clarification of these interpretations. The IR spectra

TABLE 6.5

Least squares planes defined by $lx + my + nz = p$ for $(CH_2)_2CHTl-[OCOCH(CH_3)_2]_2$

Plane	Atoms defining plane	l	m	n	p
1	O(1), O(2), C(4), C(5), Tl	-0.954	0.227	-0.196	-0.522
2	O(3), O(4), C(8), C(9), Tl	0.020	0.127	-0.992	-1.983

Deviations from planes (\AA)

1	O(1), -0.064; O(2) -0.051; C(4), 0.023; C(5), 0.073; Tl, 0.065
2	O(3), -0.076; O(4), -0.088; C(8), 0.117; C(9), 0.007; Tl, 0.038

Angle between planes; 78.3°

of I, bis(cyclopropyl)isobutyrothallium(III) and other organothallium(III) carboxylates are compared in TABLES 6.6 and 6.7, and the bands are assigned as $V(\text{CO}_2)$ asymmetric or symmetric stretching frequencies. The spectra indicate that monoorganothallium(III) compounds RTlY_2 , ($\text{R} = \text{C}_3\text{H}_5; \text{CH}_3$; $\text{Y} = \text{OCOCH}(\text{CH}_3)_2$; $\text{R} = \text{CH}_3$; $\text{Y} = \text{OCOCH}_3$, (TABLE 6.6;) have similar structures in the solid state because of the similarity of the spectra in the $1300\text{-}1700\text{cm}^{-1}$ region. Similarly, the solid state structures of $(\text{CH}_3)_2\text{TlOCOCH}_3$ ¹²⁹ and $(\text{C}_3\text{H}_5)_2\text{TlOCOCH}(\text{CH}_3)_2$ would appear to be similar on the basis of the IR evidence. The crystal structure of $(\text{CH}_3)_2\text{TlOCOCH}_3$ shows only one type of carboxylate group,¹²⁹ and this is both chelating and bridging (see FIG 6.5A). A simultaneously chelating and bridging carboxylate anion is also found in the structure of I. This suggests that for all the organothallium(III) carboxylates in TABLE 6.6, strong bands in the region $1505\text{-}1540\text{cm}^{-1}$ and $1411\text{-}1428\text{cm}^{-1}$ can be assigned as $V(\text{COO})$ asym. and $V(\text{COO})$ sym- respectively in chelating and bridging anions of type A. The additional strong bands in the regions $1610\text{-}1615\text{cm}^{-1}$ and $1380\text{-}1390\text{cm}^{-1}$ for the monoorganocarboxylates are consequently assigned as $V(\text{CO}_2)$ asym. and $V(\text{CO}_2)$ sym. respectively in chelating carboxylates, FIG. 6.5B, as found in the structure of I. The higher energies of the $V(\text{CO}_2)$ asym. bands of structural type B are consistent with the lack of bridging function and, as indicated by the structure of I, with the significantly ester-type character of this group.

TABLE 6.6

Absorption bands in the region $1350-1650\text{cm}^{-1}$ of alkylthallium(III) carboxylates^a in the solid state^b and in chloroform solution^c

<u>C₃H₅TlX₂</u>		<u>(C₃H₅)₂TlX</u>		
<u>Solid</u>	<u>Solution</u>	<u>Solid</u>	<u>Solution</u>	<u>Assignment</u> ^d
1615s	1590(br, sh)			} V _{asym.} (COO)
1512vs	1540s(br)	1528s	1545s(br)	
1505vs		1518(sh)		
1480w	1473m		1480w	
1471w		1468w		
1428s	1408m	1411s	1420m	} V _{sym.} (COO)
1390m	1395sh			
1377w	1375m		1375w	
1360w	1365m	1360m		

<u>CH₃TlY₂</u>		<u>(CH₃)₂TlY</u>		
<u>Solid</u>	<u>Solution</u>	<u>Solid</u> ^f	<u>Solution</u>	<u>Assignment</u> ^d
1610s	1590s(sh)			} V _{asym.} (COO)
1539s	1560s(br)	1540vs(br)	1570s	
1420-	1415s(br)	1428vs(br)	1428s(br)	} V _{sym.} (COO)
-1380s(br)1387sh				

<u>CH₃TlX₂</u> ^g				
<u>Solid</u>	<u>Solution</u>			
1610s	1577br	} V _{asym.} (COO)		
1510s	1525s			
1468m	1469s			
1425s	1405s	} V _{sym.} (COO)		
1390s	1400sh			
1372m	1370m			
1359m	1360m			

Table 6.6. Continued

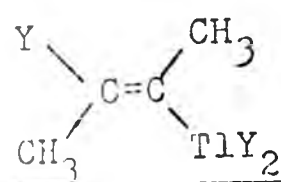
- ^aX = $\text{OCOCH}(\text{CH}_3)_2$; Y = OCOCH_3 . In cm^{-1} . vs = very strong, s = strong, m = medium, w = weak, sh = shoulder, br = broad.
- ^b Spectra obtained in Nujol or hexachlorobutadiene mulls.
- ^c Spectra obtained using CHCl_3 solution, 1%w/w.
- ^d Assignments by analogy with, or as given in, refs. 89,182, 385-388. ^e Band positions in agreement with those in ref. 388.
- ^f Band positions in good agreement with those in refs, 182,385, 388. ^g Data from ref. 89.

TABLE 6.7

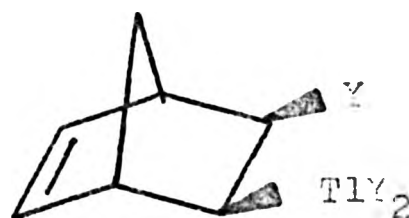
Absorption bands in the region $1350-1750\text{cm}^{-1}$ of a range of organothallium(III) carboxylates^a in the solid state^b and in chloroform solution.^c

<u>CH₃CH₂TlX₂^e</u>				<u>(CH₃CH₂)₂TlX^e</u>			
<u>Solid</u>		<u>Solution</u>		<u>Solid</u>		<u>Solution</u> <u>d</u>	
1610s	B	1587s	B				} $\nu_{\text{asym.}}$ (COO)
1518s	A	1534s	A	1531s	A	1531s	
1426m	A	1421s	A	1420s	A	1413s	} $\nu_{\text{sym.}}$ (COO)
1389m	B	1394s(sh)	B				
1474m		1475m		1476m		1474m	} Additional bands around $\nu(\text{COO})$ region
1374w				1370m		1370m	
1359w				1359w(sh)			
<u>(CH₃)₃SiCH₂TlX₂</u>				<u>[(CH₃)₃SiCH₂]₂TlX</u>			
<u>Solid</u>		<u>Solution</u>		<u>Solid</u>		<u>Solution</u> <u>d</u>	
1589s	B	1570m(s,br)	B				} $\nu_{\text{asym.}}$ (COO)
1546m(sh)		1547s(br)	A	1552s	A	1590m(sh)	
1518s	A					1543s	
						1532m(sh)	
1415s				1403s		1412m(br)	$\nu_{\text{sym.}}$ (COO)
				1472m		1470w	} Additional bands around $\nu(\text{COO})$ region
				1398w(sh)			
				1362m		1362w	
<u>[(CH₃)₃CCH₂]₂TlX</u>				<u>(cyclo-C₅H₁₁)₂TlX</u>			
<u>Solid</u>		<u>Solution</u>		<u>Solid</u>		<u>Solution</u> <u>d</u>	
1537s	A	1550s	A	1525s	A	1558s	$\nu_{\text{asym.}}$ (COO)
1417m		1411m		1405s			} $\nu_{\text{sym.}}$ (COO)
1403s							
1470s		1471s		1465w		1463w(sh)	} Additional bands around $\nu(\text{COO})$ region
1365s		1366m		1364w		1381w	
				1351w			

TABLE 6.7 Continued



<u>Solid</u>	<u>Solution</u>	<u>Solid</u>	<u>Solution</u>	<u>d</u>
1750s	1750s			V(C = O)
1674w	1672w			V(C = C)
1634w(sh)				
1609m B	1582m(sh) B			} V _{asym.} (C=O)
1524s(br)A	1532s(br) A	1535s(br)A	1557s A	
1437m	1424s	1405s A	1422s A	} V _{sym.} (C=O)
1370m	1477w 1370sh(br)	1397w(sh)	1397w(sh)	
				} Additional bands around V(C=O)region.



<u>Solid</u>	<u>Solution</u>	<u>Solid</u>	<u>Solution</u>	<u>d</u>
1750s	1750s	1744s	1744s	} V(C = O)
1732m(sh)	1733m(sh)			
1630w(sh)		1633w		
1613m B	1585m(sh) B	1615w B	1585w(br, sh)B	} V _{asym.} (C=O)
1533s(br)A	1553s A	1525s A	1554s(br) A	
			1540m(sh) A	
1420s A	1426s(br) A	1418m	1416s(br)	} V _{sym.} (C=O)
1373s	1380s(br)	1367m	1380s(br)	
				} Additional bands around V(C=O)region.

^aX = OCOCH(CH₃)₂; Y = OCOCH₃. In cm⁻¹. s = strong, m = medium, w = weak, sh = shoulder, br = broad. ^bSpectra obtained using Nujol or hexachlorobutadiene mulls. ^cSpectra obtained using CHCl₃ solution, 1% w/w. ^dAssignments by analogy with, or as given, in refs. 89, 182, 385-388. ^eBand positions in agreement with those in ref. 89.

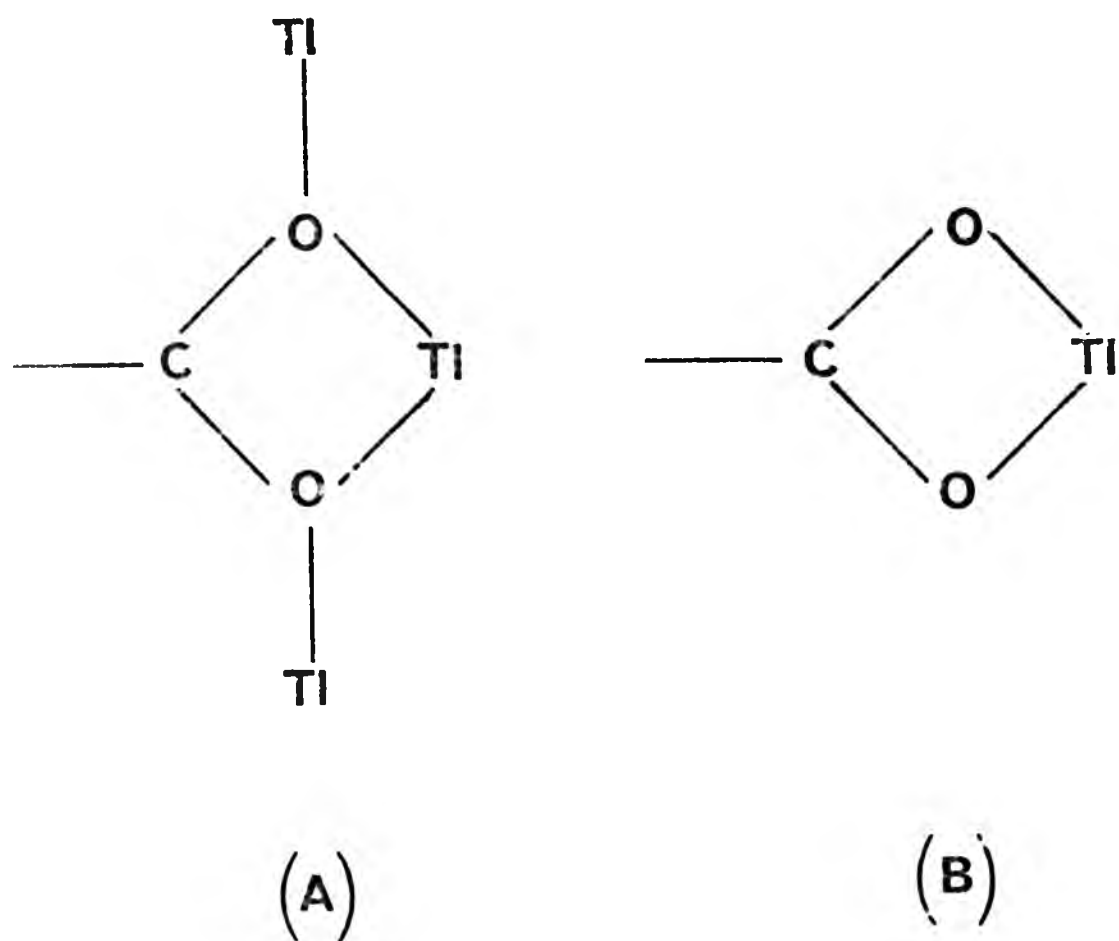


FIG. 6.5 The coordinating modes of the carboxylate anion in organothallium(III) compounds. (A) Chelating and bridging; (B) Chelating only.

On dissolution in chloroform $\nu(\text{CO}_2)$ asym. for ligands of type A increases by $15\text{--}35\text{cm}^{-1}$, consistent with partial disruption of Tl-O bonds as solvent molecules break up the polymer chains. This interpretation is also consistent with the state of aggregation (ca. 2) of $\text{CH}_3\text{Tl}(\text{OCOIC}_3\text{H}_7)_2$ in CHCl_3 solution.⁸⁹ The values of $\nu(\text{CO}_2)$ asym. for ligands of type B decrease by $20\text{--}33\text{cm}^{-1}$ for Chloroform solutions, and this may be due to the ester-like arrangement in B being altered to a more symmetrically coordinated carboxylate anion.

The infra-red spectra of a wide range of other organothallium-(III) carboxylates are compared in TABLE 6.7, both in the

solid state and in solution (CHCl_3). All the monoorganothallium(III) compounds can be seen to exhibit bands of the type B, (chelating only), in the solid state having values of $\text{Vasym}(\text{CO}_2)$ in the range $1598\text{--}1615\text{cm}^{-1}$. These values decrease by $23\text{--}30\text{cm}^{-1}$, on dissolving in chloroform as noted previously. Both mono- and diorganothallium compounds in the solid state are seen to have bands of type A, with values of $\text{Vasym}(\text{CO}_2)$ in the range $1518\text{--}1552\text{cm}^{-1}$. These values increase by $8\text{--}38\text{cm}^{-1}$ on dissolution in chloroform. Only the bands at 1552cm^{-1} and 1590cm^{-1} , in the solid state and in solution respectively, for $[(\text{CH}_3)_2\text{SiCH}_2]_2\text{TlOCO}_2\text{C}_3\text{H}_7$ are outside the range found for the compounds in TABLE 6.6.

The IR spectra of other organothallium(III) carboxylates have been reported for $\text{C}_6\text{H}_5\text{TlX}_2$,³⁸⁷ $\text{C}_6\text{H}_5\text{TlY}_2$ ^{387,388}, $(\text{C}_6\text{F}_5)_2\text{TlY}$ ¹⁸² $\text{X} = \text{OCO}_2\text{C}_3\text{H}_7$, $\text{Y} = \text{OCOCH}_3$. The similarity of their spectra (in the regions $1350\text{--}1650\text{cm}^{-1}$) to those in TABLES 6.6 and 6.7 suggest they contain carboxylate anions of type A and, for the monoorganothallium(III) species, also type B.

In the trans-acetato-(but-2-enyl)thallium(III) and norbornane-/norbornene- derivatives the third acetate group appears to play no part as a bridging or chelating group but is present as a free ester group as shown by the bands at $1732\text{--}1750\text{cm}^{-1}$.

6.3.2. Bis(trimethylsilylmethyl)chlorothallium(III). II

Numata⁸⁸ and Kurosawa¹⁴⁷ have proposed, on the basis of infra-red spectroscopic results and molecular weight measurements, that bis(trimethylsilylmethyl)chlorothallium(III), II, is dimeric in both the solid state and in chloroform solution and contains a non-linear C-Tl-C skeleton. The crystal structure of II determined here shows that whilst the dimeric formulation is confirmed in the solid state, the C-Tl-C unit is close to linear (168°).

The molecular-structure of II showing the disorder observed in one of the trimethylsilylmethyl groups and the labelling scheme used is shown in FIG.6.6. A view of the dimer unit without disorder is shown in FIG 6.7. Interatomic distances and angles are given in TABLE 6.8.

The structure consists of centrosymmetric dimers $\{[(CH_3)_3SiCH_2]_2TlCl\}_2$ with each thallium atom bonded unequally to the two bridging chlorine atoms. The thallium atom is four-coordinate with a coordination geometry based on a distorted trigonal bipyramid with one equatorial position vacant and both Tl-C bonds bent slightly towards the vacant position. The C-Tl-C angle ($168(1)^\circ$) is within the range ($163-180^\circ$) previously reported^{62,129,134-136,389,390} for R_2TlX derivatives (R = alkyl, X = uninegative anion).

The C-Tl-C angle found in II, (168°) is close to that found in the polymeric $(CH_3)_2TlCl$ ¹³² structure (180°) where thallium is six-coordinate. Thus it appears that there is no correlation between C-Tl-C angle and the extent of oligomerisation. This is supported by the following observations. $(CH_3)_2Tl$ tropolonate is polymeric with thallium six-coordinate and a C-Tl-C angle of 167° . However $(C_6H_5)_2Tl$ tropolonate is dimeric with five

TABLE 6.8

Interatomic distances and angles for $\{[(CH_3)_3SiCH_2]_2TlCl\}_2$ Distances^b

Tl...Tl ⁱ	4.308(2)	C(5) - Si(2A)	1.62(3)
Tl - Cl	2.76(1)	C(5) - Si(2B)	1.75(3)
Tl - Cl ⁱ	2.99(1)	Si(2A)... Si(2B)	(0.899)
Tl - C(1)	2.21(4)	Si(2A) - C(6)	1.86(5)
Tl - C(5)	2.17(3)	Si(2A) - C(7)	1.85(6)
C(1)-Si(1)	1.82(4)	Si(2A) - C(8A)	1.87(7)
Si(1)-C(2)	1.87(6)	Si(2B) - C(6)	1.87(5)
Si(1)-C(3)	1.82(8)	Si(2B) - C(7)	1.88(5)
Si(1)-C(4)	2.09(9)		
		Si(2B) - C(8B)	1.86(5)
		Cl...Cl ⁱ	3.87(2)

Angles^c

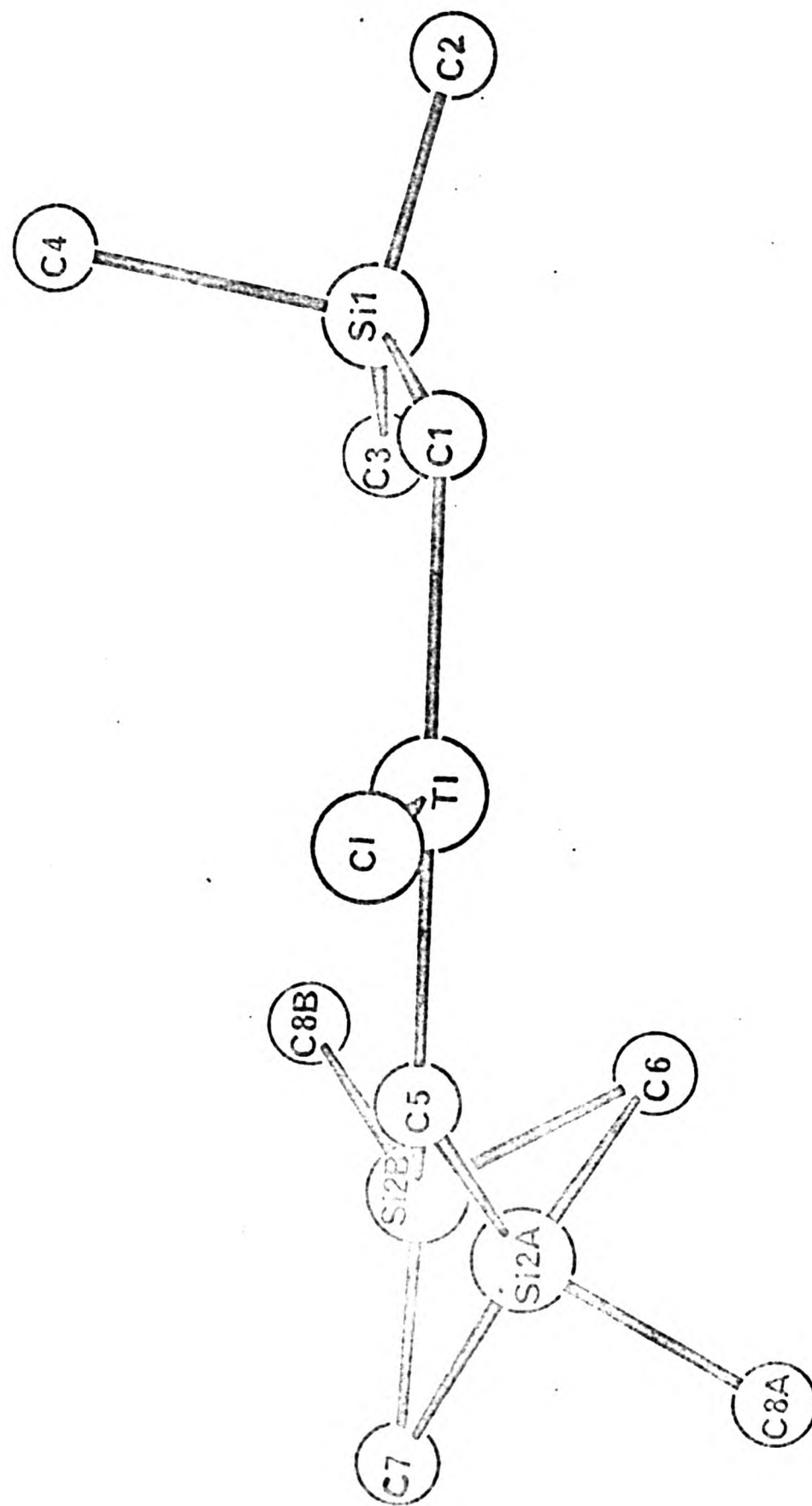
Cl-Tl-Cl ⁱ	84(1)	Tl-C(5)-Si(2A)	133(2)
Tl-Cl-Tl ⁱ	96(1)	Tl-C(5)-Si(2B)	116(2)
C(1)-Tl-Cl	97(1)	C(5)-Si(2A)-C(6)	108(2)
C(1)-Tl-Cl ⁱ	92(1)	C(5)-Si(2A)-C(7)	131(3)
C(5)-Tl-Cl	95(1)	C(6)-Si(2A)-C(7)	111(2)
C(5)-Tl-Cl ⁱ	91(1)	C(5)-Si(2A)-C(8A)	121(2)
C(1)-Si(1)-C(2)	112(2)	C(6)-Si(2A)-C(8A)	86(3)
C(1)-Si(1)-C(3)	119(3)	C(7)-Si(2A)-C(8A)	91(3)
C(2)-Si(1)-C(3)	128(3)	C(5)-Si(2B)-C(6)	102(3)
C(1)-Si(1)-C(4)	95(3)	C(5)-Si(2B)-C(7)	121(2)
C(2)-Si(1)-C(4)	87(3)	C(6)-Si(2B)-C(7)	109(2)
C(3)-Si(1)-C(4)	99(4)	C(5)-Si(2B)-C(8B)	125(3)
C(1)-Tl-C(5)	168(1)	C(6)-Si(2B)-C(8B)	79(3)
Tl-C(1)-Si(1)	116(2)	C(7)-Si(2B)-C(8B)	109(2)

^aThe superscript i refers to the symmetry transformation -x,-y,1-z.
^bIn Å. An alternative model with

constraints fixing Si(2A); Si(2B) as tetrahedra gave a refined
 Si-C bond distance of 1.834 Å and a Cl-Tl-C angle of 170.0°(11).

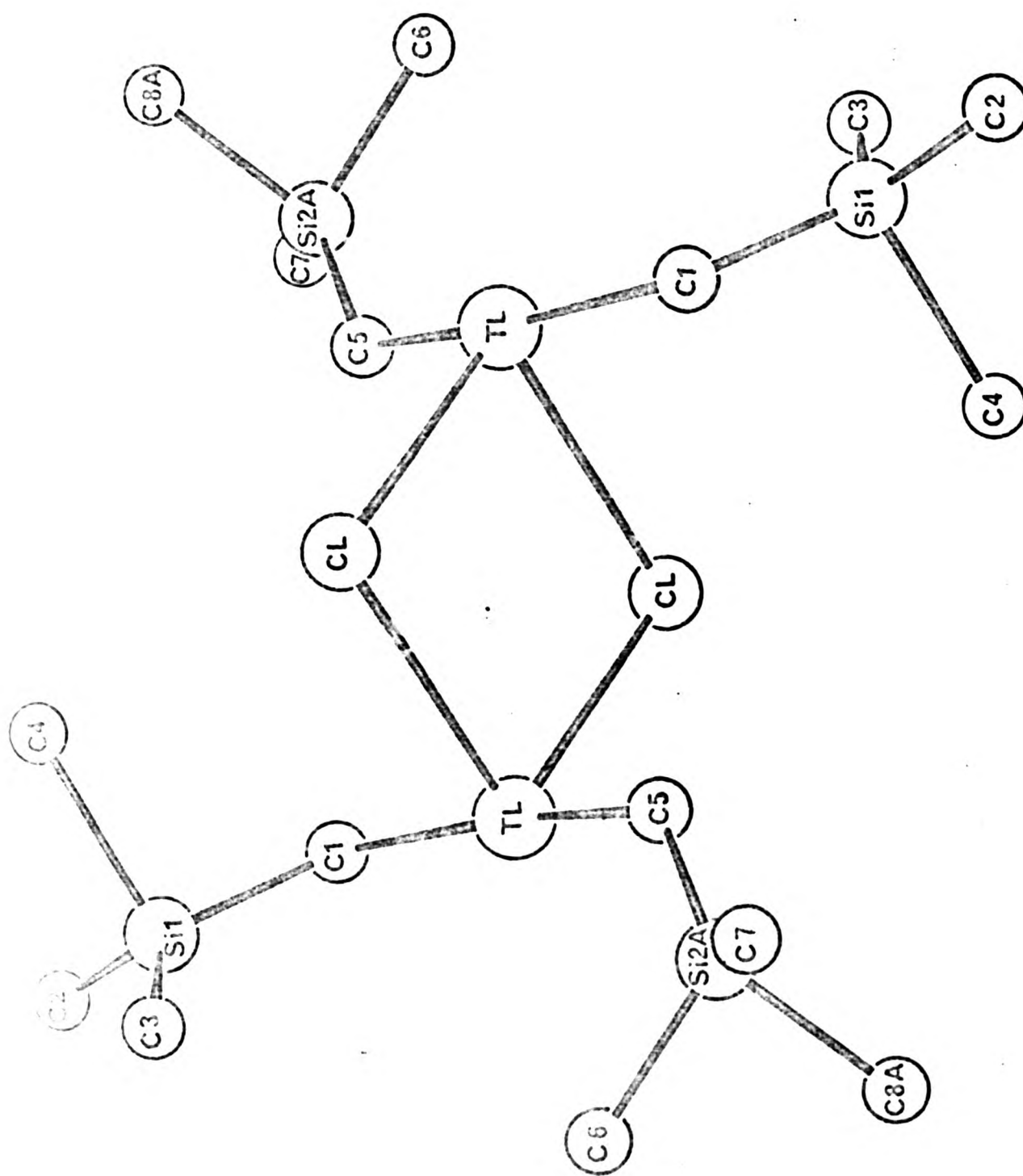
^cIn degrees.

FIG 6.6.



The structure of a monomer unit of $\{[(CH_3)_3SiCH_2]_2TiCl\}_2$ showing disorder in one of the trimethylsilylmethyl groups

FIG. 6.7.



The structure of $\{[(\text{CH}_3)_3\text{SiCH}_2]_2\text{TlCl}\}_2$ (The disorder in the trimethylsilylmethyl groups is not shown).

coordinate thallium and a C-Tl-C angle of 163° .¹⁴³ The C-Tl-C angle in the polymeric $(C_6F_5)_2TlOH$ ¹⁴¹ is 139° with five-coordinate thallium whereas in $(C_6H_5)_2Tl$ diethyldithiocarbamate thallium is four coordinate with a C-Tl-C angle of 148° .¹⁴³ This evidence suggests that electronic factors may be important in determining the C-Tl-C angle.

It has been suggested that oligomer formation in R_2TlX derivatives is strongly influenced by the nature and size of the anionic ligand X.¹⁴³ Polymerisation usually occurs in R_2TlX compounds when X is a small monodentate ligand, eg. OH ¹⁴¹, Cl ¹³³, Br ¹⁴². For larger anionic ligands eg. PhO^- , Ph^- , $o-ClC_6H_4O^-$ ⁶² and $[Al(CH_3)_3NC]^-$ ¹³⁵ association is limited to dimer formation.

Thus by analogy with $(CH_3)_2TlCl$, further association of $\{[(CH_3)_3SiCH_2]_2TlCl\}_2$ to form polymeric chains would be expected to occur through chlorine bridges. However no evidence for polymerisation in II was found and the shortest interdimer Tl.....Cl distances found are Tl.....Clⁱⁱ, 10.95Å; Tl.....Clⁱⁱⁱ, 12.91Å (superscripts ii and iii refer to the symmetry transformations $1.5-x, \frac{1}{2}+y$ and $-\frac{1}{2}+x, \frac{1}{2}-y, -\frac{1}{2}+z$ respectively). The shortest interdimer Tl.....Tl distances are Tl.....Tlⁱⁱ, 12.99Å and Tl.....Tlⁱⁱⁱ, 10.92Å. It is possible that the bulky $(CH_3)_3SiCH_2$ groups are preventing oligomerisation from proceeding beyond the dimer stage in this case. Unfortunately the exact relative orientations of the $(CH_3)_3SiCH_2$ groups in neighbouring dimer units could not be meaningfully determined due to the nature of the disorder in one of these groups. Thus it is not clear whether steric or electronic factors limit oligomer formations in this case.

Although X-ray crystal structures of several transition metal derivatives of the trimethylsilylmethyl group have been

reported eg. Cr³⁹¹, Pt³⁹², W³⁹³, Mo³⁹⁴, no main group element derivatives have been reported. Only structures of bis(trimethylsilyl)methyl-derivatives of Sn^{395,396}, Ge³⁹⁷ and Mg³⁹⁸ have been published.

REFERENCES

1. R.M. Harris, B.E. Mann eds., NMR and the Periodic Table, Academic Press, London (1978)
2. D.G. Gillies, D. Shaw, Ann. Reports NMR Spec., 5A (1972) 557.
3. I.O. Sutherland, Ann. Reports NMR Spec. 4(1971)71.
4. J.I. Musher, Adv. Mag. Res., 2(1966)177.
5. D. Shaw., Fourier Transform NMR Spectroscopy, Elsevier, Amsterdam(1976)
6. T.C. Farrar, E.D. Becker, Pulse and Fourier Transform NMR, Academic Press, New York(1971).
7. R.M. Lynden-Bell, R.K. Harris, Nuclear Magnetic Resonance Spectroscopy, Nelson, London 1969.
8. J.W. Emsley, J. Feeney, L.H. Sutcliffe, High Resolution Nuclear Magnetic Resonance Spectroscopy, Pergamon Press, Oxford (1965).
9. J.A. Pople, W.G. Schneider, J.H. Bernstein, High Resolution Nuclear Magnetic Resonance, McGraw Hill Book Co, Inc., New York (1959)
10. J.G. Schneider, A.D. Buckingham, Disc. Faraday Soc., 34(1962) 147.
11. K. Hildenbrand, H. Dreeskamp, Z. Phys. Chem; (NF) 69(1970)171.
12. C.S. Hoad, R.W. Matthews, M.M. Thakur, D.G. Gillies, J. Organometal. Chem., 124(1977)C 31.
13. H. Koppell, J. Dallorso, G. Hoffman, B. Walther, Z. Anorg. Chem. 427(1976)24.
14. J. . Hinton, R.W. Briggs, J. Magn. Reson., 22(1976)447.

15. J.I. Zink, C. Srivarnavit, J.J. Dechter, Organometal. Polymers (Symp.) 1977(Pub 1978) 323.
16. P.J. Burke, R.W. Matthews, D.G. Gillies, J. Organometal. Chem., 118(1976) 129.
17. J.F. Hinton, R.W. Briggs, J. Magn Reson., 25(1977)555.
18. P.J. Burke, PhD.Thesis, Univ, of London (1978)
19. S.O. Chan, L.W. Reeves, J. Amer. Chem. Soc., 96(1974)404 .
20. R.W. Briggs, J.F. Hinton, J. Solution Chem., 8(1979)519.
21. C. Schramm, J.I. Zink, J. Magn. Reson., 26(1977)513.
22. G.M. Sheldrick, J.P. Yesinowski, J. Chem. Soc., Dalton, 870(1975)
23. P.J. Burke, I.D. Cresshull, D.G. Gillies, R.W. Matthews, submitted to J. Chem. Soc., Dalton.
24. H.S. Gutowsky, B.R. McGarvey, Phys. Rev. 91, (1953), 81.
25. R. Freeman, R.P.H. Gasser, R.E. Richards, D.H. Wheeler, Mol. Phys., 2 (1959)75.
26. R.P.H. Gasser, R.E. Richards., Mol. Phys., 2(1959)357.
27. J.J. Dechter, J.I. Zink., J. Amer. Chem. Soc., 97(1975)2937.
28. J.F. Hinton, R.W. Briggs. J. Mag. Reson., 19(1975)393.
29. J.J. Dechter, J.I. Zink, Inorg. Chem., 15(1976) 1690.
30. H.L. Poss, Phys. Rev., 72, (1947), 637.
31. H.L. Poss, Phys. Rev., 75, (1949) 600.
32. W.G. Proctor, Phys. Rev., 75, (1949) 522.
33. R.E. Sheriff, D. Williams, Phys. Rev. 82, (1951) 651.
34. E.B. Baker, L.W. Burd, Rev. Sci, Instr. 34, (1963) 238.
35. D. Herbison-Evans, P.B.P. Phipps. R.J.P. Williams, J. Chem. Soc., (1965), 6170.

36. R. Freeman, R.P.H. Gasser, R.E. Richards, Mol.Phys.,
2,(1959)301.
37. R.W. Vaughan,D.H. Anderson, J. Chem.Phys., 52,(1970)5287.
38. N.H. Nachtrieb, R.K. Momii. Reactiv.Solids, Proc.Int.
Symp. 6th(1968)p.675. Ed. J.W. Mitchell, Wiley-Interscience
N.Y. 1969.
39. S. Hafner, N.H. Nachtrieb. J. Chem.Phys., 42,1965,631.
40. B.W. Bangerter, J. Mag. Reson., 28(1977)141.
41. R.K.Momii, N.H. Nachtrieb, J.Phys. Chem., 72,(1968),3416.
42. D. Freude, A. Hauser, H. Pankau, H. Schmiedel,
Z. Phys. Chem.(Leipzig)251,(1972)13.
43. D. Freude, U.Lohse, H. Pfeifer, W. Schmirmer, H. Schmiedel,
H. Stach, Z. Phys. Chem.,(Leipzig)255,(1974)443.
45. L.Kolditz, E. Wahner, Z.anorg. allg.Chem.400,(1973),161.
46. S.Hafner,N.H.Nachtrieb, J.Chem.Phys., 40,(1964)2891.
47. J.J. Dechter,J.I.Zink, J. Chem. Soc.,Chem.Comm.96,(1974).
48. J.J.Dechter, J.I.Zink, J. Amer.Chem.Soc., 98(1976),845.
49. J.J.Dechter, Diss.Abs.Int.B36,3944,1976.
50. J.F. Hinton, R.W.Briggs, J. Mag.Reson,25,1977,379.
51. J. Reuben,F.J.Kayne, J. Biol.Chem., 246,(1971)6227.
52. F.J. Kayne ,J. Reuben,J. Amer.Chem.Soc.,92,(1970)220.
53. K. Arnold,R.Scholl, Stud.Biophysics, 59,(1976)47.
54. C.M. Grisham, R.K.Gupta, R.E. Barnett, A.S. Mildvan,
J. Biol.Chem., 249(1974)6738.
55. C.M.Grisham,A.S. Mildvan, Fed. Proc., 23(1974)1331.
56. R.W. Briggs, J.F.Hinton, Biochemistry 17,(1978)5576.
57. R.W. Briggs J.F. Hinton, J.Mag.Reson,32,(1978)155.
58. R.W. Briggs, J.F. Hinton,J.Mag. Reson., 33(1979)363.
59. D. Gudlin, H. Schneider, Inorg. Chim.Acta,33(1979)205.

60. C. Srivnavit, J.I. Zink, J.J. Dechter, J. Amer. Chem. Soc., 99(1977)5876.
61. K. Henrick, R.W. Matthews, P.A. Tasker, Inorg. Chem., 16(1977)3293.
62. P.J. Burke, L.A. Gray, P.J.C. Hayward, R.W. Matthews, E.M. McPartlin, D.G. Gillies., J. Organometal. Chem., 136(1977) C7.
63. S. Bauer, A. Zschunke, B. Walther., Z. Anorg. allg. Chem., 70(1976)49.
64. H. Schmidbaur, H.J. Fuller, F.H. Kohler, J. Organometal. Chem., 99(1975)353.
65. H. Schmidbaur, H.J. Fuller, Chem. Ber., 107(1974)3674.
66. L. Ernst., J. Organometal. Chem., 82(1974)540.
67. L. Ernst., Org. Magn. Reson., 6(1974)540.
68. W. Kitching, D. Praeger, C.J. Moore, D. Doddrell, W. Adcock., J. Organometal. Chem., 70(1974)339.
70. W. Kitching, C.J. Moore, D. Doddrell, W. Adcock., J. Organometal. Chem., 94(1975)469.
71. J.Y. Lallemand, M. Duteil., Org. Magn. Reson., 8(1976)328.
72. V.G. Gibb, L.D. Hall., Carbohydrate Res., 63(1978)C1.
73. S. Uemura, H. Miyoshi, M. Okano, I. Morishima, T. Inubushi., J. Organometal. Chem., 165(1979)9.
74. I. Morishima, T. Inubushi, S. Uemura, H. Miyoshi, J. Amer. Chem. Soc., 100(1978)355.
75. P.R. Barron, S. Doddrell, W. Kitching., J. Organometal. Chem., 132(1977)351.
76. S. Uemura, H. Miyoshi, M. Okano, I. Morishima, T. Inubushi., J. Organometal. Chem., 171(1979)131.
77. J.Y. Lallemand, V. Michon., J. Chem. Res., 63(1978)C1.
78. A.T. Hsieh, C.A. Rogers, B.O. West Austral. J. Chem., 29(1976)49.

79. R.J.Abraham,G.E.Hawkes,K.M.Smith.,J.Chem.Soc.,Chem. Comm.,
401(1973).
80. R.J.Abraham,G.E.Hawkes,J.Chem.Soc.,Perkin II, 627,(1974)
81. R.J.Abraham,G.E.Hawkes,M.F.Hudson,K.M.Smith, J.Chem.
Soc.,Perkin II,204(1975)
82. V.F.Bystrov,Y.D.Garilov,V.T.Ivanov,Y.A.Ovchinikov.,
Eur.J.Biochem.,78(1977)63.
83. P.Krommes,J.Lorberth,J.Organometal.Chem.,74(1974)155.
84. A.F.M.J.Van Der Ploeg,G.Van Koten,K.Vrieze.,Inorg.Chim.
Acta.,39(1980)253.
85. J.F. Hinton,R.W.Briggs, in NMR and the Periodic Table.,
Eds.,R.K.Harris,B.E.Mann. Academic Press, London 1978.
86. J.P.Maher, D.F.Evans, J.Chem.Soc.,637(1965).
87. M.D.Johnson, Chem.Comm.,1037(1970).
88. S. Numata,H.Kurosawa,R.Okawara ,J.Organometal.Chem.,
70(1974)C21.
89. H.Kurosawa,R.Okawara , J.Organometal.Chem.,10(1967)211.
90. H.Kurosawa,R.Okawara.,J.Organometal.Chem.,14(1968)225.
91. H. Kurosawa,R.Okawara ,Inorg.Nucl.Chem.Letts.,3(1967)93.
92. F.A.L.Anet ,Tetrahed.Letts.,46(1964)3399.
93. H.Kurosawa,R.Kitano,T.Sasaki,J.Chem.Soc.,Dalton 234(1978)
94. E. Maxa,G.Schultz,E.Zbiral., Liebigs Ann.Chem.,933(1974)
95. J.P.Maher, D.F.Evans., Proc.Chem.Soc.,176(1963).
96. R.K.Sharma,E.D.Martinez., J.Chem.Soc.,Chem,Comm.1129(1972).
97. J.P.Maher ,PhD Thesis Univ. of London 1963.
98. S.Uemura,H.Tara,M.Okano,K.Ichikawa.,Bull.Chem.Soc. Japan
47(1974)2663.
99. S.Uemura,K.Sohma,H.Tara,M.Okano,Chem.Letts,Chem.Soc.Japan
545(1973).

100. A.N.Nesmeyanov, A.E.Borisov, N.V.Novikova, E.I.Fedin ,
Doklady Akad.Nauk SSSR 183(1968)118.
101. J.P.Maher, D.F.Evans , J. Chem.Soc., Dalton 183(1972).
102. A.McKillop, J.D.Hunt, E.C.Taylor, J.Organometal.Chem.
24(1970)77.
103. G.S.Shier, R.S.Drago, J.Organometal.Chem., 5(1966)330.
104. F.Hruska, T.Schaeffer, C.A.Reilly , Can.J.Chem., 42(1964)697.
105. J.V.Hatton , J.Chem.Phys., 40(1964)933.
106. G.S.Shier, R.S.Drago , J.Organometal.Chem., 6(1966)359.
107. H. Kurosawa, K.Yasuda, R.Okawara, Bull.Chem.Soc., Japan,
40(1967)861.
108. A.G.Lee, G.M.Sheldrick , Trans.Farad.Soc., 67(1971)7.
109. A.G.Lee, J.Chem.Soc., (A)2157(1970).
110. H.Schmidbaur, F.Schindler, Agnew.Chem.Int.Ed., 4(1965)876.
111. F.Bonati, G.Minghetti , Inorg.Chim.Acta, 3(1969)161.
112. V.S.Petrosyan, O.A.Reutov , Pure and Appl.Chem., 37(1974)147.
113. E.V.Van der Berghe, G.P.Van der Kelen , J.Organometal.
Chem., 11(1968)479.
114. J.R. Holmes, H.D.Kaes, J.Amer.Chem.Soc., 83(1961)3903.
115. G.Matsubayashi, Y.Kawasaki, T.Tanaka, R.Okawara , Bull.
Chem.Soc.Japan 40(1967)1566.
116. T.F.Bolles, R.S.Drago., J. Amer.Chem.Soc., 88(1961) 5730.
117. J.V.Hatton, W.G.Schneider, W.Siebrand , J.ChemPhys., 39(1963)
1330.
118. W.McFarlane , J.Chem.Soc., A (1967)523.
119. T.N.Mitchell, J.Organometal.Chem., 59(1973)189.
120. M.Aritomi, Y.Kawasaki , J.Organometal.Chem., 90(1975)185.
121. M.Aritomi, Y.Kawasaki , J.Organometal.Chem., 104(1976)39.
122. N.F.Ramsey , Phys.Rev., 78(1950)699.

123. M.Bacon, L.W.Reeves, J.Amer.Chem.Soc., 95(1973)272.
124. J.F.Hinton, K.H.Ladner, J.Mag. Reson., 32(1976)303.
125. B.W.Bangerter, R.N.Schwartz, J.Chem.Phys., 60(1974)333.
126. G.M.Sheldrick, W.S.Sheldrick, J.Chem.Soc., (A), 128, (1970)
127. G.H.W.Milburn, M.R.Truter, J.Chem.Soc., (A), 648(1967)
128. Y.M.Chow; D.Britton, Acta Cryst., B 31(1975)1922.
129. Y.M.Chow., D.Britton, Acta Cryst., B31(1975)1929.
130. Y.M.Chow., D. Britton, Acta Cryst., B31(1975)1934.
131. W.Schwartz, G.Mann, J.Weidlein, J.Organometal.Chem.,
122(1976)303.
132. H.M.Fowell, D.Crowfoot, Zeit.Cryst., 87(1934)370.
133. D.G.Gillies, M.Forster, Unpublished results.
134. K.Henrick, R.W.Matthews, P.A.Tasker, Acta Cryst., B34(1978)
1347.
135. S.K.Seale, J.L.Atwood, J. Organometal.Chem., 64(1974)57.
136. T.L.Blundell, H.M.Powell, Proc.Roy.Soc., London A331(1972)161.
137. T.L.Blundell, H.M.Powell, Chem.Comm., 1(1967)54.
138. K.Henrick, R.W.Matthews, P.A.Tasker, Acta Cryst., B43
(1978)935.
139. H.D.Hausen, E.Viegel, H.J.Guden, Z.Naturforsch., 29b(1974)
269.
140. N.N.Greenwood, J.A. Howard, J. Chem.Soc., Dalton 177(1976)
141. H. Luth, M.R.Truter, J. Chem.Soc., (A)(1970), 1287.
142. G.B.Deacon, R.J.Phillips, K.Henrick, M.McPartlin, Inorg.Chim.
Acta, 35(1979)L355.
143. R.T.Griffin, K. Henrick, R.W.Matthews, M.McPartlin,
J.Chem.Soc.Dalton. Accepted for publication 1980.
144. K.Henrick, M.McPartlin, G.B.Deacon, R.J.Phillips.,
Unpublished results.

145. K. Henrick, M. McPartlin, R.W. Matthews, G.B. Deacon, R.J. Phillips, J. Organometal. Chem., Accepted for publication 1980.
146. K. Henrick, R.W. Matthews, P.A. Tasker, Inorg. Chim. Acta., 25(1977) L31.
147. H. Kurosawa, S. Numata, T. Konishi, R. Okawara, Bull. Chem. Soc., Japan 51(1978) 1397.
148. A.G. Lee, The Chemistry of Thallium., Elsevier, Amsterdam, 1971.
149. A.N. Nesmeyanov, R.A. Sokilik, Methods of Elementary Organic Chemistry Vol 1, The Organic Compounds of B, Al, Ga, In, Tl. North Holland Publ. Comp., Amsterdam (1967)
150. H. Kurosawa, R. Okawara, Organometal. Chem. Rev., A, 6(1970) 65.
151. G.E. Coates, K. Wade, Organometallic Compounds 3rd ed. Vol. 1. Methuen, London (1967).
152. K. Yasuda, R. Okawara, Organometal. Chem. Rev., 2(1967) 255.
153. W. Kitching, Organometal. Chem. Rev., 24(1970) 310.
154. A.G. Lee, Quart. Rev., 24(1970) 310.
155. C. Hansen, Ber., 3(1870) 9.
156. L.I. Zakharkin, O.Yu. Okhlobystin. Izv. Akad. Nauk SSSR, Otd. Khim. Nauk, 1942(1959). Chem. Abs., 54(1960) 9738a.
157. R.T. Meyer, A. Berthelm, Chem. Ber., 37(1904) 2051.
158. E. Krause, A. Von Grosse, Ber., 58 (1925) 1933.
159. E. Krause, P. Dittmar, Ber., 63(1930) 1953.
160. A. McKillop, L.F. Elsom, E.C. Taylor, J. Organometal. Chem., 15(1968) 500.
161. A. McKillop, L.F. Elsom, E.C. Taylor, J. Amer. Chem. Soc., 90(1968) 2423.

162. H. Gilman, P.G. Jones, J. Amer. Chem.Soc., 68(1946)517.
163. A.G. Lee, G.M.Sheldrick , J. Organometal.Chem., 17(1969) 481.
164. F. Challenger, O.V. Richards, J. Chem. Soc., 405(1934).
165. D. Goddard, A.E. Goddard , J. Chem. Soc.,256(1922).
166. A.E. Goddard, D. Goddard , J. Chem.Soc.,482(1922).
167. C.R. Hart, C.K.Ingold , J. Chem.Soc., 4372(1964)
168. H. Kurosawa, T. Fukomoto, R. Okawara, Inorg.Nucl. Chem.Letts., 5(1969)473.
169. A.N.Nesmeyanov, A.E. Borisov, I.S. Savel'eva, E.I.Golubeva , Izvest. Akad. Nauk,SSSR, Otdel.Khim. Nauk 1490(1958)
170. A.N.Nesmeyanov, A.E. Borisov, N.V.Novikova, Doklady Akad. Nauk, SSSR 96(1954)289.
171. A.N.Nesmeyanov, A.E. Borisov, N.V.Novikova , Izv. Akad. Nauk,SSSR, Otdel,Khim. Nauk , 1216(1959).
172. A.E. Borisov, N.V.Novikova, Izv.Akad.Nauk,SSSR, Otdel. Khim. Nauk, 1258(1957).
173. A.N.Nesmeyanov,A.E. Borisov,N.V.Novikova, Izv. Akad. Nauk,SSSR, Otdel.Khim. Nauk,259(1959)
174. A.N.Nesmeyanov, A.E. Borisov, R.I.Shepeleva,Izv.Akad. Nauk,SSSR, Otdel.Khim. Nauk, 582(1949).
175. R.K.Freidlina, A.N.Kochetkov,A.N.Nesmeyanov,Izv.Akad. Nauk, SSSR, Otdel.Khim. Nauk,445 (1948).
176. A.E. Borisov, V.D.Vil'chevskaya, A.N.Nesmeyanov,Izv. Akad,Nauk,SSSR, Otdel.Khim. Nauk,1008(1954).
177. A.E. Borisov, N.V. Novikova,Izv. Akad. Nauk SSSR, Otdel.Khim. Nauk, 1670(1959).
178. V.A. Sazonova, N.Ya.Kronrod, Zhur.Obschc. Khim., 26(1956)1876.

179. A.N.Nesmeyanov, A.E. Borisov, M.A. Osipova, Dokl. Akad. Nauk SSSR, 169(1966)602.
180. A.E. Borisov, Izv. Akad. Nauk SSSR, Otdel.Khim.Nauk, 402(1951).
181. A.E. Borisov, M.A. Osipova, A.N.Nesmeyanov, Izv. Akad. Nauk SSSR, Ser.Khim. 1507(1963).
182. G.B. Deacon, J.H.S. Green, R.S. Nyholm, J. Chem. Soc., 3411(1965).
183. R.K. Abbott, Iowa State Coll. J. Sci., 256(1922). Chem.Abs., 38(1944)61.
184. N.N.Mel'nikov, M.S. Rokitskaya, J. Gen.Chem., USSR 7 (1937)1472. Chem. Abs., 32(1968)127.
185. F. Challenger, B. Parker, J. Chem. Soc., 1462(1931).
186. A.N.Nesmeyanov, L.G. Makarova, Doklady Akad. Nauk SSSR, 87(1952)417.
187. A.N.Nesmeyanov, T.P.Tolstaya, L.S.Isaeva, Doklady Akad.Nauk SSSR, 125 (1959)330.
188. A.McKillop, J.D.Hunt, E.C. Taylor, J.Organometal.Chem., 24(1970)77.
189. M. Tanaka, H. Kurosawa, R. Okawara, J. Organometal.Chem., 18(1967)49.
190. T. Fukumoto, H.Kurosawa, R. Okawara, J. Organometal.Chem., 22(1970)627.
191. V.P.Glushkova, K.A.Kocheshkov, Doklady Akad.Nauk SSSR, Otdel. Khim.Nauk SSSR, 1193 (1957)
192. R.K. Sharma, W.F. Fellers, J. Organometal. Chem., 49(1973)C69.
193. E.C. Pande, S. Winstein, Tet.Letts., 46(1964)3393.
194. R.G. Coombes, M.D. Johnson, D. Vamplew, J. Chem. Soc., (A) (1968)2297.

195. W. McFarlane, Proc. Roy.Soc.London Ser.A306(1968)185.
196. R.K. Harris, B.J.Kimber , J. Magn. Reson.,17(1974)174.
197. R.C. Weast, ed. Handbook of Chemistry and Physics,
53rd edn., The Chemical Rubber Co. Cleveland 1972.
198. H.H.Mantsch, H. Saito, I.C.P. Smith, Progr. in NMR Spec.,
11(1977)211.
199. R.J.Meyer, Z Anorg. allg. Chem., 24(1900)325.
200. F.A. Cotton, B.F.G. Johnson, R.M.Wing, Inorg. Chem.,
4(1965)502.
201. W.G. Palmer, Experimental Inorganic Chemistry,
Cambridge Univ. Press (1965).
202. A.E. Goddard , J. Chem. Soc., 36(1922).
203. U. Knips, F. Huber, J. Organometal. Chem.,107(1976)9.
204. A.I.Vogel , A Textbook of Practical Organic Chemistry,
3rd ed. Longmans, 1964 London (p.276).
205. F.C.Whitmore, L.H. Sommer , J. Amer. Chem. Soc.,
68(1946)481.
206. T. Abe, R. Okawara , J. Organometal. Chem.,43(1972)117.
207. A.N. Nesmeyanov, R. Kh.Freidlina, Chem.Abs., 40(1946)
3451., A.N.Nesmeyanov, Chem.Abs.,34(1940)6567.
208. F. Brady, BSc Chemistry Project, (CNAA) The Polytechnic
Of N. London. (1976).
209. T.F. Wimeitt , Phys. Rev., 91(1953)499A.
210. B.N. Figgis , Trans. Faraday Soc., 55(1959)1075.
211. T. Sidei, S. Yano, S. Sasaki, Oyo Butsuri 27(1958)513.
212. A. Saika, C.P. Slichter , J. Chem.Phys.,22(1954)26.
213. J.C. Slater , Phys. Rev.,36(1930)57.
214. J.D. Kennedy, W. McFarlane, Rev. Silicon, Germanium Tin
and Lead Compounds 1(1974)235.

215. P.J. Smith, A.P.Tupciauskas, *Ann. Rep.NMR Spec.*3(1978) 291.
216. J.S. Griffith, L.E. Orgel *Trans. Faraday Soc.*, 53(1957) 601.
217. L.E. Orgel *Mol.Phys.*, 1(1958)322.
218. C.J.Jameson, H.S. Gutowsky, *J. Chem. Phys.*,40(1964)1714.
219. J.A.Pople, *J. Chem. Phys.* 37(1962)5360.
220. M. Karplus, J.A. Pople , *J. Chem.Phys.*, 38(1963)2803.
221. Y.M.Cahen, P.R.Handy, E.T. Roach, A.I. Popov , *J. Phys. Chem.*,79(1975) 80.
222. M.S.Greenberg, R.L. Bodner, A.I.Popov,*J. Phys. Chem.*, 77(1973)2449.
223. V. Gutmann , *Coordination Chemistry in Non-Aqueous Solutions*, Springer-Verlag, New York 1968.
224. R.H. Erlich, A.I.Popov , *J. Amer. Chem. Soc.*,93(1971) 5620.
225. W.J.Dewitte, R.C.Schoening, A.I.Popov,*Inorg.Nucl.Chem. Lett.*,12(1976)251.
226. J.S. Shih, A.I.Popov, *Inorg. Nucl. Chem.Lett.*, 13(1977) 105.
227. F. Brady, K.Henrick, R.W. Matthews, D.G.Gillies , *J. Organometal.Chem.*, Accepted for publication 1980.
228. M.A. Sens, N.K. Wilson, P.D. Ellis, J.D. Odom,*J. Mag. Res.*,19(1975)323.
229. A.J.Brown, O.W. Howarth, P. Moore , *J. Chem.Soc.,Dalton*, 1589(1976).
230. T.N.Mitchell, J. Gmehling, F. Huber , *J. Chem. Soc., Dalton* 960(1978).
231. J.B. Kennedy, W.McFarlane, G.S. Pyne, *J. Chem.Soc., Dalton*, 2332(1977).

232. J.D. Kennedy, W. McFarlane, J. Chem.Soc., Perkin(II) 1257(1974).
233. R.W. Taft Jnr., in Steric Effects in Organic Chemistry, Ed. M.S. Newman, Wiley, New York, 1956. Chapter 13.
234. T.N. Mitchell, G. Walter, J. Chem.Soc., Perkin 1842(1977)
235. W. McFarlane, R.J. Wood, J. Chem.Soc., Dalton 1397(1972)
236. T.M. Krygowski, W.R. Fawcett, J. Amer. Chem.Soc. 97(1975) 2143.
237. C.J. Turner, R.F.M. White, J. Mag. Reson., 26(1977)1.
238. G. Kidd, R.J. Goodfellow, in NMR and the Periodic Table, eds. R.K. Harris, B.E. Mann, Academic Press, London 1978, p.269.
239. R.E. Dessy, T.J. Flautt, H.H. Jaffe, G.F. Reynolds, J. Chem Phys., 30(1959)1422.
240. G.C. Maciel, J.L. Dallas, J. Amer. Chem. Soc., 95(1973)3039.
241. P.J. Burke, R.W. Matthews, D. Gillies, J. Chem. Soc., Dalton Submitted for publication 1980.
- 241a. G. Klose, Ann. Phys., 9(1962)262.
242. A. Rahm, M. Pereye, M. Petraud, B. Barbe, J. Organometal. Chem., 139(1977)49.
243. L. Smith, PhD. Thesis, Univ. of London, 1972.
244. J.D. Kennedy, W. McFarlane., J. Chem.Soc., Perkin(II) 146(1974).
245. W. McFarlane, R.J. Wood, J. Organometal. Chem., 40(1972)C.17.
246. P. Smith, R.F.M. White, L. Smith, J. Organometal. Chem., 40 (1972)341.
247. P.F. Barron, D. Doddrell, J. Organometal. Chem., 139(1977) 361.
248. E. Kitching, D. Praeger, D. Doddrell, F.A.L. Anet, J. Krane, Tetrahedron Letts, 10(1975)759.

249. T.N. Mitchell, C. Kummetat, J. Organometal. Chem., 157(1978)275.
250. W. McFarlane, J. Chem. Soc., A, 2280(1968).
251. A.P. Tupciauskas, N.M. Sergeyev, Yu.A. Ustnyuk, A.N. Kashin, J. Mag. Reson., 7(1972)124.
252. G.B. Deacon, R.M. Slade, D.G. Vince, J. Fluorine Chem., 11(1978)57.
253. M.M. Thakur, R.W. Matthews. Unpublished results.
254. P.J. Banney, M.Sc., thesis Univ. of Queensland 1969.
Quoted by P.R. Wells in Determination of Organic Structures by Physical Methods. Vol 4. Ch.5, Academic Press New York, 1971. Eds. F.C. Nachod, J.J. Zuckerman.
255. V.S. Petrosyan, Progr. NMR Spec., 11(1977)115.
256. R.K. Harris, J.D. Kennedy, W. McFarlane, in NMR and the Periodic Table, Eds. R.K. Harris, B.E. Mann, Academic Press, London 1978.
257. T.N. Mitchell, J. Organometal. Chem., 141(1977)289.
258. B. de Poorter, M. Gielen, J. Organometal. Chem., 124(1977)161.
259. H. Von Kerner, H. Blank, K. Yasufuku, J. Organometal. Chem. 165(1979)187.
260. V.S. Petrosyan, O.A. Reutov, J. Organometal. Chem., 76(1974)123.
261. J. Casanova, H.R. Rogers, K.L. Servis, Org. Mag. Reson., 7(1975)57.
262. N.K. Wilson, R.D. Zehr, P.D. Ellis, J. Magn. Reson., 21(1976)437.
263. V.G. Gibb, L.D. Hall, Carbohydr. Res., 50(1976)C3.
264. Y. Kawasaki, M. Aritomi, J. Iyoda, Bull. Chem. Soc. Japan 49(1976)3428.

265. A.J. Canty, A. Marker, P. Barron, P.C. Healy ,
J. Organometal.Chem., 144(1978)371.
266. R.H.Cox , J. Mag.Reson., 33(1979)61.
267. J.D. Kennedy, W. McFarlane, B. Wrackmeyer , Inorg. Chem.,
15(1976)1299.
268. D.de Vos, J. Organometal.Chem., 104(1976)193.
269. D.C. Van Beelen, J. Walters, A. Van der Gen, J. Organometal.
Chem., 145(1978)359.
270. D.C. Van Beelen, D. de Vos, G.J.M.Bots, L.J.Van Doorn,
J. Walters, Inorg. Nucl. Chem. Letts., 12(1976)581.
271. Y. Kawasaki , J. Organometal.Chem., 9(1967)549.
272. F.J.Weigert, M. Winokur, J.D. Roberts, J. Amer.Chem.Soc.,
90(1968)1566.
273. H. Muller, L. Rosch, W. Erb , J. Organometal. Chem.,
140(1977)C17.
274. H.D. Vissier, L.P.Stodulski, J.P.Oliver , J. Organometal.
Chem., 24(1970)563.
275. A.D. Cardin, P.D. Ellis, J.D. Odom , J.W.Howard ,
J. Amer.Chem.Soc., 97(1975)1672.
276. H.Kurosawa, R.kitano, R. Okawara , Chem. Letts, Chem.Soc.
Japan 6(1976)605.
277. P.J. Burke, R.W. Matthews , Unpublished results.
278. Laocoon 1968. NMR spectroscopy, R. K. Harris, M.Kinns,
Atlas Computer Laboratory, Chilton, Didcot. 1974.
279. F.A.L. Anet, J.L. Sudmeir , J. Mag.Reson, 1(1969)124.
280. A. Saupe, G. Englert., Phys. Rev.Lett., 11(1963)462.
281. A.D. Buckingham, K.A.Mc Lauchlan, Proc. Chem.Soc., (1963)144.
282. M. Karplus , J. Amer. Chem. Soc., 84, (1962)2458.
283. R.K. Harris in NMR and the Periodic Table, eds. R.K. Harris,
B.E. Mann. Academic Press, London 1978.

284. M. Karplus , J. Chem. Phys.,30(1959)11.
285. K. Kuhlmann, J.D. Baldeschwieler , J. Amer. Chem. Soc.,
85(1963)100.
286. P.A.Scherr, J.P. Cliver, J. Amer. Chem. Soc.,94(1972) 8026.
287. A.T. Wiebel, J.P. Oliver, J. Organometal. Chem.,74(1974)
155.
288. H.M. Hutton, T. Schaeffer , Can. J.Chem.,41(1963)684.
289. P.A. Scherr, J.P. Oliver, J. Molec. Spec.,31(1969)109.
290. N.F. Ramsey, Phys. Rev., 91(1953)303.
291. J.A. Pople, D.P. Santry , Mol.Phys., 8(1964)1.
292. H. McConnell, J. Chem. Phys., 24(1956)460.
293. J.D. Kennedy, W. McFarlane, G.S. Pyne, B. Wrackmeyer,
J. Chem. Soc., Dalton (1975)386.
294. C.J. Jameson, H.S. Gutowsky, J. Chem. Phys., 51(1969)2790.
295. W. McFarlane., Quart. Rev.,23(1969)187.
296. D.K. Dalling, H.S. Gutowsky , U.S. Clearing house Fed.
Sci.Tech. Inform, AD721717,32(1971). Chem. Abs.,75(1971)
82238.
297. B.E. Mann in Advances in Organometallic Chemistry, Vol.12,
eds., F.G.A. Stone, R. West, Academic Press 1974.
298. T.Iwayanagi, T.Ibusuki, Y.Saito, J.Organometal. Chem.,
126(1977)145.
299. H.F. Henneke , J. Amer. Chem. Soc.,94(1972)5945.
300. G.Barbieri, R. Benassi, F. Taddei, J. Organometal.Chem.
129(1977)27.
301. T.N.Mitchell, J. Organometal. Chem., 70(1974)C1.
302. T.N.Mitchell, G. Walter, J. Organometal.Chem, 121(1976)
177.
303. K. Kamienska-Trela, J. Organometal.Chem,159(1978)15.

304. G. Singh , J. Organometal.Chem.99(1975)251.
305. M. Aritomi, Y. Kawasaki , J. Organometal.Chem.,81(1974)363.
306. G. Breit, Phys. Rev., 42(1932)348.
307. J.V. Hatton , W.G.Schneider, W.Siebrand ,J. Chem.Phys ., 39(1963)1330.
308. T. Ibusuki, Y. Saito, Chem.Lett.,Chem.Soc.,Japan (1974)311.
309. T.N.Mitchell, H.C. Marsmann ,J. Organometal.Chem.,150 (1978)171.
310. C.S.Hoad, R.W. Matthews. Unpublished results.
311. M. Charton in The Chemistry of Alkenes, Vol.2 Ch. 10. Ed. J. Zabicky. Interscience 1970.
312. J.D. Kennedy, W. McFarlane ,J. Organometal.Chem., 80(1974)C47.
313. L.A.Fedorov, L.A. Stumbrevichute, A.K.Prokofyev, E.I.Fedin, Dokl.Akad Nauk SSSR, 209 (1973)134.
314. T. Schaeffer, Can.J.Chem.,40(1962)1.
315. S.Cawley, S.S.Danyluk, J. Phys.Chem.,68(1964)1240.
316. G. Singh, G.S. Reddy , J. Organometal.Chem.,42(1972)267.
317. F.Glocking, N.S. Hosmane,V.B.Mahale, J.J. Swindall, L. Magos, T.J. King , J. Chem. Res.(S)(1977) 116.
318. K.A.McLauchlan, D.H. Wifren, Mol. Phys.,10(1966)131.
319. G. Singh , J. Organometal.Chem.,5(1966)577.
320. F. Glocking, S.R. Stobart, J.J. Sweeney, J. Chem.Soc, Dalton (1973)2029.
321. H.A. Bent , J. Inorg. Nucl.Chem., 19(1961)43.
322. C.N.Rao , Ultraviolet and Visible Spectroscopy , 2nd edn., Butterworths, London (1967).
323. K. Tokita, S. Kondo, M.Takeda , J. Chem.Res.,(S)63(1980)
324. J.E. Sarneski, Luther E. Erickson, C.N. Reilley, J. Mag. Reson., 37(1980)155.

325. F.R. Jensen, C.H. Bushweller, *Advan. Alicyclic Chem.*,
3, (1971)139.
326. J. Hirsch, *Top. Stereochem.*,1(1967)199.
327. F.R. Jensen, C.H. Bushweller, B.H. Beck, *J. Amer. Chem.Soc.*,
91(1969)344.
328. F.R. Jensen, L.H. Gale, *J. Amer.Chem.Soc.*,81(1959)1261.
329. F.R. Jensen, L.H. Gale, *J. Amer.Chem.Soc.*,81(1959)6337.
330. F.A.L. Anet, J. Krane, W.Kitching, D.Doddrell, D. Praeger,
Tet.Letts., 37(1974)3255.
331. W. Kitching, D. Doddrell, J.B.Grutzner, *J. Organometal.*
Chem.,107(1976)C5.
332. M. Hanack(Translated H.C. Neumann), *Conformation Theory*,
Academic Press, London 1965.
333. A. McKillop, M.E. Ford, E.C. Taylor, *J. Org. Chem.*,39
(1974)2434.
334. R.A. Hoffman, S. Forsen, B. Gestblom in *NMR Basic Principles
and Progress Vol. 5.*, eds.,P. Diehl, E. Fluck, R. Kosfield,
Springer-Verlag,Berlin (1971).
335. M. Karplus, *J. Amer.Chem.Soc.*,85(1963)2870.
336. R.J. Abraham,K.M.Smith,*Tet.Letts.*,36(1971)335.
337. C.A.Busby,D. Dolphin, *J. Mag.Reson.*,23(1976)211.
338. S. Uemura, K. Zushi, A. Tabata,A. Toshimitsu, M. Okano,
Bull. Chem. Soc. Japan. 47(1974)920.
339. G.C. Levy, *Topics in Carbon-13 NMR Spectroscopy. Vol.2.*
Wiley-Interscience., New York 1976.
340. G.E. Maciel, M. Borzo, *J. Chem. Soc., Chem Comm.*,
394(1973).
341. Y.C. Pushkar, T.A. Saluvere, E.T. Lippmaa, A.B. Pernin,
V.S. Petrosyan, *Dokl. Akad. Nauk.SSSR* 220 (1975)112.

342. C.R.G. Lassigne, E.J. Wells, J. Mag. Reson., 26(1977)55.
343. A. Frangou, Ph.D. Thesis, Univ. of London. 1979.
344. C.R. Lassigne, E.J. Wells, Can. J. Chem., 55(1977)1303,927.
345. J.D. Kennedy, W. McFarlane, J. Chem.Soc., Faraday II, 72(1976)1653.
346. G.E. Maciel, in Nuclear Magnetic Resonance Spectroscopy of Nuclei Other than Protons, eds. T. Axenrod, G.A. Webb, Wiley-Interscience, New York 1974.
347. A. Abragam, The Principles of Nuclear Magnetism, Oxford, London 1961.
348. A. Briquet, J.C. Duplan, J. Delmau, Mol. Phys., 29(1975) 837.
349. R.K. Harris, B.J. Kimber, Adv. Molec. Relax. Process. 8(1976)15.
350. P.S. Hubbard, Phys. Rev., 131(1963)1155.
351. R.E.D. McClung, J. Chem. Phys., 51(1969)3842.
352. G.A. Webb, in NMR and the Periodic Table, eds. R.K. Harris, B.E. Mann, Academic Press, London (1978)
353. A.A. Marynott, T.C. Farrar, M.S. Malmberg, J. Chem. Phys., 54(1971)64.
354. W. Freeman, P.S. Pregosin, S.N. Sze, L.M. Venazi, J. Mag. Reson., 22(1976)473.
355. M. Holts, R.B. Jordan, M.D. Zeidler, J. Mag. Reson., 22(1976)47
356. E.L. Macknor, C. Maclean, Prog. in NMR Spec., 3(1967)152.
357. G.C. Levy, D.M. White, F.A.L. Anet, J. Mag. Reson., 6(1972)453.
358. W.H. Pan, J. P. Packler Jnr, J. Amer. Chem. Soc., 100 (1978)5783.
359. W.E. Vernon, Ph.D. Thesis, Michigan State Univ. U.S.A. (1975)
360. R.N. Schwartz, J. Mag. Reson., 24(1976)205.

361. D.G. Gillies , Unpublished results.
362. E.D. Becker in Nuclear Magnetic Resonance Spectroscopy of Nuclei Other than Protons, eds., T. Axenrod, G.A. Webb, Wiley-Interscience , New York 1974.
363. L. Simerai, G.E. Maciel, J. Phys. Chem., 80(1976)552.
364. M. Eisenstadt, H.L. Friedman, J. Chem. Phys., 44(1966) 1407.
365. G. Balimann, P.S. Pregosin, J. Mag. Reson., 26(1977)283.
366. V.I. Chizhik, L.V. Olenina, Yu.S. Chernyshev, V.V. Frolov, V.P. Matveev, I.I. Puchkov, Kompleksn Ispol'z-Miner Syr'ya 3(1978)31. Chem. Abs., 90(1979)96918n.
367. A.W. Overhauser, Phys. Rev., 92(1953)411.
368. P.L. Goggin, L.A. Woodward, Trans. Faraday Soc., 56(1960) 1591.
369. M.G. Miles, J.H. Patterson, C.W. Hobbs , M.J. Hopper, J. Overend. R.S. Tobias , Inorg. Chem., 7(1968)1721.
370. D.G. Gillies, I.C. Cresshall. Unpublished results.
371. T.N. Mitchell, Org. Mag. Reson., 7(1975)59.
372. M. Forster, BSc. Project, Royal Holloway College, Univ. of London(1979)
373. M.F.C. Ladd, R.A. Palmer, Structure Determination by X-Ray Crystallography, Plenum Press, New York 1977.
374. G.H.W. Milburn , X-Ray Crystallography: An Introduction to the Theory and Practice of Single-Crystal Structure Analysis, Butterworths, London(1973)
375. A.L. Patterson, Zeit. Kryst., 90(1935)517.
376. J. Hornstra, B. Stubbe, PW1100 Data Processing Program, 1972. Philips Research Laboratories , Eindhoven, The Netherlands.

377. P.W.R. Corfield, R.J. Doedens, J.A. Ibers, *Inorg. Chem.*, 6(1967)197.
378. Programs for crystal structure determinations were kindly supplied by G.M. Sheldrick, University of Cambridge.
379. D.T. Cromer, J.B. Mann, *Acta Cryst.*, A24 (1968)321.
380. D.T. Cromer, *Acta Cryst.*, 18(1965)17.
381. C.K. Johnson, Oak Ridge National Laboratory Tenn., USA.
382. J.W. Moore, D.A. Sanders, P.A. Scherr, M.D. Glick, J.P. Oliver *J. Amer. Chem. Soc.*, 93(1971) 1035.
383. D.B. Chestnut, R.E. Marsh, *Acta Cryst.*, 11(1958)413.
384. J. Elaker, C. Rømming, *Acta Chem. Scand.*, 21(1967)2761
385. G.B. Deacon, J.H.S. Green, *Spectrochim. Acta* 24A(1968)885.
386. G.B. Deacon, R.J. Phillips, *Aust. J. Chem.*, 31(1978)1709.
387. A.G. Lee, *J. Organometal. Chem.*, 22(1970)537.
388. H. Kurosawa, R. Okawara, *J. Organometal. Chem.* 19(1969)253.
389. J.M. Chow, D. Britton, *Acta Cryst.*, B31 (1975)1929.
390. J.M. Chow, D. Britton, *Acta Cryst.*, B31(1975)1934.
391. M. B. Hursthouse, K.M.A. Malik, K.D. Sales, *J. Chem Soc., Dalton* 1314(1978).
392. B. Jovanovic, L. Manojlovic-Muir, K.W. Muir, *J. Chem. Soc., Dalton* 195(1974).
393. M.H. Chisholm, F.A. Cotton, M.W. Extine, C.A. Murrillo, *Inorg. Chem.*, 17(1978)696.
394. E. Guzman, G. Wilkinson, J.L. Atwood, R.D. Rogers, W.E. Hunter, M.J. Zaworotko, *J. Chem. Soc., Chem. Comm.*, 465(1978)
395. D.E. Goldberg, D.H. Harris, M. Lappert, K. M. Thomas, *J. Chem. Soc., Chem Comm.*, (1976) 261.
396. M.G.S. Gynane, M.F. Lappert, S.J. Miles, A.J. Carty, N.J. Taylor, *J. Chem. Soc., Dalton* (1977)2009.

397. M.F. Lappert, S.J. Miles, P.P. Power, A.J. Carty,
N.J. Taylor, J.Chem. Soc., Chem. Comm., (1977)458.
398. R. Shakir, J. L. Atwood, Amer. Cryst. Assoc., Ser 2,6,
(1978)11.
399. H.G. Kuivila, J.L. Considine, R. H. Sharma, R.J. Mynott, .
J. Organometal. Chem., 111(1976)179.
400. W. McFarlane, Poster. Fourth International Meeting on
NMR Spectroscopy, University of York, July 1978.

PUBLICATIONS

1. Monoalkylthallium(III) derivatives: Preparation and X-Ray crystal structure of cyclopropylbis(isobutyrate) thallium(III). F. Brady, K. Henrick, R.W. Matthews, J. Organometal. Chem., 165(1979)21.
2. Carbon-13 and proton NMR parameters of Neopentyl- and Trimethylsilylmethylthallium(III) derivatives and the X-ray crystal structure of bis(trimethylsilylmethyl)chlorothallium(III). F. Brady, K. Henrick, R.W. Matthews, D.G. Gillies, J. Organometal.Chem. (accepted for publication 1980).

Journal of Organometallic Chemistry, 165 (1979) 21-30
 © Elsevier Sequoia S.A., Lausanne -- Printed in The Netherlands

MONOALKYLTHALLIUM(III) DERIVATIVES: PREPARATION AND X-RAY CRYSTAL STRUCTURE OF CYCLOPROPYLBIS(ISOBUTYRATO)THALLIUM(III)

F. BRADY, K. HENRICK and R.W. MATTHEWS *

Department of Chemistry, The Polytechnic of North London, Holloway Road, London N7 8DB (Great Britain)

(Received July 3rd, 1978)

Summary

Cyclopropylbis(isobutyrate)thallium(III) has been synthesised and its crystal structure determined. The compound crystallises in the orthorhombic space group $Pna2_1$, with a 7.316, b 12.079, c 16.19 Å. Linear polymers are present in which thallium is seven-coordinate. Two types of carboxylate ligands are present; one weakly chelating and the other both chelating and bridging.

This structure allows clarification of infrared spectroscopic data, presented for mono- and diorganothallium(III) carboxylates, in the solid state and in solution.

Introduction

Synthetic procedures are now available for several types of monoorganothallium species, $RTiX_2$ (R = aryl [1]; vinyl [2]; norbornane derivatives [3]; and groups of the types $ClCH_2$ [4], $(CH_3)_3SiCH_2$ [5], $(pyH^+Cl^-)CH_2$ [6], $PhCH(OCH_3)CH_2$ [7]; X = anionic species). In contrast to this wide range of stable derivatives, monoalkylthallium(III) compounds appear to have been reported with only four types of alkyl group; R = CH_3 [8-16], C_2H_5 [8,9,12,13,16], $n-C_3H_7$ [12] and $(CH_3)_3CCH_2$ [17]. A variety of potentially bidentate [8,9], quadridentate [15] and quinquidentate [16] anionic ligands has been used to stabilise these monoalkyl compounds but the precursor compounds [8,14] (where X = carboxylate for R = CH_3 , C_2H_5 , $n-C_3H_7$) and $\{(CH_3)_3CCH_2\}_2TlBr$ [17] are apparently less stable in solution and in the solid state. As part of an investigation of monoalkylthallium(III) compounds we have isolated the cyclopropyl derivative, $C_3H_5Ti[OCOCH(CH_3)_2]_2$ (I), which appears to be remarkably stable.

Little is known about the structures of monoorganothallium(III) com-

ounds. The two available structure determinations are of complexes of CH_3TI^+ with quadri- [15] and quinquidentate [16] ligands respectively. The structures involving these multidentate ligands give little indication of the preferred co-ordination around thallium in the precursor monoalkylthallium(III) carboxylates. Our previous attempts to isolate crystalline samples of (alkyl)- $\text{TI}X_2$ ($X = \text{OCOCH}_3, \text{OCOCH}(\text{CH}_3)_2$) failed due to crystal disintegration on removal of solvent during isolation of the products. The cyclopropyl derivative, I, proved exceptional in this respect, and an X-ray crystal structure determination was therefore undertaken.

Experimental

Preparation of dicyclopropylbromothallium(III). Cyclopropylmagnesium bromide [18] (0.13 mol) in THF (100 cm³) was added slowly (45 min) with stirring to a cooled (-20°C) freshly prepared solution of thallium(III) bromide [2a] (0.06 mol) in THF (100 cm³) under dry nitrogen. Stirring was continued for a further 20 min at -20°C and then, after being allowed to warm to room temperature, the mixture was hydrolysed with aqueous ammonium bromide solution (5%). The crude product was collected by filtration, washed with water and ether and dried over P_2O_5 . Extraction of this material (14.5 g) with pyridine (500 cm³) at 45°C and concentration to ca. 25 cm³, followed by addition of petroleum ether, gave the product as a white solid. (Found: C, 20.2; H, 2.8. $\text{C}_6\text{H}_{10}\text{TlBr}$ calc.: C, 19.7; H, 2.7%.)

Preparation of dicyclopropylisobutyrate-thallium(III). Dicyclopropylbromothallium(III) (5.9 mmol) and isobutyrate-silver(I) (1.6 mmol) were mixed in methanol solution. Silver bromide was removed by filtration, and evaporation of the solvent gave the product as a white solid (75%), which was used without further purification.

Preparation of cyclopropylbis(isobutyrate)-thallium(III), I. A solution of dicyclopropylisobutyrate-thallium(III) (0.8 g; 0.002 mol) and bis(isobutyrate)-mercury(II) (0.8 g; 0.002 mol) in methanol (100 cm³) was stirred for 4 h. The mixture was filtered and evaporation of the filtrate at 20°C under reduced pressure gave a white solid. The mercury salts were removed by washing with benzene (50 cm³). Recrystallisation from methanol gave I (0.4 g; 44%) as colourless needles. (Found: C, 31.6; H, 4.6. $\text{C}_{11}\text{H}_{19}\text{O}_4\text{Tl}$ calc.: C, 31.5; H, 4.5%.)

Dimethylacetatothallium(III) and methylbis(acetate)-thallium(III) were prepared as previously reported [8].

Physical measurements

Microanalyses were carried out by the Butterworth Microanalytical Service, London. IR spectra were recorded on a Pye Unicam SP2000 spectrophotometer as mulls in Nujol and HCB, and in chloroform solution.

Crystallography

Weissenberg photographs of I indicated orthorhombic symmetry. The systematically absent reflections were those required for either the space group

$Pna2_1$ or $Pnma$. The non-centrosymmetric space group, $Pna2_1$, was found to be the correct one.

Unit cell calibration was carried out for the sample by a least squares fit of the angular parameters for 25 reflections with 2θ ca 20° on a Philips PW1100 automatic four-circle diffractometer using graphite monochromatised Mo- K_α radiation (λ 0.7107 Å). A $\theta - 2\theta$ scan mode was used for data collection and reflections with $3.0 \leq \theta \leq 26.0^\circ$ were examined. Weak reflections which gave $I_t - 2(I_b)^{1/2} < I_b$ on the first scan were not further examined. (I_t is the intensity at the top of the reflection peak and I_b is the mean of two preliminary 5 s background measurements on either side of the peak.) Of the remaining reflections, those for which the total intensity recorded in the first scan of the peak (I_t) was < 500 counts were scanned twice to increase their accuracy. A constant scan speed of $0.05^\circ \text{ s}^{-1}$ and a variable scan width of $(0.70 + 0.05 \tan \theta)^\circ$ was used, with a background measuring time proportional to I_b/I_t . Three standard reflections were measured every 6 h. These showed a decrease of ca. 21% during data collection and were used to scale the data to a common level. See Table 1 for pertinent crystal information and details of data collection.

Reflections in an octant (761) were measured after the preliminary test (see above). The reflection intensities were calculated from the peak and background measurements using a program written for the PW1100 diffractometer [19]. The variance of the intensity, I , was calculated as the sum of the variance due to counting statistics and $(0.04I)^2$, where the term in I^2 was introduced to allow for other sources of error [20]. I and $\sigma(I)$ were corrected for Lorentz and polarisation factors and reflections for which $I \leq 3\sigma(I)$ were rejected. The transmission factors estimated for the crystal along the non-equivalent edge lengths were (0.336) and (0.065). No absorption corrections were applied. Equivalents were averaged to give 749 unique reflections of which 54 were considered to be unobserved. The structure was solved by the heavy atom method and refined by full matrix least-squares.

The Patterson function and an initial difference map were solved in the centrosymmetric space group $Pnma$ and showed peaks corresponding to an isobutyrate ligand lying on a mirror plane and a second isobutyrate ligand oblique to the mirror plane, inconsistent with the space group symmetry elements. Subsequent difference maps with the non-centrosymmetric space group $Pna2_1$ revealed all the atom positions and the presence of disorder both in the methyl groups of the isobutyrate ligands and in one atom of the cyclopropane ring. See Fig. 1 for the atom labelling scheme. Two positions for C(2) [C(2a), C(2b)] and for C(7)

TABLE 1

SUMMARY OF CRYSTAL DATA AND INTENSITY COLLECTION FOR CYCLOPROPYLBIS(ISOBUTYRATO)THALLIUM(III)

Formula weight	419.4	Z	4
Space group	$Pna2_1$	$F(000)$	792
a (Å)	7.316	Crystal dimensions (mm)	$0.1 \times 0.1 \times 0.25$
b (Å)	12.679	μ (cm^{-1})	108.90
c (Å)	16.119	Total no. of variables	82
V (Å ³)	1424.43	Unique data used,	695
		$I > 3\sigma(I)$	

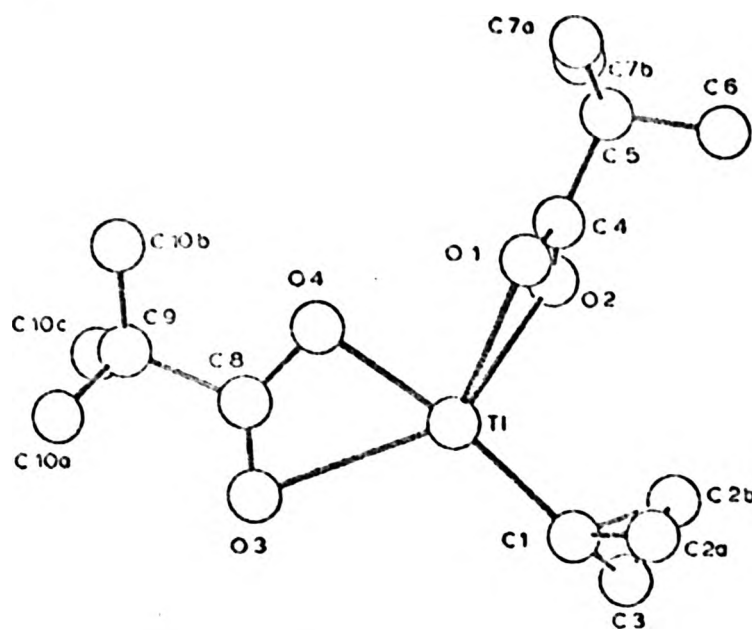


Fig. 1. The structure of **1** showing the disorder in atoms C(2), C(7), and C(10).

[C(7a), C(7b)] were found, together with a three-fold disorder for the atoms C(10) and C(11) [C(10a), C(10b), C(10c)]. It was necessary to constrain isotropic thermal parameters to be equal for the disordered sets of atoms. Based on these restrictions $R = \Sigma ||F_o| - |F_c|| / \Sigma |F_o|$ was 0.045. However, the bond lengths obtained from this model were not chemically reasonable within the

TABLE 2

FINAL FRACTIONAL COORDINATES (TI $\times 10^5$; C, O $\times 10^4$) AND ISOTROPIC THERMAL PARAMETERS ($\times 10^3$) FOR **1**^a

Atom	x	y	z	U (\AA^2)	s.o.f. ^b
Ti	-1130	-6260	25000	^c	1
O(1)	591(25)	674(11)	1061(10)	86(10)	1
O(2)	234(19)	740(9)	4031(37)	65(7)	1
O(3)	-1994(16)	-1519(14)	2333(68)	95(8)	1
O(4)	-1744(15)	-145(12)	2751(128)	89(5)	1
C(1)	1447(23)	-1275(22)	2707(102)	107(10)	1
C(3)	2411(28)	-822(20)	2269(75)	117(15)	1
C(4)	513(21)	1113(16)	2522(44)	74(6)	1
C(5)	763(23)	2047(17)	2230(32)	100(11)	1
C(6)	2023(26)	2123(26)	2301(137)	145(18)	1
C(8)	2398(28)	839(21)	2257(220)	93(14)	1
C(9)	-3670(27)	-669(19)	2412(53)	151(14)	1
C(2a)	2258(56)	-1128(45)	4056(86)	72(19)	1/2
C(2b)	2117(55)	-1525(33)	1226(102)	72(15)	1/2
C(7a)	270(59)	2499(65)	3885(195)	110(20)	1/2
C(7b)	341(60)	2459(67)	485(101)	110(20)	1/2
C(10a)	-1211(46)	-1290(23)	3131(56)	102(10)	2/3
C(10b)	3986(47)	-723(24)	548(42)	102(10)	2/3
C(10c)	3988(40)	129(22)	3097(63)	102(10)	2/3

^a Values of e.s.d.'s in parentheses. ^b Site occupation factor. ^c Anisotropic thermal parameters ($\times 10^3$) for Ti: U_{11} , 67(0); U_{22} , 84(0); U_{33} , 57(0); U_{12} , 0(0); U_{13} , 9(1); U_{23} , -1(5).

disordered parts of the molecule, with chemically equivalent bonds showing a long/short pattern with average values at the expected values.

The chemically equivalent distances in the disordered parts of the molecule were then constrained to be equal within an e.s.d. of 0.005 Å by the addition of extra observational equations to the least-square matrix [21]. The bond lengths were initially set at the average values obtained from the previous model and acceptable values were then obtained at completion of refinement. In the final cycle of refinement the mean and maximum shift/ σ were (0.33) and (1.58) respectively. The final R was 0.045 and $R_w = 0.050$ where: $R_w = [\sum w(|F_o| - |F_c|)^2 / \sum w|F_o|^2]^{1/2}$; with $w = 0.8217(\sigma^2|F_o| + 2.015 \times 10^{-3}|F_o|^2)^{-1}$. Neutral atom scattering factors were used [22], and those for Tl were corrected for anomalous dispersion effects ($\Delta f'$, $\Delta f''$) [23]. Computation was carried out using the SHELX [21] system and ORTEP2 [24]. A list of the observed and calculated structure amplitudes for the data used in the refinements is available from the authors. The final atomic positional and thermal parameters are listed in Table 2.

Results and discussion

Cyclopropylbis(isobutyrate)thallium(III), I, was obtained as colourless crystals from dicyclopropylisobutyrate-thallium(III) by an exchange reaction with bis(isobutyrate)mercury(II) in a manner similar to that described for the preparation of other monoalkylthallium(III) carboxylates [8,12]. The crystals were suitable for X-ray crystal structure analysis and the results obtained represent the first available for a monoorganothallium(III) derivative with a simple anionic ligand. Structural details for only one other cyclopropyl-metal derivative $\text{Al}_2(\text{C}_3\text{H}_5)_6$, appear to have been published [25].

A view of I illustrating the disorder observed and the atomic numbering scheme is shown in Fig. 1. The principal bond lengths and angles are listed in Table 3 and the co-ordination geometry around thallium is shown in Fig. 2. The $\text{C}_3\text{H}_5\text{Tl}(\text{O}_2\text{C}_4\text{H}_7)_2$ units exist in the crystal as infinite linear polymers in which one of the isobutyrate groups, while chelating the Tl atom, also forms oxygen bridges to the Tl atoms of adjacent units. A section of the polymer chain is shown in Fig. 3.

In the $\text{C}_3\text{H}_5\text{Tl}(\text{O}_2\text{C}_4\text{H}_7)_2$ unit (Fig. 1) the thallium atom is five co-ordinate. Polymerisation via the bridging oxygen atoms, however, increases the co-ordination to seven (Fig. 2). The co-ordination geometry of the Tl atom is irregular but may be derived from a pentagonal bipyramid by bending the equatorial atom O(3) towards the O(4) axial position. Seven co-ordinate thallium is unusual but has been found previously in dimethylxanthogenatothallium(III) [26], although bridging S-Tl distances of 3.19 to 3.35 Å were found compared to S-Tl distances of 2.96 Å within the planar TlS_2C unit. In the case of $[\text{C}_3\text{H}_5\text{Tl}(\text{O}_2\text{C}_4\text{H}_7)_2]_n$ the bridging O-Tl distances are not overly long (2.57 to 2.67 Å) compared to the chelating O-Tl distances of 2.50 Å within the same isobutyrate group. The Tl-Tl distance between adjacent monomer units is 4.187 Å.

The non bridging isobutyrate ligand acts as a weak chelate to the thallium atom, showing considerable ester-type character with two very different O-Tl distances of 2.12 and 2.71 Å to oxygen atoms O(1) and O(3) respectively. The

TABLE 3
INTERATOMIC DISTANCES AND ANGLES FOR I^a

Distances ^b					
O(1)-C(1)	1.285(16)	C(1)-C(2a)	1.410(30) ^c	C(5)-C(7b)	1.527(30) ^c
O(2)-C(4)	1.235(16)	C(1)-C(2b)	1.410(30) ^c	C(8)-C(9)	1.675(15)
O(3)-C(8)	1.207(22)	C(4)-C(5)	1.550(35)	C(9)-C(10a)	1.419(28) ^c
O(4)-C(8)	1.359(61)	C(5)-C(6)	1.527(28)	C(9)-C(10b)	1.420(28) ^c
C(1)-C(3)	1.411(30) ^c	C(5)-C(7a)	1.533(27) ^c	C(9)-C(10c)	1.419(28) ^c
Angles ^d					
C(1)-C(3)-C(2a)	60.0(3)	Tl-C(1)-C(2a)	125.0(49)		
C(1)-C(3)-C(2b)	60.0(3)	Tl-C(1)-C(2b)	125.8(49)		
C(1)-C(2a)-C(3)	60.0(3)	O(1)-Tl-O(2)	52.2(6)		
C(1)-C(2b)-C(3)	60.0(4)	O(4)-Tl-O(3)	55.2(7)		
C(3)-C(1)-C(2a)	60.0(3)	C(1)-Tl-O(1)	98.0(13)		
C(3)-C(1)-C(2b)	60.0(3)	C(1)-Tl-O(4)	163.3(26)		
C(4)-C(5)-C(6)	105.5(27)	C(1)-Tl-O(3)	117.9(10)		
C(4)-C(5)-C(7a)	106.1(56)	C(1)-Tl-O(2)	104.4(13)		
C(4)-C(5)-C(7b)	118.2(55)	O(1)-Tl-O(3)	136.5(11)		
C(8)-C(9)-C(10a)	111.4(43)	O(2)-Tl-O(4)	78.2(13)		
C(8)-C(9)-C(10b)	100.7(63)	O(1)-Tl-O(4)	92.6(13)		
C(8)-C(9)-C(10c)	116.4(36)	O(2)-Tl-O(3)	130.0(9)		
C(10a)-C(9)-C(10b)	109.2(13) ^e	O(1 ⁱⁱ)-Tl-O(1)	120.6(6)		
C(10a)-C(9)-C(10c)	109.3(13) ^e	O(1 ⁱⁱ)-Tl-O(2)	68.4		
C(10b)-C(9)-C(10c)	109.3(13) ^e	O(1 ⁱⁱ)-Tl-O(3)	81.2(11)		
O(1)-C(4)-O(2)	117.6(22)	O(1 ⁱⁱ)-Tl-O(4)	74.0(13)		
O(1)-C(4)-C(5)	114.0(32)	O(1 ⁱⁱ)-Tl-C(1)	96.1(13)		
O(2)-C(4)-C(5)	128.5(33)	O(1 ⁱⁱ)-Tl-O(2 ⁱ)	163.3(6)		
O(3)-C(8)-O(4)	127.7(58)	O(2 ⁱ)-Tl-O(1)	70.1(6)		
O(3)-C(8)-C(9)	117.9(31)	O(2 ⁱ)-Tl-O(2)	120.7(6)		
O(4)-C(8)-C(9)	109.4(41)	O(2 ⁱ)-Tl-O(3)	82.5(9)		
C(6)-C(5)-C(7a)	108.8(11) ^e	O(2 ⁱ)-Tl-O(4)	93.5(13)		
C(6)-C(5)-C(7b)	109.0(12) ^e	O(2 ⁱ)-Tl-C(1)	94.9(13)		
Tl-C(1)-C(3)	117.0(29)				

^a The superscripts i and ii refer to the symmetry transformations $-x, -y, -1/2 + z$ and $-x, -y, 1/2 + z$ respectively (see Fig. 3). ^b In Å; e.s.d.'s in parentheses. ^c Constrained bond lengths. ^d In degrees; e.s.d.'s in parentheses. ^e Constrained angles.

shorter of these two bonds makes an angle of 168° with the Tl-C bond to the cyclopropyl ring and strikingly demonstrates that the dominant characteristic of dialkylthallium(III) chemistry whereby thallium tends to form a near-linear arrangement with two strongly bonded groups [1a, 26-28] persists into monoalkylthallium(III) systems. Indeed, the polymeric pattern of I is very similar to that found for dimethylacetatothallium(III), $(\text{CH}_3)_2\text{TlO}_2\text{CCH}_3$ [28], and the structural arrangement of I can be considered to be derived from the latter by replacing one of the alkyl groups with the non-bridging isobutyrate group. The C-Tl-C angle in $(\text{CH}_3)_2\text{TlO}_2\text{CCH}_3$ is 172(2)° [28] (cf. C(1)-Tl-O(4) in I 168(3)°). The least squares plane through O(1), O(2), C(4), C(5), Tl of the bridging ligand and that through O(3), O(4), C(8), C(9), Tl of the non-bridging ligand intersect at an angle of 78° (see Table 4). This is close to the angle (86°) made between the Tl-CH₃ bond and the TlC₂O₂ plane of the chelating and bridging acetate ligand in dimethylacetatothallium(III).

The Tl-C bond length of 2.160 Å is similar to that found in the two other reported structures of monoalkylthallium(III) compounds (Tl-C = 2.147 Å in

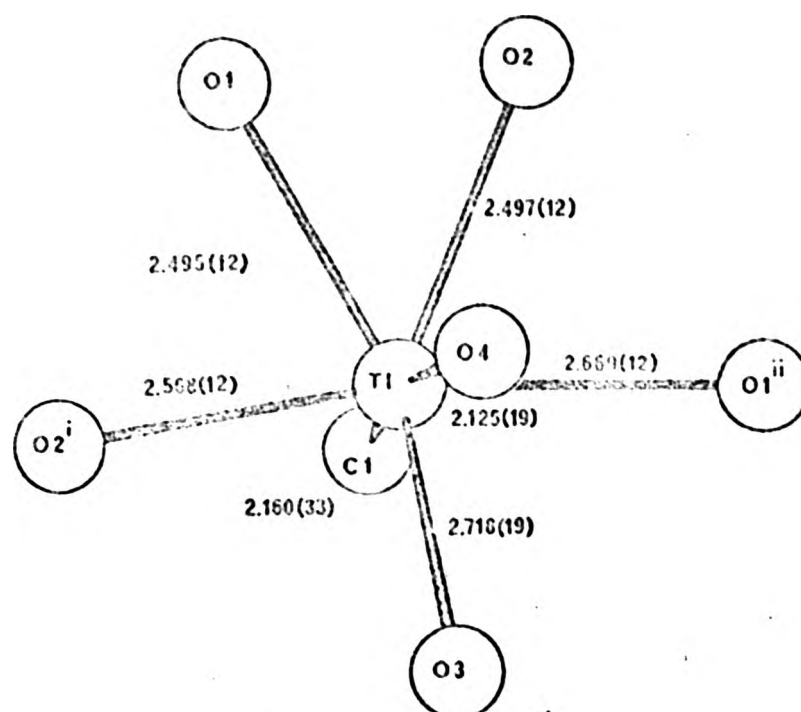


Fig. 2. Coordination geometry around Tl in I showing bond lengths (Å) with e.s.d.s. in parentheses. (See footnote to Table 3 for definitions of superscripts i and ii.)

methyl-5,10,15,20-tetraphenylporphinatothallium(III) [15]; Tl-C = 2.073 Å in a methylthallium(III) complex of 2,6-bis(2-methyl-2-benzothiazolynyl)pyridine [16]). The Tl-C distance in I also in the range (2.01–2.20 Å) found

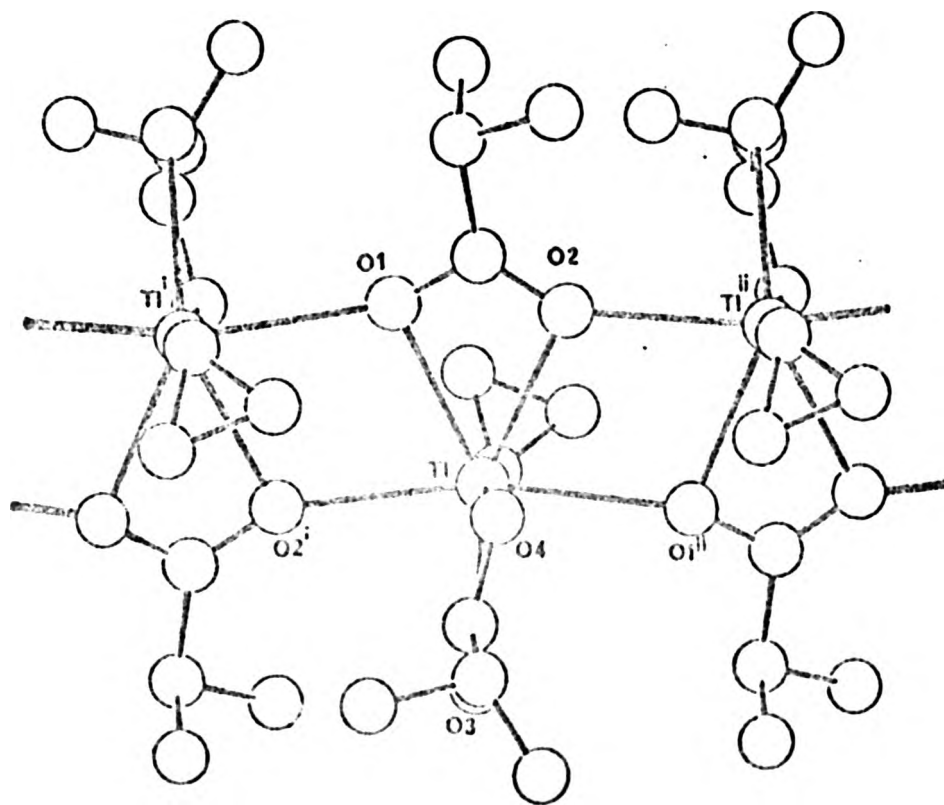


Fig. 3. A section of the polymer chain in I. For clarity, only one position for each disordered atom is shown. (See footnote to Table 3 for definitions of superscript i and ii.)

TABLE 4
LEAST SQUARES PLANES DEFINED BY $lx + my + nz = p$

Plane	Atoms defining plane	<i>l</i>	<i>m</i>	<i>n</i>	<i>p</i>
1	O(1), O(2), C(4), C(5), Tl	-0.954	0.227	-0.196	-0.522
2	O(3), O(4), C(8), C(9), Tl	0.020	0.127	-0.992	-1.983

Deviations from planes (Å)

1	O(2), -0.064; O(2), -0.051; C(4), 0.023; C(5), 0.073; Tl, 0.065
2	O(3), -0.076; O(4), -0.088; C(8), 0.117; C(9), 0.007; Tl, 0.038

Angle between planes 78.3°

for Tl-C bonds in neutral dialkylthallium(III) species [26-28].

The short C-C distances found in the cyclopropyl group (1.41 Å) are a result of the crystallographic treatment of the disorder and are not comparable to the values found in other monosubstituted cyclopropyl derivatives.

Infrared spectra

The role of the carboxylate anions (bridging and/or chelating) in organothallium(III) carboxylates has previously been suggested from assignments of their IR spectra [8,11,29-31]. Consideration of the structure of I, together with that of $(\text{CH}_3)_2\text{TlO}_2\text{C}_2\text{H}_3$ [28] allows clarification of these interpretations.

The IR spectra in the region 1350-1650 cm^{-1} for I and other alkylthallium(III) carboxylates are compared in Tables 5 and 6, and the bands are assigned as $\nu(\text{CO}_2)$ asymmetric or symmetric stretching frequencies. The spectra indicate that the monoalkylthallium(III) compounds have similar structures in the solid state. Likewise, the solid state structures of $(\text{CH}_3)_2\text{TlO}_2\text{C}_2\text{H}_3$ and $(\text{C}_3\text{H}_5)_2\text{TlO}_2\text{C}_4\text{H}_7$ appear to be similar. The crystal structure of $(\text{CH}_3)_2\text{TlO}_2\text{C}_2\text{H}_3$ shows only one type of acetate group [28], and this is both chelating and bridg-

TABLE 5
IR ABSORPTION BANDS IN THE REGION 1350-1650 cm^{-1} OF ALKYLTHALLIUM(III) CARBOXYLATES IN THE SOLID STATE ^{a, b}

$\text{C}_3\text{H}_5\text{TlX}_2$ (I)	$(\text{C}_3\text{H}_5)_2\text{TlX}$	CH_3TlX_2 ^c	CH_3TlY_2 ^d	$(\text{CH}_3)_2\text{TlY}$ ^e	Assignment ^f	
1615s		1610s	1610s	1540vs(br)	$\nu(\text{CO}_2)_{\text{asym}}$	
1512vs	1520s	1510s	1539s			
1505vs(sh)	1518s(sh)					
1480w				1428vs(br)	$\nu(\text{CO}_2)_{\text{sym}}$	
1471w	1468w	1468m	1420—1380s(br)			
1428s	1411s	1425s				
1390m		1390s				
1377w		1372m				
1360w	1360m	1359m				

^a X = $\text{O}_2\text{C}_2\text{H}_3$; Y = $\text{O}_2\text{C}_2\text{H}_3$. cm^{-1} . vs very strong, s strong, m medium, w weak, sh shoulder, br broad.

^b Spectra obtained using Nujol or hexachlorobutadiene mulls. ^c Data from ref. 8. ^d Band positions in agreement with those in ref. 11. ^e Band positions in good agreement with those in refs. 11, 29 and 30.

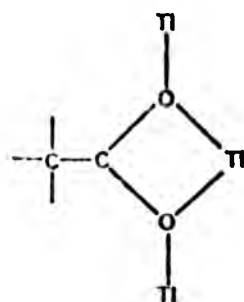
^f Assignments by analogy with, or as given in refs. 8, 11, 29-31.

TABLE 6
IR ABSORPTION BANDS IN THE REGION 1350–1650 cm^{-1} OF ALKYLTHALLIUM(III) CARBOXY-
LATES IN SOLUTION ^{a, b}

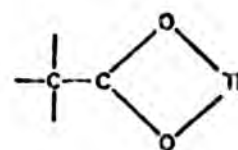
$\text{C}_3\text{H}_7\text{TlX}_2$ (I)	$(\text{C}_3\text{H}_7)_2\text{TlX}$	CH_3TlX_2 ^c	CH_3TlY_2	$(\text{CH}_3)_2\text{TlY}$	Assignment ^d
1590s(br,sh)		1577(br)	1590s(sh)		$\nu(\text{CO}_2)_{\text{asym.}}$
1540s(br)	1545s(br)	1525s	1560s(br)	1570s	
1473m	1480w	1469s			
1408m	1420m	1405s	1415s(br)	1428s(br)	$\nu(\text{CO}_2)_{\text{sym.}}$
1395(sh)		1400(sh)	1337(sh)		
1375m	1375w	1370m			
1365m		1360m			

^a See footnote a, Table 5. ^b Spectra obtained in CHCl_3 solution, 1% w/w. ^c Data from ref. 8. ^d Assignment by analogy with, or as given in, ref. 8.

ing (A). A simultaneously chelating and bridging carboxylate anion is also



(A)



(B)

found in the structure of I. This indicates that for all the alkylthallium(III) carboxylates in Table 5, strong bands in the regions 1505–1540 and 1411–1428 cm^{-1} can be assigned as $\nu(\text{CO}_2)_{\text{asym.}}$ and $\nu(\text{CO}_2)_{\text{sym.}}$ respectively in chelating and bridging anions of type A. The additional strong bands in the regions 1610–1615 and 1380–1390 cm^{-1} for the monoalkylthallium(III) carboxylates are consequently assigned as $\nu(\text{CO}_2)_{\text{asym.}}$ and $\nu(\text{CO}_2)_{\text{sym.}}$ respectively in chelating carboxylates (B) as found in the structure of I. The higher energies of the $\nu(\text{CO}_2)_{\text{asym.}}$ bands of structural type B are consistent with the lack of bridging function and, as indicated by the structure of I, with the significantly ester type character of this group.

On dissolution in chloroform $\nu(\text{CO}_2)_{\text{asym.}}$ for ligands of type A increases by 15–35 cm^{-1} , consistent with partial disruption of bridging $\text{Tl}-\text{O}$ bonds as solvent molecules break up the polymer chains. This interpretation is also consistent with the state of aggregation (ca. 2) of $\text{CH}_3\text{Tl}(\text{OC}_4\text{H}_9)_2$ in CHCl_3 solution [8]. The values of $\nu(\text{CO}_2)_{\text{asym.}}$ for ligands of type B decrease by 20–33 cm^{-1} for chloroform solutions, and this may be due to ester-like arrangement in B being altered to for a more symmetrically coordinated carboxylate anion.

The IR spectra of other organothallium(III) carboxylates have been reported ($\text{C}_2\text{H}_5\text{TlX}_2$, $(\text{C}_2\text{H}_5)_2\text{TlX}$ [8], $\text{C}_6\text{H}_5\text{TlX}_2$ [31], $\text{C}_6\text{H}_5\text{TlY}_2$ [11,31], $(\text{C}_6\text{F}_5)_2\text{TlY}$ [20]; $\text{X} = \text{O}_2\text{C}_4\text{H}_9$; $\text{Y} = \text{O}_2\text{C}_3\text{H}_7$) and the similarity of their spectra (in the region 1350–1650 cm^{-1}) to those in Table 5 suggests that they contain carboxylate anions of type A and, for the mono-organothallium(III) species, also type B.

Acknowledgements

We thank the S.P.C. for financial support for purchase of X-ray diffractometer equipment and for a Research Studentship (to F.B.). We thank Dr. M. McPartlin for her interest in this work.

References

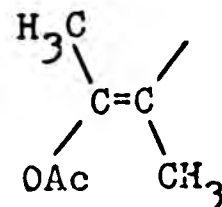
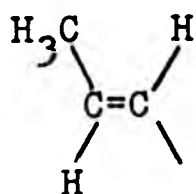
- 1 (a) A.G. Lee, *The Chemistry of Thallium*, Elsevier Amsterdam, 1971, ch. 7; (b) J.P. Maher, M. Evans and M. Harrison, *J. Chem. Soc. Dalton*, (1972) 188.
- 2 (a) J.P. Maher and D.F. Evans, *J. Chem. Soc.*, (1965) 637; (b) A.E. Borisov and N.V. Novikova, *Izvest. Akad. Nauk S.S.S.R., Otdel. Khim. Nauk*, (1959) 1670; (c) S. Uemura, K. Sohma, H. Tara and M. Okano, *Chem. Lett.*, (1973) 545.
- 3 E. Maxa, G. Schulz and E. Zbiral, *Liebigs Ann. Chem.*, (1974) 933.
- 4 T. Abe and R. Okawara, *J. Organometal. Chem.*, 43 (1972) 117.
- 5 S. Namata, H. Kurosawa and R. Okawara, *J. Organometal. Chem.*, 70 (1974) C21.
- 6 R.G. Coombes, M.D. Johnson and D. Vamplew, *J. Chem. Soc. (A)*, (1968) 2297.
- 7 S. Uemura, A. Toshimitsu and M. Okano, *Bull. Chem. Soc. Japan*, 49 (1976) 2762; H. Kurosawa, R. Kitano and T. Sasaki, *J. Chem. Soc. Dalton*, (1978) 234.
- 8 H. Kurosawa and R. Okawara, *J. Organometal. Chem.*, 10 (1967) 211.
- 9 H. Kurosawa and R. Okawara, *J. Organometal. Chem.*, 11 (1968) 225; Y. Kawasaki, *Organic Magn. Res.*, 2 (1970) 165; K. Tanaka, H. Kurosawa and R. Okawara, *J. Organometal. Chem.*, 30 (1971) 1.
- 10 H. Kurosawa, M. Tanaka and R. Okawara, *J. Organometal. Chem.*, 12 (1968) 241; H. Kurosawa, T. Fukumoto and R. Okawara, *Inorg. Nucl. Chem. Letters*, 3 (1969) 473; C.S. Hoad, R.W. Matthews, M.M. Thakur and D.G. Gillies, *J. Organometal. Chem.*, 124 (1977) C31.
- 11 H. Kurosawa and R. Okawara, *J. Organometal. Chem.*, 19 (1969) 253.
- 12 M. Tanaka, H. Kurosawa and R. Okawara, *J. Organometal. Chem.*, 18 (1969) 49.
- 13 T. Fukumoto, H. Kurosawa and R. Okawara, *J. Organometal. Chem.*, 22 (1970) 627.
- 14 U. Pebl and F. Huber, *J. Organometal. Chem.*, 116 (1976) 141; 135 (1977) 301.
- 15 K. Henrick, R.W. Matthews and P.A. Tasker, *Inorg. Chem.*, 16 (1977) 3293.
- 16 K. Henrick, R.W. Matthews and P.A. Tasker, *Inorg. Chim. Acta*, 25 (1977) 131.
- 17 M.D. Johnson, *Chem. Commun.*, (1970) 1037.
- 18 D. Seyferth and H.M. Cohen, *Inorg. Chem.*, 1 (1962) 913.
- 19 J. Hornstra and B. Stubbe, *PW1100 Data Processing Program*, 1972, Philips Research Laboratories, Eindhoven, The Netherlands.
- 20 P.W.R. Corfield, R.J. Doedens and J.A. Ibers, *Inorg. Chem.*, 6 (1967) 197.
- 21 Programs for crystal structure determinations were kindly supplied by G.M. Sheldrick, University of Cambridge, England.
- 22 D.T. Cromer and J.B. Mann, *Acta Crystallogr., Sect. A*, 24 (1968) 321.
- 23 D.T. Cromer, *Acta Crystallogr.*, 13 (1965) 17.
- 24 C.K. Johnson, Oak Ridge National Laboratory, Tenn., U.S.A.
- 25 J.W. Moore, D.A. Sanders, P.A. Scherr, N.D. Glick and J.P. Oliver, *J. Amer. Chem. Soc.*, 93 (1971) 1035.
- 26 W. Schwartz, G. Mann and J. Wiedlein, *J. Organometal. Chem.*, 122 (1976) 303.
- 27 P.J. Burke, L.A. Gray, D.G. Gillies, P.J.C. Harwood, R.W. Matthews and M. McPartlin, *J. Organometal. Chem.*, 136 (1977) C7; Y.F. Chow and D. Britton, *Acta Crystallogr.*, B31 (1975) 1922, 1934; K. Henrick, R.W. Matthews and P.A. Tasker, *Acta Crystallogr.*, B31 (1975) 955, 1347; T.L. Blundell and H.M. Powell, *Proc. Roy. Soc. Lond.*, A331 (1972) 161; S.K. Seal and J.L. Atwood, *J. Organometal. Chem.*, 61 (1974) 1; G.H.W. Milburn and M.R. Fother, *J. Chem. Soc., (A)* (1967) 648.
- 28 Y.M. Cheu and D. Britton, *Acta Crystallogr.*, B31 (1975) 1929.
- 29 G.B. Deacon, J.H.S. Green and R.S. Nyholm, *J. Chem. Soc.*, (1965) 3411.
- 30 G.B. Deacon and J.H.S. Green, *Spectrochim. Acta*, 24A (1978) 885.
- 31 A.G. Lee, *J. Organometal. Chem.*, 22 (1970) 537.

APPENDIX I

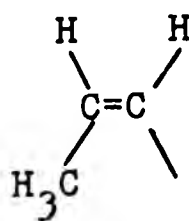
ABBREVIATIONS USED

<u>iso</u> -propyl	$(\text{CH}_3)_2\text{CH}$	
<u>iso</u> -butyl	$(\text{CH}_3)_2\text{CHCH}_2$	
<u>sec</u> -butyl	$\text{CH}_3\text{CH}_2(\text{CH}_3)\text{CH}$	
<u>iso</u> -amyl	$(\text{CH}_3)_2\text{CHCH}_2\text{CH}$	
<u>sec</u> -amyl	$\text{CH}_3\text{CH}_2\text{CH}_2(\text{CH}_3)\text{CH}$	
<u>neo</u> -pentyl	$(\text{CH}_3)_3\text{CCH}_2$	
trimethylsilylmethyl	$(\text{CH}_3)_3\text{SiCH}_2$	
cyclohexylmethyl	$\text{cyclo-C}_6\text{H}_{11}\text{CH}_2$	
vinyl	$\text{H}_2\text{C}=\text{CH}-$	
<u>iso</u> -propenyl	$\text{H}_2\text{C}=\text{C}(\text{CH}_3)$	<u>trans</u> -2-acetato, but-2-enyl

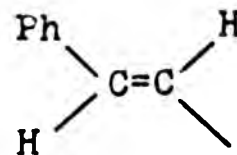
trans-propenyl



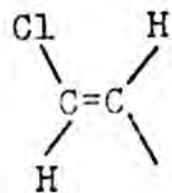
cis-propenyl



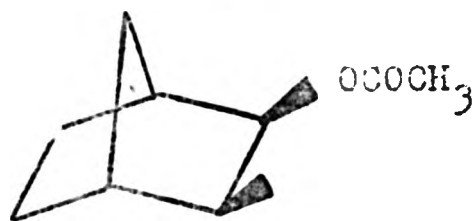
trans- β -styryl



trans-chlorovinyl



bornane



norbornene



APPENDIX II

COMPUTER OUTPUT FROM ITERATIVE CALCULATION

OF ^1H SPECTRUM OF BIS(CYCLOPROPYL)ISOBUTYRATO-THALLIUM(III)

COMP 1 DICYCLOPENTHENE 19973

NUM 6 FREQUENCY RANGE -228.000 372.000 MINIMUM INTENSITY 0.02000

100 VALUE CHEMICAL SHIFT

1	U(1)=	67.960
1	U(2)=	51.760
1	U(3)=	73.100
1	U(4)=	51.760
1	U(5)=	73.100
2	U(6)=	10000.000

COUPLING CONSTANTS

J(1,2)=	9.360
J(1,3)=	6.320
J(1,4)=	9.360
J(1,5)=	6.320
J(1,6)=	605.130
J(2,3)=	7.000
J(2,4)=	8.670
J(2,5)=	4.900
J(2,6)=	340.060
J(3,4)=	4.900
J(3,5)=	7.860
J(3,6)=	562.820
J(4,5)=	7.000
J(4,6)=	340.060
J(5,6)=	562.820

PARAMETER SETS

1 U(1)

2 U(2)
U(4)

3 U(3)
U(5)

ITERATION	0	R M S ERROR =	2.466
ITERATION	1	R M S ERROR =	2.333
ITERATION	2	R M S ERROR =	2.300
ITERATION	3	R M S ERROR =	2.291

Best values Case1.

1	$\mu(1) =$	66.702
1	$\mu(2) =$	50.904
1	$\mu(3) =$	72.532
1	$\mu(4) =$	50.904
1	$\mu(5) =$	72.532
2	$\mu(6) =$	10000.000
	$J(1,2) =$	9.360
	$J(1,3) =$	6.320
	$J(1,4) =$	9.360
	$J(1,5) =$	6.320
	$J(1,6) =$	408.130
	$J(2,3) =$	3.800
	$J(2,4) =$	8.670
	$J(2,5) =$	4.900
	$J(2,6) =$	340.060
	$J(3,4) =$	4.900
	$J(3,5) =$	7.860
	$J(3,6) =$	562.320
	$J(4,5) =$	3.800
	$J(4,6) =$	340.060
	$J(5,6) =$	562.320

ERROR VECTORS AND STANDARD ERRORS

0.0037	0.0410	0.0294	
	STANDARD ERROR =	1.495	
0.0437	0.0984	0.0392	
	STANDARD ERROR =	0.851	
0.0010	0.0340	0.0008	
	STANDARD ERROR =	1.027	

PROBABLE ERRORS OF PARAMETER SETS

1	1.608
2	0.576
3	0.603

**REPRODUCED
FROM THE
BEST
AVAILABLE
COPY**

[illegible]

1911	1,000,000	1,000,000	1912	1,000,000	1,000,000	
1913	1,000,000	1,000,000	1914	1,000,000	1,000,000	
1915	1,000,000	1,000,000	1916	1,000,000	1,000,000	
1917	1,000,000	1,000,000	1918	1,000,000	1,000,000	
1919	1,000,000	1,000,000	1920	1,000,000	1,000,000	
1921	1,000,000	1,000,000	1922	1,000,000	1,000,000	
1923	1,000,000	1,000,000	1924	1,000,000	1,000,000	
1925	1,000,000	1,000,000	1926	1,000,000	1,000,000	
1927	1,000,000	1,000,000	1928	1,000,000	1,000,000	
1929	1,000,000	1,000,000	1930	1,000,000	1,000,000	
1931	1,000,000	1,000,000	1932	1,000,000	1,000,000	
1933	1,000,000	1,000,000	1934	1,000,000	1,000,000	
1935	1,000,000	1,000,000	1936	1,000,000	1,000,000	
1937	1,000,000	1,000,000	1938	1,000,000	1,000,000	
1939	1,000,000	1,000,000	1940	1,000,000	1,000,000	
1941	1,000,000	1,000,000	1942	1,000,000	1,000,000	
1943	1,000,000	1,000,000	1944	1,000,000	1,000,000	
1945	1,000,000	1,000,000	1946	1,000,000	1,000,000	
1947	1,000,000	1,000,000	1948	1,000,000	1,000,000	
1949	1,000,000	1,000,000	1950	1,000,000	1,000,000	
1951	1,000,000	1,000,000	1952	1,000,000	1,000,000	
1953	1,000,000	1,000,000	1954	1,000,000	1,000,000	
1955	1,000,000	1,000,000	1956	1,000,000	1,000,000	
1957	1,000,000	1,000,000	1958	1,000,000	1,000,000	
1959	1,000,000	1,000,000	1960	1,000,000	1,000,000	
1961	1,000,000	1,000,000	1962	1,000,000	1,000,000	
1963	1,000,000	1,000,000	1964	1,000,000	1,000,000	
1965	1,000,000	1,000,000	1966	1,000,000	1,000,000	
1967	1,000,000	1,000,000	1968	1,000,000	1,000,000	
1969	1,000,000	1,000,000	1970	1,000,000	1,000,000	
1971	1,000,000	1,000,000	1972	1,000,000	1,000,000	
1973	1,000,000	1,000,000	1974	1,000,000	1,000,000	
1975	1,000,000	1,000,000	1976	1,000,000	1,000,000	
1977	1,000,000	1,000,000	1978	1,000,000	1,000,000	
1979	1,000,000	1,000,000	1980	1,000,000	1,000,000	
1981	1,000,000	1,000,000	1982	1,000,000	1,000,000	
1983	1,000,000	1,000,000	1984	1,000,000	1,000,000	
1985	1,000,000	1,000,000	1986	1,000,000	1,000,000	
1987	1,000,000	1,000,000	1988	1,000,000	1,000,000	
1989	1,000,000	1,000,000	1990	1,000,000	1,000,000	
1991	1,000,000	1,000,000	1992	1,000,000	1,000,000	
1993	1,000,000	1,000,000	1994	1,000,000	1,000,000	
1995	1,000,000	1,000,000	1996	1,000,000	1,000,000	
1997	1,000,000	1,000,000	1998	1,000,000	1,000,000	
1999	1,000,000	1,000,000	2000	1,000,000	1,000,000	
2001	1,000,000	1,000,000	2002	1,000,000	1,000,000	
2003	1,000,000	1,000,000	2004	1,000,000	1,000,000	
2005	1,000,000	1,000,000	2006	1,000,000	1,000,000	
2007	1,000,000	1,000,000	2008	1,000,000	1,000,000	
2009	1,000,000	1,000,000	2010	1,000,000	1,000,000	
2011	1,000,000	1,000,000	2012	1,000,000	1,000,000	
2013	1,000,000	1,000,000	2014	1,000,000	1,000,000	
2015	1,000,000	1,000,000	2016	1,000,000	1,000,000	
2017	1,000,000	1,000,000	2018	1,000,000	1,000,000	
2019	1,000,000	1,000,000	2020	1,000,000	1,000,000	
2021	1,000,000	1,000,000	2022	1,000,000	1,000,000	
2023	1,000,000	1,000,000	2024	1,000,000	1,000,000	
2025	1,000,000	1,000,000	2026	1,000,000	1,000,000	
2027	1,000,000	1,000,000	2028	1,000,000	1,000,000	
2029	1,000,000	1,000,000	2030	1,000,000	1,000,000	
2031	1,000,000	1,000,000	2032	1,000,000	1,000,000	
2033	1,000,000	1,000,000	2034	1,000,000	1,000,000	
2035	1,000,000	1,000,000	2036	1,000,000	1,000,000	
2037	1,000,000	1,000,000	2038	1,000,000	1,000,000	
2039	1,000,000	1,000,000	2040	1,000,000	1,000,000	
2041	1,000,000	1,000,000	2042	1,000,000	1,000,000	
2043	1,000,000	1,000,000	2044	1,000,000	1,000,000	
2045	1,000,000	1,000,000	2046	1,000,000	1,000,000	
2047	1,000,000	1,000,000	2048	1,000,000	1,000,000	
2049	1,000,000	1,000,000	2050	1,000,000	1,000,000	
2051	1,000,000	1,000,000	2052	1,000,000	1,000,000	
2053	1,000,000	1,000,000	2054	1,000,000	1,000,000	
2055	1,000,000	1,000,000	2056	1,000,000	1,000,000	
2057	1,000,000	1,000,000	2058	1,000,000	1,000,000	
2059	1,000,000	1,000,000	2060	1,000,000	1,000,000	
2061	1,000,000	1,000,000	2062	1,000,000	1,000,000	
2063	1,000,000	1,000,000	2064	1,000,000	1,000,000	
2065	1,000,000	1,000,000	2066	1,000,000	1,000,000	
2067	1,000,000	1,000,000	2068	1,000,000	1,000,000	
2069	1,000,000	1,000,000	2070	1,000,000	1,000,000	
2071	1,000,000	1,000,000	2072	1,000,000	1,000,000	
2073	1,000,000	1,000,000	2074	1,000,000	1,000,000	
2075	1,000,000	1,000,000	2076	1,000,000	1,000,000	
2077	1,000,000	1,000,000	2078	1,000,000	1,000,000	
2079	1,000,000	1,000,000	2080	1,000,000	1,000,000	
2081	1,000,000	1,000,000	2082	1,000,000	1,000,000	
2083	1,000,000	1,000,000	2084	1,000,000	1,000,000	
2085	1,000,000	1,000,000	2086	1,000,000	1,000,000	
2087	1,000,000	1,000,000	2088	1,000,000	1,000,000	
2089	1,000,000	1,000,000	2090	1,000,000	1,000,000	
2091	1,000,000	1,000,000	2092	1,000,000	1,000,000	
2093	1,000,000	1,000,000	2094	1,000,000	1,000,000	
2095	1,000,000	1,000,000	2096	1,000,000	1,000,000	
2097	1,000,000	1,000,000	2098	1,000,000	1,000,000	
2099	1,000,000	1,000,000	2100	1,000,000	1,000,000	

APPENDIX III

τ VALUES USED IN THALLIUM-205 SPIN-LATTICE
RELAXATION MEASUREMENTS.

1. $\frac{1}{\tau} = \frac{1}{\tau_0} \left[\frac{c}{c_0} \right]^2$ 0.22 mol dm^{-3} in DMSO-d6

2. 1.1

Temp = 36.5°C

τ (sec)	τ_T (mm)
0.001	-115
0.005	-137
0.01	-125
0.03	-95.5
0.03	-72
0.13	60.5
0.15	71.5
0.17	88.5
0.17	105
1.0	176

$\omega = 176$
 $\tau_1 = 0.112s$

Temp = 36.5°C

τ (sec)	τ_T (mm)
0.001	-143
0.01	-115
0.03	-77.5
0.05	-45
0.07	-18
0.13	42
0.15	61
0.17	74
0.19	87
1.0	164

$\tau_\infty = 164$
 $\tau_1 = 0.139s$

Temp = 50.7°C

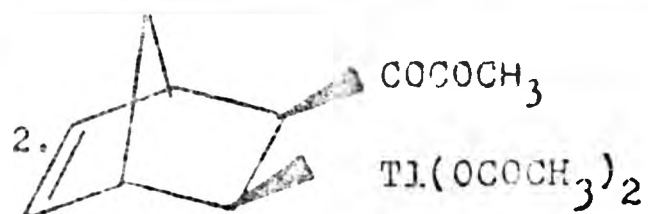
τ (sec)	τ_T (mm)
0.001	-155.5
0.01	-132
0.03	-100
0.07	-67.5
0.07	-41.5
0.15	20
0.17	29
0.19	36.5
1.0	170

$\omega = 170$
 $\tau_1 = 0.177s$

Temp = 52.8°C

τ (sec)	τ_T (mm)
0.001	-96
0.01	-84.5
0.05	-45
0.07	-29
0.09	-16.5
0.15	20.5
0.17	32
0.19	41
0.21	50.5
1.50	127.5

$\tau_\infty = 127.5$
 $\tau_1 = 0.199s$



0.56 mol dm^{-3} in DMSO-d_6

Table 5.1.

Temp = 16.3°C		Temp = 30.3°C	
$\tau(\text{sec})$	$M_\tau(\text{mm})$	$\tau(\text{sec})$	$M_\tau(\text{mm})$
0.001	-371	0.001	-141.5
0.01	-282	0.01	-123
0.03	-151	0.07	-45
0.05	-45	0.09	-10.5
0.07	38	0.11	46.0
0.09	107	0.15	58
0.11	165.5	0.19	81
0.13	214	0.25	107.5
0.15	250	2.0	157.0
1.50	416		
M_∞ = 416		M_∞ = 157	
T_1 = 0.097s		T_1 = 0.137s	

Temp = 45.6°C	
$\tau(\text{sec})$	$M_\tau(\text{mm})$
0.001	-286
0.01	-287
0.03	-227
0.05	-164.5
0.07	-108
0.13	17.5
0.15	53
0.19	112
0.30	217
1.50	362
M_∞ = 362	
T_1 = 0.192s	

3. $[(CH_3)_2N]_2TiCl_2CH(CH_3)_2$ 0.25 mol dm⁻³ in pyridine -d₅

Table 5.2.

Temp = 45.5°C		Temp = 58.0°C	
τ (sec)	M_τ (mm)	τ (sec)	M_τ (mm)
0.03	-75	0.001	-134.5
0.05	-51	0.01	-104
0.07	-25	0.03	-79.5
0.11	10	0.05	-58
0.13	23	0.07	-37
0.15	36	0.15	26
0.17	49.5	0.17	36.5
1.00	141.5	0.19	47
		0.21	57
		1.25	142.5
M_∞	= 141.5	M_∞	= 142.5
T_1	= 0.166s	T_1	= 0.185s

Temp = 64.5°C		Temp = 81.5°C	
τ (sec)	M_τ (mm)	τ (sec)	M_τ (mm)
0.001	-125.5	0.001	-125
0.03	-79.5	0.01	-114.5
0.05	-60.5	0.03	-85.5
0.09	-22	0.05	-65
0.15	20	0.07	-43.5
0.18	37.5	0.13	0
0.20	47.5	0.15	13
0.22	55	0.17	25
0.25	136	0.20	39.5
		1.25	145.5
M_∞	= 136	M_∞	= 145.5
T_1	= 0.188s	T_1	= 0.213s

0. (7.2) HCl 0.2 mol $\Delta - 3$ in DMSO d. (Table 5.2)

Temp = 22.0°C			Temp = 20.7°C		
$\tau(\text{sec})$	$M_\tau(\text{mm})$	$\tau(\text{sec})$	$M_\tau(\text{mm})$	$\tau(\text{sec})$	$M_\tau(\text{mm})$
0.001	-78	0.001	-81	0.01	-85.5
0.005	-88	0.01	-68	0.02	-70.5
0.01	-59.5	0.02	-50	0.03	-56
0.02	-38	0.03	-31	0.05	-33.5
0.03	-21	0.04	-20.5	0.11	21
0.05	44	0.05	30.5	0.13	34
0.10	53	0.10	39.5	0.14	40
0.11	59	0.11	47	0.15	44.5
0.12	62.5	0.12	51	1.00	103
1.00	91	1.00	94		

$\infty = 91$ $M_\infty = 94$ $M_\infty = 108$
 $T_1 = 0.056$ $T_1 = 0.083$ $T_1 = 0.125$

Temp = 62.8°C		Temp = 80.7°C	
$\tau(\text{sec})$	$M_\tau(\text{mm})$	$\tau(\text{sec})$	$M_\tau(\text{mm})$
0.02	-80	0.01	-71
0.03	-68	0.03	-51.5
0.05	-59	0.05	-37
0.07	-47	0.07	-26
0.11	13	0.20	23.5
0.12	19	0.21	27
0.13	19	0.23	31
0.15	20.5	0.25	35
1.00	101	1.25	79
$\infty = 101$		$M_\infty = 79$	
$T_1 = 0.199$		$T_1 = 0.199$	

APPENDIX IV

OBSERVED AND CALCULATED STRUCTURE FACTORS FOR
CYCLOPROPYLBIS(ISOBUTYRATO)THALLIUM(III)

AND

BIS(TRIMETHYLSILYLMETHYL)CHLOROTHALLIUM(III)

[illegible]

[The page contains extremely faint, illegible markings that appear to be bleed-through from the reverse side of the document.]

[illegible]

[illegible]

[illegible]

[illegible]

[illegible]

[illegible]

Attention is drawn to the fact that the copyright of this thesis rests with its author.

This copy of the thesis has been supplied on condition that anyone who consults it is understood to recognise that its copyright rests with its author and that no quotation from the thesis and no information derived from it may be published without the author's prior written consent.

I

D 37667'81

END

D37668'81

END